

FACILITY FORM 602

N 66-10684

(ACCESSION NUMBER)	(THRU)
168	1
(PAGES)	(CODE)
30, 375, 3	29
(NASA CR OR TMX OR AD NUMBER)	(CATEGORY)

GPO PRICE \$ _____

CFSTI PRICE(S) \$ _____

Hard copy (HC) 5.00

Microfiche (MF) 1.00

ff 653 July 65

JET PROPULSION LABORATORY
CALIFORNIA INSTITUTE OF TECHNOLOGY
PASADENA, CALIFORNIA

NSL 65-5
JANUARY 1965

FINAL REPORT FOR

CONTRACT NO. JPL 950229

**JET PROPULSION LABORATORY
PASADENA, CALIFORNIA**

BY CONSTANTINO CAFARO, MERL K. FAIRCCHILD,
HERBERT J. HARRIS, ARNOLD P. GHLOSINGER
AND VINCENT M. URBAN

**ENGINEERING STUDY TO DETERMINE
FEASIBLE METHODS OF SIMULATING
PLANETARY ALBEDO AND RADIATION
EFFECTS UPON THE THERMAL
BALANCE OF SPACECRAFT**

*This work was performed for the Jet Propulsion Laboratory,
California Institute of Technology, sponsored by the
National Aeronautics and Space Administration under
Contract NAS7-100.*

NORTHROP SPACE LABORATORIES
3401 WEST BROADWAY, HAWTHORNE, CALIFORNIA 90047

NORTHROP CORPORATION

NSL 65-5
JANUARY 1965

This work was performed for the Jet Propulsion Laboratory,
California Institute of Technology, sponsored by the
National Aeronautics and Space Administration under
Contract N722-104.

FINAL REPORT FOR

CONTRACT NO. JPL 950829

**JET PROPULSION LABORATORY
PASADENA, CALIFORNIA**

BY CONSTANTINO CAFARO, MERL K. FAIRCHILD,
HERBERT J. HARRIS, ARNOLD P. SHLOSINGER
AND VINCENT M. URRAN

**ENGINEERING STUDY TO DETERMINE
FEASIBLE METHODS OF SIMULATING
PLANETARY ALBEDO AND RADIATION
EFFECTS UPON THE THERMAL
BALANCE OF SPACECRAFT**

APPROVED BY



DR. V. W. HOWARD
VICE PRESIDENT
AND
MANAGER
SYSTEMS DEPARTMENT

NORTHROP SPACE LABORATORIES
3401 WEST BROADWAY, HAWTHORNE, CALIFORNIA 90250

NORTHROP CORPORATION

NORTHROP SPACE LABORATORIES

FOREWORD

This study was conducted from 25 June, 1964 to 25 January, 1965 by the Systems Department of the Northrop Space Laboratories, Hawthorne, California. All work was conducted under Contract JPL 950829 for the Jet Propulsion Laboratory, Pasadena, California. Ralph E. Bartera served as technical representative for JPL.

Arnold P. Shlosinger, Supervisor of the Temperature and Environmental Control Systems Branch at Northrop Space Laboratories was Program Manager. Mr. C. Cafaro, Senior Engineer, Temperature and Environmental Control Systems Branch, was the principal investigator. Major contributions to the study effort and preparation of this report were made by H. J. Harris, Senior Engineer of the Temperature and Environmental Control Branch, and M. K. Fairchild, Supervisor; V. M. Urban, Member of the Technical Staff, of the Space Simulation Branch.

SUMMARY

N 66 10 684

This report presents the results of an engineering study and analysis to determine the effects of planetary albedo and radiation from Mars and Venus on the thermal balance of spacecraft orbiting these planets, and to study feasible methods of simulating Mars and Venus planetary albedo and radiation in a space simulation chamber. The existing literature for Mars and Venus provides a multiplicity of planetary albedo values. This study used the range of published albedo values to effectively bound the thermal effects on vehicles orbiting these planets.

The results of the thermal analysis indicate that the effects of planetary albedo and radiation are significant. Therefore, the albedo and radiation should be considered in the design and test of spacecraft whose mission includes close orbit of these planets.

Previously, only limited consideration has been given to planetary albedo and radiation simulation. However, some advanced concepts have recently been proposed. The concepts do not provide exact spectral match or variation of orbital altitude and position simulation. The extreme variation of environment for Mars and Venus and the conflicting simulation features desired for planetary radiation simulations makes it impractical to devise one simulator system for both Mars and Venus. Simulator design should be tailored to the specific requirements of the spacecraft and its mission.

Author

NORTHROP SPACE LABORATORIES

TABLE OF CONTENTS

	PAGE
SUMMARY	ii
INTRODUCTION	1
SECTION I - DATA SURVEY	I-1
Planetary Temperature	I-1
Spectral Distribution of Planetary Radiation	I-4
Albedo	I-4
Planetary Physical Elements	I-5
Figures	I-7
SECTION II - THERMAL ANALYSIS	II-1
Discussion of Analysis	II-1
Assumptions Made in the Analysis	II-4
Computer Program Modification	II-5
Variables Considered in the Analysis	II-7
Results of Thermal Analysis	II-12
Figures	II-18
SECTION III - SIMULATION TECHNIQUES	III-1
Desired Simulation Characteristics	III-1
Current Techniques	III-6
Components or Elements of a Radiosity Simulator System	III-8
Simulation Philosophy	III-13
Suggested Simulator Approaches	III-18
Concepts for Specific Applications	III-25
Figures	III-33
SECTION IV - CONSLUSION AND RECOMMENDATIONS	IV-1
APPENDIX - ALBEDO SIMULATION SURVEY	A-1
REFERENCES	R-1

NORTHROP SPACE LABORATORIES

LIST OF ILLUSTRATIONS

<u>Figure No.</u>	<u>Title</u>	<u>Page</u>
I-1	Mars Monochromatic Power Versus Wavelength for Grey Body Albedo and Planetary Radiation.	I-7
I-2	Venus Monochromatic Power Versus Wavelength for Grey Body Albedo and Planetary Radiation.	I-8
II-1	The Effect of Mass Variations on Temperature for an Earth Orbiting Spherical Spacecraft.	II-18
II-2	The Effect of Albedo on Temperature of a Spherical Satellite Orbiting Mars.	II-19
II-3	The Effect of Albedo on Temperature of a Spherical Satellite Orbiting Venus.	II-20
II-4	Mean Temperature of a Spherical Satellite in Mars Circular Polar Orbits Neglecting Planetary Radiation and Albedo Effects, for a Spacecraft Emissivity of 0.1.	II-21
II-5	Mean Temperature of a Spherical Satellite in Mars Circular Polar Orbits Including the Effects of Planetary Radiation and an Albedo of 0.148, for a Spacecraft Emissivity of 0.1.	II-22
II-6	Mean Temperature Increase of Spherical Spacecraft due to Planetary Albedo and Radiation Effects.	II-23
II-7	Mean Temperature of a Spherical Satellite in Mars Circular Polar Orbits Including the Effects of Planetary Radiation and an Albedo of .295, for a Spacecraft Emissivity of 0.1.	II-24
II-8	Mean Temperature of a Spherical Satellite in Mars Circular Polar Orbits Neglecting Planetary Radiation and Albedo Effects, for a Spacecraft Emissivity of 0.3.	II-25
II-9	Mean Temperature of a Spherical Satellite in Mars Circular Polar Orbits Including the Effects of Planetary Radiation and an Albedo of 0.148, for a Spacecraft Emissivity of 0.3.	II-26

<u>Figure No.</u>	<u>Title</u>	<u>Page</u>
II-10	Mean Temperature of a Spherical Satellite in Mars Circular Polar Orbits Including the Effects of Planetary Radiation and an Albedo of 0.295, for a Spacecraft Emissivity of 0.3.	II-27
II-11	Mean Temperature of a Spherical Satellite in Mars Circular Polar Orbits Neglecting Planetary Radiation and Albedo Effects, for a Spacecraft Emissivity of 0.6.	II-28
II-12	Mean Temperature of a Spherical Satellite in Mars Circular Polar Orbits Including the Effects of Planetary Radiation and an Albedo of 0.148, for a Spacecraft Emissivity of 0.6.	II-29
II-13	Mean Temperature of a Spherical Satellite in Mars Circular Polar Orbits Including the Effects of Planetary Radiation and an Albedo of 0.295, for a Spacecraft Emissivity of 0.6.	II-30
II-14	Mean Temperature of a Spherical Satellite in Mars Circular Polar Orbits Neglecting Planetary Radiation and Albedo Effects, for a Spacecraft Emissivity of 0.9.	II-31
II-15	Mean Temperature of a Spherical Satellite in Mars Circular Polar Orbits Including the Effects of Planetary Radiation and an Albedo of 0.148, for a Spacecraft Emissivity of 0.9.	II-32
II-16	Mean Temperature of a Spherical Satellite in Mars Circular Polar Orbits Including the Effects of Planetary Radiation and an Albedo of 0.295, for a Spacecraft Emissivity of 0.9.	II-33
II-17	Average Incident Radiation per Square Foot of Surface Area on a 1 foot Diameter Sphere in Circular Polar Orbits Around Mars with an Albedo of 0.148.	II-34
II-18	Average Incident Radiation per Square Foot of Surface Area on a 1 foot Diameter Sphere in Circular Polar Orbits Around Mars with an Albedo of 0.295.	II-35
II-19	Mean Temperature of a Spherical Satellite in Venus Circular Polar Orbits Neglecting Planetary Radiation and Albedo Effects for a Spacecraft Emissivity of 0.1.	II-36
II-20	Mean Temperature of a Spherical Satellite in Venus Circular Polar Orbits Including the Effects of Planetary Radiation and an Albedo of 0.59, for a Spacecraft Emissivity of 0.1.	II-37

<u>Figure No.</u>	<u>Title</u>	<u>Page</u>
II-21	Mean Temperature of a Spherical Satellite in Venus Circular Polar Orbits Including the Effects of Planetary Radiation and an Albedo of 0.77, for a Spacecraft Emissivity of 0.1.	II-38
II-22	Mean Temperature of a Spherical Satellite in Venus Circular Polar Orbits Neglecting Planetary Radiation and Albedo Effects for a Spacecraft Emissivity of 0.3.	II-39
II-23	Mean Temperature of a Spherical Satellite in Venus Circular Polar Orbits Including the Effects of Planetary Radiation and an Albedo of 0.59, for a Spacecraft Emissivity of 0.3.	II-40
II-24	Mean Temperature of a Spherical Satellite in Venus Circular Polar Orbits Including the Effects of Planetary Radiation and an Albedo of 0.77, for a Spacecraft Emissivity of 0.3.	II-41
II-25	Mean Temperature of a Spherical Satellite in Venus Circular Polar Orbits Neglecting Planetary Radiation and Albedo Effects for a Spacecraft Emissivity of 0.6.	II-42
II-26	Mean Temperature of a Spherical Satellite in Venus Circular Polar Orbits Including the Effects of Planetary Radiation and an Albedo of 0.59, for a Spacecraft Emissivity of 0.6.	II-43
II-27	Mean Temperature of a Spherical Satellite in Venus Circular Polar Orbits Including the Effects of Planetary Radiation and an Albedo of 0.77, for a Spacecraft Emissivity of 0.6.	II-44
II-28	Mean Temperature of a Spherical Satellite in Venus Circular Polar Orbits Neglecting Planetary Radiation and Albedo Effects for a Spacecraft Emissivity of 0.9.	II-45
II-29	Mean Temperature of a Spherical Satellite in Venus Circular Polar Orbits Including the Effects of Planetary Radiation and an Albedo of 0.59, for a Spacecraft Emissivity of 0.9.	II-46
II-30	Mean Temperature of a Spherical Satellite in Venus Circular Polar Orbits Including the Effects of Planetary Radiation and an Albedo of 0.77, for a Spacecraft Emissivity of 0.9.	II-47

<u>Figure No.</u>	<u>Title</u>	<u>Page</u>
II-31	Average Incident Radiation per Square Foot of Surface Area on a 1 foot Diameter Sphere in Circular Polar Orbits Around Venus with an Albedo of 0.59.	II-48
II-32	Average Incident Radiation per Square Foot of Surface Area on a 1 Foot Diameter Sphere in Circular Polar Orbits Around Venus with an Albedo of 0.77.	II-49
II-33	Spherical Satellite Temperature Determination for Circular Polar Orbits as a Function of Azimuth Angle.	II-50
II-34	Mean Temperature of a Planetary Oriented Flat Plate Satellite in Mars Circular Polar Orbits Neglecting Planetary Radiation and Albedo Effects, for a Spacecraft Emissivity of 0.1.	II-51
II-35	Mean Temperature of a Planetary Oriented Flat Plate Satellite in Mars Circular Polar Orbits Including the Effects of Planetary Radiation and an Albedo of 0.148, for a Spacecraft Emissivity of 0.1.	II-52
II-36	Mean Temperature of a Planetary Oriented Flat Plate Satellite in Mars Circular Polar Orbits Including the Effects of Planetary Radiation and an Albedo of 0.295, for a Spacecraft Emissivity of 0.1.	II-53
II-37	Mean Temperature of a Planetary Oriented Flat Plate Satellite in Mars Circular Polar Orbits Neglecting Planetary Radiation and Albedo Effects, for a Spacecraft Emissivity of 0.3.	II-54
II-38	Mean Temperature of a Planetary Oriented Flat Plate Satellite in Mars Circular Polar Orbits Including the Effects of Planetary Radiation and an Albedo of 0.148, for a Spacecraft Emissivity of 0.3.	II-55
II-39	Mean Temperature of a Planetary Oriented Flat Plate Satellite in Mars Circular Polar Orbits Including the Effects of Planetary Radiation and an Albedo of 0.295, for a Spacecraft Emissivity of 0.3.	II-56
II-40	Mean Temperature of a Planetary Oriented Flat Plate Satellite in Mars Circular Polar Orbits Neglecting Planetary Radiation and Albedo Effects, for a Spacecraft Emissivity of 0.6.	II-57

<u>Figure No.</u>	<u>Title</u>	<u>Page</u>
II-41	Mean Temperature of a Planetary Oriented Flat Plate Satellite in Mars Circular Polar Orbits Including the Effects of Planetary Radiation and an Albedo of 0.148, For a Spacecraft Emissivity of 0.6.	II-58
II-42	Mean Temperature of a Planetary Oriented Flat Plate Satellite in Mars Circular Polar Orbits Including the Effects of Planetary Radiation and an Albedo of 0.295, for a Spacecraft Emissivity of 0.6.	II-59
II-43	Mean Temperature of a Planetary Oriented Flat Plate Satellite in Mars Circular Polar Orbits Neglecting Planetary Radiation and Albedo Effects, for a Spacecraft Emissivity of 0.9.	II-60
II-44	Mean Temperature of a Planetary Oriented Flat Plate Satellite in Mars Circular Polar Orbits Including the Effects of Planetary Radiation and an Albedo of 0.148, for a Spacecraft Emissivity of 0.9.	II-61
II-45	Mean Temperature of a Planetary Oriented Flat Plate Satellite in Mars Circular Polar Orbits Including the Effects of Planetary Radiation and an Albedo of 0.295, for a Spacecraft Emissivity of 0.9.	II-62
II-46	Incident Radiation on Planet Oriented Side of a 1 Foot Square Flat Plate in Circular Polar Orbits Around Mars with an Albedo of 0.148.	II-63
II-47	Incident Radiation on Side Opposite Planet Oriented Side of a 1 Foot Square Flat Plate in Circular Polar Orbits Around Mars.	II-64
II-48	Incident Radiation on Planet Oriented Side of a 1 Foot Square Flat Plate in Circular Polar Orbits Around Mars with an Albedo of 0.295.	II-65
II-49	Mean Temperature of a Planetary Oriented Flat Plate Satellite in Venus Circular Polar Orbits Neglecting Planetary Radiation and Albedo Effects, for a Spacecraft Emissivity of 0.1.	II-66

<u>Figure No.</u>	<u>Title</u>	<u>Page</u>
II-50	Mean Temperature of a Planetary Oriented Flat Plate Satellite in Venus Circular Polar Orbits Including the Effects of Planetary Radiation and an Albedo of 0.59, for a Spacecraft Emissivity of 0.1.	II-67
II-51	Mean Temperature of a Planetary Oriented Flat Plate Satellite in Venus Circular Polar Orbits Including the Effects of Planetary Radiation and an Albedo of 0.77, for a Spacecraft Emissivity of 0.1.	II-68
II-52	Mean Temperature of a Planetary Oriented Flat Plate Satellite in Venus Circular Polar Orbits Neglecting Planetary Radiation and Albedo Effects, for a Spacecraft Emissivity of 0.3.	II-69
II-53	Mean Temperature of a Planetary Oriented Flat Plate Satellite in Venus Circular Polar Orbits Including the Effects of Planetary Radiation and an Albedo of 0.59, for a Spacecraft Emissivity of 0.3.	II-70
II-54	Mean Temperature of a Planetary Oriented Flat Plate Satellite in Venus Circular Polar Orbits Including the Effects of Planetary Radiation and an Albedo of 0.77, for a Spacecraft Emissivity of 0.3.	II-71
II-55	Mean Temperature of a Planetary Oriented Flat Plate Satellite in Venus Circular Polar Orbits Neglecting Planetary Radiation and Albedo Effects, for a Spacecraft Emissivity of 0.6.	II-72
II-56	Mean Temperature of a Planetary Oriented Flat Plate Satellite in Venus Circular Polar Orbits Including the Effects of Planetary Radiation and an Albedo of 0.59, for a Spacecraft Emissivity of 0.6.	II-73
II-57	Mean Temperature of a Planetary Oriented Flat Plate Satellite in Venus Circular Polar Orbits Including the Effects of Planetary Radiation and an Albedo of 0.77, for a Spacecraft Emissivity of 0.6.	II-74
II-58	Mean Temperature of a Planetary Oriented Flat Plate Satellite in Venus Circular Polar Orbits Neglecting Planetary Radiation and Albedo Effects, for a Spacecraft Emissivity of 0.9.	II-75

<u>Figure No.</u>	<u>Title</u>	<u>Page</u>
II-59	Mean Temperature of a Planetary Oriented Flat Plate Satellite in Venus Circular Polar Orbits Including the Effects of Planetary Radiation and an Albedo of 0.59, for a Spacecraft Emissivity of 0.9.	II-76
II-60	Mean Temperature of a Planetary Oriented Flat Plate Satellite in Venus Circular Polar Orbits Including the Effects of Planetary Radiation and an Albedo of 0.77, for a Spacecraft Emissivity of 0.9.	II-77
II-61	Incident Radiation on Planet Oriented Side of a 1 Foot Square Flat Plate in Circular Polar Orbits Around Venus with an Albedo of 0.59.	II-78
II-62	Incident Radiation on Side Opposite Planet Oriented Side of a 1 Foot Square Flat Plate in Circular Polar Orbits Around Venus.	II-79
II-63	Incident Radiation on Planet Oriented Side of a 1 Foot Square Flat Plate in Circular Polar Orbits Around Venus with an Albedo of 0.77.	II-80
II-64	Flat Plate Temperature Determination for Circular Polar Orbits as a Function of Azimuth Angle.	II-81
III-1	Energy Characteristics - Mars Orbits	III-33
III-2	Energy Characteristics - Venus Orbits	III-34
III-3	Spacecraft Orbital Coordinates	III-35
III-4	Elemental Area Illumination Factors - Maximum Albedo and Planetary Emission	III-36
III-5	Elemental Area Illumination Factors - Planetary Albedo	III-37
III-6	Polar Energy Distributions - 1000 Km Mars Orbit	III-38
III-7	Energy Contributions - Mars Orbits	III-39
III-8	Energy Contributions - Venus Orbits	III-40
III-9	Radiosity Field Simulator	III-41

<u>Figure No.</u>	<u>Title</u>	<u>Page</u>
III-10	Shroud Simulator	III-41
III-11	Lamp Beams	III-42
III-12	Incandescent Lamp Characteristics	III-42
III-13	Window Type Filter	III-42
III-14	Simulation Energy Distribution Approaches	III-43
III-15	Beam Shaping	III-44
III-16	Planetary Simulation Near Eclipse	III-45
III-17	Distributed Radiation Simulator	III-45
III-18	Method for Programming 360° Rotation Simulation	III-46
III-19	Comparison of Mars Albedo & 3000°K Source	III-47
III-20	Filtering for Mars Albedo	III-48
III-21	Beam Reflector	III-48
III-22	Mars Albedo Simulator	III-49
III-23	Comparison of Venus Albedo and Tungsten Filament Sources	III-50
III-24	Venus Simulator	III-51

NORTHROP SPACE LABORATORIES

LIST OF TABLES

<u>TABLE NO.</u>	<u>TITLE</u>	<u>PAGE</u>
I-1	Observed Venus Temperatures	I-2
I-2	Observed Mars Temperatures	I-3
I-3	Planetary Dimensions for Mars and Venus	I-5
I-4	Planetary Distance From the Sun	I-6
II-1	Planetary Data Used in the Thermal Analysis	II-8
II-2	Typical Values of Surface Coating Properties Analyzed	II-10
II-3	Weight and Geometric Dimensions of Typical Spacecraft	II-11
II-4	Orbital Time and Max Shadow Time	II-17
III-1	Desired Radiosity Simulation Features	III-17

NORTHROP SPACE LABORATORIES

INTRODUCTION

This report presents the results of Northrop Space Laboratories' engineering study to (1) perform a literature survey to determine the best current data regarding planetary albedo and radiation of Mars and Venus, (2) define the effects of planetary albedo and radiation on the thermal balance of spacecraft orbiting Mars and Venus, and (3) determine feasible methods of simulating planetary albedo and radiation of Mars and Venus in a space simulation chamber. For the purpose of this study, the combined phenomena of albedo and planetary radiation are referred to by the term "Radiosity".

Included is a discussion of the technical problem areas, the approximations and assumptions made to define or simplify problems, and the results of the study effort.

A range of planetary albedo values was obtained from the literature for both planets. Grey body reflectance curves of energy versus wavelength are presented spanning this range. Superimposed on these curves are the observed planetary spectral reflectance data. Data for planetary diameter and mean distance from the sun were obtained from various sources and tabulated. Specific values for each were adopted for use in the thermal analysis.

The spacecraft configurations analyzed were a one-foot diameter sphere and a one-foot square flat plate. Both were assumed to be planetary oriented in circular polar orbits around the two planets, at altitudes between 1000 Km and 2500 Km. Circular polar orbits perpendicular and parallel to the Sun's rays are investigated. The resulting temperature data are supplemented by a method of extrapolating the results of this investigation to circular polar orbits other than those resulting in maximum and minimum temperatures.

Simulator characteristics necessary to reproduce the thermal environment for space vehicles orbiting Mars and Venus are presented. A survey was conducted to determine currently employed planetary albedo and radiation simulation techniques and solicit recommendations for new approaches. Several proposed methods are analyzed and discussed. One simulation technique for the

Mars environment and two for the Venus environment are presented and discussed.

The conclusions resulting from the study are presented in Section IV along with specific recommendations of promising areas for future development.

NORTHROP SPACE LABORATORIES

SECTION I

DATA SURVEY

A literature search was conducted for the purpose of obtaining the following information: (1) the planetary temperature, (2) the spectral distribution of the planetary radiation, (3) the planetary albedo, (4) the average distance of the planet from the sun, and (5) the dimensions of the planets Mars and Venus.

PLANETARY TEMPERATURE

Published literature provided a sufficient quantity of planetary temperature information to enable a reasonable assessment of these values for Mars and Venus. Tables I-1 and I-2 present a listing of the perused data in chronological order for the two subject planets; the major portion of which was obtained by observation (Reference 1 through 23). It is to be noted that these data represent the effective planetary temperature when the planet is viewed from deep space.

This effective temperature may also be determined analytically for a steady state condition of a planet. A heat balance between incoming and outgoing radiation yields for a planet, radiating as a black body (Reference 24):

$$T_p = \left[\frac{(1-a) G_s}{4\sigma} \right]^{1/4} \quad (^\circ R) \quad (I-1)$$

where

a = albedo of the planet

G_s = solar irradiation flux at the planet (Btu/Hr-Ft²)

σ = Stefan-Boltzmann Constant = $.1713 \times 10^{-8}$ Btu/Hr-Ft² - $^\circ R^4$

Under thermal steady state conditions a planet reradiates that portion of radiation which it absorbs. This requires that the planet is neither a source of, nor stores thermal energy. This assumption is valid for earth, where the amount of solar energy converted and stored by photo synthesis and the amount of energy generated by chemical and nuclear processes is insignificantly small.

TABLE I-1

OBSERVED VENUS TEMPERATURES

	TEMPERATURE			AUTHOR(S) AND YEAR
	<u>°K</u>	<u>°R</u>		
1.	220-230	397--414	(eff. blk. body)	Sinton and Strong (1960a)(Ref. 1)
2.	234	421.4	(center of disk)	Sinton and Strong (1960b)(Ref. 2)
3.	293	527.4	(probable)	General Electric-Space Facts (1960) (Ref. 3)
4.	225	405	(eff. blk. body)	Kaplan (1961) (Ref. 4)
5.	235	423	(average i.r. emission)	Kellogg and Sagan (1961)(Ref. 5)
6.	233-240	419.4-432		Pettit and Sinton (1961) (Ref. 6)
7.	230	414	(probable)	Stevenson and Grafton (1961) (Ref. 7)
8.	234	421.2	(clouds)	Warner (1961) (Ref. 8)
9.	230	414	(black body effec- tive)	Jastrow and Rasool (1962) (Ref. 9)
10.	234	421.2	(upper cloud layer black body)	Opik (1962) (Ref 10)
11.	236	424.8		Sinton (1962) (Ref. 11)
12.	235	423		Wyckoff (1962) (Ref. 12)
13.	250	450	(upper atmosphere)	Briggs & Mamikunian (1963) (Ref. 13)
14.	240	432	(clouds by Mariner II data)	Briggs & Mamikunian (1963) (Ref. 13)
15.	235	423	(average radiation temperature)	Chase, Kaplan, Neugebauer (1964) (Ref. 14)
16.	209 [±] 2	374.4 [±] 3.6	(uncertain data)	Murray, Wildey, and Westphal (1963) (Ref. 15)
17.	235	423	(effective)	Rasool (1963) (Ref. 16)
18.	240	432	(center of disk, Mariner II)	Rea & Welch (1963) (Ref. 17)
19.	235	423	(top of cloud layer)	Sinton (1963) (Ref. 18)

TABLE I-2

OBSERVED MARS TEMPERATURES

	<u>TEMPERATURE</u>			<u>AUTHOR(S) AND YEAR</u>
	<u>°K</u>	<u>°R</u>		
1.	250	450	(measured average)	Pettit and Nicholson (1924) (Ref. 19)
2.	275	495	(black body)	Coblentz (1925) (Ref. 20)
3.	223	401.4	(Polar-Tropical Arithmetic av.)	deVaucouleurs (1954) (Ref. 21)
4.	289	520.2	(probable)	General Electric-Space Facts (1960) (Ref. 3)
5.	288	518.4	(center of disk)	Sinton and Strong (1960b) (Ref. 2)
6.	240	432	(average)	Kellogg & Sagan (1961) (Ref. 1)
7.	218	382.4	(probable)	Stevenson & Grafton (1961) (Ref. 7)
8.	230	414	(estimated mean)	Jastrow & Rasool (1962) (Ref. 15)
9.	253	455.4	(surface temp.)	Öpik (1962) (Ref. 10)
10.	250	450	(arithmetic average)	Schilling (1962) (Ref. 22)
11.	230	414	(mean)	Rasool (1963) (Ref. 16)
12.	240	432	(mean daytime temp.)	Kellogg and Sagan (1963) (Ref. 23)

SPECTRAL DISTRIBUTION OF PLANETARY RADIATION

A planet does not radiate energy as a black body. However, as actual emissivity and temperature are unknown, a Planckian black body distribution can be used to express the planetary emissive power when the known effective planetary black body temperature is used. Figures I-1* and I-2 show planetary emission curves of Planckian distribution (Reference 24). The T_{\max} and T_{\min} are the maximum and minimum values of effective planetary black body temperature, the numerical value being obtained by performing a heat balance on the planets with Equation I-1. T_{\max} corresponds to the minimum albedo and T_{\min} corresponds to the maximum albedo values that were obtained from the literature survey. Mariner II information is shown on Figure I-2 and lends additional credence to the data presented.

ALBEDO

The literature survey (References 9, 21, 26-35) shows that a considerable amount of conflicting albedo data had been published. The range of published albedo values is for Mars .148 to 0.295 and for Venus 0.59 to 0.77. The value of .148 for Mars and the values of .59 to .77 for the planet Venus are visual albedo values. Visual albedo is the ratio of radiation reflected in the visible portion of the spectrum to the total radiation incident at the planet. The albedo value for Mars of 0.295 (reference 25) was derived from radiometric measurements. Venus appears to be a "grey" reflector and thus equal albedo or reflectance factors can be applied over the entire spectrum.

Curves shown as Figure I-1 and I-2 have been plotted by use of a constant percentage reduction by the albedo values shown, of the solar black body curve. A black body temperature of the Sun of 10,400°R was used. The energy level at each planetary distance was varied according to the Inverse Square Law and the planet was considered to be a grey reflector. Published spectral reflectance data are superimposed on the curves to indicate essential agreement with values based on above simplifications.

*Referenced figures are grouped as the final entry in this section.

PLANETARY PHYSICAL ELEMENTS

Planetary data were abstracted from various sources to yield the diameters and planet-sun average distance for Mars and Venus. These data are listed in Tables I-3 and I-4, respectively.

TABLE I-3

PLANETARY DIMENSIONS FOR MARS AND VENUS

Planet	Diameter (Km)	Radius (Km)	References
Mars	6828 \pm 7 (equatorial) 6756 \pm 7 (polar)	3291 - 3359 (polar) 3323 - 3438 (equatorial) 3380 (equatorial)	Schilling(Ref. 22) Allen (Ref. 36) deVaucouleurs (1964) (Ref. 25)
Venus	12,060 - 12,640 12,240 \pm 15	6100 (equatorial) 6100 \pm 30	Briggs & Mamikunian (Ref.13) Allen (Ref. 36) deVaucouleurs (1964)(Ref.25) Martynov (Ref. 37)

The values used in this report are:

Mars planetary diameter = 6792 Km

Mars distance from the Sun = 1.5237 A.U.

Venus planetary diameter = 12,240 Km

Venus distance from Sun = .72333 A.U.

TABLE I-4

PLANETARY DISTANCE FROM THE SUN

Planet	Distance (Km)	A. U.*	Reference
Mars	227.8 x 10 ⁶	1.52369 1.52369 1.524	American Ephemeris (Ref. 38) Allen (Ref. 36) Space Facts (Ref. 3)
Venus	108.1 x 10 ⁶	.723332 .72333 .72333	Briggs & Mamikunian (Ref. 13) American Ephemeris (Ref. 38) Allen (Ref. 36)
*1 A.U. = 149,525,000 Km.			

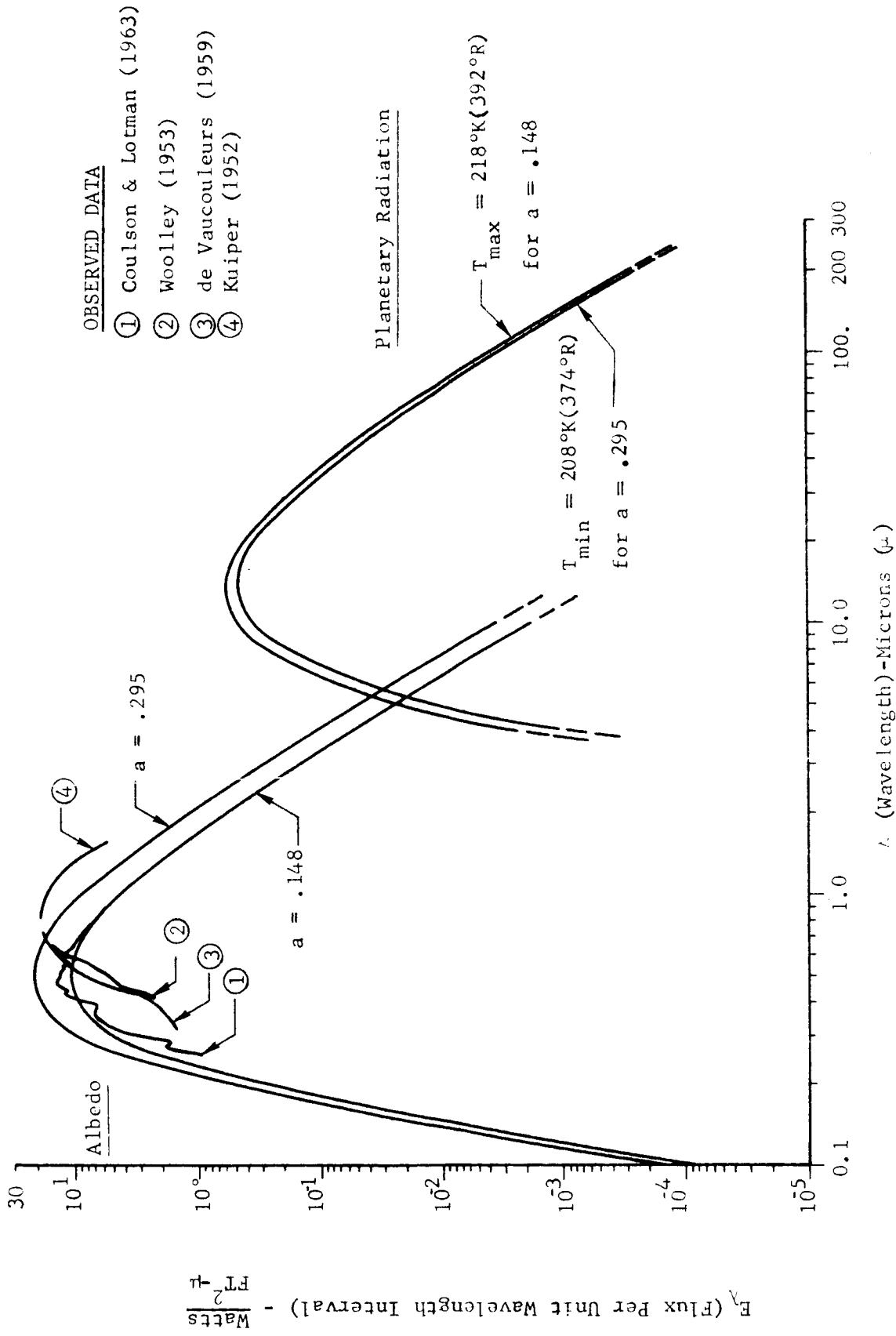
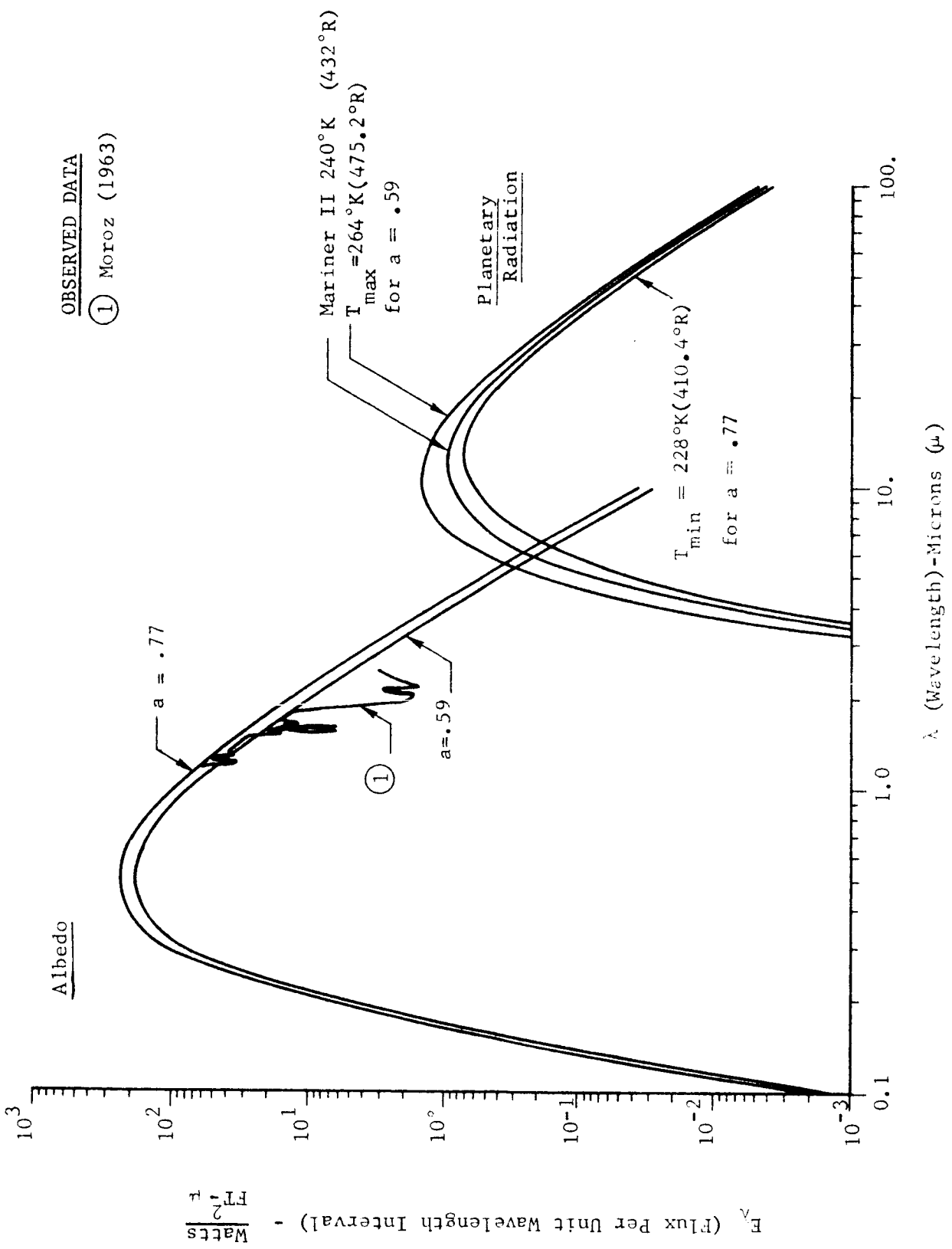


FIGURE I-1 - MARS MONOCHROMATIC POWER VERSUS WAVELENGTH FOR GREY BODY ALBEDO AND PLANETARY RADIATION



OBSERVED DATA

① Moroz (1963)

FIGURE I-2 VENUS MONOCHROMATIC POWER VERSUS WAVELENGTH FOR GREY BODY ALBEDO AND PLANETARY RADIATION

SECTION II

THERMAL ANALYSIS

The temperature of a space vehicle in orbit around a planet is determined by the heat balance between the space vehicle and its environment, which includes the sun, the planet and its atmosphere, and space. The spacecraft receives solar energy directly from the sun and indirectly (reflected) from the planet and its atmosphere. It further receives thermal radiation emitted by the planet and its atmosphere.

DISCUSSION OF ANALYSIS

The external environment factors that influence the heat balance are: the solar radiation constant at the planetary distance from the sun; the planetary albedo; and the thermal emission resulting from the apparent temperature of the planet as seen from space. In writing an instantaneous heat balance equation for a space vehicle, the sum of all incident radiant energy minus the sum of all radiation leaving the space vehicle, will equal the rate of change in stored thermal energy and hence the temperature of the space vehicle. Aerodynamic heating can be neglected at the altitudes to be considered.

The rate of change of temperature of an orbiting vehicle may be obtained from the following expression:

$$\underbrace{\alpha F_s G_s A}_{\text{direct solar input}} + \underbrace{\epsilon F_p \epsilon_p \sigma T_p^4 A}_{\text{planetary input}} + \underbrace{\alpha F_r a G_s A}_{\text{reflected solar input}} - \underbrace{\epsilon \sigma T_v^4 A}_{\text{energy emitted by vehicle}} = \underbrace{m c_p \frac{dT_v}{dt}}_{\text{rate of change in stored thermal energy}} \quad (\text{Eq. II-1})$$

where:

- A = Total surface area of vehicle
- a = Planetary albedo
- c_p = Specific heat of vehicle

- F_{ep} = Shape factor for planetary emission
- F_{rs} = Shape factor for planetary reflected solar radiation
- F_s = Shape factor for direct solar radiation
- G_s = Solar radiation on a plane normal to sun at the planetary distance from the sun
- m = Mass of vehicle
- T_p = Temperature of planet
- T_v = Temperature of vehicle
- t = Time
- α = Solar absorptivity of vehicle's exterior coating
- ϵ = Emissivity of vehicle's exterior coating
- ϵ_p = Emissivity of planet
- σ = Stefan-Boltzmann thermal radiation constant $(.1713 \times 10^{-8} \frac{\text{BTU/hr}}{\text{Ft}^2 \cdot \text{R}^4})$

As discussed in Section I - Data Survey, available data of the solid planetary surface temperatures are not of interest here. A satellite orbiting a planet with a surrounding atmosphere will actually see the planet including it's atmosphere envelope. The planetary radiation reaching the satellite will be the result of the properties of the atmosphere as well as of the planetary surface temperature and emissivity. For this analysis, the apparent temperature of the planet as seen from space and the thermal radiation resulting therefrom is required. Changes in atmospheric conditions, topography and time of day can introduce variation in planetary thermal radiation.

It is possible to compute the average planetary radiation by performing a thermal balance on the planet -plus- atmosphere combination based on the solar radiation absorbed by the planet -plus- atmosphere system and the assumption that no significant amounts of energy are stored or generated by the planet.

The thermal balance can be written:

Total energy absorbed by the planet and its atmosphere = Energy emitted from the planet and atmosphere

$$(1 - a) G_s (\pi R^2) = (4 \pi R^2) E_p \text{ from which the planetary emission } (E_p)$$

$$E_p = \frac{(1 - a)}{4} G_s = \epsilon_p \sigma T_p^4$$

(πR^2) = Projected Area of Planet seen from Sun, R = Radius of Planet

$(4 \pi R^2)$ = Total surface area of Planet

The planetary input term in Equation II-1 above is then written

$$\epsilon F_e E_p A = \epsilon F_e \frac{(1 - a)}{4} G_s A$$

and Equation II-1 becomes

$$m c_p \frac{dT}{dt} = \alpha F_s G_s A + \epsilon F_e \frac{(1 - a)}{4} G_s A + \alpha F_r a G_s A - \epsilon \sigma T^4 A$$

(Equation II-2)

This expression is solved numerically in a digital computer program technique presented in Reference 39. This computer program is set up to analyze Earth orbiting spacecraft. For application to this analysis, several modifications to the program were made by N.S.L. which enable it to handle other planets.

Computation is begun by providing approximate values of the satellite temperature at the perigee point in orbit. The program will then compute temperatures at successive intervals around the orbit until it has returned to perigee. Chances are that the approximate value and the newly computed temperature at perigee do not agree. The program then repeats the computation, utilizing the newly calculated temperature at the initial value. This iteration process continues until initial and final temperatures converge to within an acceptable tolerance.

Although the foregoing discussion was confined to temperature determination, the amount of radiant energy incident to the satellite from the

space environment is also calculated by the program. This information may be utilized, if desired, as input data in a general heat transfer program such as the SHARE Thermal Network Analyzer Program (MLFTHAN) if it is required to obtain a detailed thermal analysis of the surface and interior temperatures of a vehicle.

ASSUMPTIONS MADE IN THE THERMAL ANALYSIS

1. It is assumed that the two satellites considered have a high thermal conductivity and that the entire satellite is at an uniform temperature. This assumption greatly simplifies the analysis and although it is not entirely realistic, it is acceptable for the scope of this work.

2. A rigorous specification of the position at which the satellite enters and exists the planets true shadow leads to extremely complicated expressions. The following simplifications of shadow geometry which provide acceptable accuracy are made:

- a. The planets were assumed to be perfectly spherical.
- b. The planet's shadow was assumed cylindrical and umbral (sun at infinity).
- c. Penumbral effects were ignored.

From the thermal analysis standpoint the error introduced by the assumption of a cylindrical umbral shadow is essentially zero.

3. It is assumed that all thermal radiation considered in the analysis, except direct solar radiation, is in diffuse form. In fact, most thermal radiation is in diffuse form. Neglect of the small specular fractions will not introduce significant errors to this study, and greatly simplifies the analysis.

4. It is assumed that direct solar radiation impinges upon the planet and upon the satellite with parallel rays, due to the great distance between the sun and its planets. The error introduced into the analysis by this assumption is practically zero.

5. In all cases, it is assumed that the planet emits as a black body at an equivalent black body temperature calculated from a thermally steady

state condition (i.e., the planetary-emitted energy is equal to the absorbed solar energy). It is also assumed that the planetary emission is a constant at any point on the surface and does not vary from day to night. These are necessary assumptions because little is known of the actual spectral and local variations in the planetary emitted radiation. Convection in planetary atmospheres and planet rotation tend to equalize the effective planetary temperatures.

6. In all cases, the planetary albedo is assumed to be constant over the surface of the planet, and the planet is assumed to be a diffuse reflector. This is done because of the complications of analyzing a non-diffuse reflector and because it is not possible to accurately define local variations from present knowledge of Mars and Venus.

7. Conduction and convection between the satellite and its surroundings are neglected. This is reasonable because orbital heights are usually too far above the atmosphere for these thermal effects to appear.

8. It is assumed that the absorptivity of the vehicle surface to planetary thermal emission is equal to the emissivity of the vehicle surface. Since the effective temperature of the planet and the temperatures of most vehicle surfaces are nearly the same, this assumption is valid according to Kirchhoff's law.

9. Any scattering effects of direct solar radiation upon the satellite due to the planet's atmosphere are ignored. It is felt that this will introduce a negligible error into the analysis.

10. The thermal radiation shape factor from the spherical satellite to the planet was calculated with the assumption that the satellite is a point source in space. The assumption is valid if the satellite is uniform in temperature; as it would be if it were spinning or if it had a very high thermal conductivity as assumed in this study.

COMPUTER PROGRAM MODIFICATIONS

In order to handle spacecraft orbiting Mars and Venus, modifications

to the original earth orbiting spacecraft program were necessary. The planetary diameters and gravitational parameters (GM) of the planets were made input variables in the computer program. These changes were required for calculation of orbital parameters for Mars and Venus which had to be substituted for the Earth constants used in the original program.

It was further necessary to make a change in the program to improve the method of calculating the reflected solar shape factor. The method of calculating this reflected solar shape factor in the existing program used the following simplifying expression:

$$Fr_s = Fe_p \cos \theta_s$$

where:

- Fr_s = Reflected solar shape factor
- Fe_p = Planetary emission shape factor
- θ_s = Angle between the planet-Sun line and a line drawn from the planet center to the satellite.

The angle θ_s was permitted to vary from zero to ± 90 degrees. If the angle is outside this range the reflected solar shape factor was set equal to zero. This simplifying expression is a reasonably good approximation only for θ_s angles up to approximately 60 degrees. For angles greater than 60 degrees the expression deviates significantly from the correct values. When the vehicle is above the terminator ($\theta_s = 90^\circ$ & $\cos \theta_s = 0$, hence $Fr_s =$ zero), the satellite, at the altitudes of interest, will still view a planet cap, half of which is sunlit and the approximation is obviously far from the correct value.

The existing method of reflected solar shape factor calculation was therefore replaced by the data appearing in Table 6 of Appendix B of Reference 7. Table 6 presents solar reflected shape factor as a function of altitude and the angle formed by the Sun, planet and spacecraft for an Earth orbiting spacecraft. An altitude correction factor defined for several planets in Table 1 of Appendix B in Reference 7, was used in the modified program. An additional correction was necessary because the

reflected solar shape factors of Reference 7 were based on the projected area of the sphere (πr^2) and the computer program utilizes a shape factor based on the total surface area of the sphere ($4 \pi r^2$). The altitudes were also converted into statute miles and programmed into a computer routine that interpolates between the tabulated values to handle any given variation of altitude or Sun, planet, spacecraft angle.

For the space vehicle shaped like a flat plate, a similar technique was programmed for the reflected solar shape factor using Table 66 of Reference 7 which is for a flat plate oriented such that the flat side is facing directly at the planet.

One other computer program modification was necessary since the existing program did not have a subroutine to handle the flat plate shaped space vehicle radiating from both sides. It was necessary to modify an existing subroutine in order to handle the flat plate configuration of spacecraft.

VARIABLES CONSIDERED IN THE ANALYSIS

In analyzing the temperature history of a spacecraft in orbit, there are three classes of variables which must be considered. These are: (1) planetary variables, (2) orbital variables, and (3) spacecraft variables.

For purposes of this study the variables were considered as follows:

Planetary Variables

The planetary variable considered in this analysis is the range of albedo values as determined by the literature survey portion of this report and as previously discussed. Table II-1 summarizes the range of values that have been used in this analytic task for both Mars and Venus.

TABLE II-1

PLANETARY DATA USED IN THE THERMAL ANALYSIS

	MARS	VENUS
Mean Diameter (From Data Survey)	6,792 Km 4,220 Stat. Miles	12,240 Km 7,606 Stat. Miles
Albedo (From Data Survey)	.148 - .295	.59 - .77
Mean Solar Constant Calculated from Distance between Sun and Planet	55.9 Watts/Ft ² 190.8 BTU/(Hr-Ft ²)	247.9 Watts/Ft ² 846.7 BTU/(Hr-Ft ²)
Mean Distance From Sun (From Data Survey) (Astronomical Units)	1.524 A.U.	0.723 A.U.
Gravitational Parameter GM	42,906 Km ³ /Sec ²	324,230 Km ³ /Sec ²
Orbital Eccentricity of Planet (e = 0.0 is a circular orbit)	e = 0.09337	e = 0.006791

Table II-1 also presents information on other factors which influence the heat balance, namely the value of the solar constant and planetary albedo. The value of the solar constant and distance from the Sun are average values for the planetary orbit. Since the orbits are elliptical, these values vary during a revolution of the planet around the Sun. For Mars, the orbit eccentricity is greater than for Venus, but still not as large as that of Earth (e = 0.1673). The assumption of a constant value for the solar constant is permissible for purpose of this study which concerns itself primarily with the significance of the albedo of these planets.

Orbital Variables

This study is concerned with circular polar orbits around Mars and Venus. More specifically, two types of polar orbits have been considered; the first is a polar orbit perpendicular to the Sun's rays (no shadow time), and the second is a polar orbit parallel to the solar rays (maximum shadow time). Four orbital altitudes were analyzed in each of the two types of orbits for both Mars and Venus. The four orbital altitudes are: 1000, 1500, 2000, and 2500 Kilometer orbits around the planets.

Spacecraft Variables

The spacecraft variables considered in the analysis are concerned with the thermo-optical properties, the configuration, and the orientation of the spacecraft. The thermo-optical properties selected for the analysis span the range of typical coatings used for spacecraft. A large range of properties was used to permit interpolation and extrapolation of the temperature data developed for these coatings in order to predict temperatures for any thermal control coating properties (See Table II-2).

The thermal mass (mc_p) of the satellite affects the temperature variation and average temperature of an orbiting spacecraft. Figure II-1* indicates the typical effect of varying the mass, for an Earth orbiting spacecraft. A thermal mass typical of existing or planned spacecraft, scaled down to the size and shape of spacecraft studied in this analysis was determined for the analysis. Table II-3 is a summary of approximate weight and external surface area of ten spacecraft.

*Referenced Figures are grouped as the final entry in this section.

TABLE II-2

TYPICAL VALUES OF SURFACE COATING PROPERTIES ANALYZED

IDENTIFICATION NUMBER	EMISSIVITY ϵ	SOLAR ABSORBTIVITY α	α/ϵ
1	.10	.05	0.5
2	.10	.20	2.0
3	.10	.50	5.0
4	.10	.90	9.0
5	.30	.10	0.33
6	.30	.30	1.00
7	.30	.60	2.00
8	.30	.90	3.00
9	.60	.10	0.166
10	.60	.30	0.50
11	.60	.60	1.00
12	.60	.90	1.500
13	.90	.10	0.11
14	.90	.30	0.33
15	.90	.60	0.66
16	.90	.90	1.0

TABLE II-3

WEIGHT AND GEOMETRIC DIMENSIONS OF TYPICAL SPACECRAFT

SPACECRAFT	WEIGHT (LBS)	APPROXIMATE DIMENSIONS (FT)	APPROXIMATE EXTERNAL SURFACE AREA (FT ²)	WEIGHT/UNIT SURFACE AREA (LB/FT ²)
Explorer 16	225	Cylinder 2 Dia X 6.25	45.6	4.9
Explorer 17	405	Sphere 2.92 Dia.	26.8	15.1
Injun	114	Sphere 2 Dia.	12.6	9.0
Syncom 1	86	Cylinder 2-1/3 dia X 1.29	18.0	4.8
Telstar 2	175	Sphere 2.875 Dia.	26.0	6.7
OAO	3600	7 Octagon X 10 Long	313.0	11.5
OGO	1000	2.7 Square X 5.6 Long	75.1	13.3
Nimbus	750	Cylinder 5 Dia. X 3	86.4	8.7
Advanced Syncom	700	Cylinder 4.8 Dia. X 4.16	98.9	7.1
Pioneer	130	Cylinder 3 Dia. X 3	42.4	3.1
			AVERAGE	8.4

The average weight per unit surface area is 8.4 lbs/ft². An average specific heat for the spacecraft of 0.18 $\frac{\text{BTU}}{\text{Lb} \cdot ^\circ\text{F}}$ was used assuming a combination of aluminum, plastics and insulating materials. An average thermal mass per unit area of spacecraft of 1.5 BTU/(^oF-ft²) results from these assumptions.

For the one foot diameter sphere, the mass used in the analysis is equal to the surface area of the one foot diameter sphere multiplied by the average weight per unit surface area (3.1416 ft² x 8.4 lbs/ft² = 26.39 lbs).

For the one foot square flat plate, the plate was assumed to have negligible thickness and a surface area of 2.0 ft² x 8.4 lbs/ft² = 16.8 lbs

total weight.

The flat plate can be oriented in an infinite number of possible directions in a particular orbit. In this analysis, one flat side of the plate is constantly oriented directly at the planet.

THERMAL ANALYSIS RESULTS

The modified computer program was used, in conjunction with the previously described assumptions for analytical variables, to define the thermal effects of planetary albedo and radiation on the temperature of the two configurations of planet-oriented spacecraft (sphere and flat plate) orbiting Mars or Venus. In order to identify the significance of the albedo and planetary radiation on the spacecraft it was practical to first determine the temperature of these spacecraft, assuming that the planetary radiosity (i.e., planetary albedo plus radiation) were zero. For this purpose, it is assumed that the spacecraft are orbiting a fictitious planet with the same physical dimensions and gravitational effects as Mars or Venus, but with zero planetary albedo and at an effective radiating temperature equal to that of deep space. The spacecraft temperature data obtained from orbiting these zero radiosity planets then establishes a datum from which the steady state temperatures, including effects of planetary radiosity, can be evaluated.

Spherical Satellites

In analyzing the one foot diameter spherically shaped spacecraft in circular orbit around Mars or Venus, the polar orbit perpendicular to the solar rays (no shadow) results in the maximum temperature the satellite will experience. The circular orbit parallel to the solar rays (maximum shadow) results in the minimum temperatures. A method of estimating the temperatures for circular polar orbits between these two extreme conditions is presented in a later part of this section.

Typical temperature information obtained from the computer program is presented in Figure II-2 for the spherical spacecraft orbiting Mars with

the noted set of thermophysical properties. This figure presents the spacecraft temperature history in two 1000 Kilometer circular orbits. It also presents temperature information assuming the planetary radiosity is zero, and with Martian planetary albedos of 0.15 and 0.295.

It should be noted that for the particular thermo-optical properties selected for Figure II-2 ($\alpha/\epsilon = 5.0$), the higher albedo value results in a higher satellite temperature. Since the effective planetary emission decreases with an increasing value of albedo (a), i.e.

$$\text{Planetary Emission } E_p = \frac{(1-a)}{4} G_s$$

satellites with thermal control coatings that are more sensitive to the planetary radiation than they are to solar and reflected (albedo) radiation, (i.e. low α/ϵ coatings) will show an increase in temperature with decreasing albedo. This is shown in Figure II-3 for the spherical satellite orbiting Venus. In this case, the thermal control coating properties are more sensitive to the planetary radiation, than to the solar or reflected solar energy, ($\alpha/\epsilon = 0.5$) and the smaller albedo value results in a higher satellite temperature. For both Figure II-2 and II-3, there is a significant increase in temperature of the spherical spacecraft, in either polar orbit, above the fictitious spacecraft temperature assuming no planetary albedo and radiation.

In order to span a range of thermo-optical properties encountered in spacecraft temperature control, orbiting satellite temperature data are presented in parametric form such as to permit interpolation and extrapolation of temperature data for any thermal control coating. For the circular polar orbits parallel to the solar rays (i.e., orbits that have a shadow period), an average or mean temperature for the total orbit period is plotted versus the solar absorptivity to emissivity (α/ϵ) ratio. An insert graph on these plots shows the maximum temperature variation from the mean temperature during one orbit as function of the α/ϵ ratio.

Since the temperature of a satellite in a shadow orbit around a planet

is a function of both the solar absorptivity to emissivity ratio (α/ϵ) and of the emissivity, it is necessary to present the satellite temperature in orbit as a function of both of these variables. Computer runs were made for all the conditions analyzed for orbit altitudes of 2500, 2000, 1500, and 1000 Km. In plotting of the data, altitudes between 2500 Km and 1000 Km have sometimes been omitted for the sake of easier readability of curves.

Figures II-4 and II-5 present the average temperature of a satellite orbiting Mars, as a function of (α/ϵ) ratio and altitude for an emissivity of 0.10. Figure II-4 shows the fictitious temperatures assuming zero radiosity (assuming no planetary radiation or albedo) for Mars orbits. Figure II-5 indicates the satellite temperatures for the same orbits with an albedo of 0.148.

When the temperature variations (ΔT) presented in the insert figure is added or subtracted from the mean orbiting temperature, for a given α/ϵ ratio, the maximum (or minimum) temperatures experienced by the satellite in orbit is obtained. Figure II-6 has been included to indicate how information presented on Figures such as II-4 and II-5 can be used to predict the increase in temperature of the spherical spacecraft due to planetary radiation and albedo effects. Figure II-7 shows the same data as Figure II-5, for an albedo of 0.295.

Figures II-8, II-9 and II-10 are similar to Figures II-4, II-5 and II-7 for a thermal emissivity of 0.3.

Figures II-11, II-12 and II-13 are for a thermal emissivity of 0.6, and Figures II-14, II-15 and II-16 are for a thermal emissivity of 0.9.

Figure II-17 shows the average level of radiation incident to each square foot of surface area on the spherical satellite orbiting Mars with an assumed albedo of 0.148. The total radiation incident on the satellite may thus be obtained by multiplying the average incident radiation by the total surface area of the spherical satellite. Figure II-18 is similar to Figure II-17, for an albedo value of 0.295. This decreases the level of the planetary

radiation while increasing the level of solar reflected or albedo radiation incident on the satellite. The identical method of data presentation (temperature and incident radiation) as used for Mars, is repeated for the spherical satellite orbiting Venus in Figures II-19 through II-32. The albedo values used for the planet Venus were 0.59 and 0.77.

In order to estimate the change in temperature of the spherical satellite for polar orbits between the orbit parallel and that perpendicular to the solar rays, Figure II-33 was prepared. This curve presents a correction factor as a function of the polar orbit angle (θ) from the parallel orbit position, toward the orbit perpendicular to solar rays. The correction factor can be used to predict the temperature of the spherical satellite in a circular polar orbit other than the two considered in the study thus far, as shown in the figure.

Flat Plate Satellites

The analytical results for the flat plate configuration are presented in Figures II-34 to II-65. This manner of presentation is the same as used for the spherical satellite. A significant difference in the one square foot flat plate configuration results from the fact that the flat plate is assumed to have negligible thickness and is oriented such that the flat side is always parallel to the planet surface. This means that when the flat plate is in the polar orbit perpendicular to the solar rays, the flat plate receives no direct solar radiation. For this reason, the orbit perpendicular to the solar rays in this case does not represent the maximum temperature but rather the minimum temperature orbit. On the other hand, because of the orientation in orbit, the polar orbit parallel to the solar rays represents the one with the maximum solar insolation and thus the maximum temperature orbit.

The zero planetary radiosity curves used to compare the effects of planetary radiation and albedo on the flat plate, do not contain the orbit perpendicular to the solar rays curves because the temperature of the flat plate with zero incident energy from the sun (viewing the plate on edge)

is absolute zero. With a finite albedo value for the planet there is energy input to the plate from both planetary albedo and planetary radiation, for the flat plate in an orbit perpendicular to the solar rays.

The first set of temperature curves for the flat plate orbiting Mars with a thermal emissivity of 0.1 are shown in Figures II-34, II-35, and II-36. Figure II-34 is the zero radiosity planet figure, while Figures II-35 and II-36 are for albedo values of 0.148 and 0.295, respectively.

The additional sets of temperature curves for the flat plate spacecraft orbiting Mars appear in Figures II-37 through II-45 for emissivity values of 0.3, 0.6 and 0.9.

Figure II-46 depicts the radiation incident to the one square foot flat plate facing the planet Mars for an albedo of 0.148. This side of the plate sees the planetary albedo, planetary thermal radiation and direct solar radiation. Figure II-47 indicates the level of solar energy incident to the side of the flat plate facing away from the planet. Figure II-48 indicates the level of solar, planetary albedo and planetary radiation incident on the flat plate facing Mars, assuming an albedo value of 0.295 for Mars.

The four sets of mean temperature data for the flat plate orbiting Venus are presented in Figures II-49 through II-60 for the thermal emissivity values considered.

Figure II-61 indicates the intensity of the radiation incident to the Venus-facing-side of the flat plate assuming an albedo of 0.59. Figure II-62 indicates the intensity of incident radiation from the Sun onto the opposite side of the flat plate. Figure II-63 indicates the level of intensity of radiation incident on the planet-facing-side assuming the albedo value for the planet Venus is as high as 0.77.

Figure II-64 can be used to establish the flat plate temperatures for circular polar orbits other than those perpendicular or parallel to the solar rays.

The total orbital time and shadow time data resulting from the computer

runs is presented in Table II-4.

TABLE II-4
ORBITAL TIME AND MAXIMUM SHADOW TIME

Circular Orbit Altitude (Km)	Orbital Period (Minutes)	Maximum Shadow Circular Orbit	
		Shadow Time (Minutes)	Percent of Time in Shadow
<u>MARS</u>			
1000	147.4	41.4	28.0
1500	173.2	42.3	24.4
2000	200.4	43.4	21.7
2500	228.9	44.7	19.5
<u>VENUS</u>			
1000	110.5	36.3	32.9
1500	122.3	36.3	29.7
2000	134.6	36.6	27.2
2500	147.2	37.0	25.1

It is interesting to note that there is a significant decrease in the percent of orbit time spent in the shadow as the orbit altitude increases, whereas, the time spent in the shadow remains relatively constant.

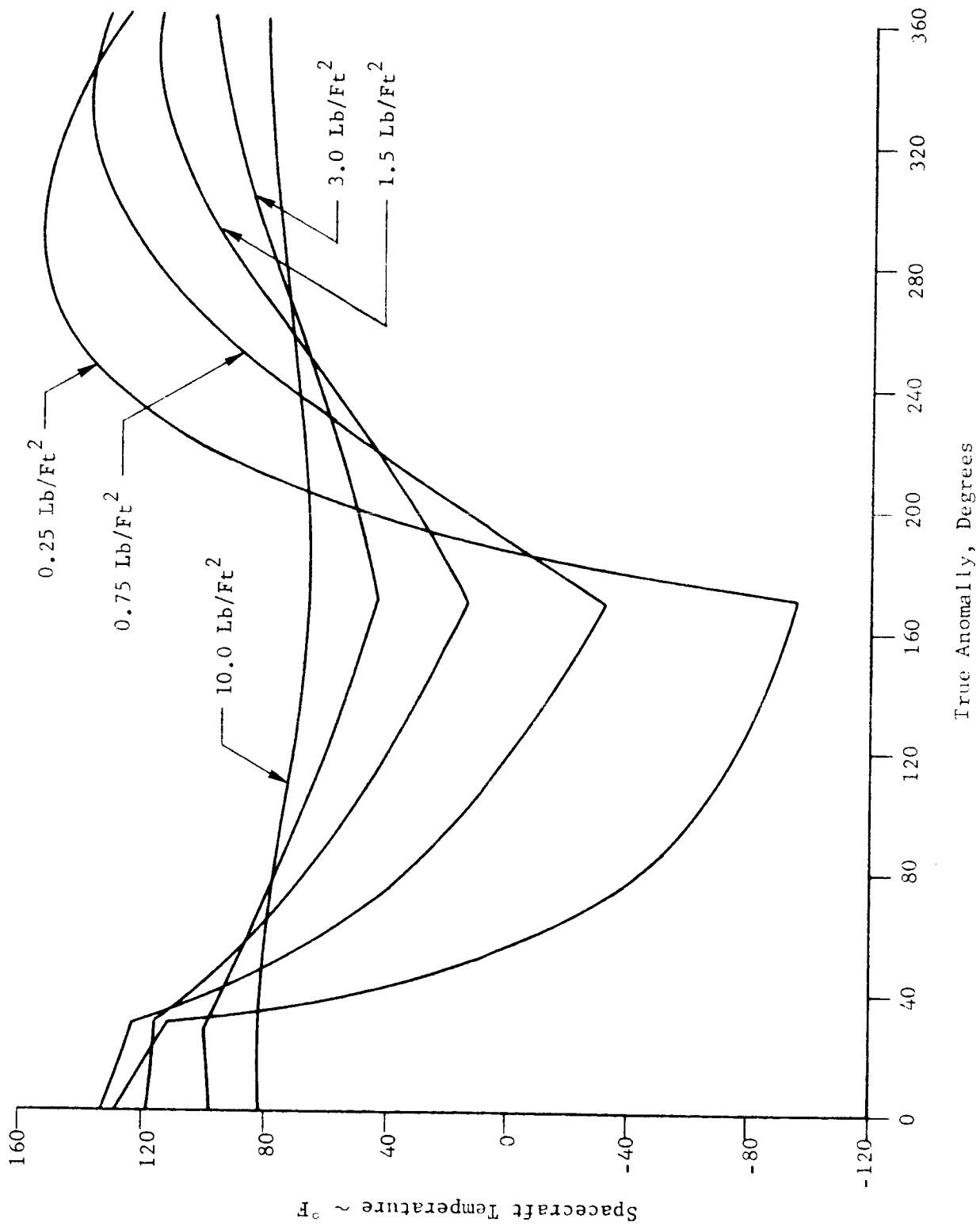


FIGURE II-1 THE EFFECT OF MASS VARIATIONS ON TEMPERATURE FOR AN EARTH ORBITING SPHERICAL SPACECRAFT (From Reference 7)

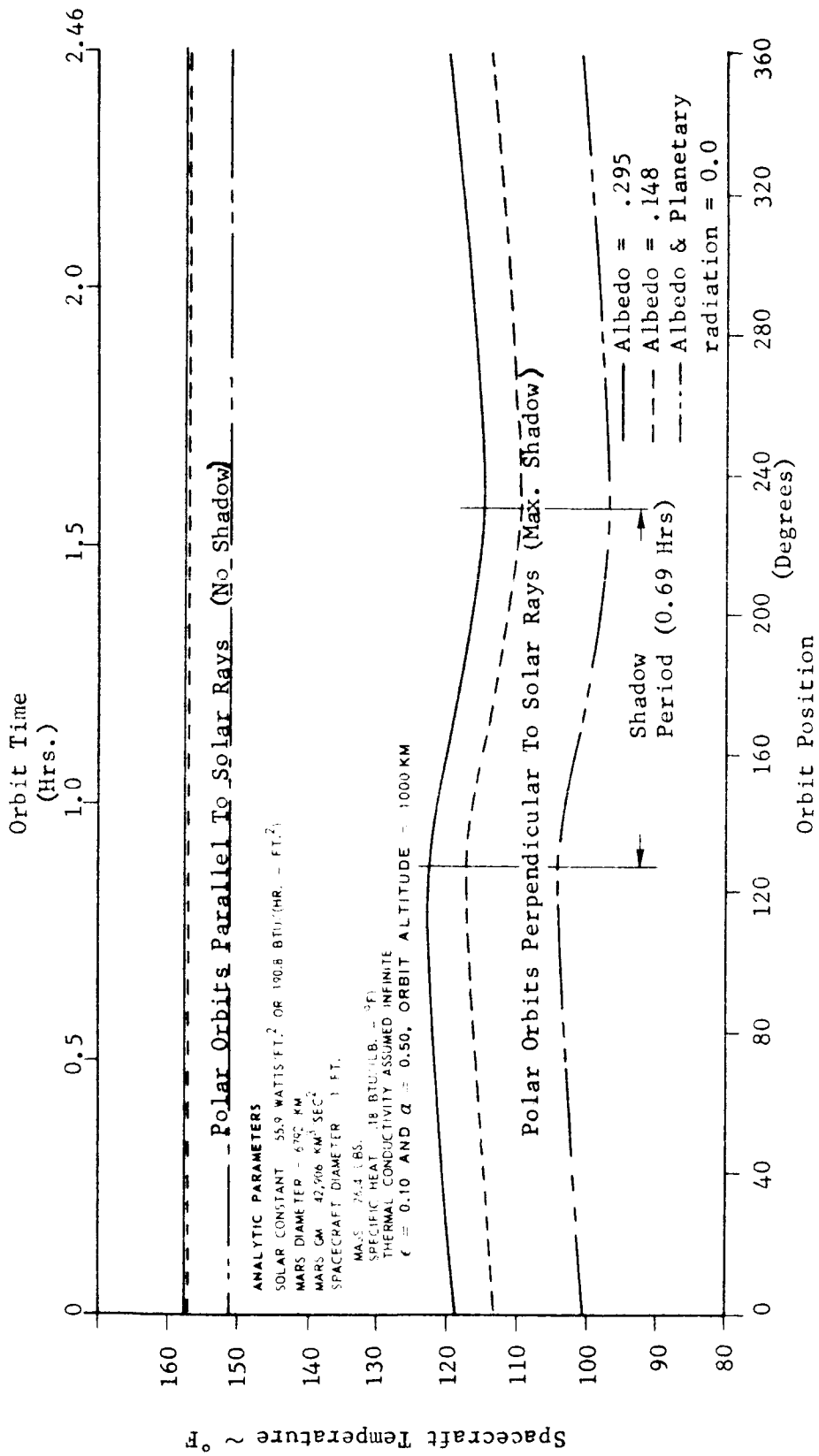


FIGURE II-2 - THE EFFECT OF ALBEDO ON TEMPERATURE OF A SPHERICAL SATELLITE ORBITING MARS

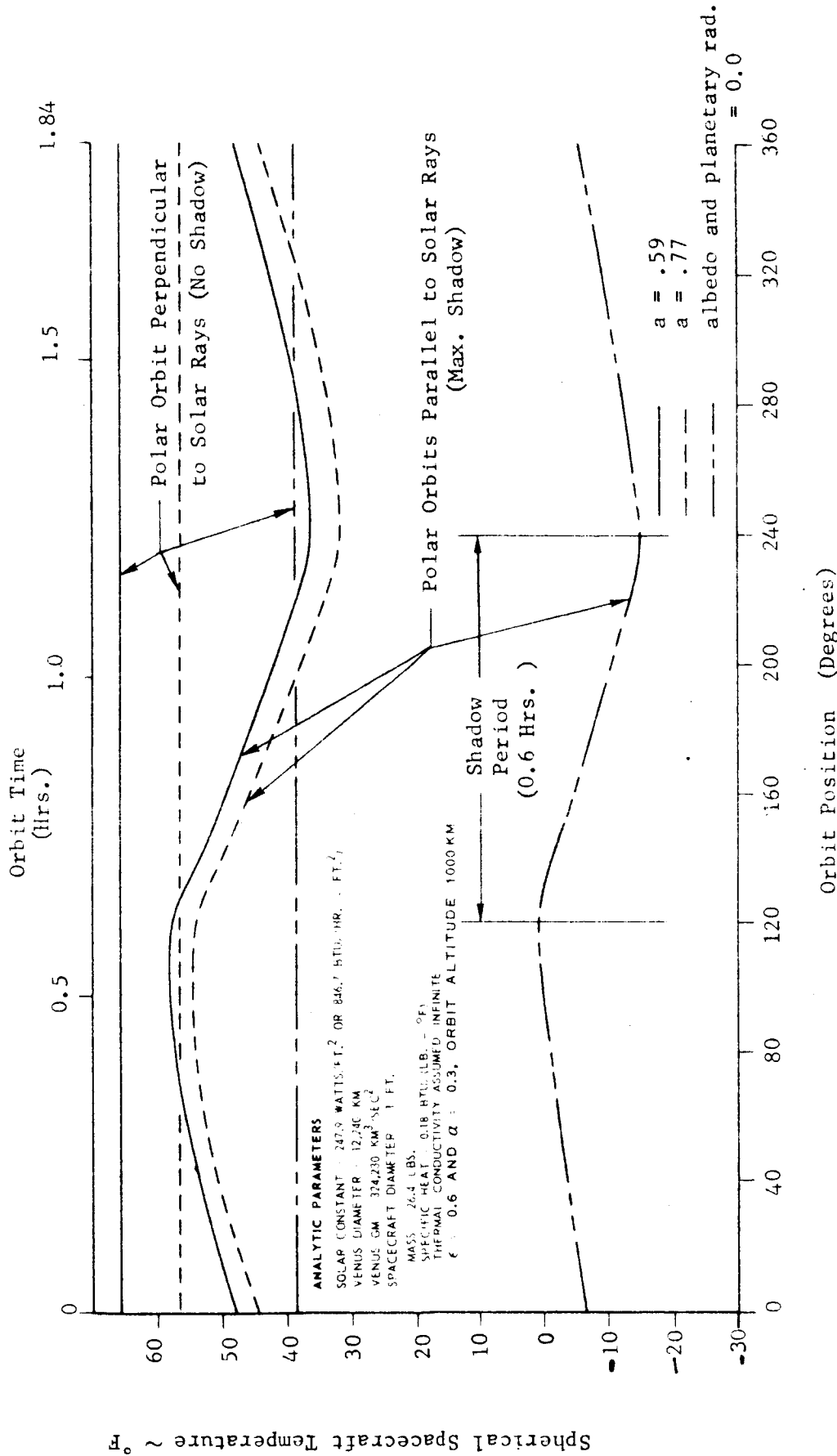
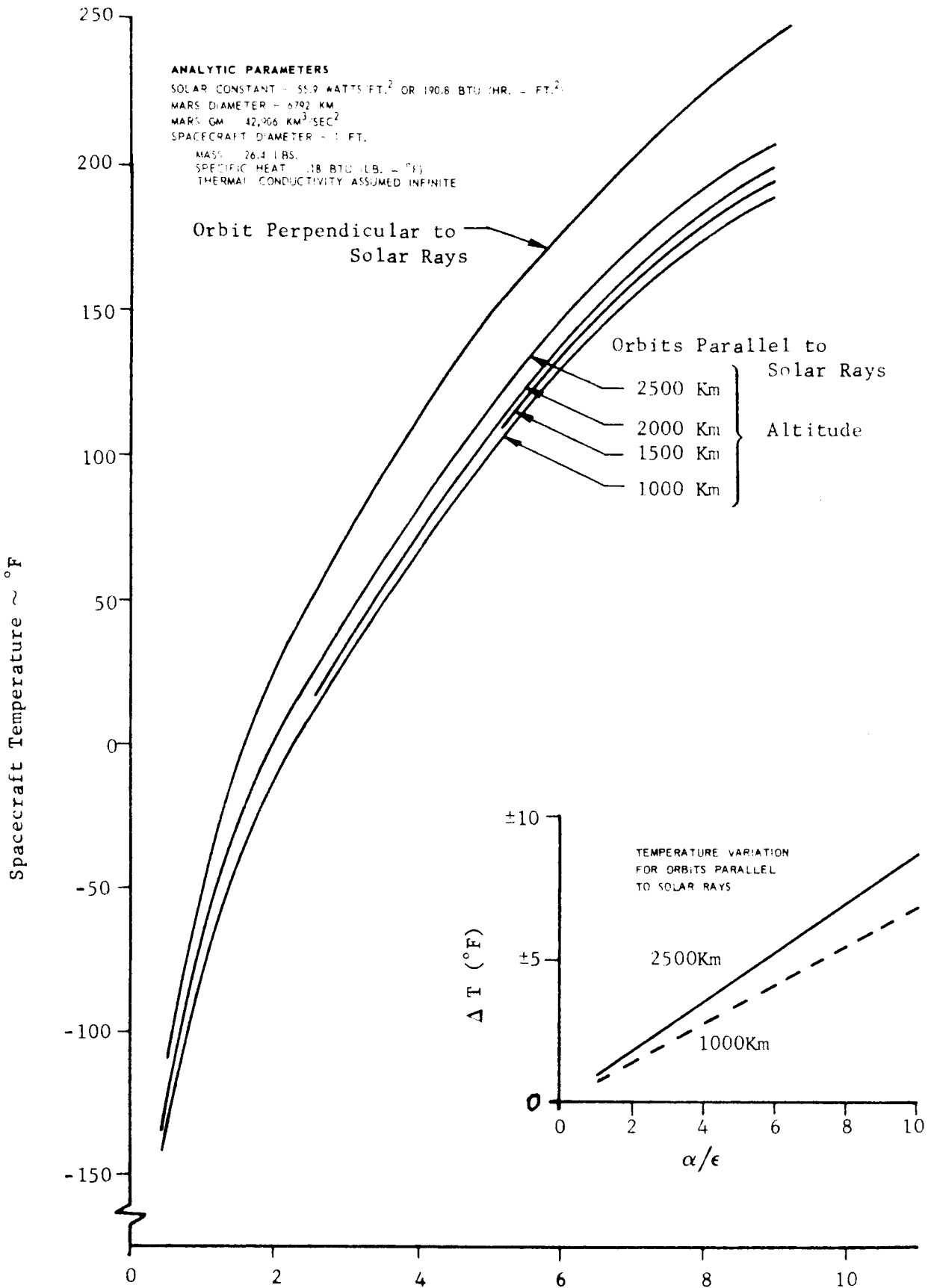
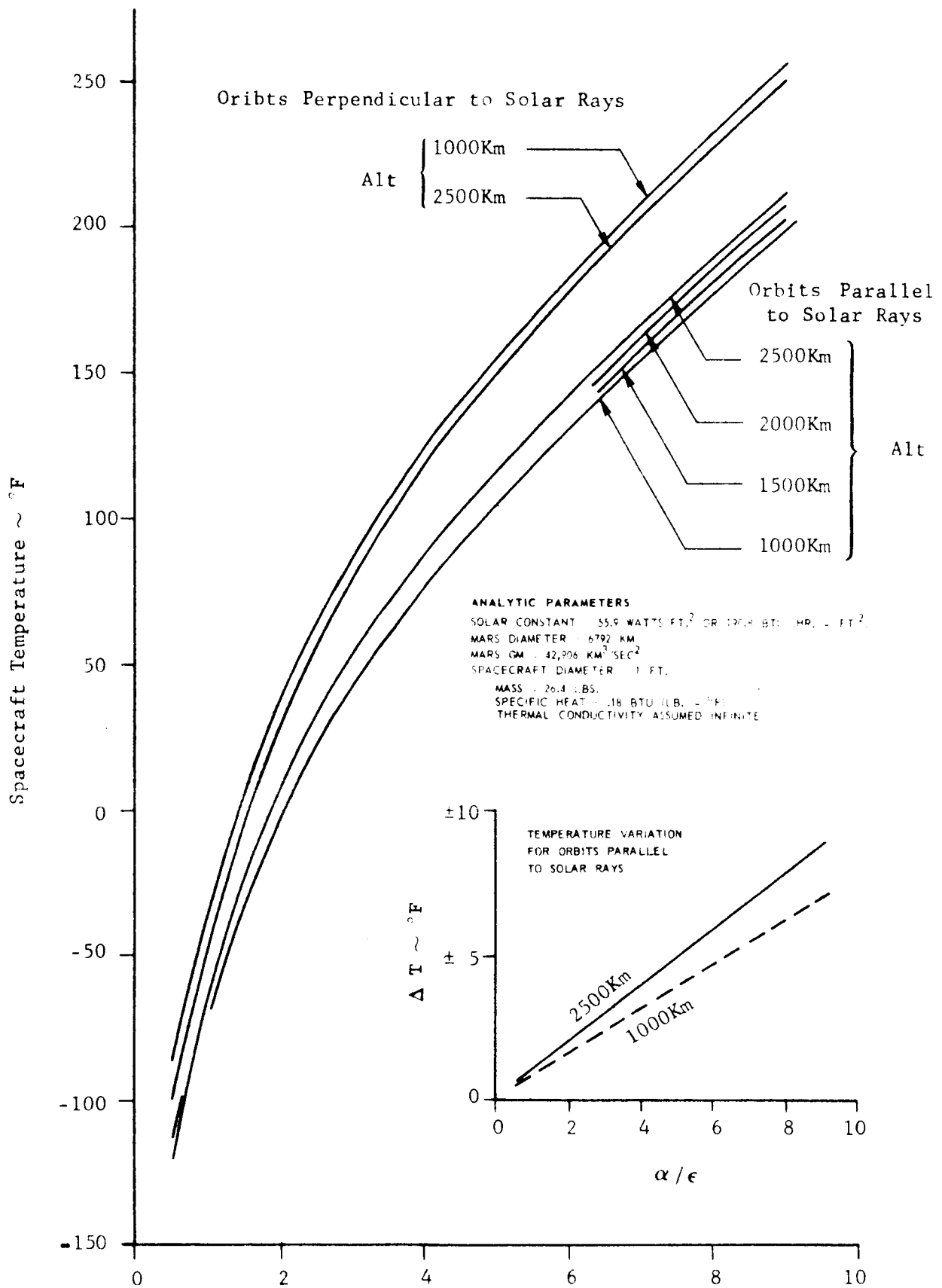


FIGURE II-3 - THE EFFECT OF ALBEDO ON TEMPERATURE OF A SPHERICAL SATELLITE ORBITING VENUS



Spacecraft Coating Solar Absorptivity to Emissivity Ratio (α/ϵ)

FIGURE II-4 MEAN TEMPERATURE OF A SPHERICAL SATELLITE IN MARS CIRCULAR POLAR ORBITS NEGLECTING PLANETARY RADIATION AND ALBEDO EFFECTS, FOR A SPACECRAFT EMISSIVITY OF 0.1.



Spacecraft Coating Solar Absorptivity to Emissivity Ratio (α/ϵ)

FIGURE II-5 MEAN TEMPERATURE OF A SPHERICAL SATELLITE IN MARS CIRCULAR POLAR ORBITS INCLUDING THE EFFECTS OF PLANETARY RADIATION AND AN ALBEDO OF 0.148, FOR A SPACECRAFT EMISSIVITY OF 0.1.

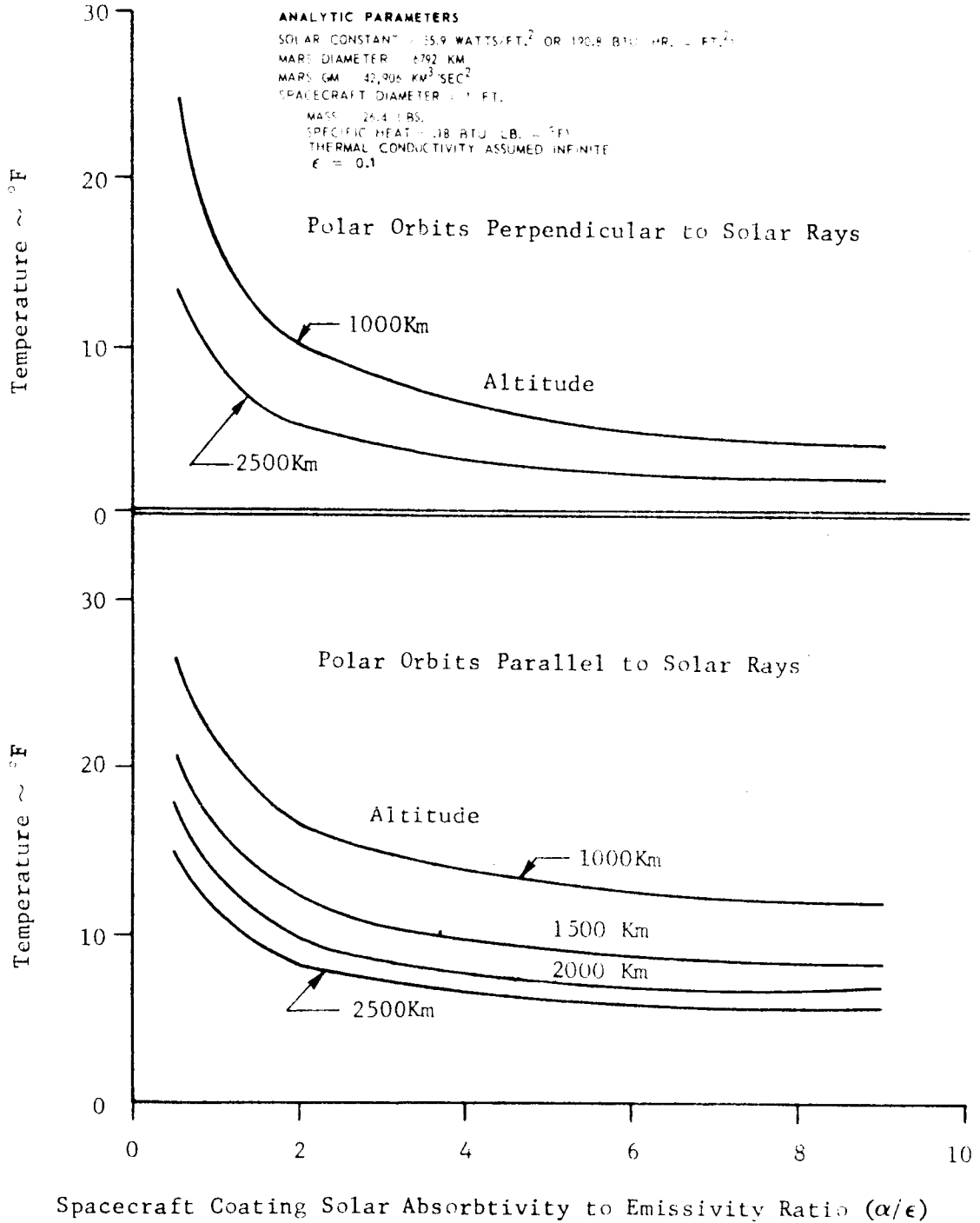
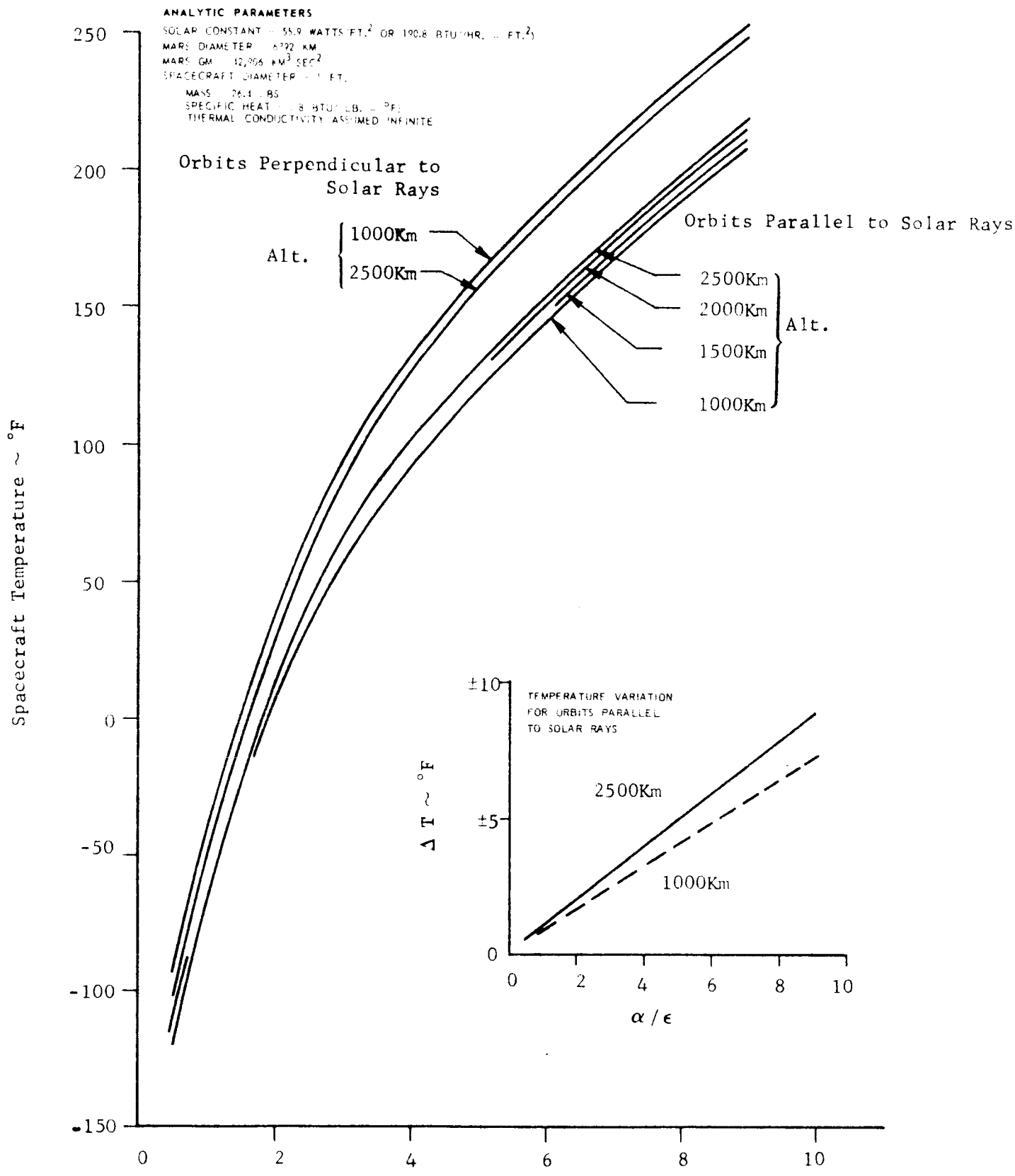


FIGURE II-6 MEAN TEMPERATURE INCREASE OF SPHERICAL SPACECRAFT DUE TO PLANETARY ALBEDO AND RADIATION EFFECTS.

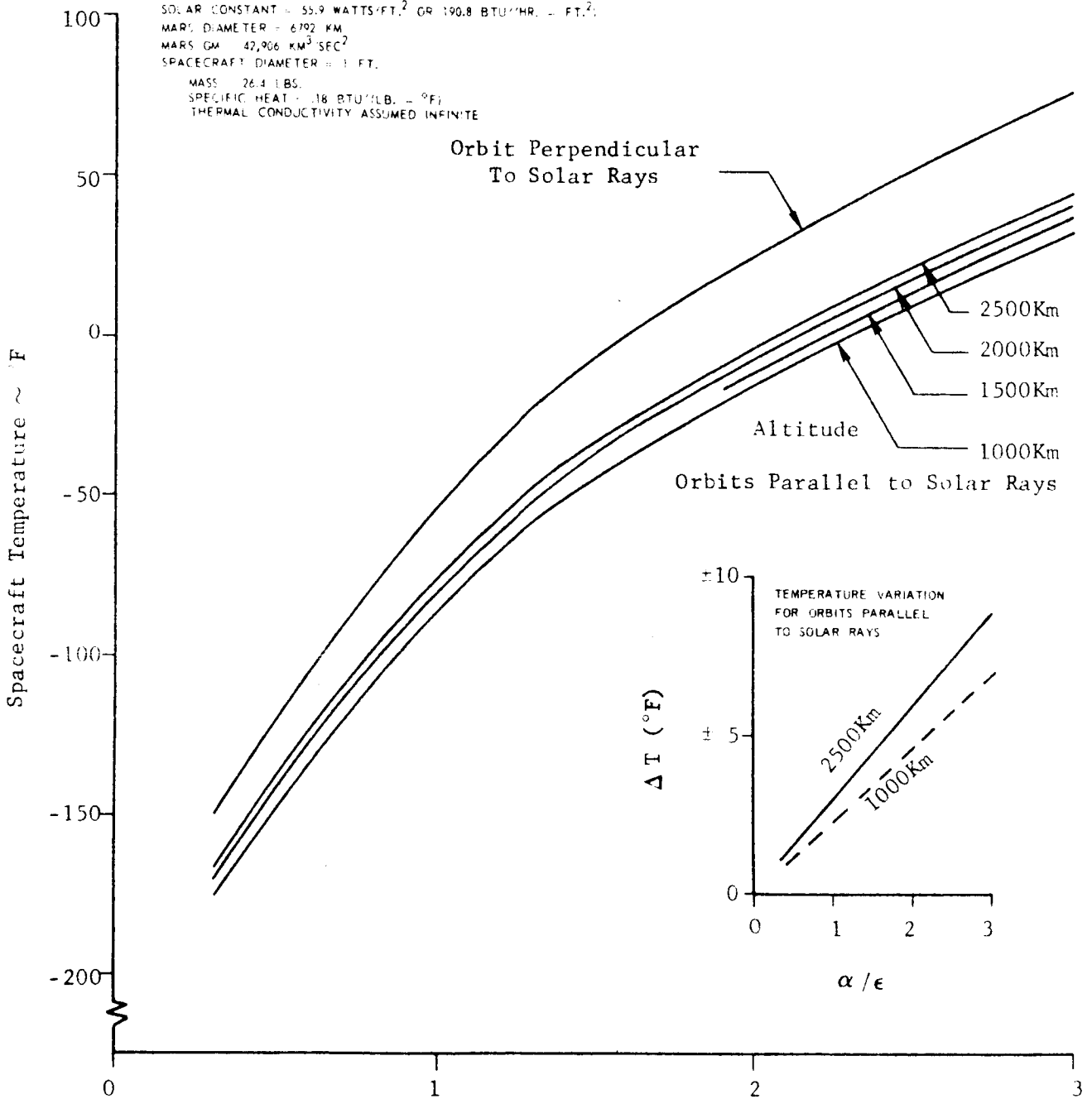


Spacecraft Coating Solar Absorptivity to Emissivity Ratio (α/ϵ)

FIGURE II-7 MEAN TEMPERATURE OF A SPHERICAL SATELLITE IN MARS CIRCULAR POLAR ORBITS INCLUDING THE EFFECTS OF PLANETARY RADIATION AND AN ALBEDO OF .295, FOR A SPACECRAFT EMISSIVITY OF 0.1.

ANALYTIC PARAMETERS

SOLAR CONSTANT = 55.9 WATTS/FT.² OR 190.8 BTU/HR. - FT.²;
 MARS DIAMETER = 6792 KM
 MARS GM = 42,906 KM³/SEC²
 SPACECRAFT DIAMETER = 3 FT.
 MASS = 26.4 LBS.
 SPECIFIC HEAT = .18 BTU/(LB. - °F)
 THERMAL CONDUCTIVITY ASSUMED INFINITE



Spacecraft Coating Solar Absorptivity to Emissivity Ratio (α/ϵ)

FIGURE II-8 MEAN TEMPERATURE OF A SPHERICAL SATELLITE IN MARS CIRCULAR POLAR ORBITS NEGLECTING PLANETARY RADIATION AND ALBEDO EFFECTS, FOR A SPACECRAFT EMISSIVITY OF 0.3.

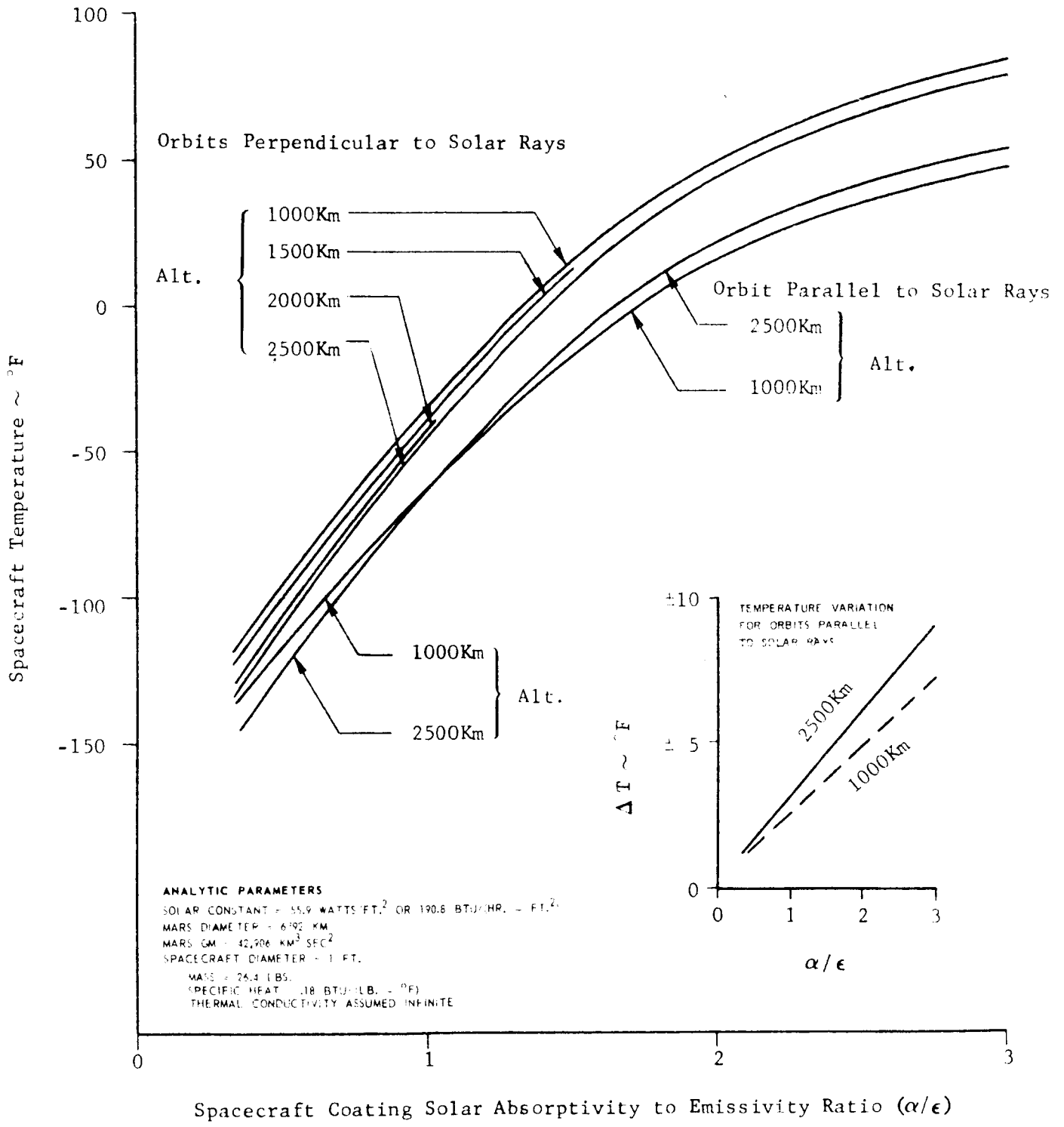


FIGURE II-9 MEAN TEMPERATURE OF A SPHERICAL SATELLITE IN MARS CIRCULAR POLAR ORBITS INCLUDING THE EFFECTS OF PLANETARY RADIATION AND AN ALBEDO OF 0.148, FOR A SPACECRAFT EMISSIVITY OF 0.3.

ANALYTIC PARAMETERS

SOLAR CONSTANT = 550 WATTS/FT.² OR 190.8 BTU/HR. / FT.²
 MARS DIAMETER = 6792 KM
 MARS GM = 42,906 KM³/SEC²
 SPACECRAFT DIAMETER = 1 FT.
 MASS = 26.4 LBS.
 SPECIFIC HEAT = .18 BTU/(LB. - °F)
 THERMAL CONDUCTIVITY ASSUMED INFINITE

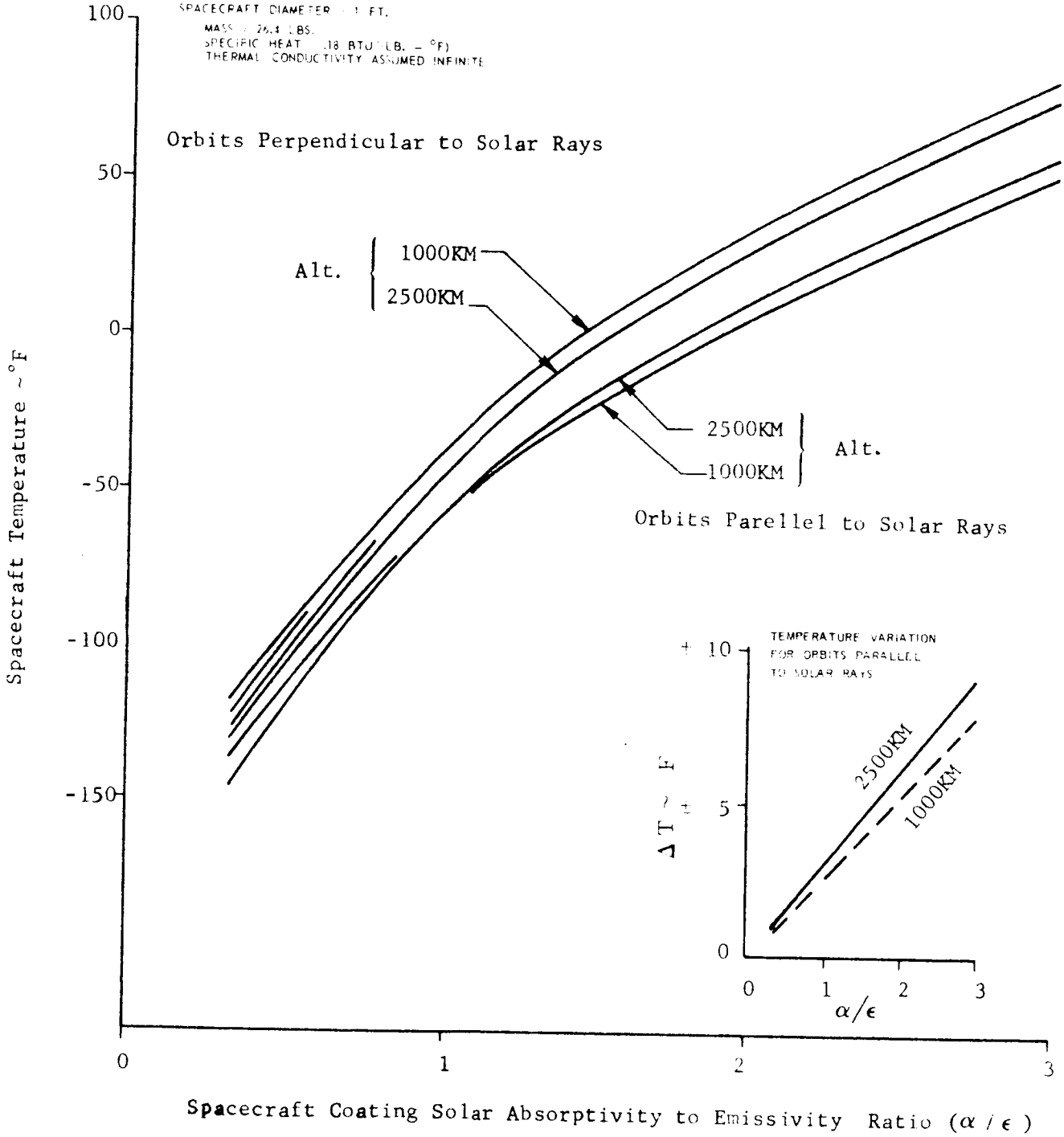


FIGURE II-10 MEAN TEMPERATURE OF A SPHERICAL SATELLITE IN MARS CIRCULAR POLAR ORBITS INCLUDING THE EFFECTS OF PLANETARY RADIATION AND AN ALBEDO OF 0.295, FOR A SPACECRAFT EMISSIVITY OF 0.3.

ANALYTIC PARAMETERS

SOLAR CONSTANT = 55.9 WATTS FT.² OR 190.8 BTU (HR. - FT.)²

MARS DIAMETER = 6792 KM

MARS GM = 42,906 KM³ SEC²

SPACECRAFT DIAMETER = 1 FT.

MASS = 76.4 LBS.

SPECIFIC HEAT = .18 BTU (LB. - °F)

THERMAL CONDUCTIVITY ASSUMED INFINITE

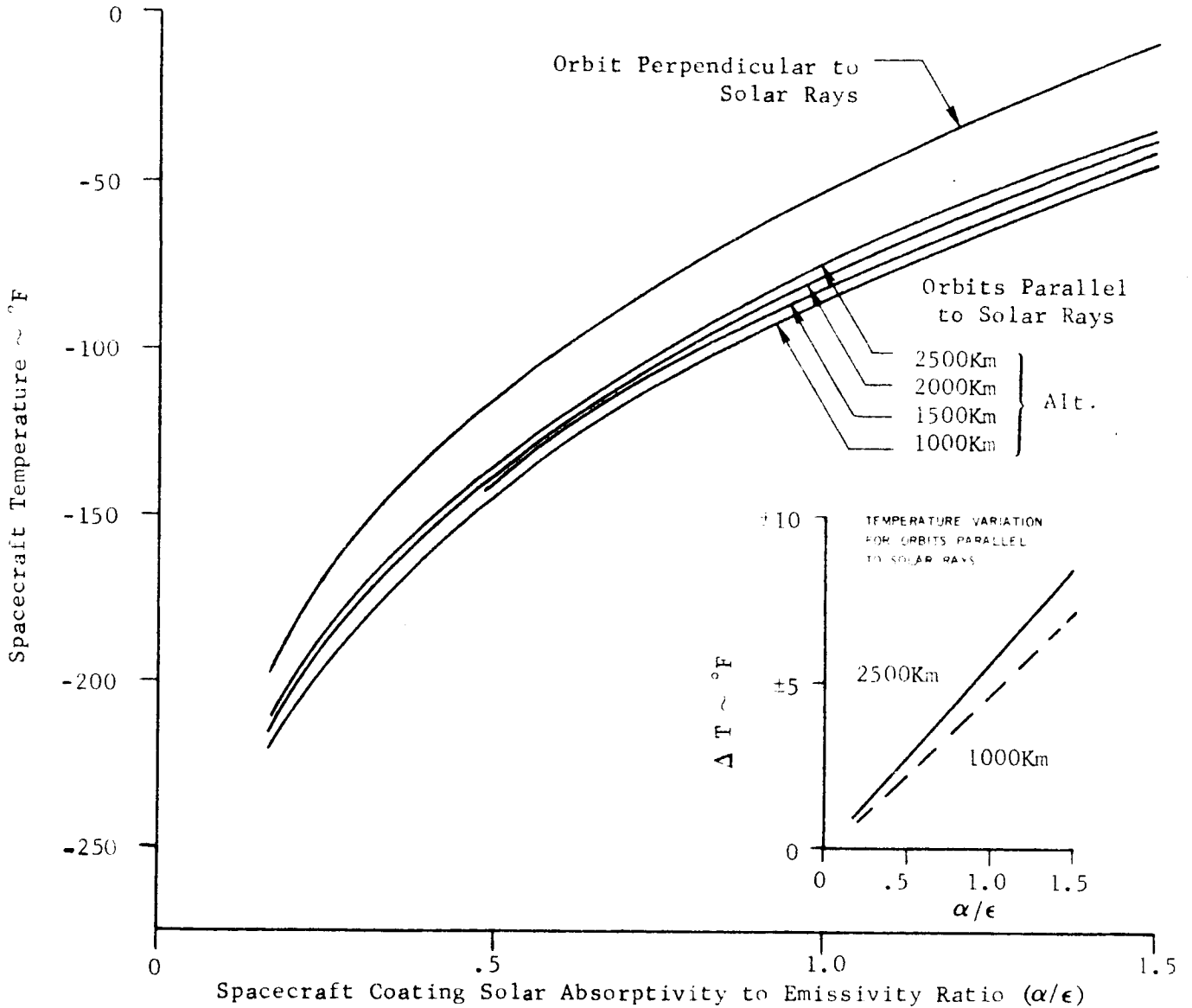


FIGURE II-11 MEAN TEMPERATURE OF A SPHERICAL SATELLITE IN MARS CIRCULAR POLAR ORBITS NEGLECTING PLANETARY RADIATION AND ALBEDO EFFECTS, FOR A SPACECRAFT EMISSIVITY OF 0.6.

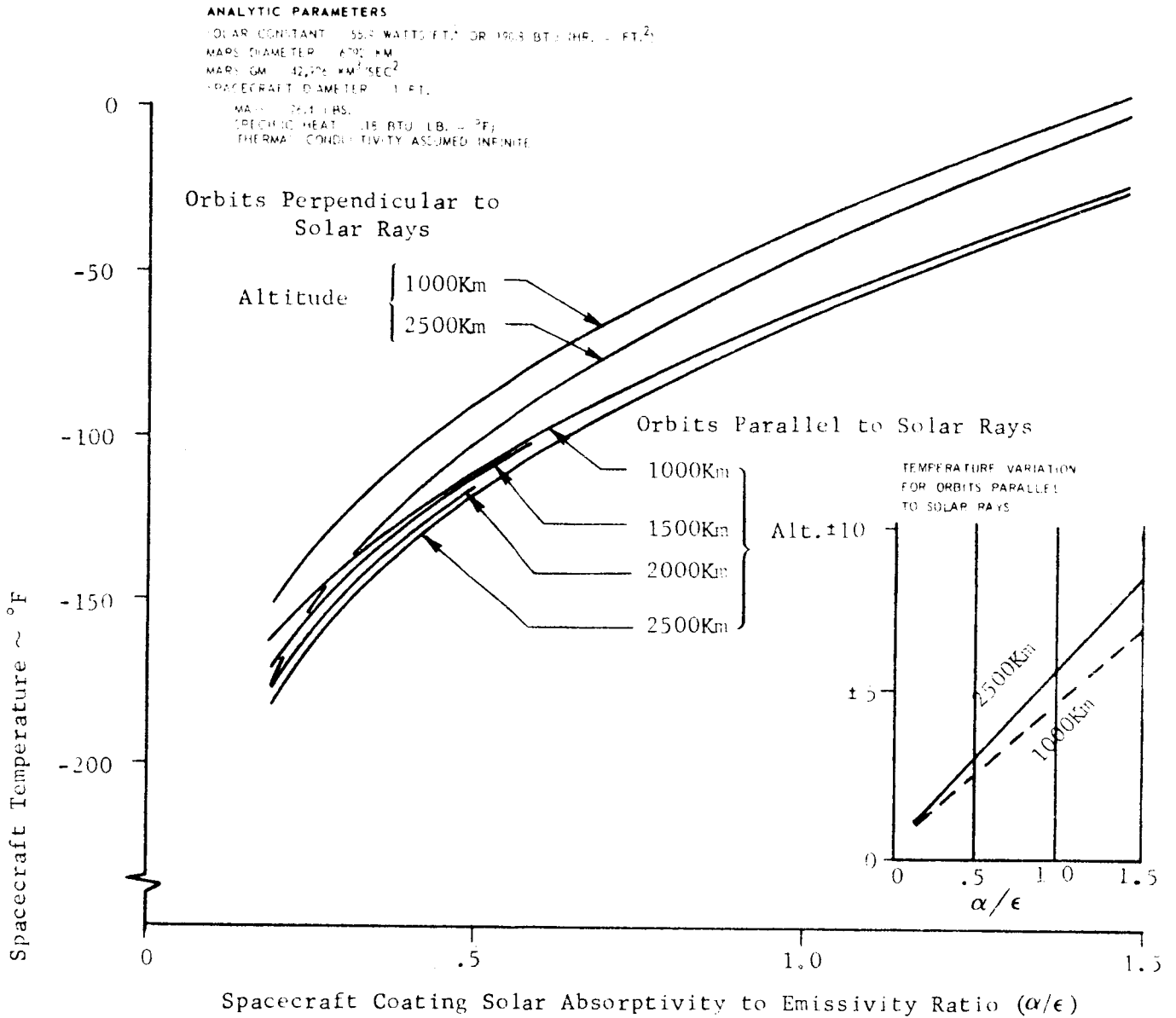


FIGURE II-12 MEAN TEMPERATURE OF A SPHERICAL SATELLITE IN MARS CIRCULAR POLAR ORBITS INCLUDING THE EFFECTS OF PLANETARY RADIATION AND AN ALBEDO OF 0.148, FOR A SPACECRAFT EMISSIVITY OF 0.6.

ANALYTIC PARAMETERS

SOLAR CONSTANT = 587 WATTS/FT.² OR 190.8 BTU/HR./FT.²
 MARS DIAMETER = 4792 KM
 MARS GM = 42,406 KM³/SEC.²
 SPACECRAFT DIAMETER = 1 FT.
 MASS = 24.3 LBS.
 SPECIFIC HEAT = .18 BTU/LB./°F
 THERMAL CONDUCTIVITY ASSUMED INFINITE

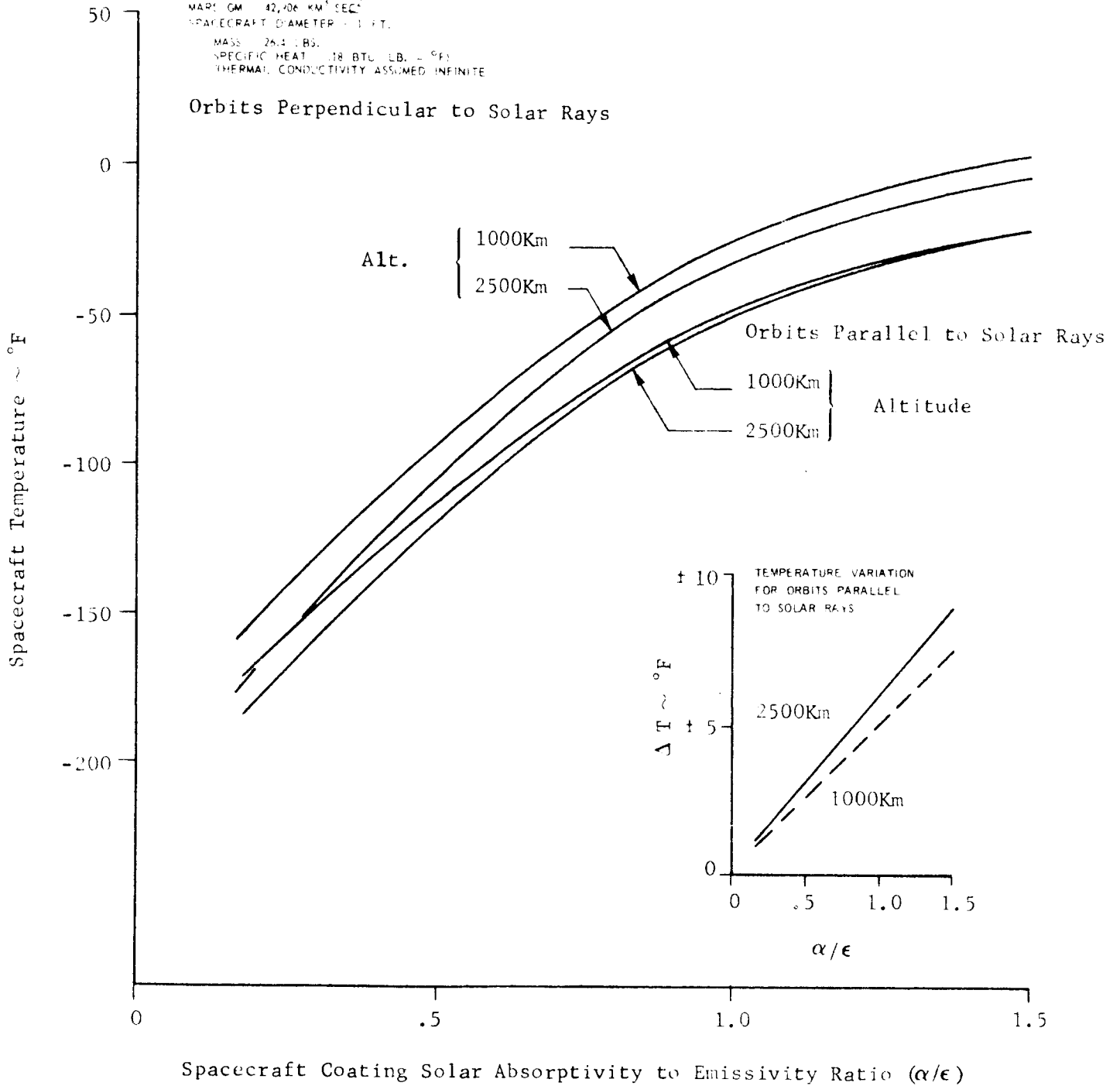


FIGURE II-13 MEAN TEMPERATURE OF A SPHERICAL SATELLITE IN MARS CIRCULAR POLAR ORBITS INCLUDING THE EFFECTS OF PLANETARY RADIATION AND AN ALBEDO OF 0.295, FOR A SPACECRAFT EMISSIVITY OF 0.6.

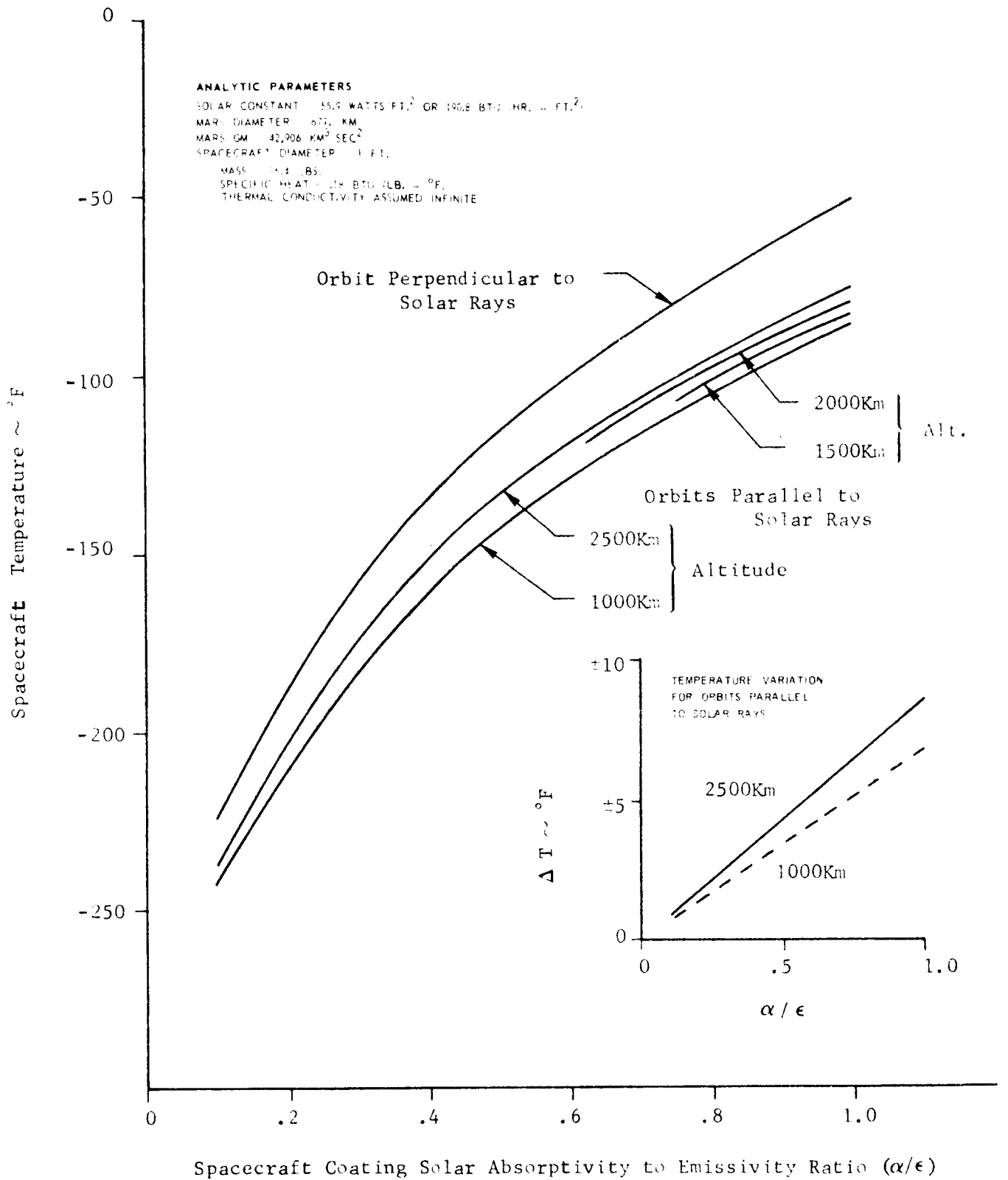


FIGURE II-14 MEAN TEMPERATURE OF A SPHERICAL SATELLITE IN MARS CIRCULAR POLAR ORBITS NEGLECTING PLANETARY RADIATION AND ALBEDO EFFECTS, FOR A SPACECRAFT EMISSIVITY OF 0.9.

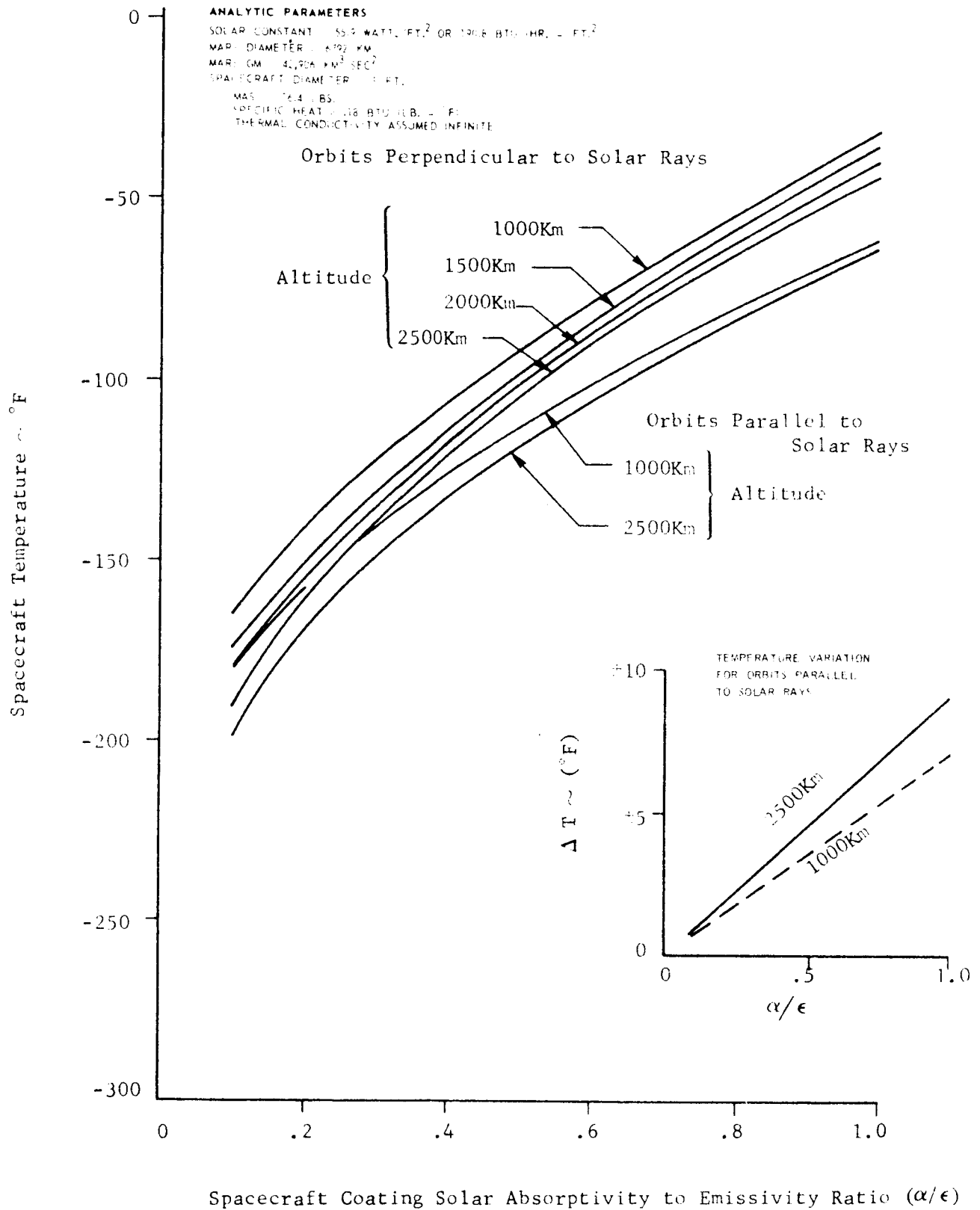
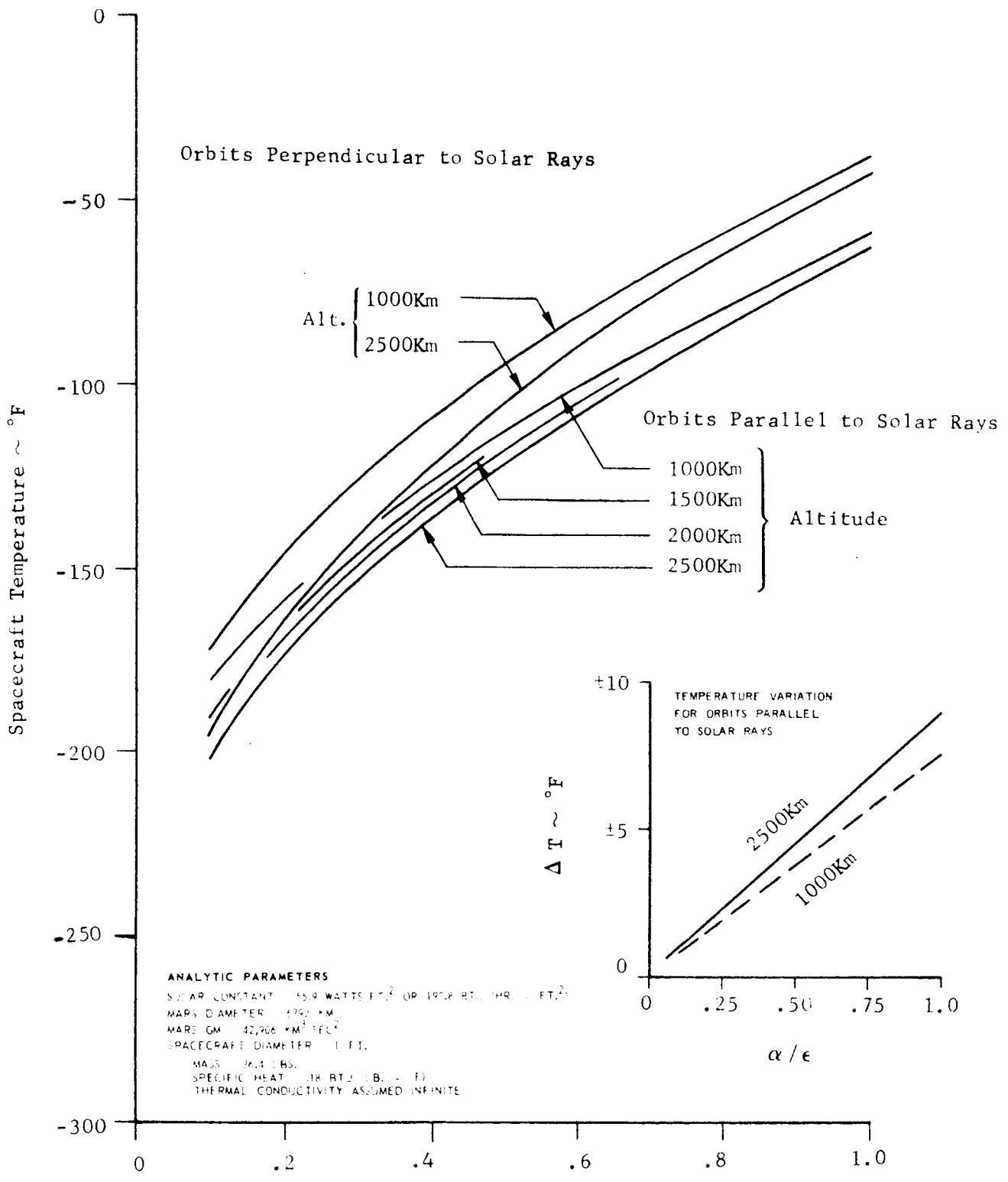


FIGURE II-15 MEAN TEMPERATURE OF A SPHERICAL SATELLITE IN MARS CIRCULAR POLAR ORBITS INCLUDING THE EFFECTS OF PLANETARY RADIATION AND AN ALBEDO OF 0.148, FOR A SPACECRAFT EMISSIVITY OF 0.9.



Spacecraft Coating Solar Absorptivity to Emissivity Ratio (α/ϵ)

FIGURE II-16 MEAN TEMPERATURE OF A SPHERICAL SATELLITE IN MARS CIRCULAR POLAR ORBITS INCLUDING THE EFFECTS OF PLANETARY RADIATION AND AN ALBEDO of 0.295, FOR A SPACECRAFT EMISSIVITY OF 0.9.

- - - Orbits Perpendicular to Solar Rays
 — Orbits Parallel to Solar Rays

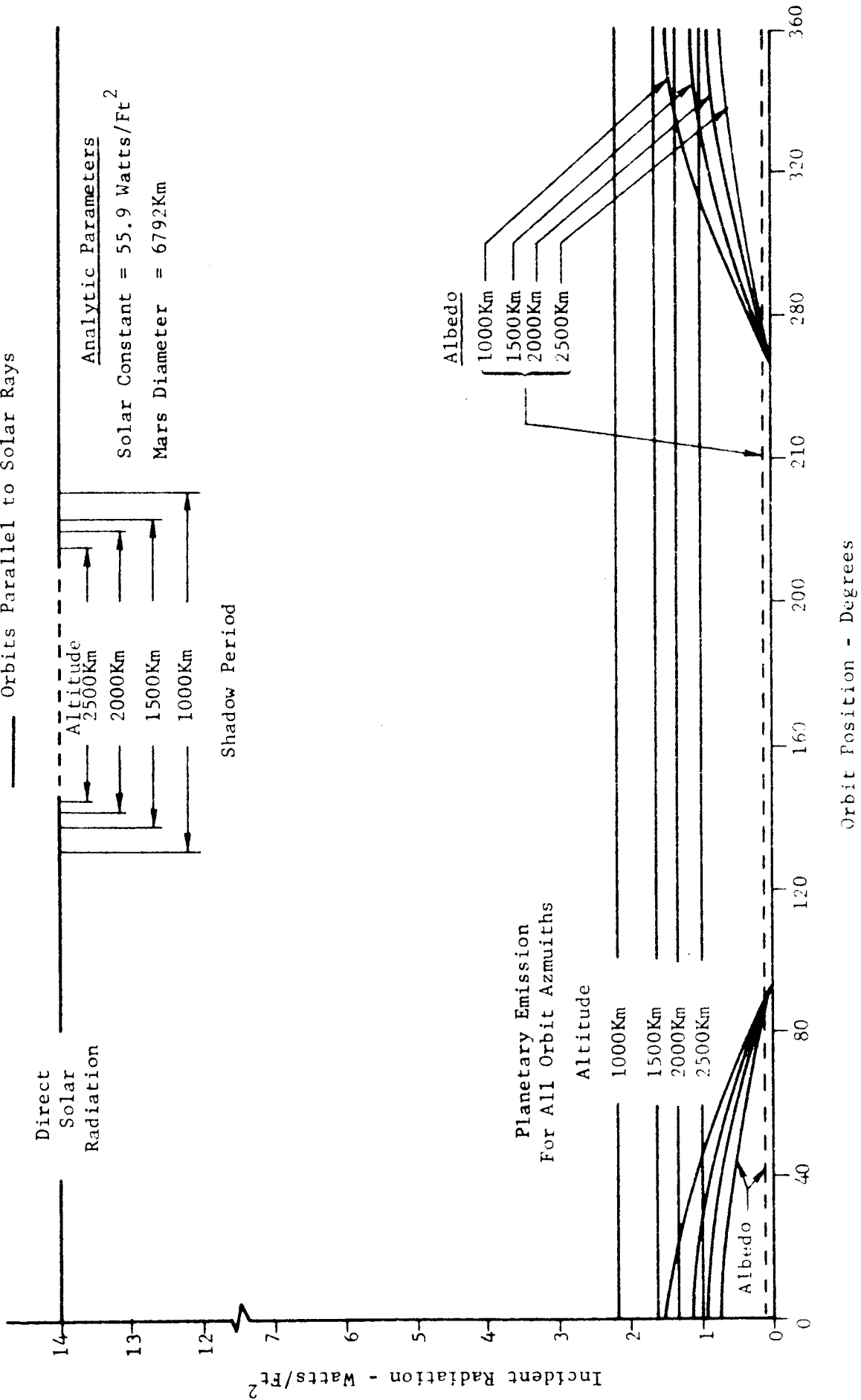


FIGURE II-17 AVERAGE INCIDENT RADIATION PER SQUARE FOOT OF SURFACE AREA ON A 1 FOOT DIAMETER SPHERE IN CIRCULAR POLAR ORBITS AROUND MARS WITH AN ALBEDO OF 0.148.

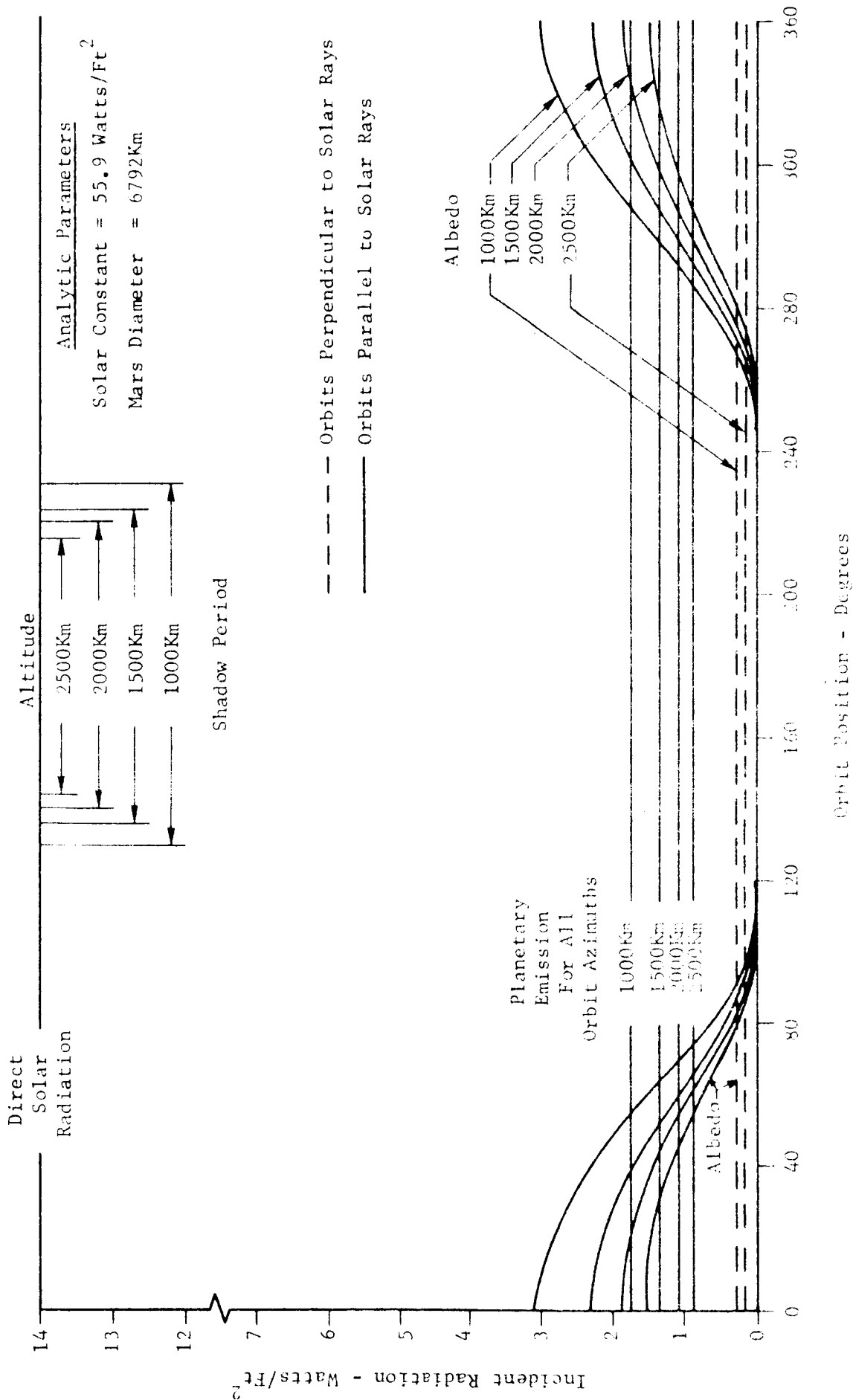


FIGURE II-18 AVERAGE INCIDENT RADIATION PER SQUARE FOOT OF SURFACE AREA ON A 1 FOOT DIAMETER SPHERE IN CIRCULAR POLAR ORBITS AROUND MARS WITH AN ALBEDO OF .295.

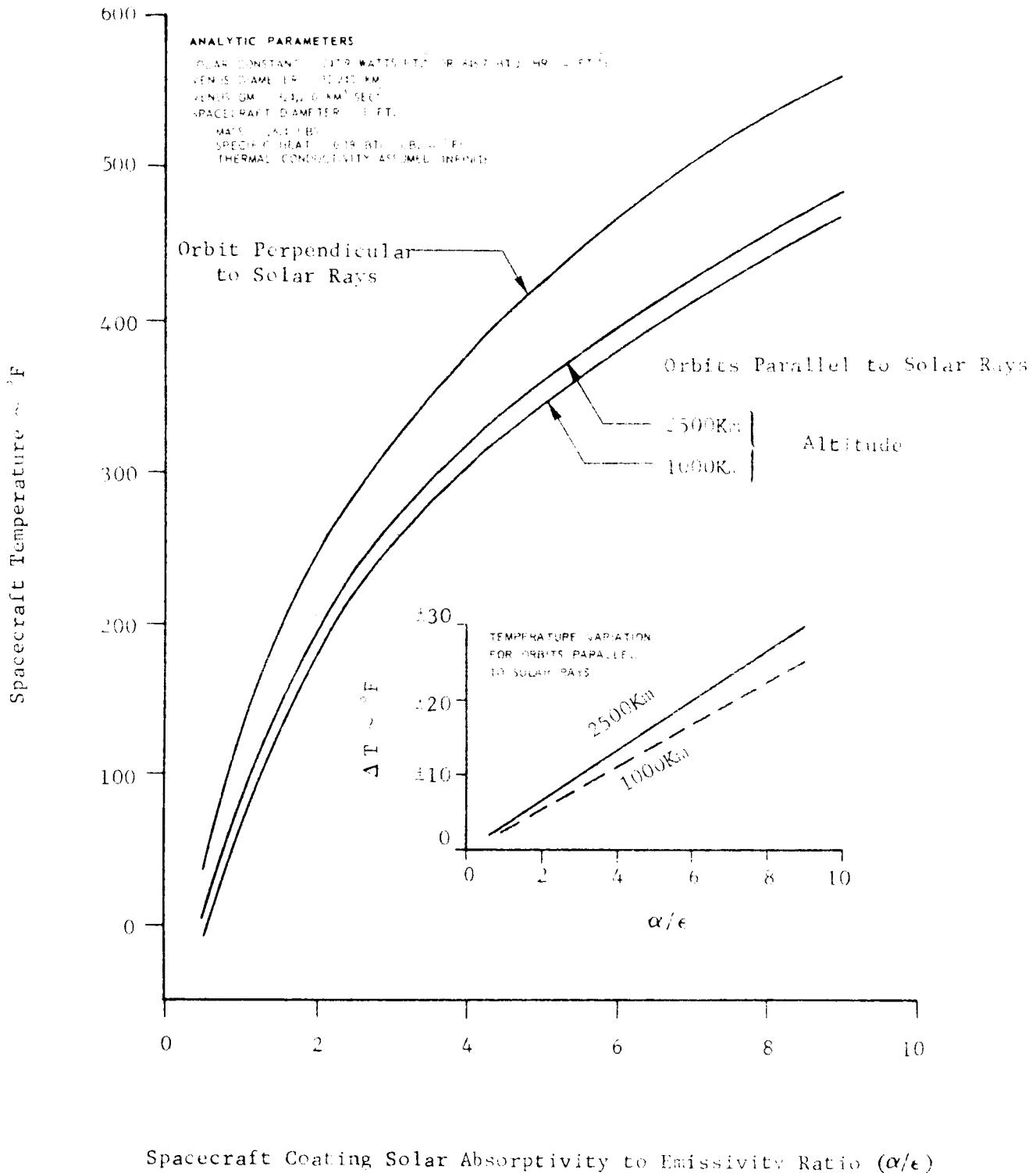


FIGURE II-19 MEAN TEMPERATURE OF A SPHERICAL SATELLITE IN VENUS CIRCULAR POLAR ORBITS NEGLECTING PLANETARY RADIATION AND ALBEDO EFFECTS FOR A SPACECRAFT EMISSIVITY OF 0.1.

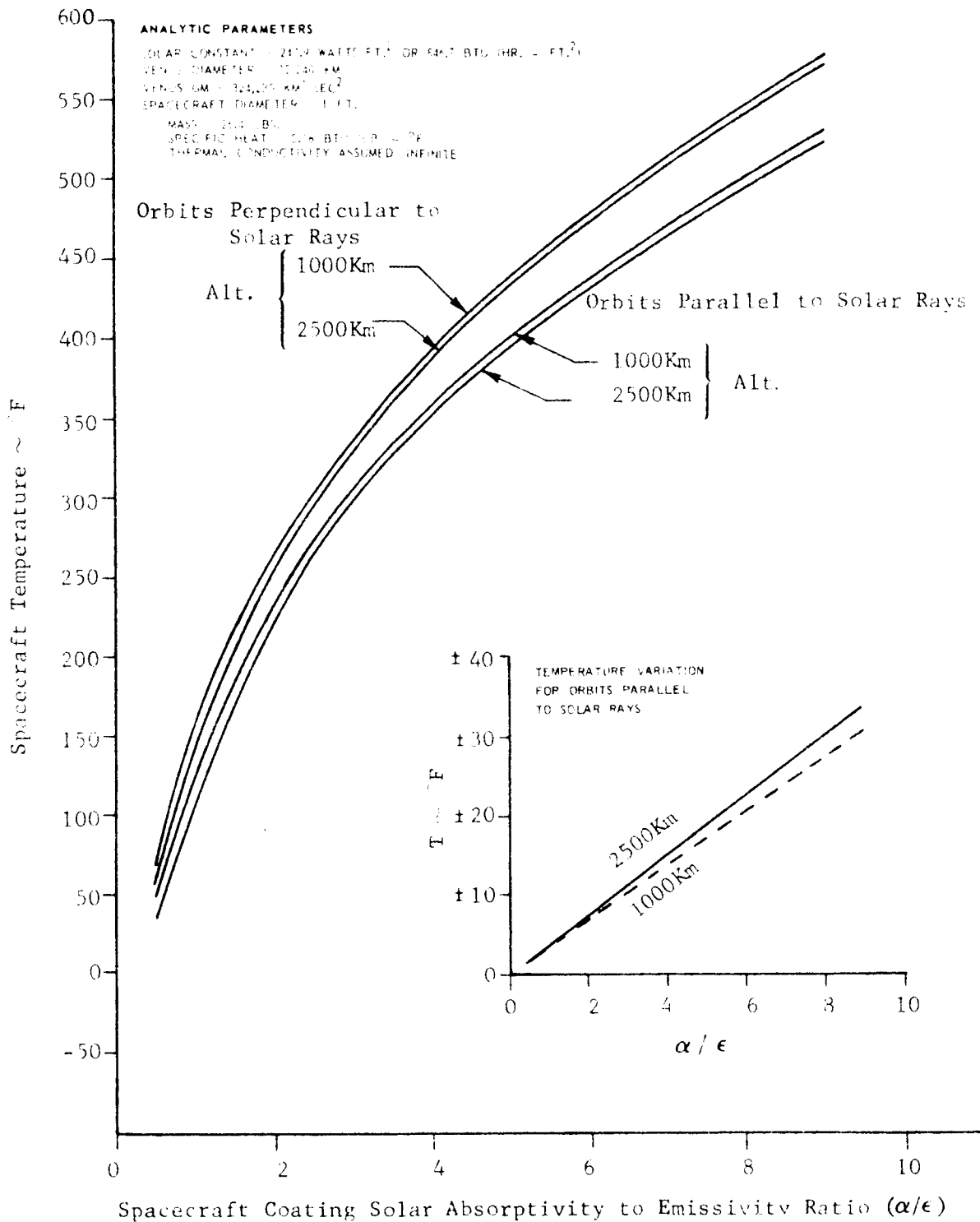


FIGURE II-20 MEAN TEMPERATURE OF A SPHERICAL SATELLITE IN VENUS CIRCULAR POLAR ORBITS INCLUDING THE EFFECTS OF PLANETARY RADIATION AND AN ALBEDO OF 0.59, FOR A SPACECRAFT EMISSIVITY OF 0.1.

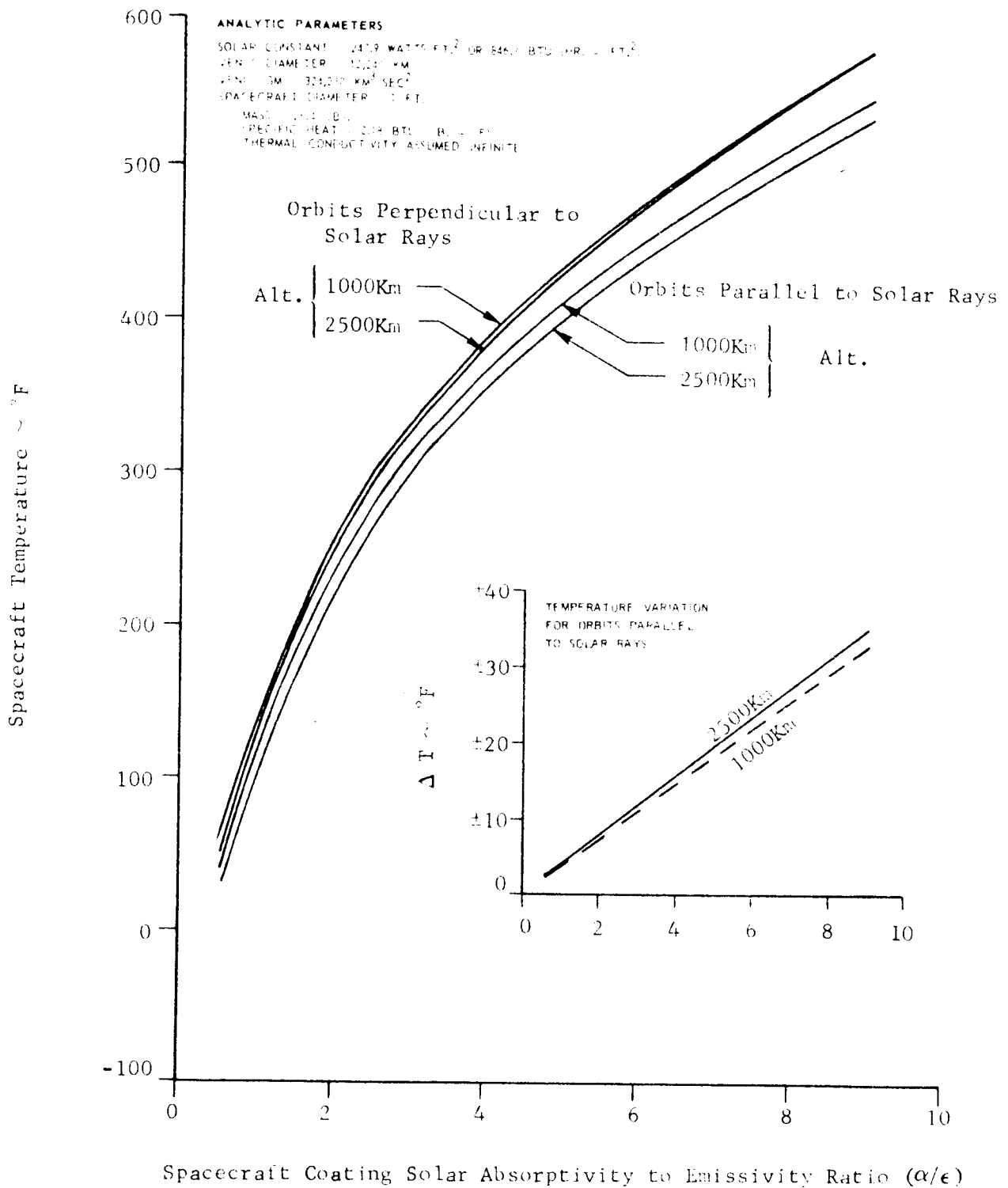


FIGURE II-21 MEAN TEMPERATURE OF A SPHERICAL SATELLITE IN VENUS CIRCULAR POLAR ORBITS INCLUDING THE EFFECTS OF PLANETARY RADIATION AND AN ALBEDO OF 0.77, FOR A SPACECRAFT EMISSIVITY OF 0.1.

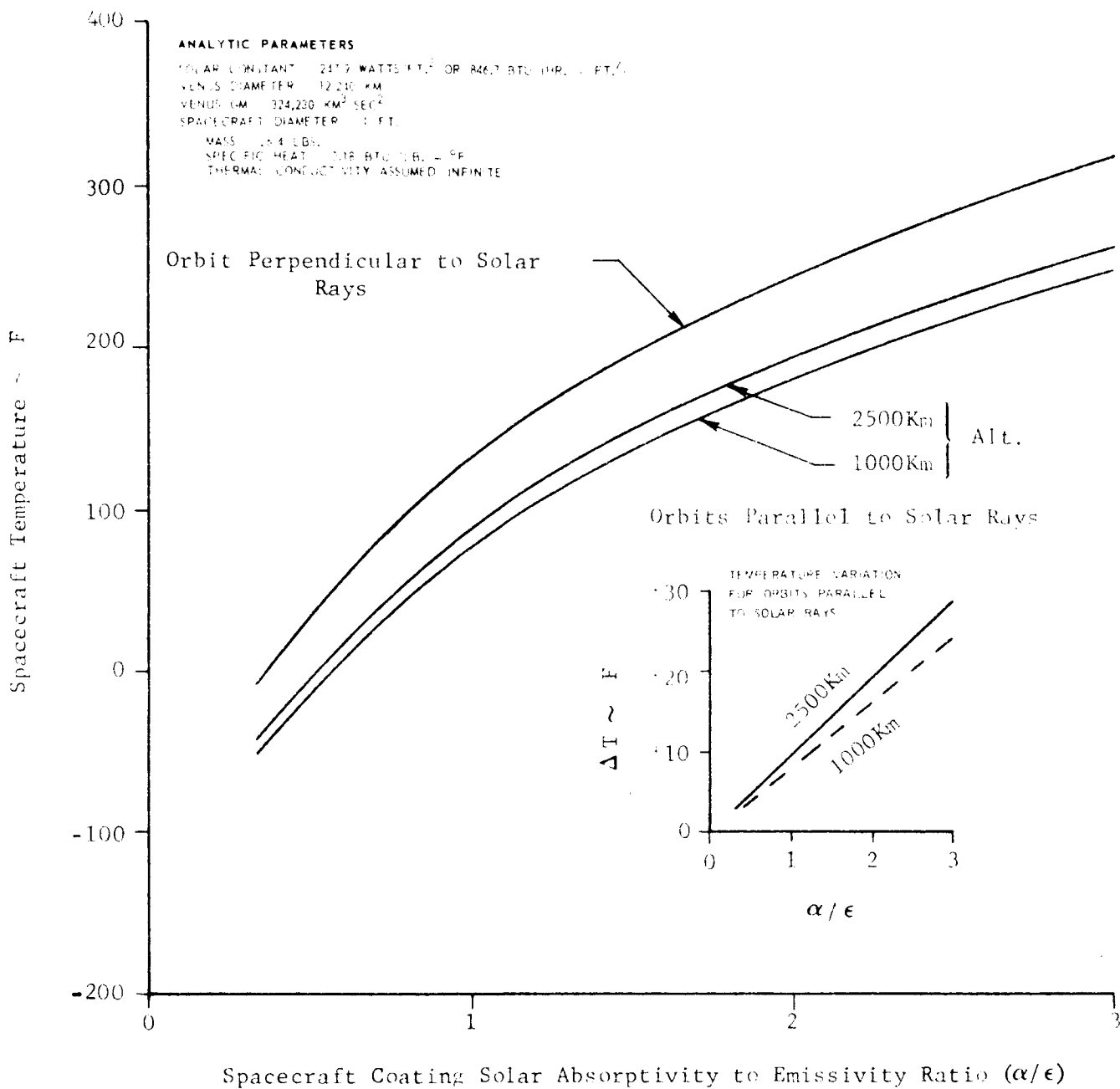


FIGURE II-22 MEAN TEMPERATURE OF A SPHERICAL SATELLITE IN VENUS CIRCULAR POLAR ORBITS NEGLECTING PLANETARY RADIATION AND ALBEDO EFFECTS FOR A SPACECRAFT EMISSIVITY OF 0.3.

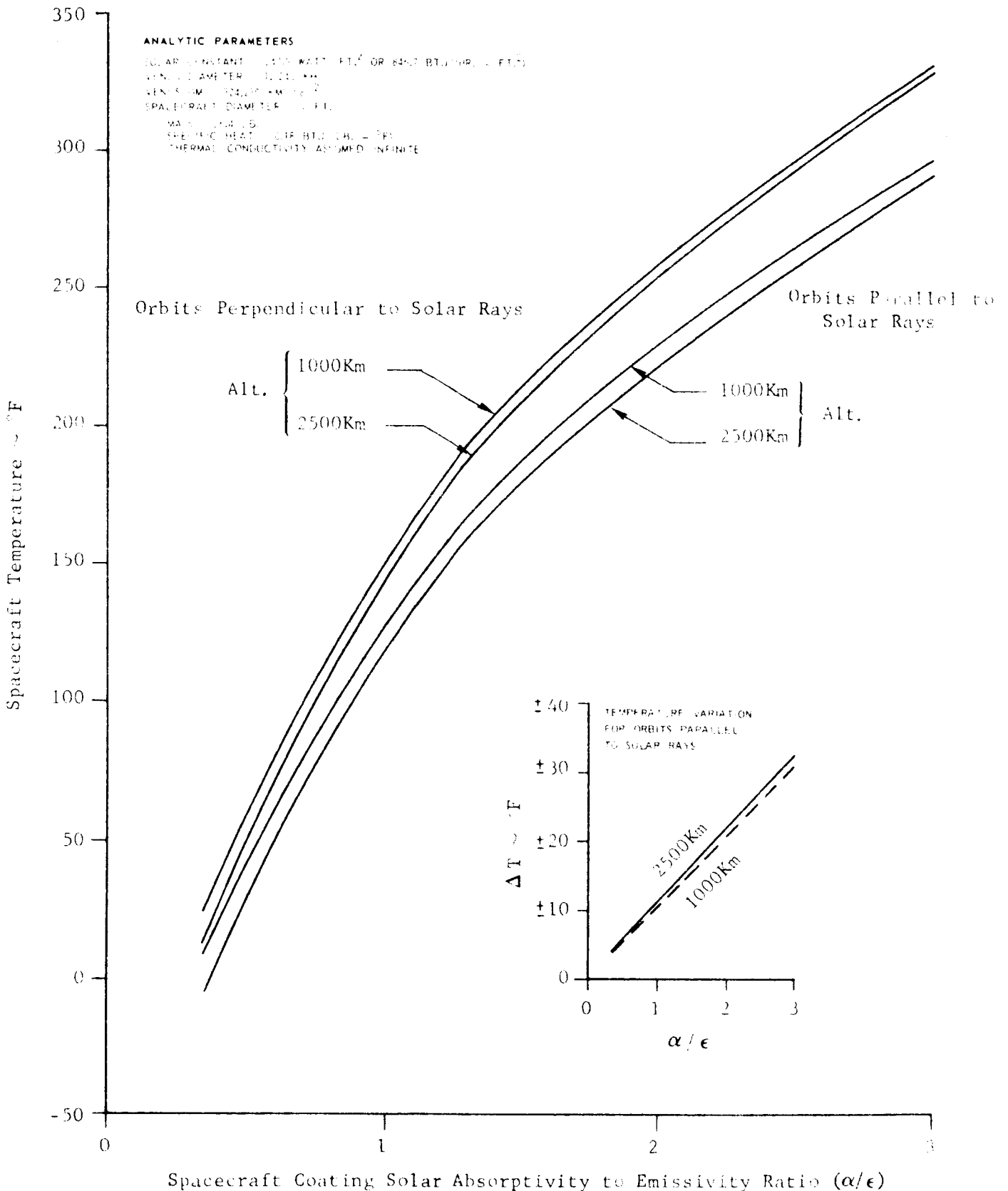


FIGURE II-23 MEAN TEMPERATURE OF A SPHERICAL SATELLITE IN VENUS CIRCULAR POLAR ORBITS INCLUDING THE EFFECTS OF PLANETARY RADIATION AND AN ALBEDO OF 0.59, FOR A SPACECRAFT EMISSIVITY OF 0.3.

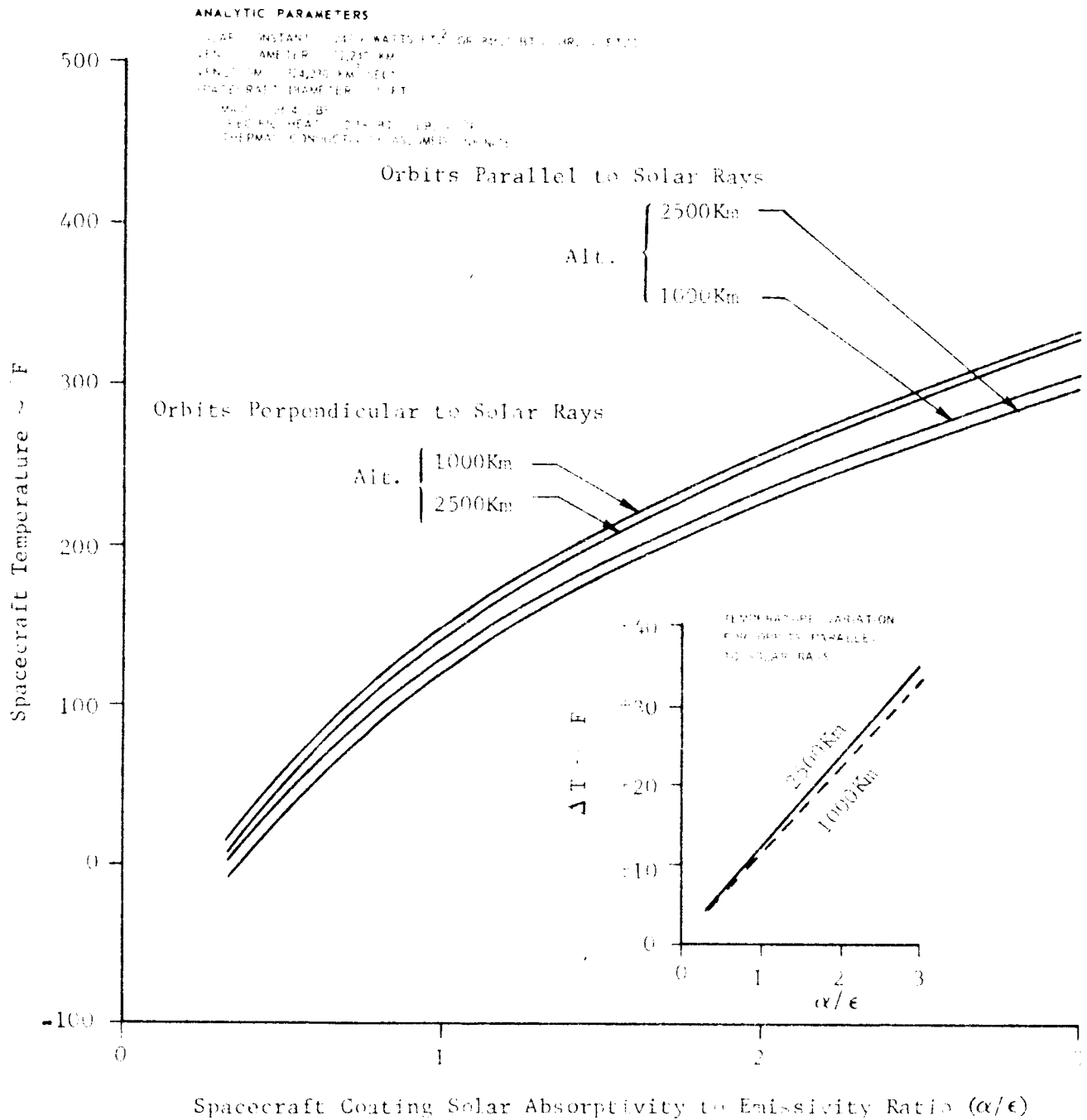


FIGURE II-24 MEAN TEMPERATURE OF A SPHERICAL SATELLITE IN VENUS CIRCULAR POLAR ORBITS INCLUDING THE EFFECTS OF PLANETARY RADIATION AND AN ALBEDO OF 0.77, FOR A SPACECRAFT EMISSIVITY OF 0.3.

ANALYTIC PARAMETERS

SOLAR CONSTANT = 2400 WATTS/FT.² OR 846.7 BTU (HR. - FT.²)
 VENUS DIAMETER = 7,680 KM
 VENUS GM = 125,230 KM³/SEC.²
 SPACECRAFT DIAMETER = 1 FT.

MASS = 200 LBS.
 SPECIFIC HEAT = 0.18 BTU (LBS. - °F)
 THERMAL CONDUCTIVITY ASSUMED INFINITE

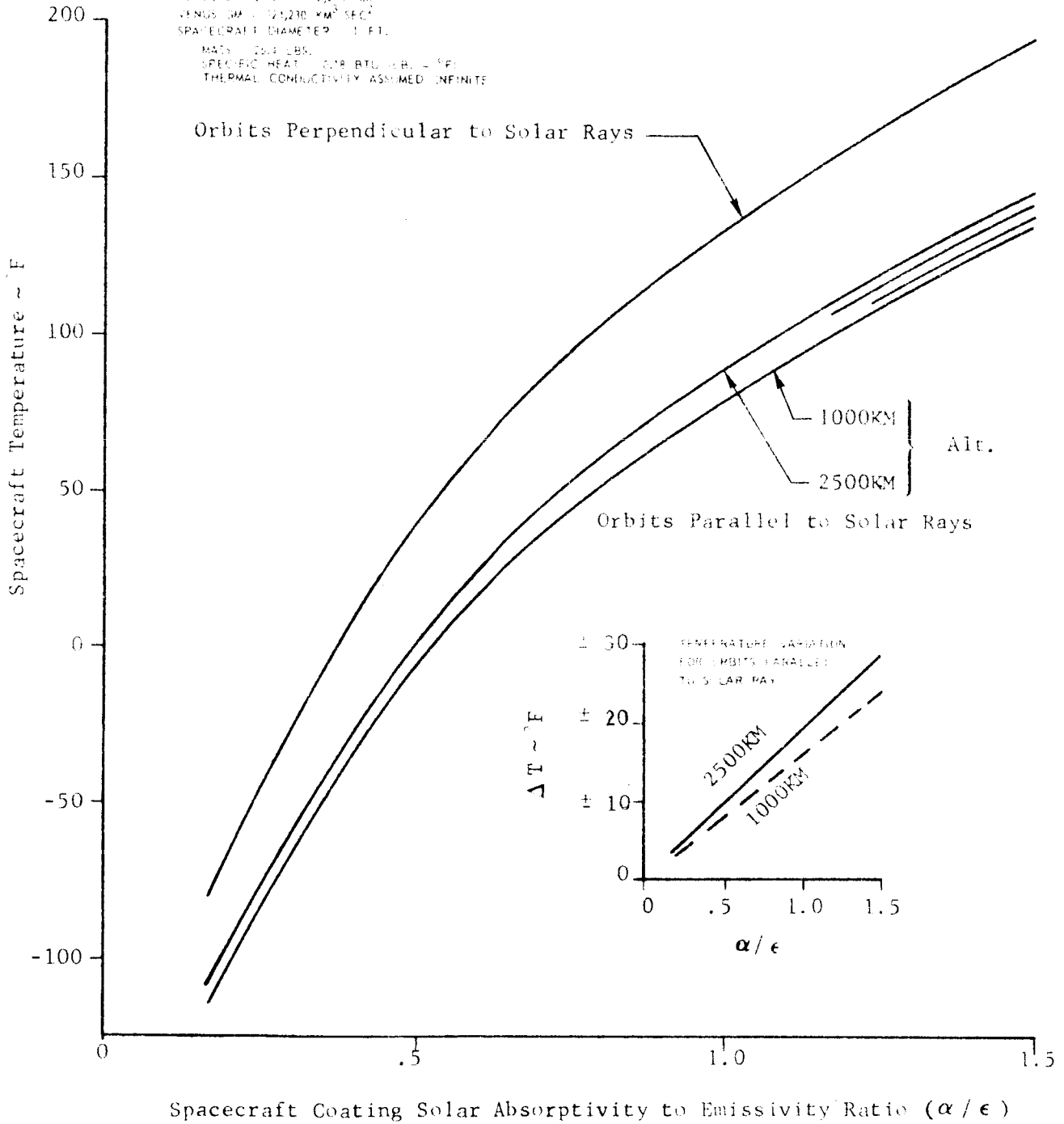


FIGURE II-25 MEAN TEMPERATURE OF A SPHERICAL SATELLITE IN VENUS CIRCULAR POLAR ORBITS NEGLECTING PLANETARY RADIATION AND ALBEDO EFFECTS FOR A SPACECRAFT EMISSIVITY OF 0.6.

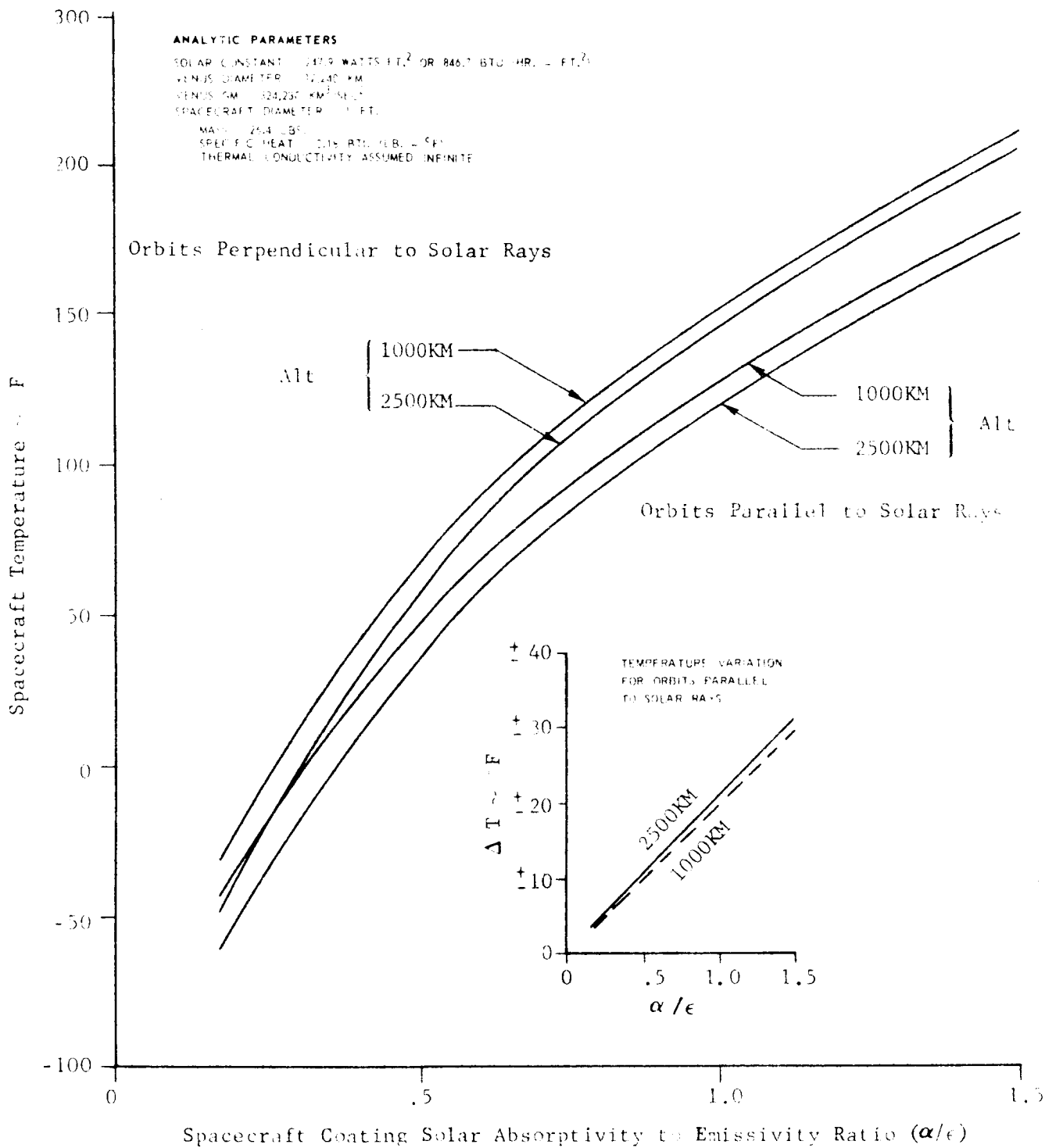


FIGURE II-26 MEAN TEMPERATURE OF A SPHERICAL SATELLITE IN VENUS CIRCULAR POLAR ORBITS INCLUDING THE EFFECTS OF PLANETARY RADIATION AND AN ALBEDO OF 0.59, FOR A SPACECRAFT EMISSIVITY OF 0.6.

ANALYTIC PARAMETERS

SOLAR CONSTANT = 247.9 WATTS/FT.² OR 916.7 BTU/HR. - FT.²
 VENUS DIAMETER = 12,240 KM
 VENUS GM = 324,030 KM²/SEC.²
 SPACECRAFT DIAMETER = 1 FT.

MASS = 254 LBS.
 SPECIFIC HEAT = 0.76 BTU/LB. - °F
 THERMAL CONDUCTIVITY ASSUMED INFINITE

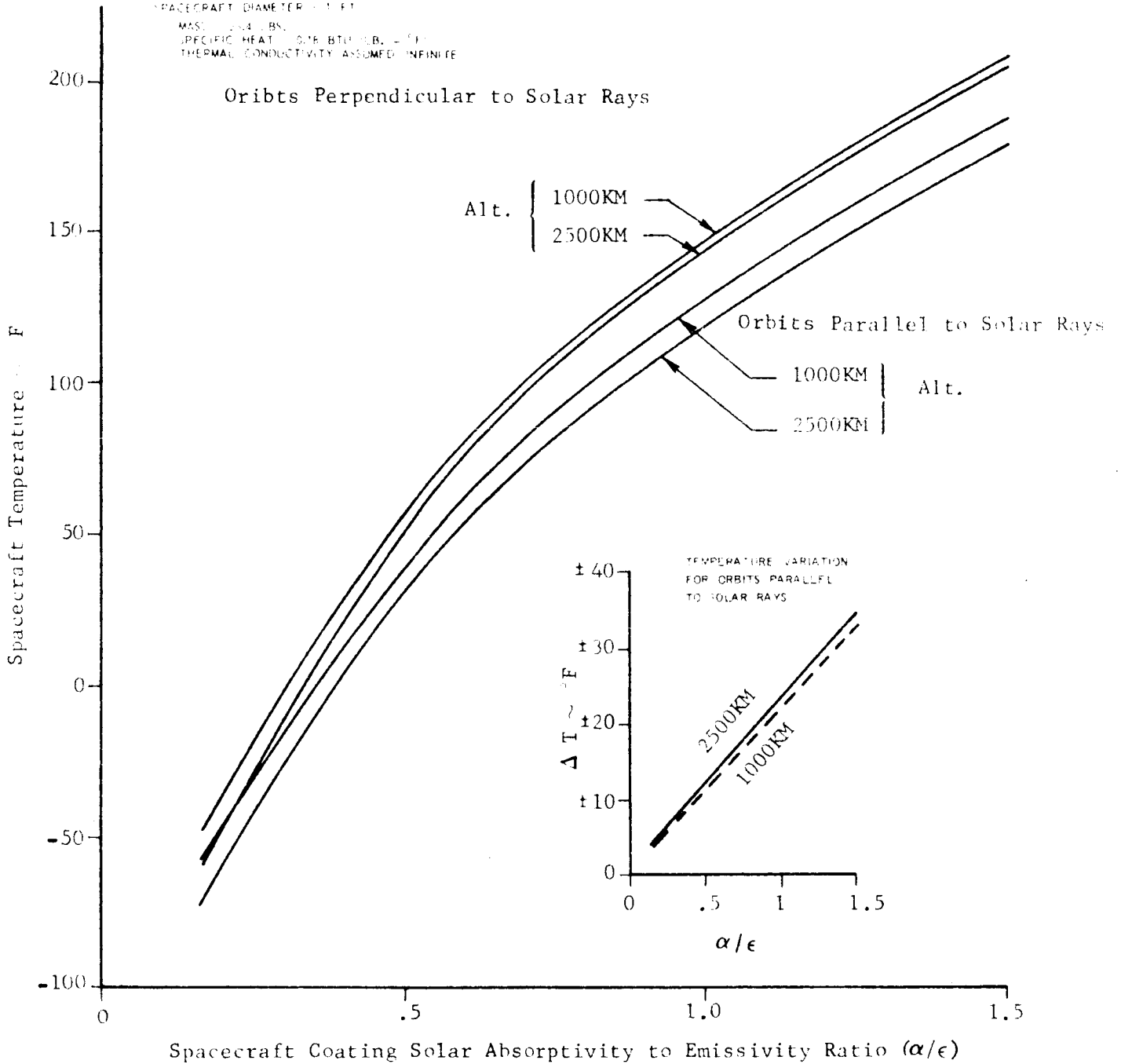


FIGURE II-27 MEAN TEMPERATURE OF A SPHERICAL SATELLITE IN VENUS CIRCULAR POLAR ORBITS INCLUDING THE EFFECTS OF PLANETARY RADIATION AND AN ALBEDO OF 0.77, FOR A SPACECRAFT EMISSIVITY OF 0.6.

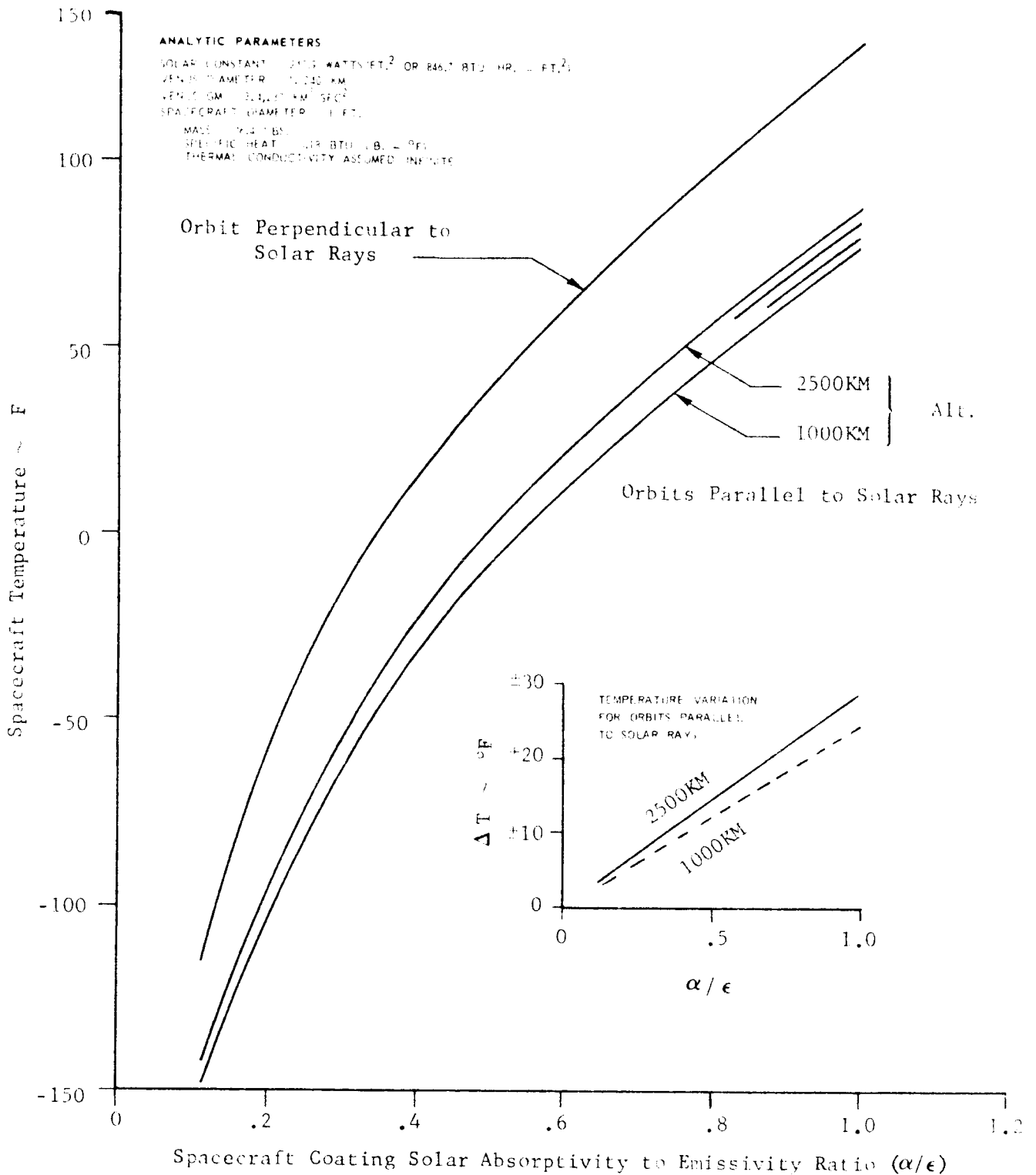


FIGURE II-28 MEAN TEMPERATURE OF A SPHERICAL SATELLITE IN VENUS CIRCULAR POLAR ORBITS NEGLECTING PLANETARY RADIATION AND ALBEDO EFFECTS FOR A SPACECRAFT EMISSIVITY OF 0.9.

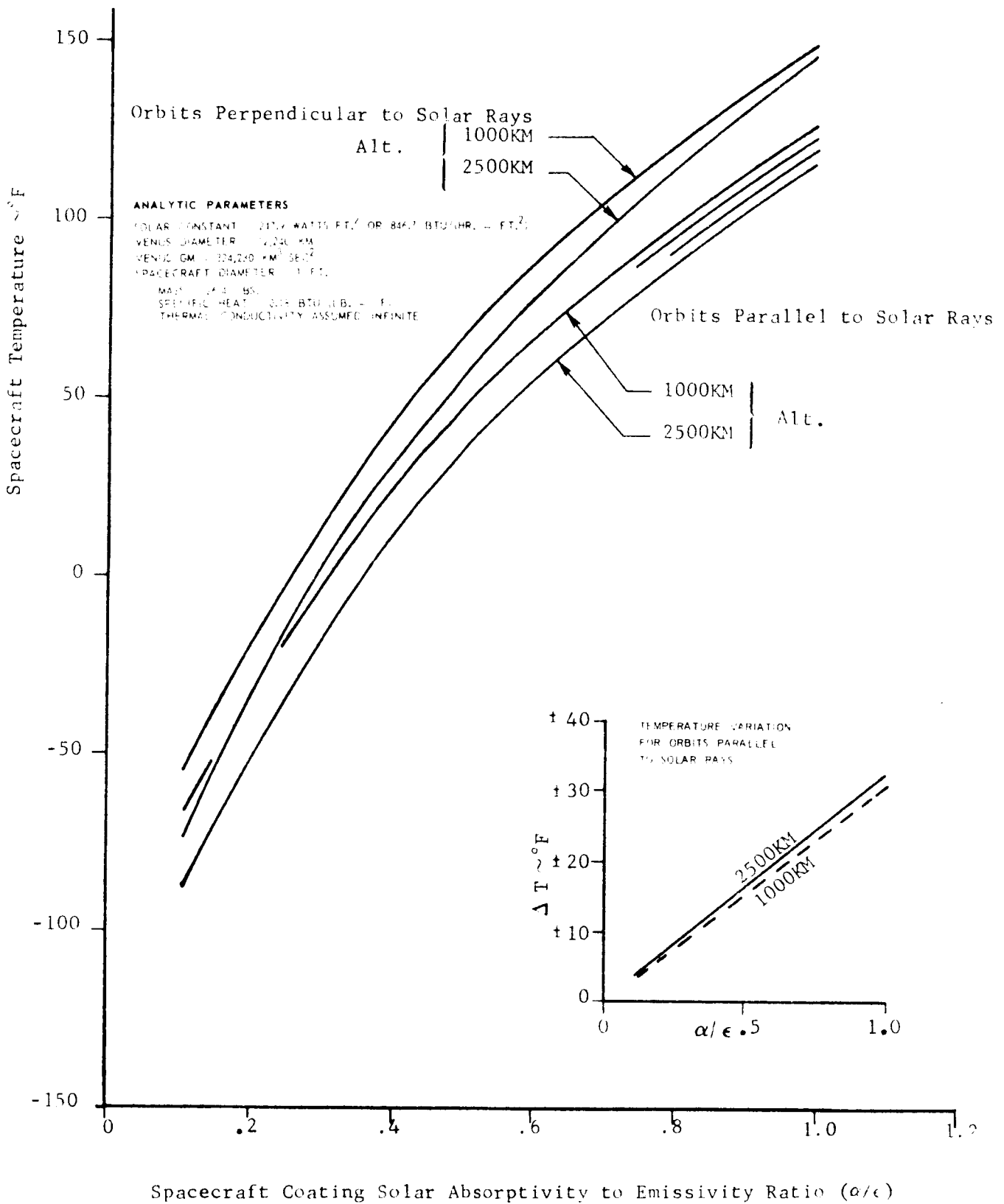
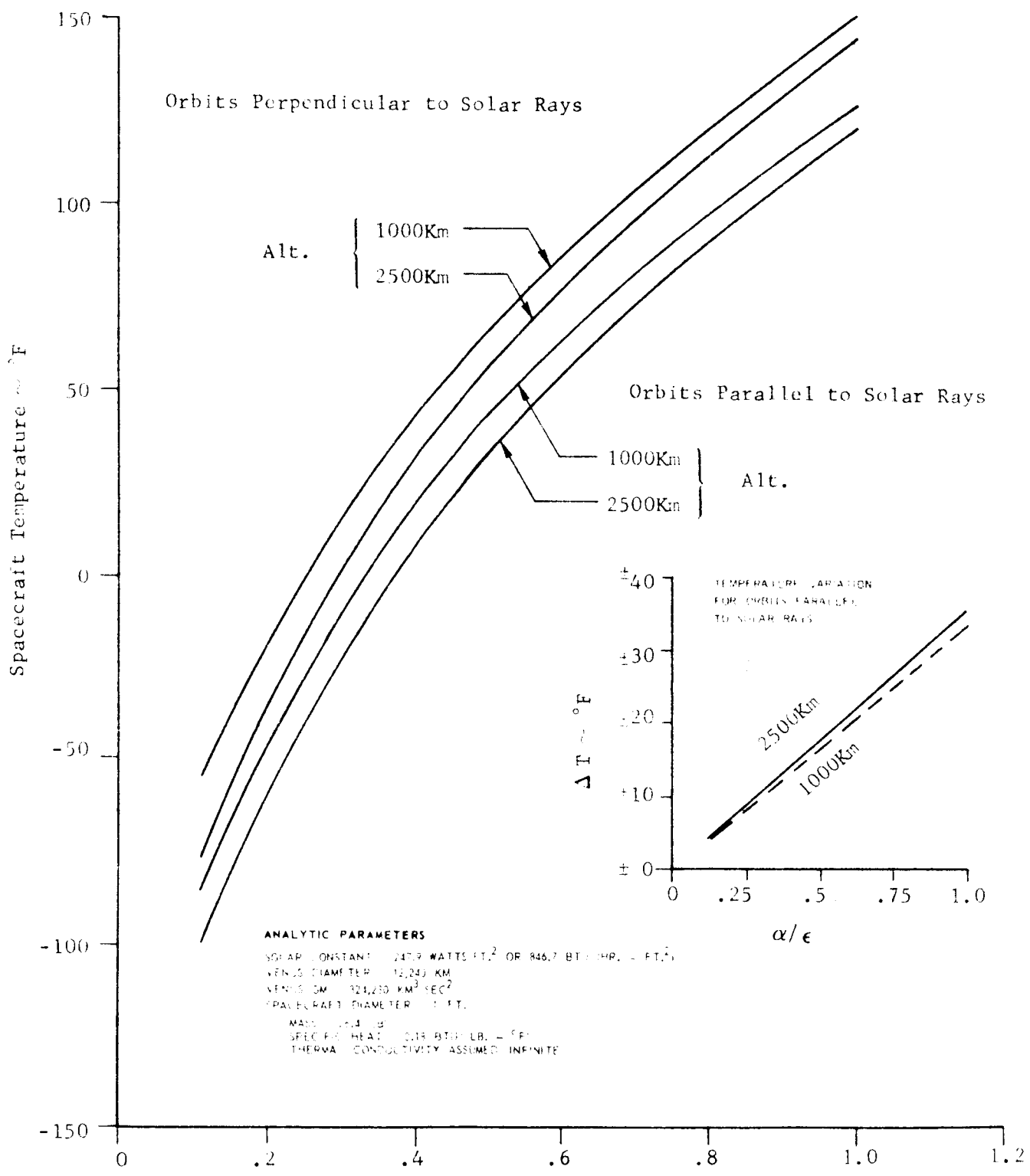


FIGURE II-29 MEAN TEMPERATURE OF A SPHERICAL SATELLITE IN VENUS CIRCULAR POLAR ORBITS INCLUDING THE EFFECTS OF PLANETARY RADIATION AND AN ALBEDO OF 0.59, FOR A SPACECRAFT EMISSIVITY OF 0.9.



Spacecraft Coating Solar Absorptivity to Emissivity Ratio (α/ϵ)

FIGURE II-30 MEAN TEMPERATURE OF A SPHERICAL SATELLITE IN VENUS CIRCULAR POLAR ORBITS INCLUDING THE EFFECTS OF PLANETARY RADIATION AND AN ALBEDO OF 0.77, FOR A SPACECRAFT EMISSIVITY OF 0.9.

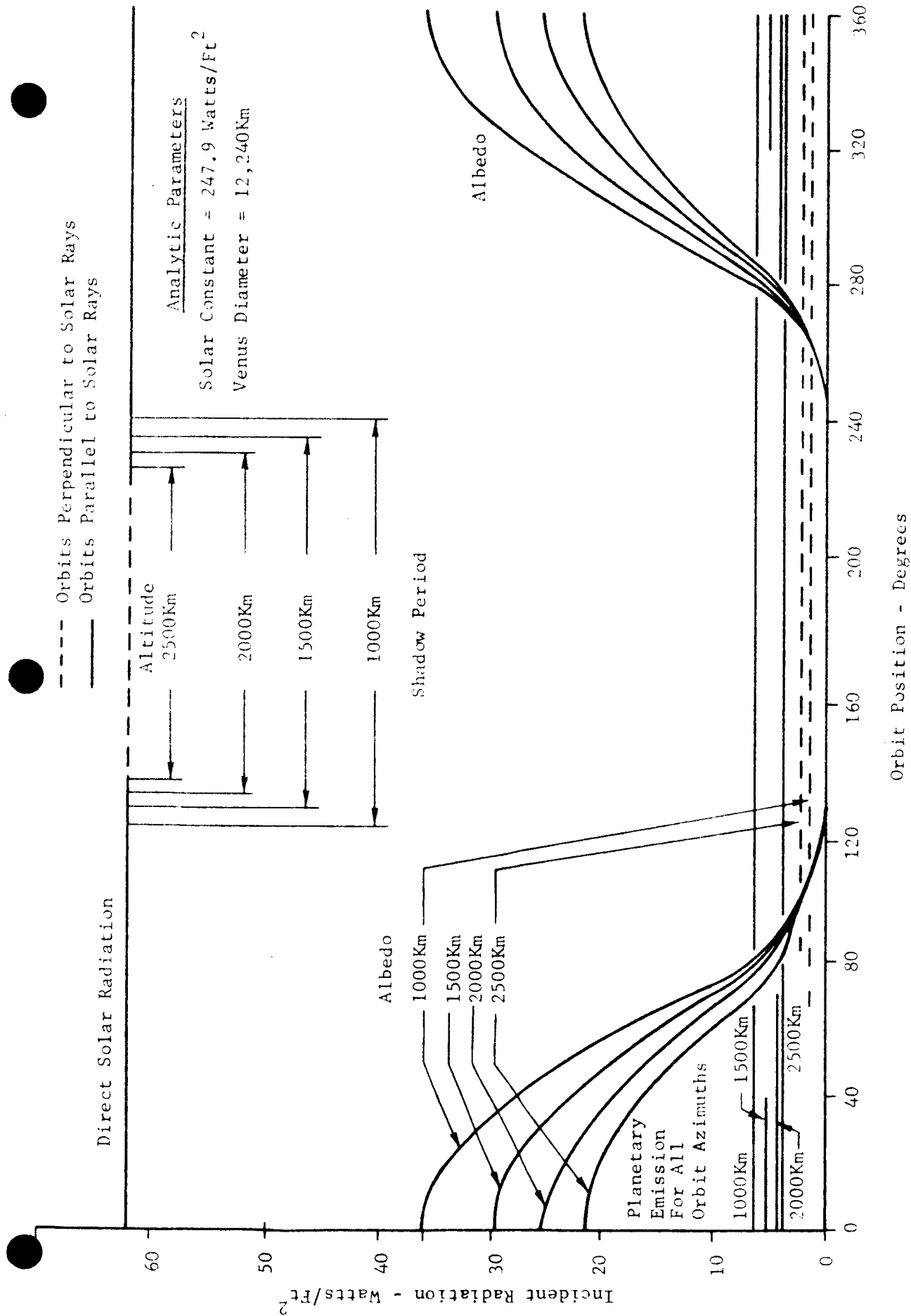


FIGURE II-31 AVERAGE INCIDENT RADIATION PER SQUARE FOOT OF SURFACE AREA ON A 1 FOOT DIAMETER SPHERE IN CIRCULAR POLAR ORBITS AROUND VENUS WITH AN ALBEDO OF 0.59.

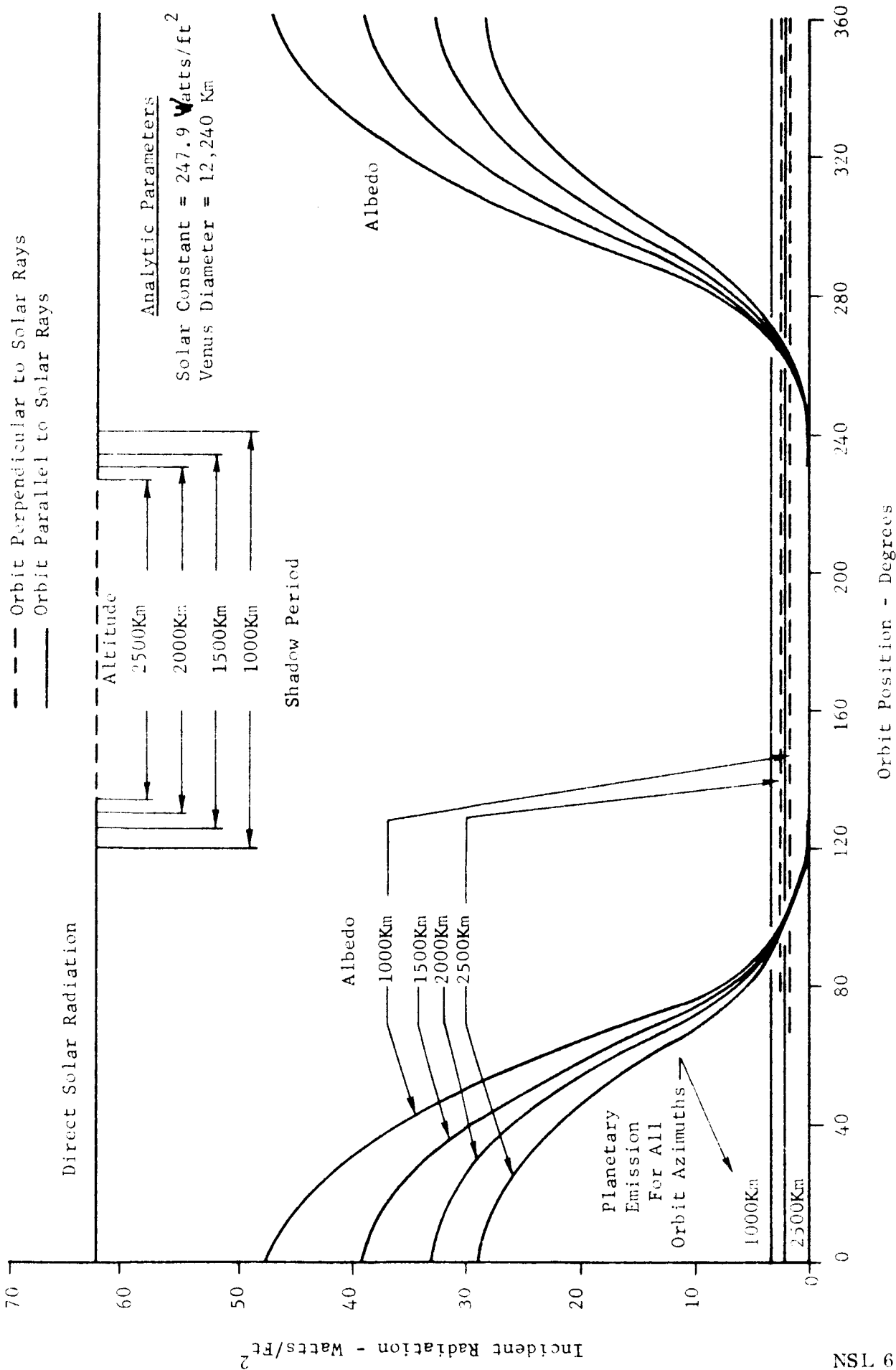
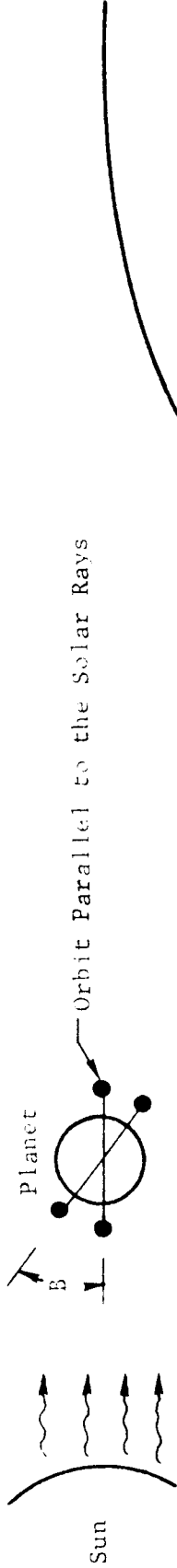


FIGURE II-32 AVERAGE INCIDENT RADIATION PER SQUARE FOOT OF SURFACE AREA ON A 1 FOOT DIAMETER SPHERE IN CIRCULAR POLAR ORBITS AROUND VENUS WITH AN ALBEDO OF 0.77.

Azimuth Angle B = Angle of Polar Orbit Plane from the Orbit Parallel to Solar Rays
 Rays Toward the Orbit Perpendicular to Solar Rays



T = Spacecraft Mean Temperature

T_{11} = Spacecraft Mean Temperature in Orbit Parallel to Solar Rays

T_{\perp} = Spacecraft Mean Temperature in Orbit Perpendicular
 Solar Rays

The Approximate Spacecraft Mean Temperature at any
 Polar Orbit Angle B may be calculated from:

$$T = T_{11} + (T_{\perp} - T_{11}) \times C.F.$$

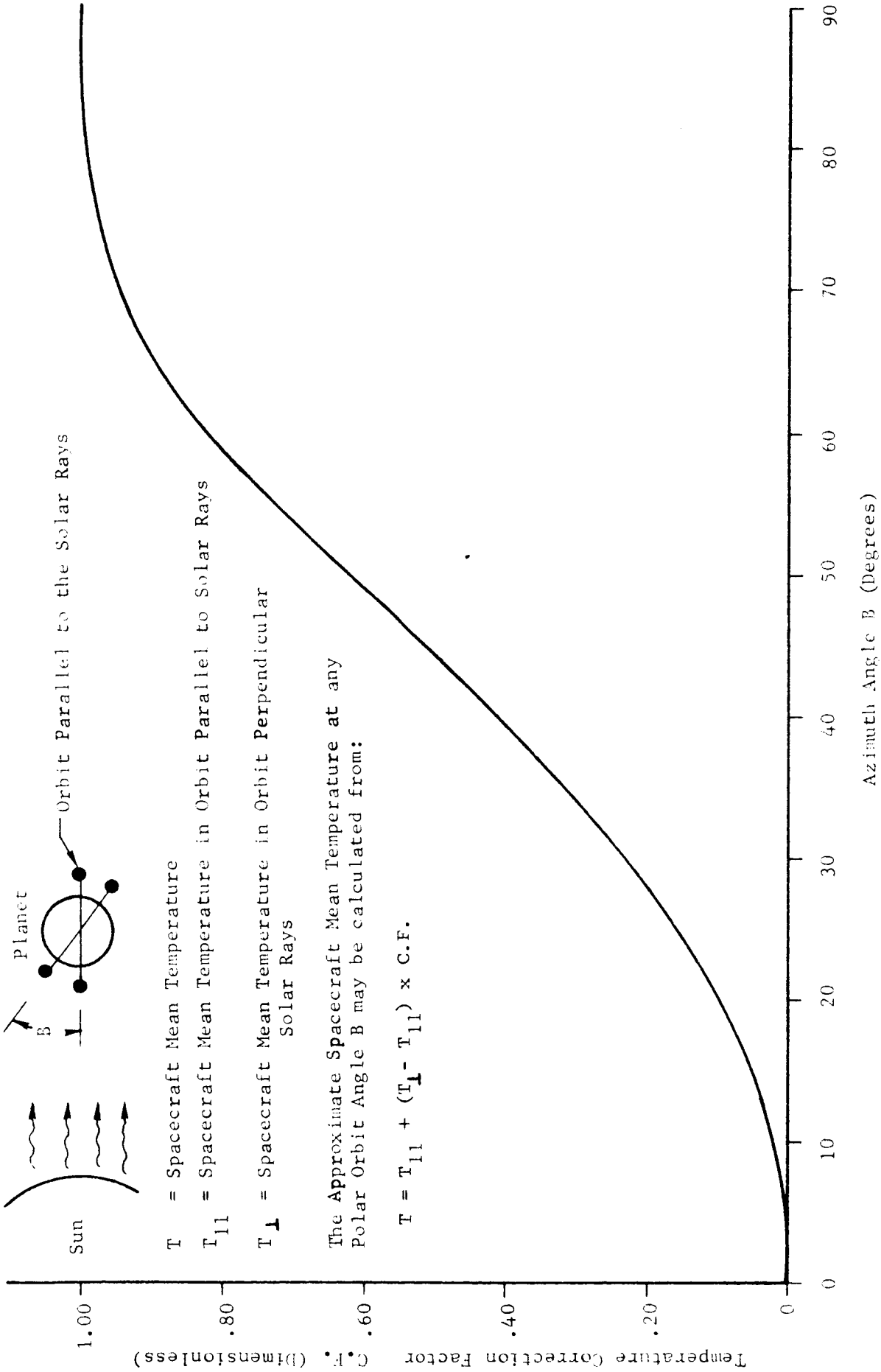


FIGURE II-33 - SPHERICAL SATELLITE TEMPERATURE DETERMINATION FOR
 CIRCULAR POLAR ORBITS AS A FUNCTION OF AZIMUTH ANGLE

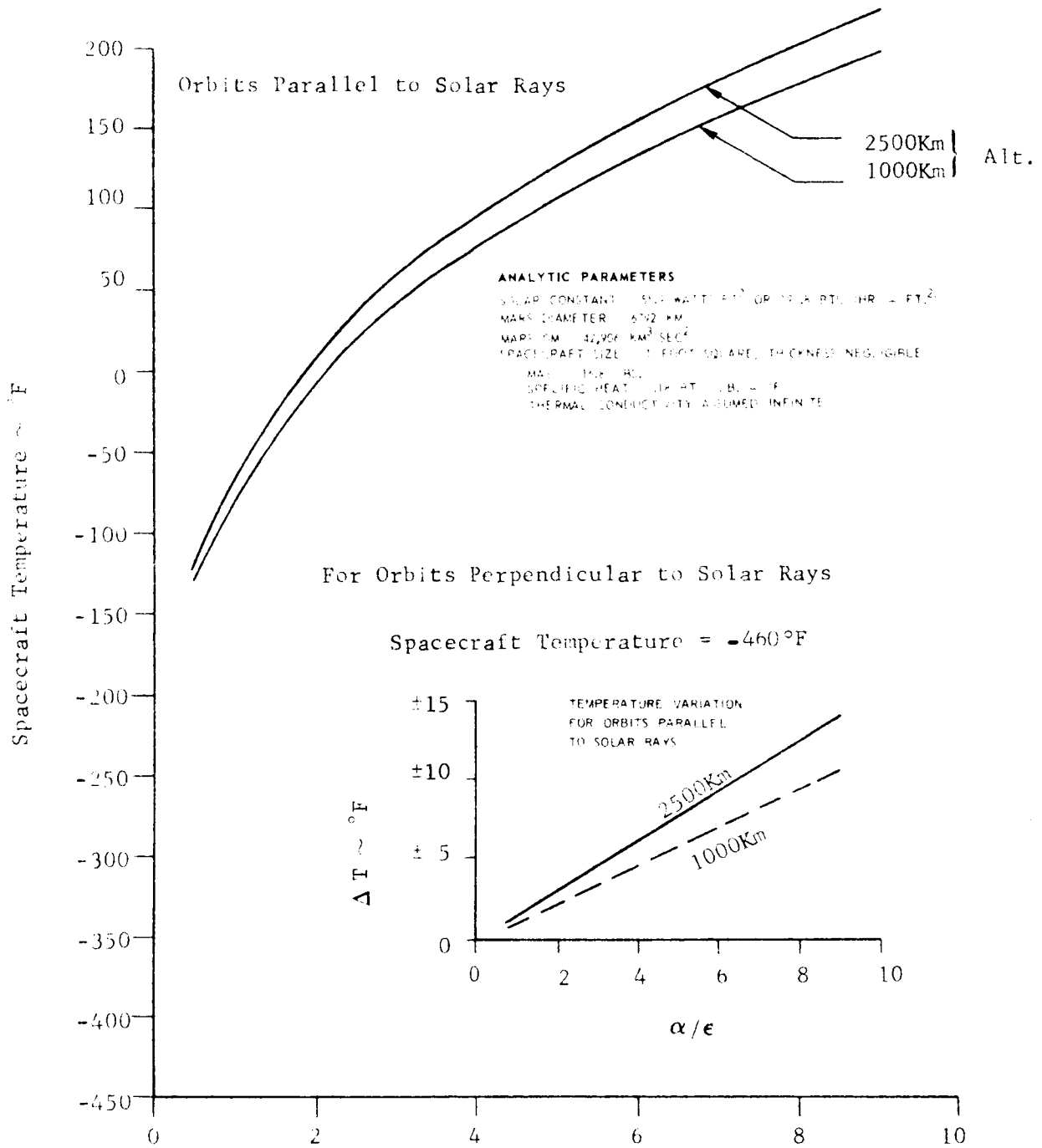
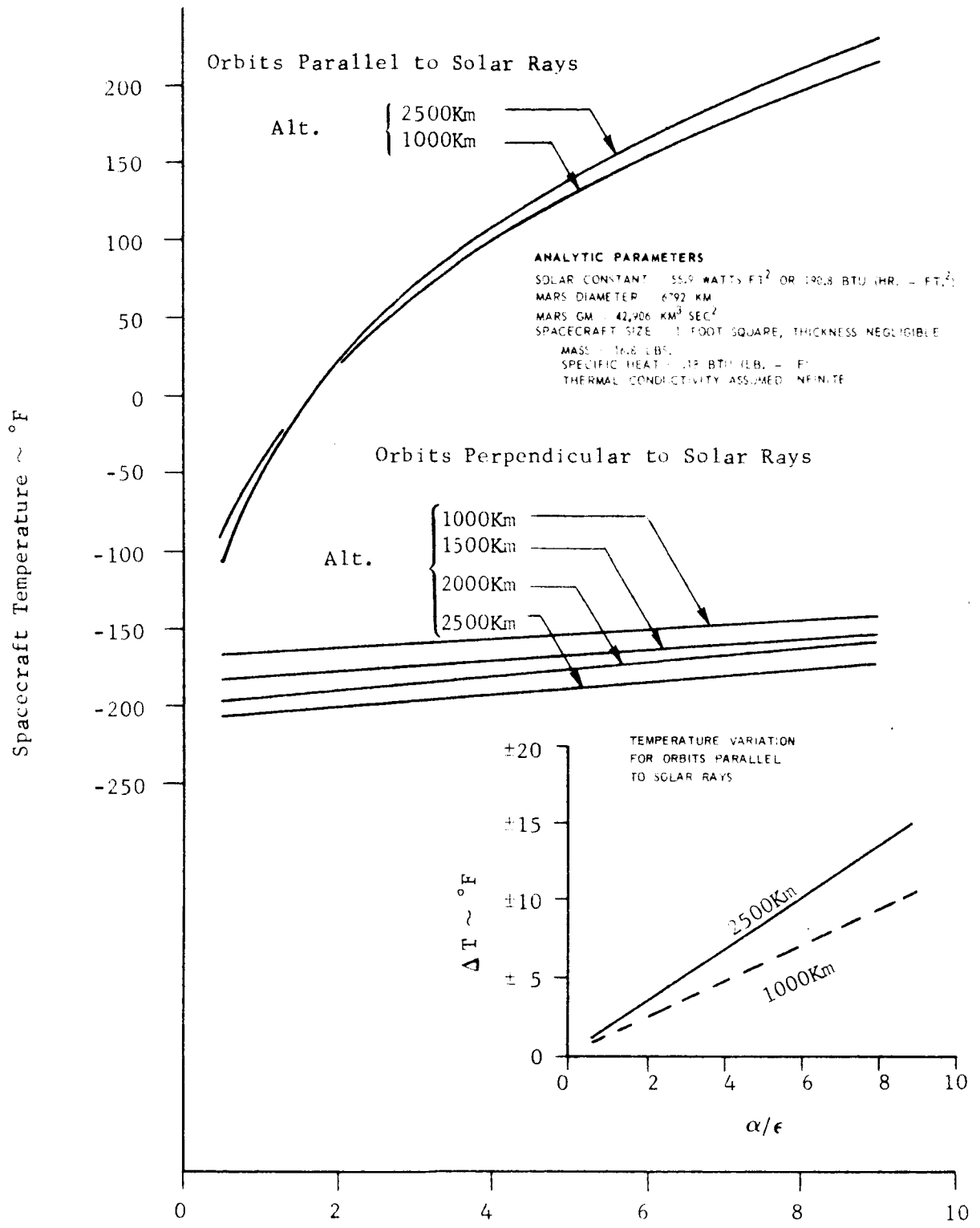


FIGURE II-34 MEAN TEMPERATURE OF A PLANETARY ORIENTED FLAT PLATE SATELLITE IN MARS CIRCULAR POLAR ORBITS NEGLECTING PLANETARY RADIATION AND ALBEDO EFFECTS, FOR A SPACECRAFT EMISSIVITY OF 0.1.



Spacecraft Coating Solar Absorptivity to Emissivity Ratio (α/ϵ)

FIGURE II-35 MEAN TEMPERATURE OF A PLANETARY ORIENTED FLAT PLATE SATELLITE IN MARS CIRCULAR POLAR ORBITS INCLUDING THE EFFECTS OF PLANETARY RADIATION AND AN ALBEDO OF 0.148, FOR A SPACECRAFT EMISSIVITY OF 0.1.

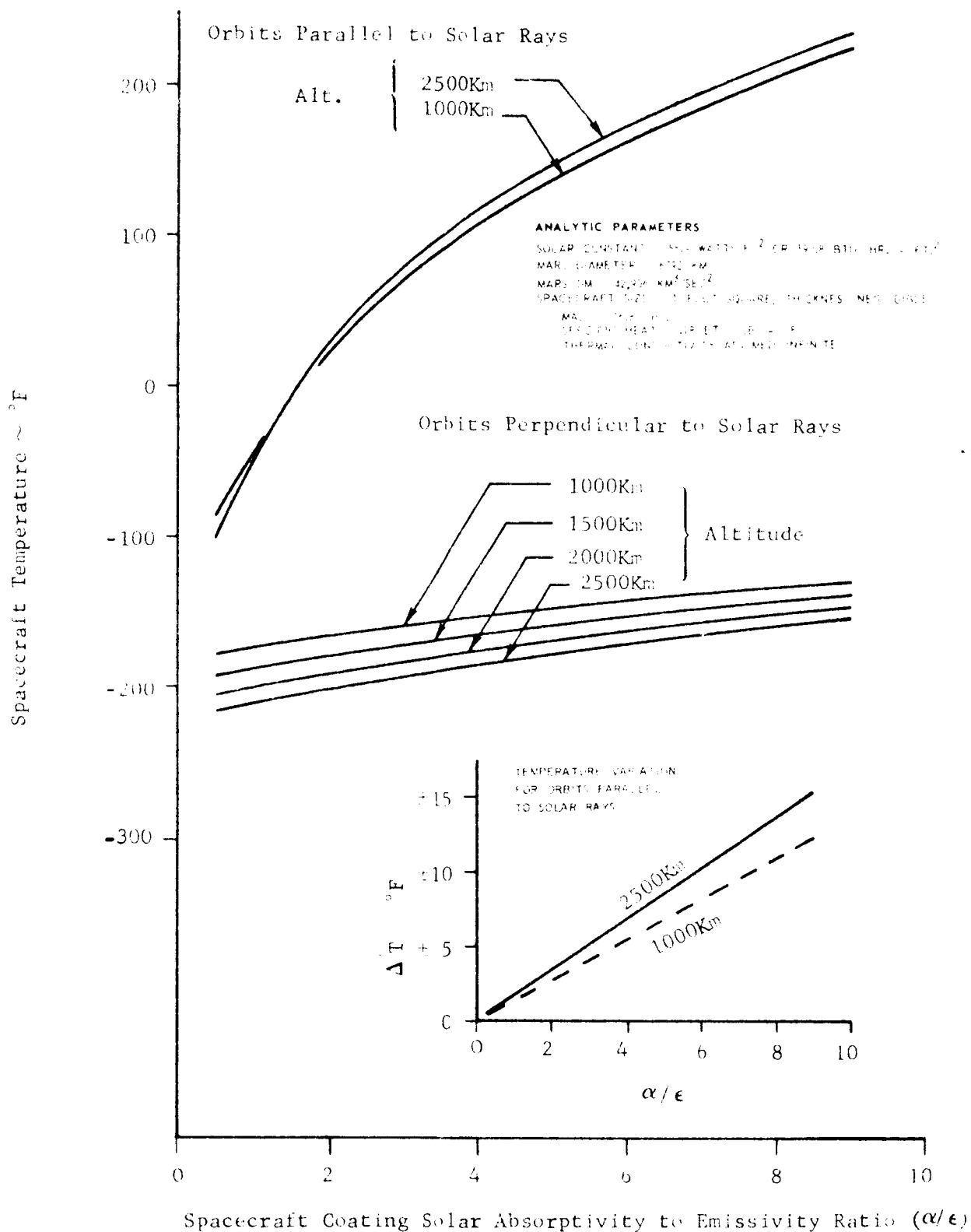


FIGURE II-36 MEAN TEMPERATURE OF A PLANETARY ORIENTED FLAT PLATE SATELLITE IN MARS CIRCULAR POLAR ORBITS INCLUDING THE EFFECTS OF PLANETARY RADIATION AND AN ALBEDO OF 0.295, FOR A SPACECRAFT EMISSIVITY OF 0.1.

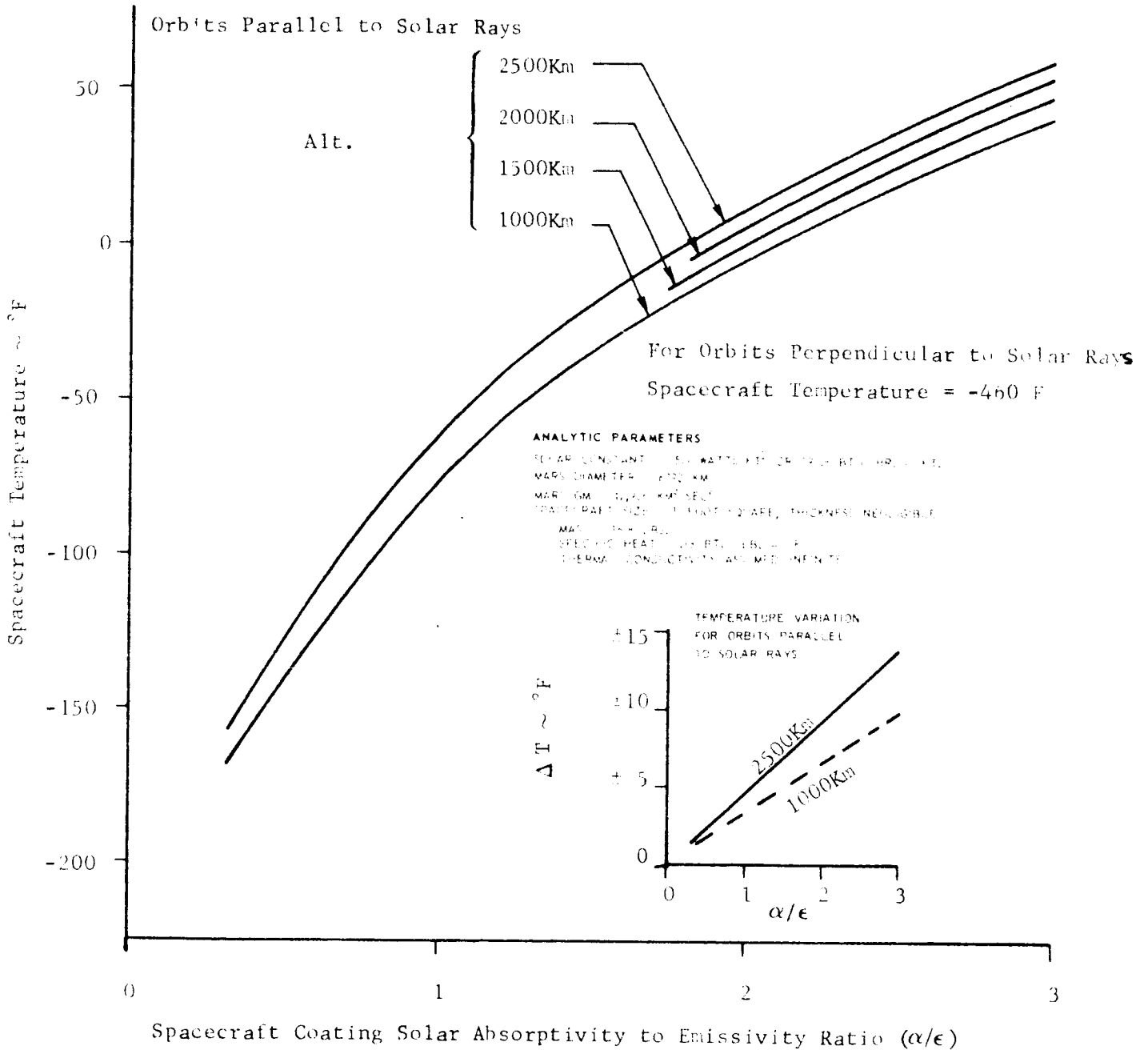


FIGURE II-37 MEAN TEMPERATURE OF A PLANETARY ORIENTED FLAT PLATE SATELLITE IN MARS CIRCULAR POLAR ORBITS NEGLECTING PLANETARY RADIATION AND ALBEDO EFFECTS, FOR A SPACECRAFT EMISSIVITY OF 0.3.

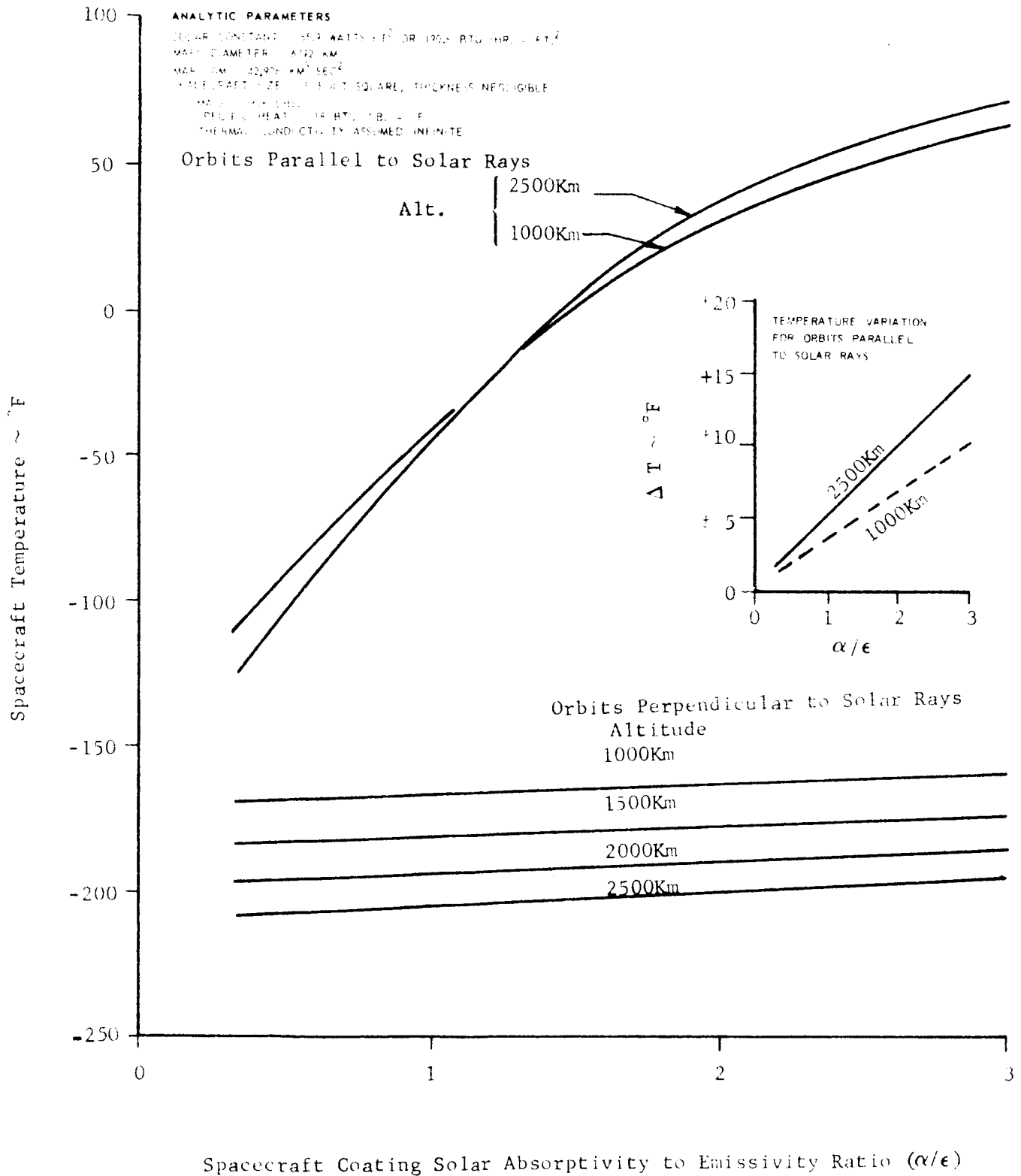
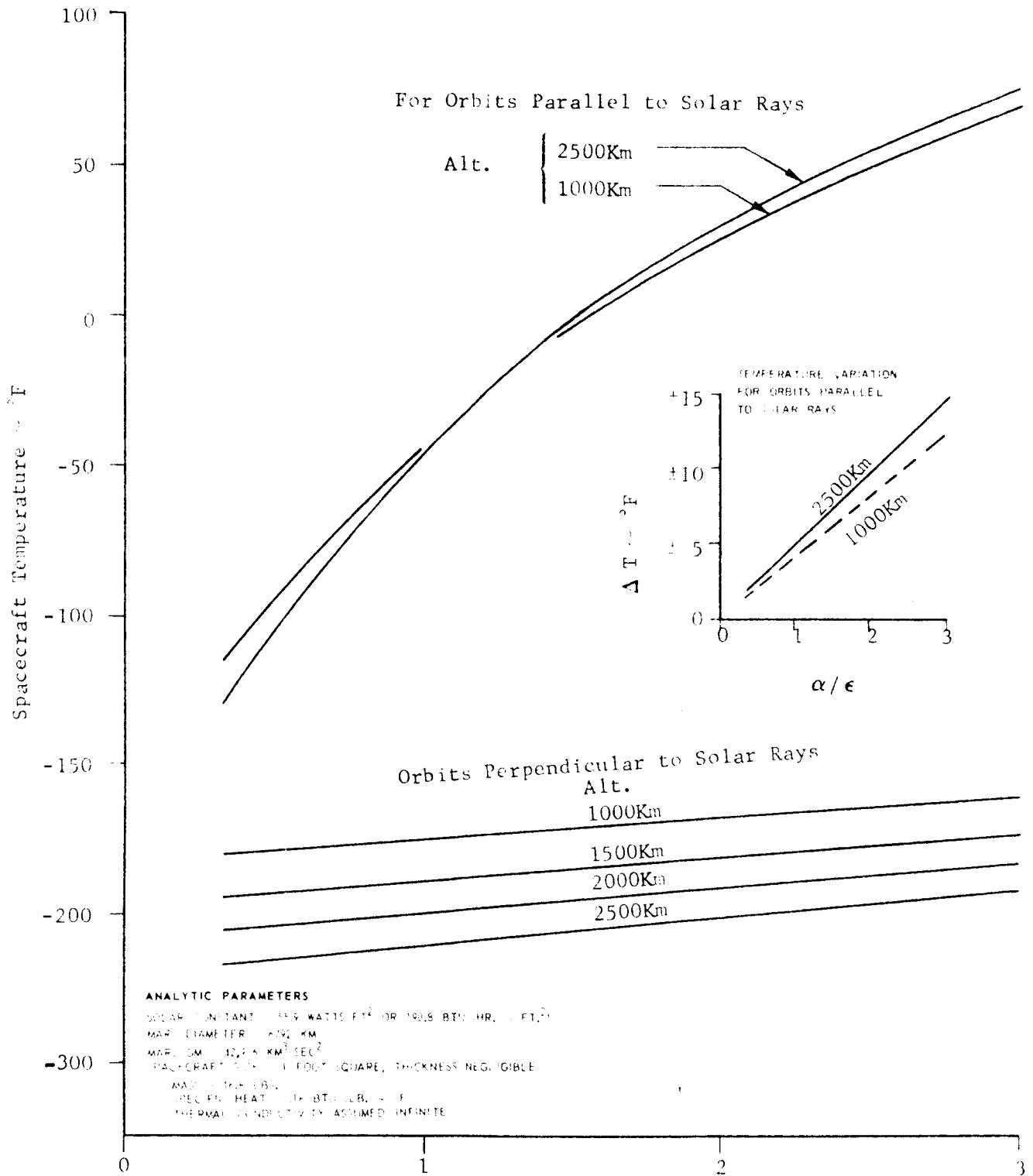


FIGURE II-38 MEAN TEMPERATURE OF A PLANETARY ORIENTED FLAT PLATE SATELLITE IN MARS CIRCULAR POLAR ORBITS INCLUDING THE EFFECTS OF PLANETARY RADIATION AND AN ALBEDO OF 0.148, FOR A SPACECRAFT EMISSIVITY OF 0.3.



Spacecraft Coating Solar Absorptivity to Emissivity Ratio (α/ϵ)

FIGURE II-39 MEAN TEMPERATURE OF A PLANETARY ORIENTED FLAT PLATE SATELLITE IN MARS CIRCULAR POLAR ORBITS INCLUDING THE EFFECTS OF PLANETARY RADIATION AND AN ALBEDO OF 0.295, FOR A SPACECRAFT EMISSIVITY OF 0.3.

ANALYTIC PARAMETERS

SOLAR CONSTANT = 593 WATT/FT² OR 190.8 BTU/HR. - FT.²
 MARS DIAMETER = 6792 KM
 MARS GM = 12,296 KM³ SEC⁻²
 SPACECRAFT SIZE = 1 FOOT SQUARE, THICKNESS NEGLECTIBLE
 MASS = 100 LBS.
 SPECIFIC HEAT = 0.18 BTU/LB. - F.
 THERMAL CONDUCTIVITY ASSUMED INFINITE

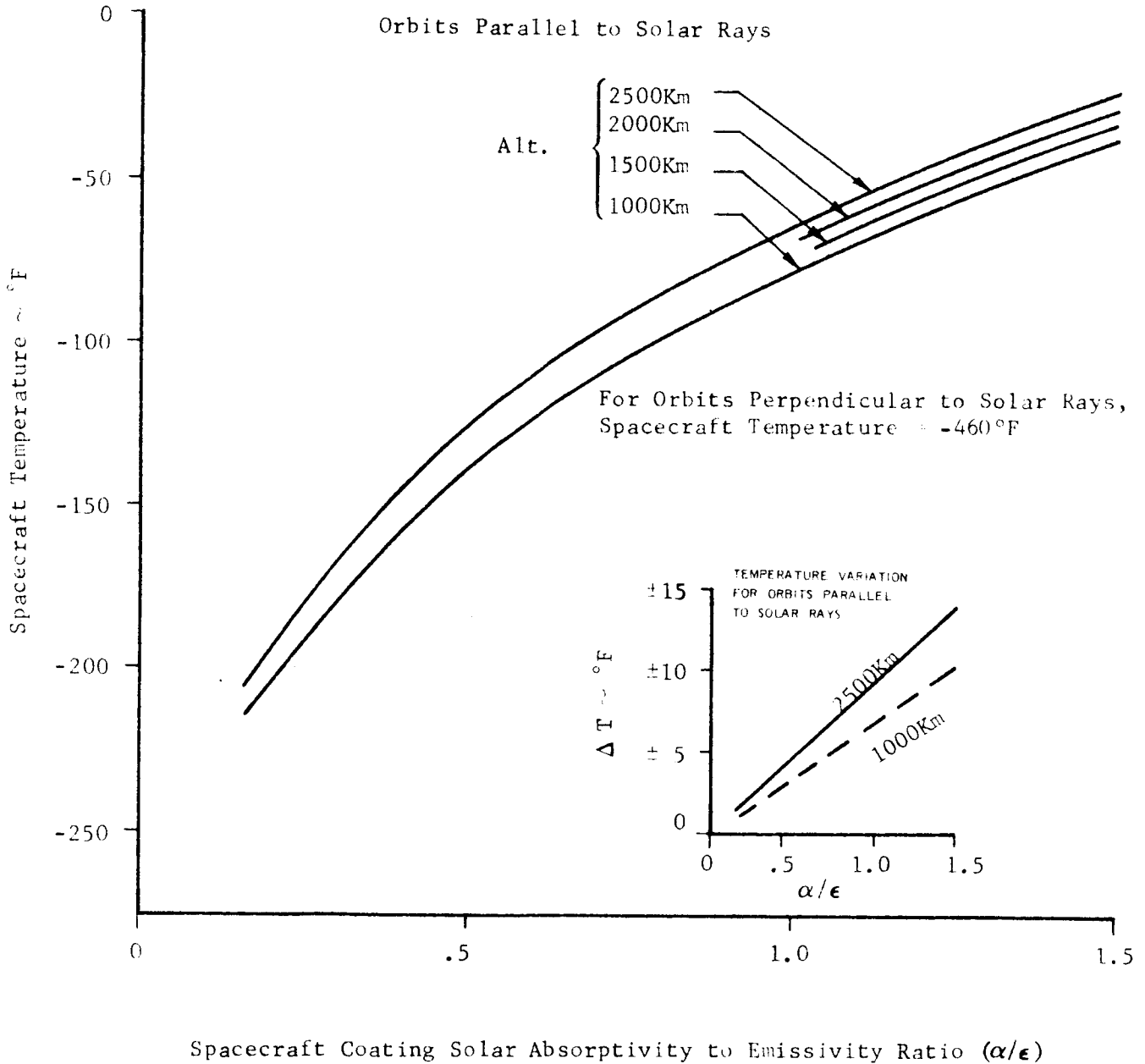
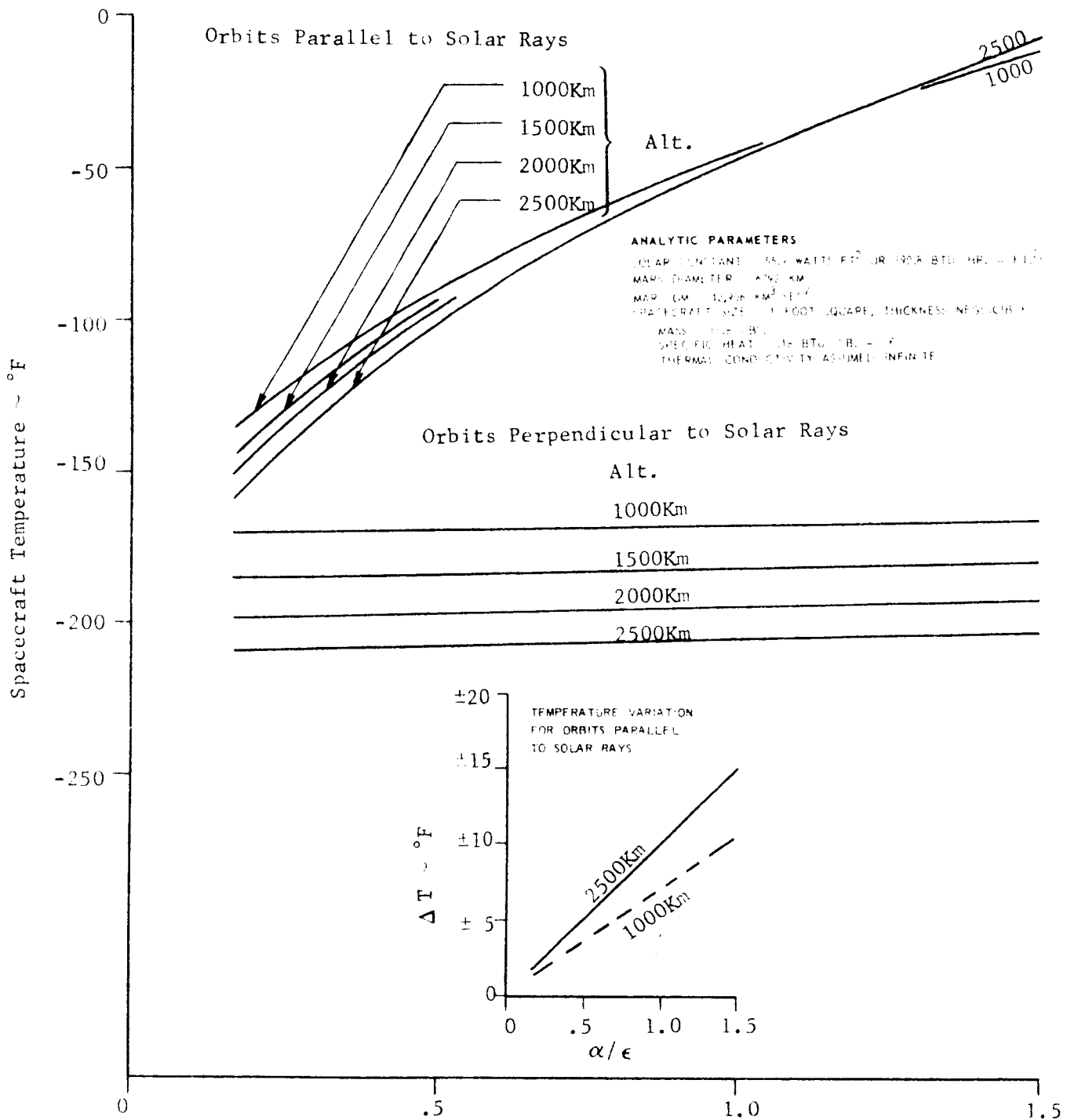


FIGURE II-40 MEAN TEMPERATURE OF A PLANETARY ORIENTED FLAT PLATE SATELLITE IN MARS CIRCULAR POLAR ORBITS NEGLECTING PLANETARY RADIATION AND ALBEDO EFFECTS, FOR A SPACECRAFT EMISSIVITY OF 0.6.

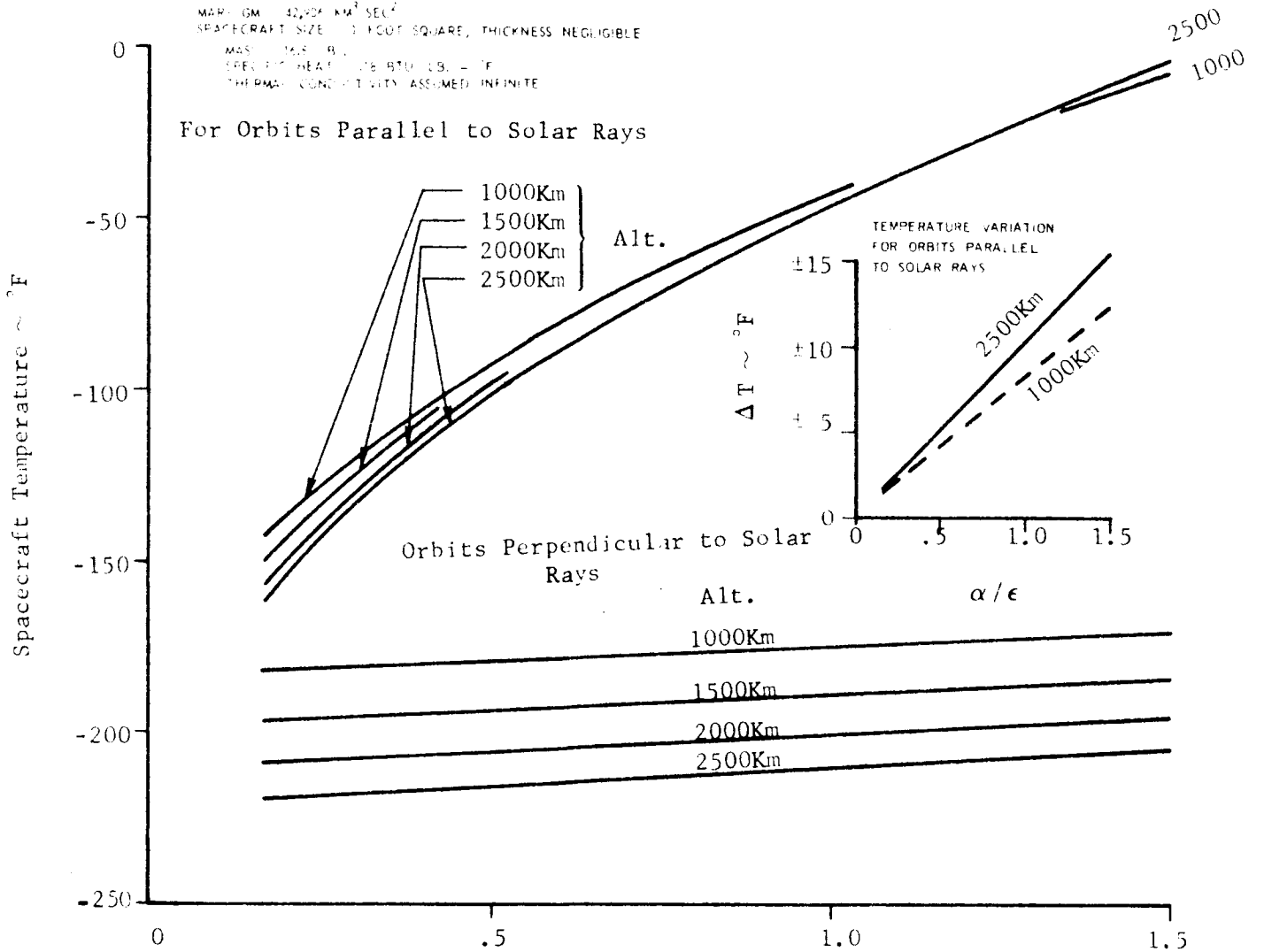


Spacecraft Coating Solar Absorptivity to Emissivity Ratio (α/ϵ)

FIGURE II-41 MEAN TEMPERATURE OF A PLANETARY ORIENTED FLAT PLATE SATELLITE IN MARS CIRCULAR POLAR ORBITS INCLUDING THE EFFECTS OF PLANETARY RADIATION AND AN ALBEDO OF 0.148, FOR A SPACECRAFT EMISSIVITY OF 0.6.

ANALYTIC PARAMETERS

SOLAR CONSTANT = 593 WATTS/FT² OR 190.8 BTU/HR. - FT.²
 MARS DIAMETER = 4192 KM
 MARS GM = 42204 KM²/SEC²
 SPACECRAFT SIZE = 1 FOOT SQUARE, THICKNESS NEGLECTIBLE
 MARS ALBEDO = 0.295
 SPECIFIC HEAT = 0.16 BTU/LB. - °F
 THERMAL CONDUCTIVITY ASSUMED INFINITE



Spacecraft Coating Solar Absorptivity to Emissivity Ratio (α/ϵ)

FIGURE II-42 MEAN TEMPERATURE OF A PLANETARY ORIENTED FLAT PLATE SATELLITE IN MARS CIRCULAR POLAR ORBITS INCLUDING THE EFFECTS OF PLANETARY RADIATION AND AN ALBEDO OF 0.295, FOR A SPACECRAFT EMISSIVITY OF 0.6.

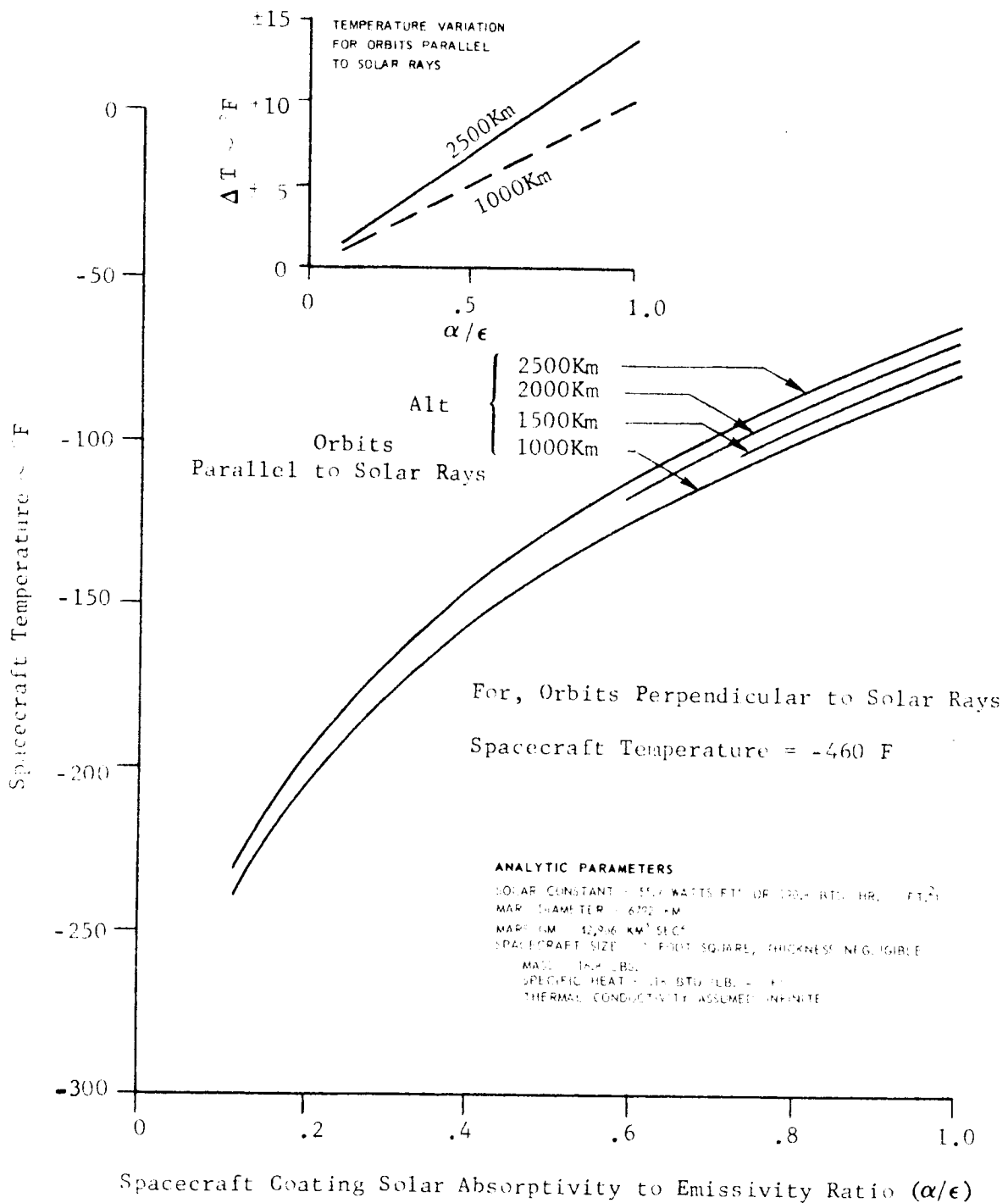


FIGURE II-43 MEAN TEMPERATURE OF A PLANETARY ORIENTED FLAT PLATE SATELLITE IN MARS CIRCULAR POLAR ORBITS NEGLECTING PLANETARY RADIATION AND ALBEDO EFFECTS, FOR A SPACECRAFT EMISSIVITY OF 0.9.

ANALYTIC PARAMETERS

SOLAR CONSTANT = 557 WATTS/FE² OR 140.8 BTU/HR./FE²
 MARS DIAMETER = 4092 KM
 MARS GM = 4,936 KM³ SEC²
 SPACECRAFT SIZE = 1 FOOT SQUARE, THICKNESS NEGLECTIBLE
 MASS = 100 LBS.
 SPECIFIC HEAT = .18 BTU/LB./°F
 THERMAL CONDUCTIVITY ASSUMED INFINITE

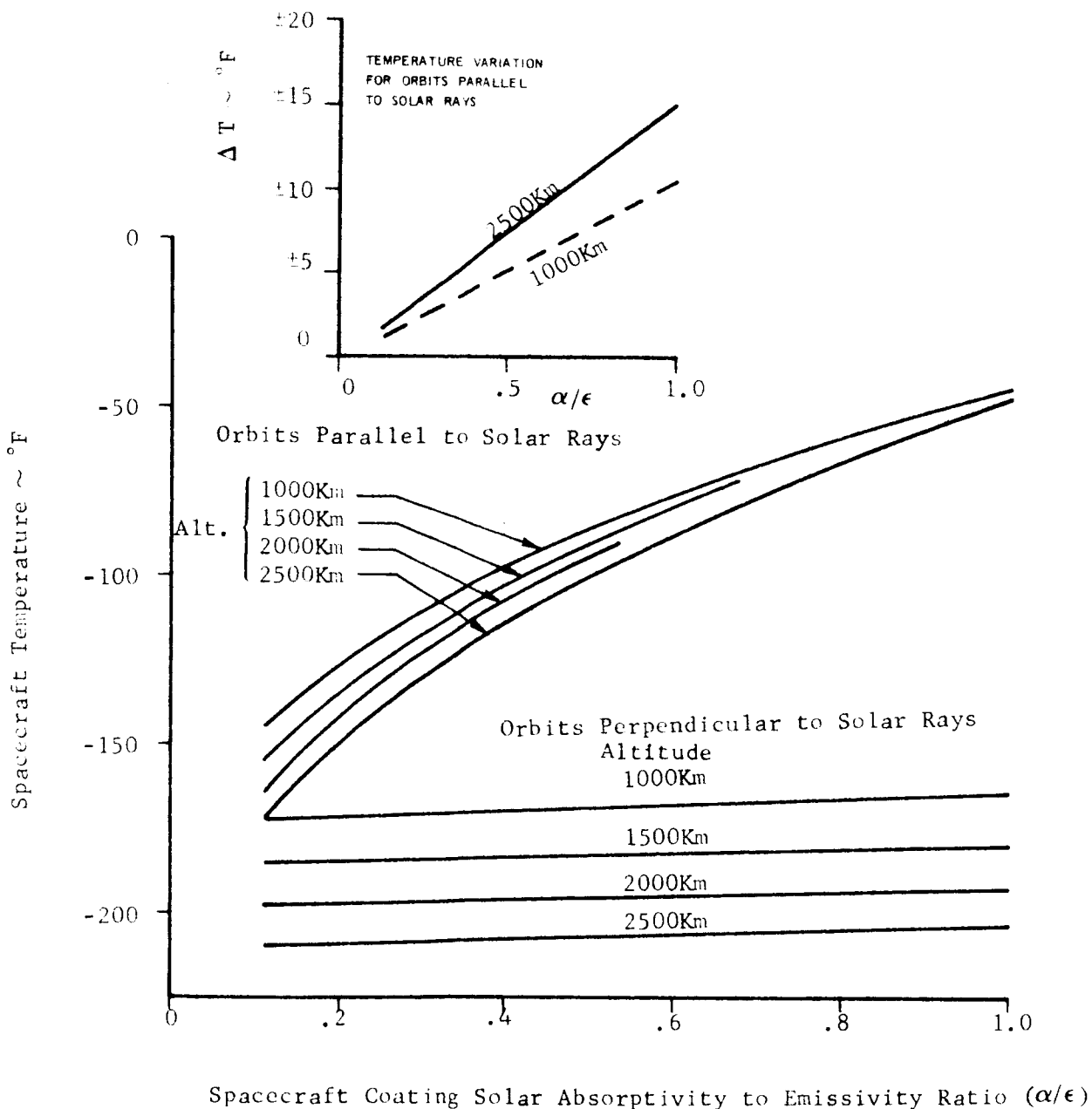


FIGURE II-44 MEAN TEMPERATURE OF A PLANETARY ORIENTED FLAT PLATE SATELLITE IN MARS CIRCULAR POLAR ORBITS INCLUDING THE EFFECTS OF PLANETARY RADIATION AND AN ALBEDO OF 0.148, FOR A SPACECRAFT EMISSIVITY OF 0.9.

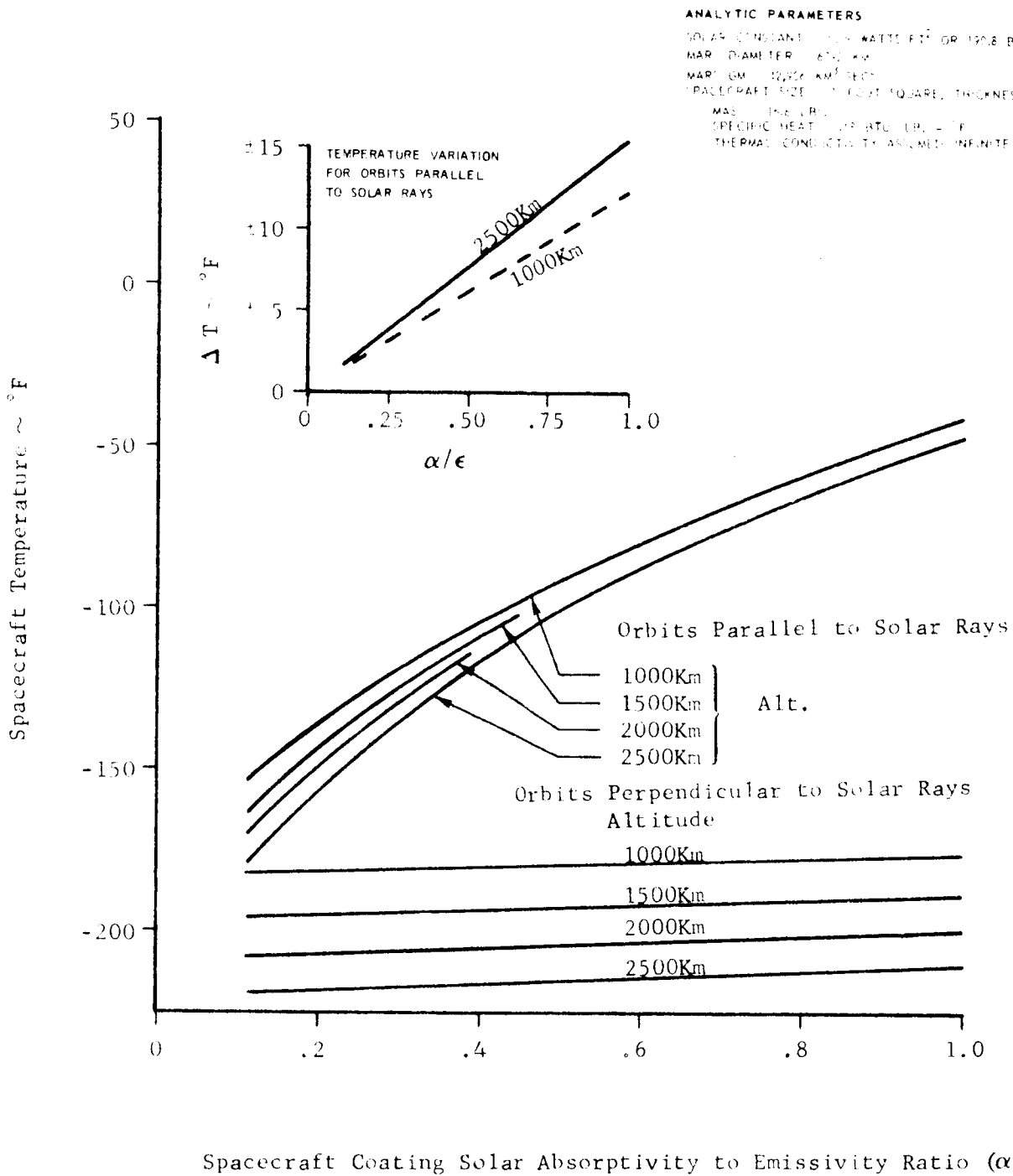


FIGURE II-45 MEAN TEMPERATURE OF A PLANETARY ORIENTED FLAT PLATE SATELLITE IN MARS CIRCULAR POLAR ORBITS INCLUDING THE EFFECTS OF PLANETARY RADIATION AND AN ALBEDO OF 0.295, FOR A SPACECRAFT EMISSIVITY OF 0.9.

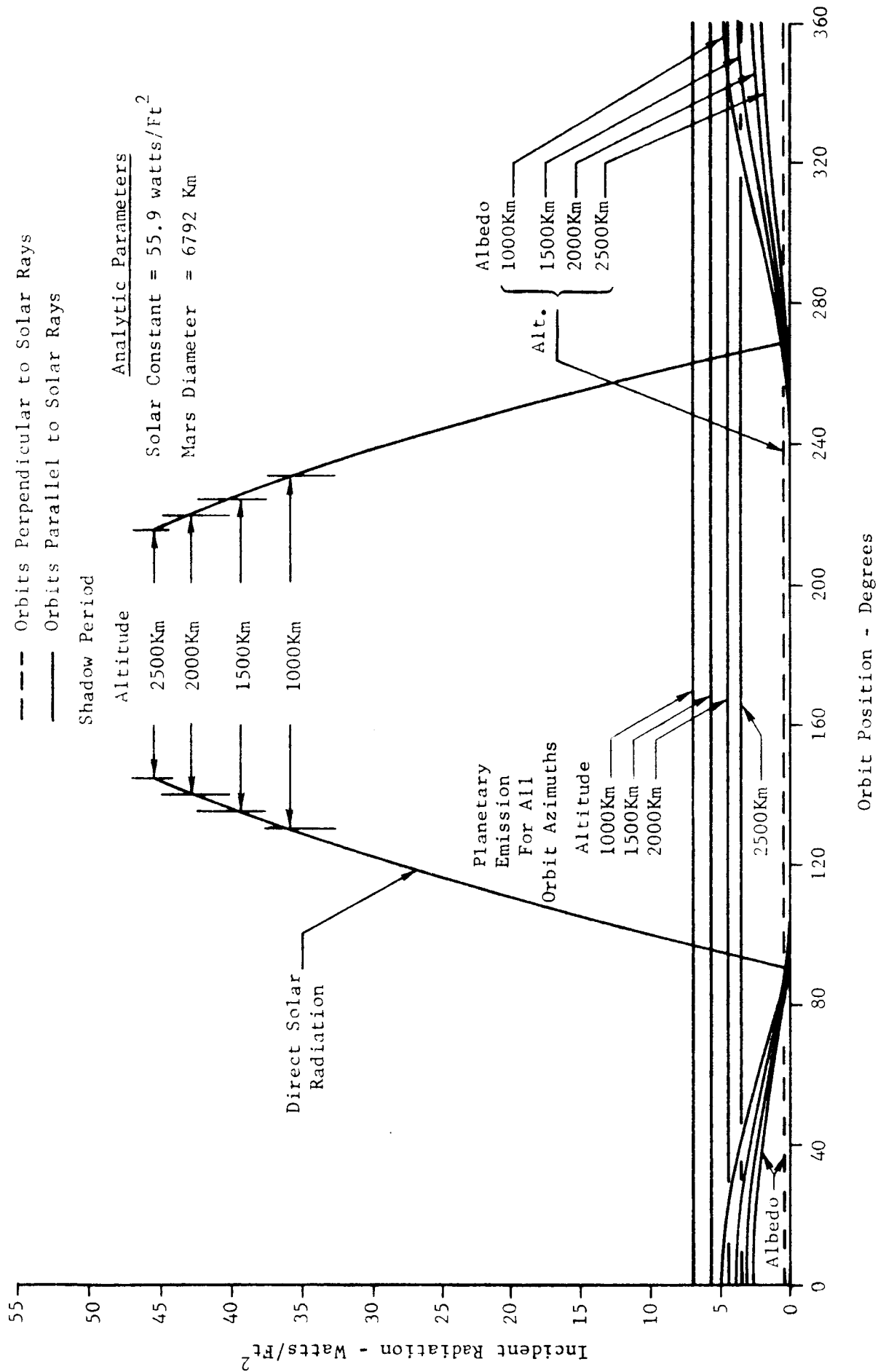


FIGURE II-46 INCIDENT RADIATION ON PLANET ORIENTED SIDE OF A 1 FOOT SQUARE FLAT PLATE IN CIRCULAR POLAR ORBITS AROUND MARS WITH AN ALBEDO OF 0.148.

Analytic Parameters

Solar Constant = 55.9 Watts/Ft²

Mars Diameter = 6792Km

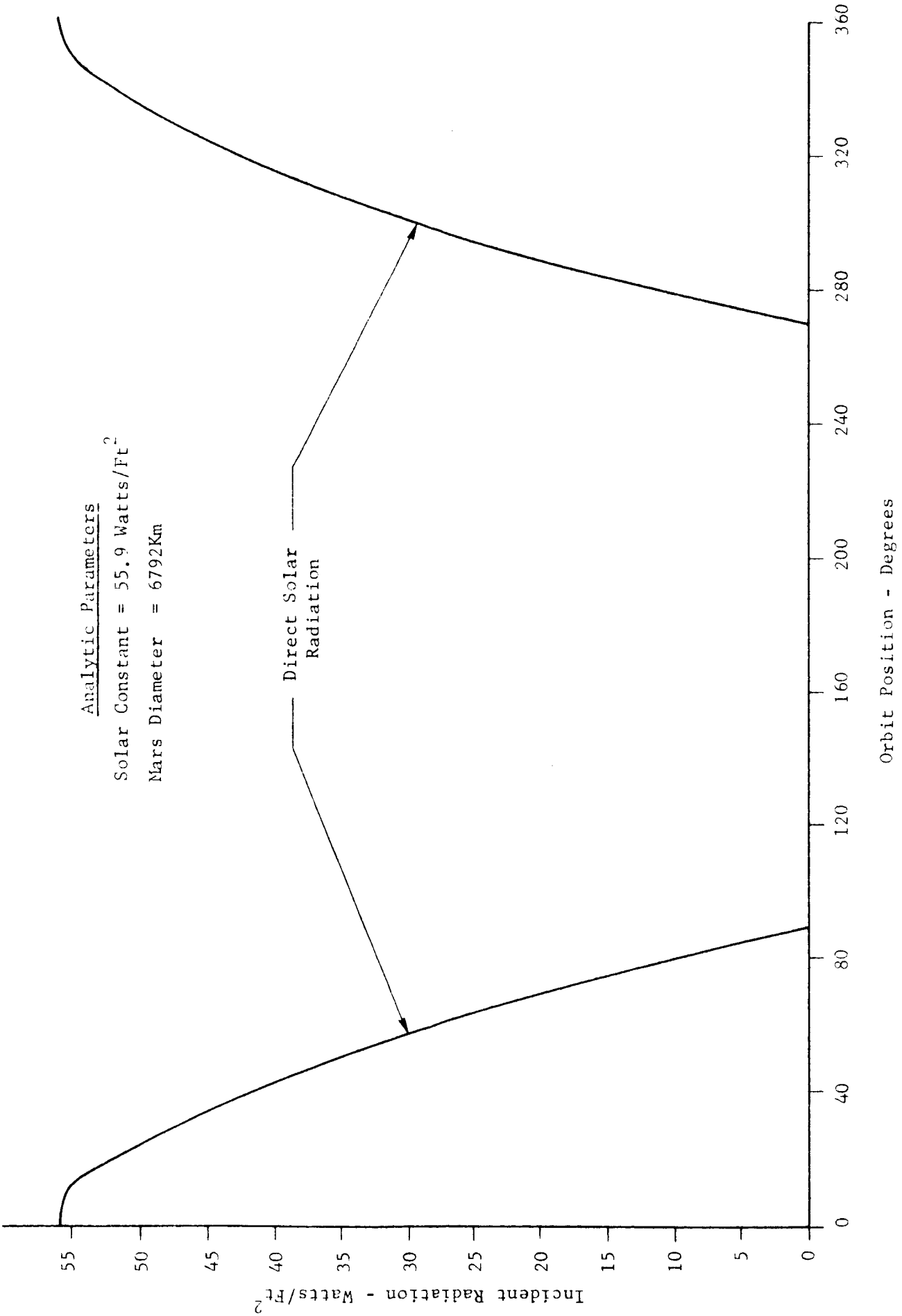


FIGURE II-47 INCIDENT RADIATION ON SIDE OPPOSITE PLANET ORIENTED SIDE OF A 1 FOOT SQUARE FLAT PLATE IN CIRCULAR POLAR ORBIT'S AROUND MARS.

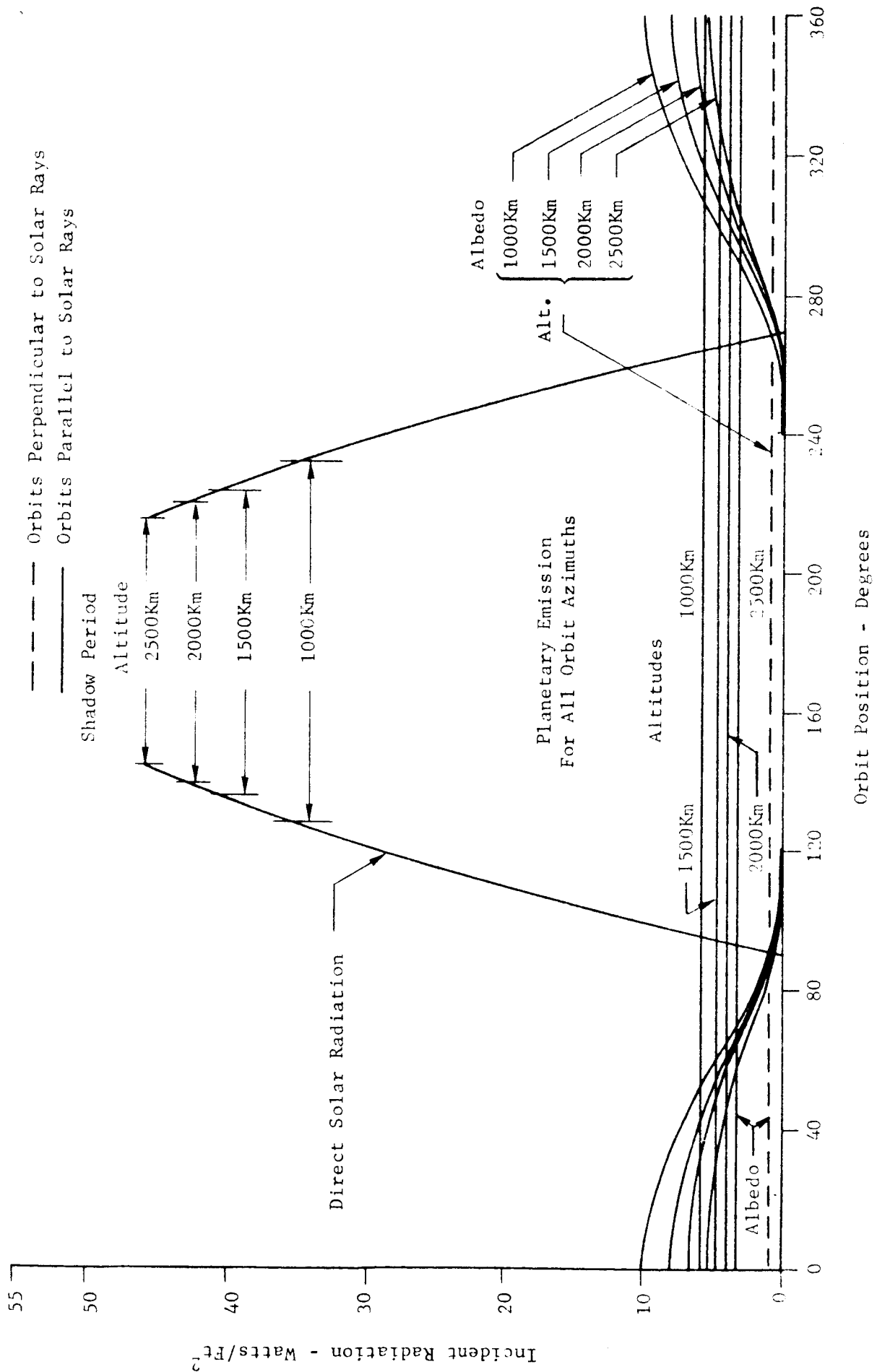


FIGURE II-48 INCIDENT RADIATION ON PLANET ORIENTED SIDE OF A 1 FOOT SQUARE FLAT PLATE IN CIRCULAR POLAR ORBITS AROUND MARS WITH AN ALBEDO OF 0.295.

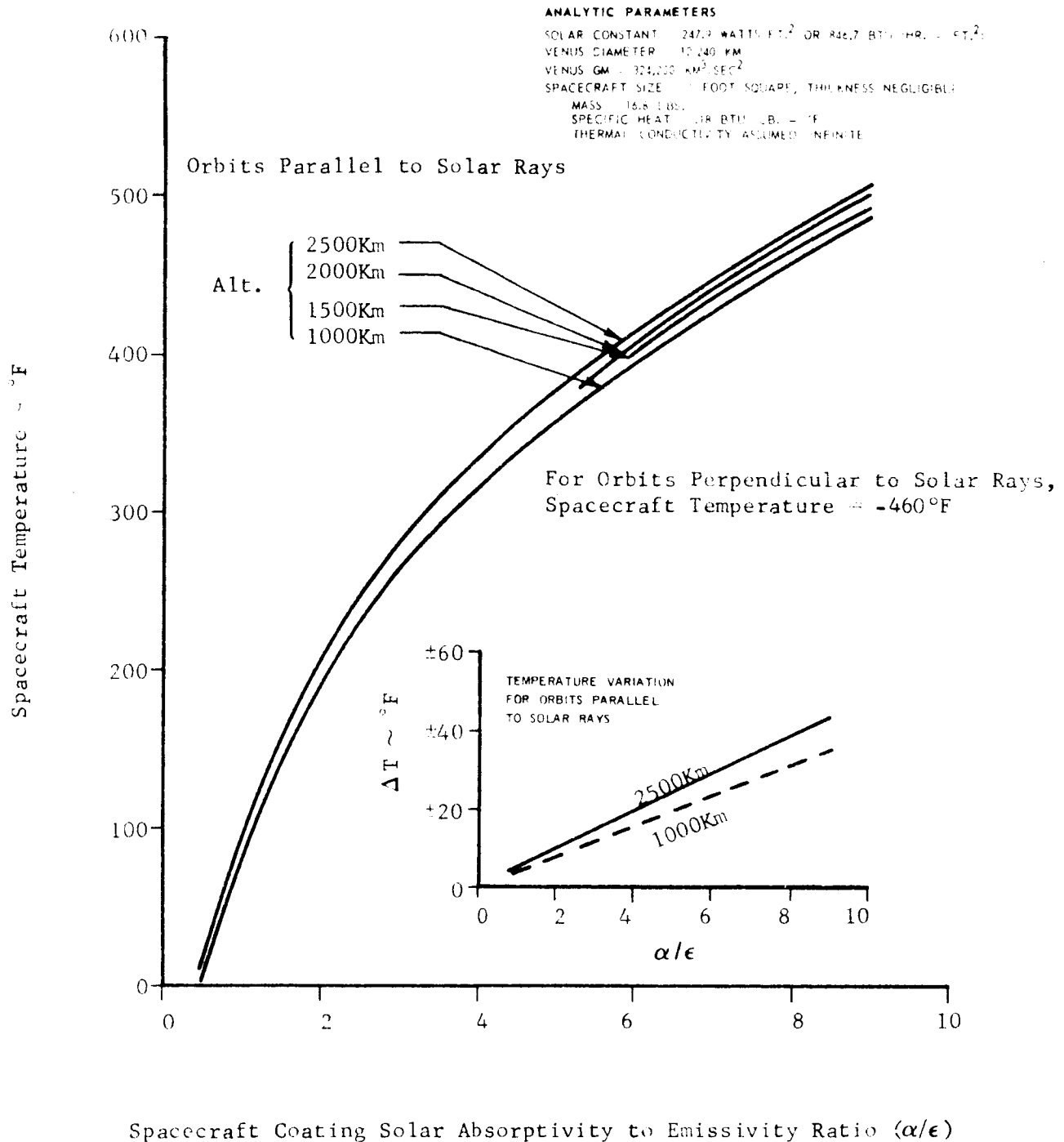


FIGURE II-49 MEAN TEMPERATURE OF A PLANETARY ORIENTED FLAT PLATE SATELLITE IN VENUS CIRCULAR POLAR ORBITS NEGLECTING PLANETARY RADIATION AND ALBEDO EFFECTS, FOR A SPACECRAFT EMISSIVITY OF 0.1.

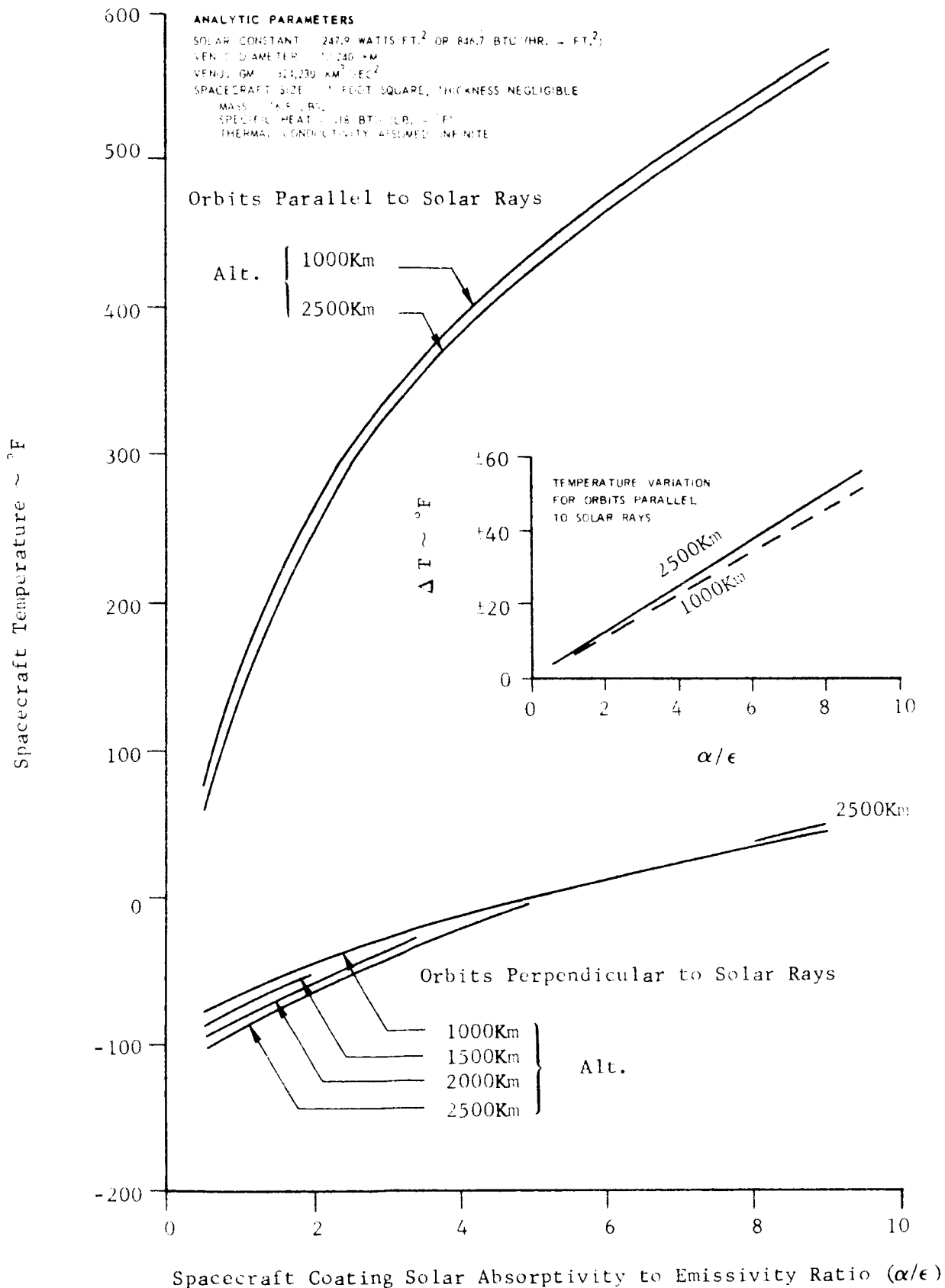


FIGURE II-50 MEAN TEMPERATURE OF A PLANETARY ORIENTED FLAT PLATE SATELLITE IN VENUS CIRCULAR POLAR ORBITS INCLUDING THE EFFECTS OF PLANETARY RADIATION AND AN ALBEDO OF 0.59, FOR A SPACECRAFT EMISSIVITY OF 0.1.

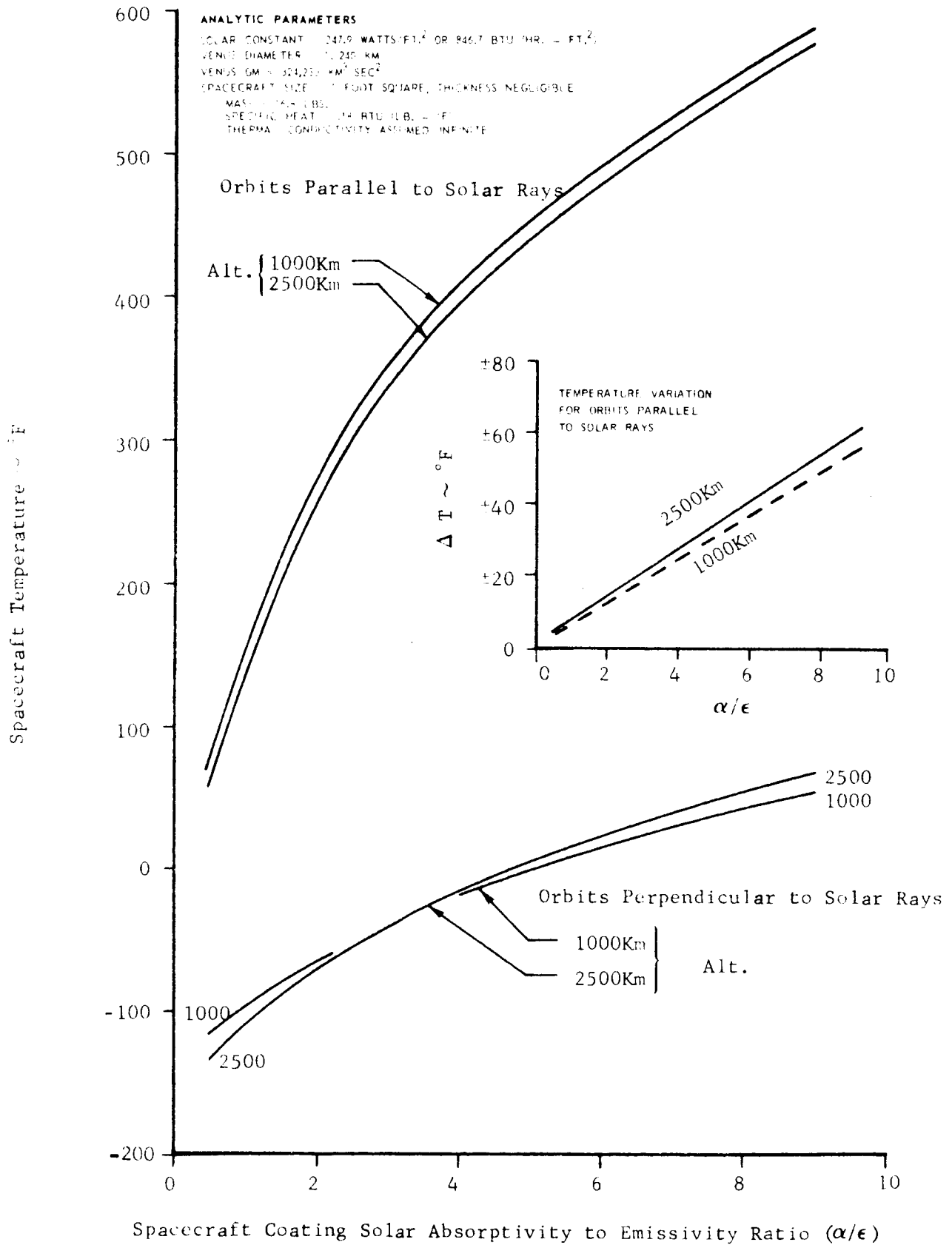


FIGURE II-51 MEAN TEMPERATURE OF A PLANETARY ORIENTED FLAT PLATE SATELLITE IN VENUS CIRCULAR POLAR ORBITS INCLUDING THE EFFECTS OF PLANETARY RADIATION AND AN ALBEDO OF 0.77, FOR A SPACECRAFT EMISSIVITY OF 0.1.

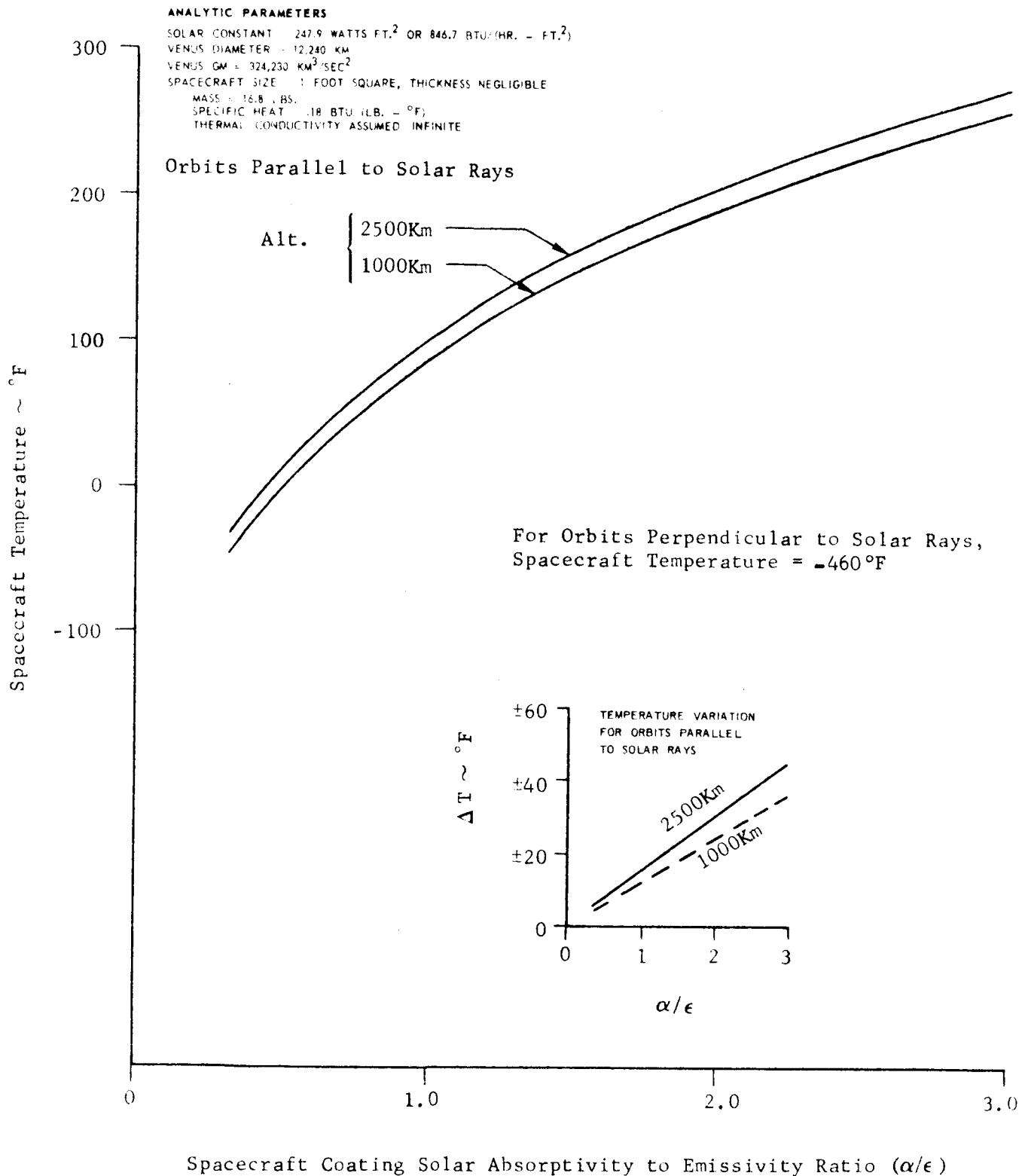


FIGURE II-52 MEAN TEMPERATURE OF A PLANETARY ORIENTED FLAT PLATE SATELLITE IN VENUS CIRCULAR POLAR ORBITS NEGLECTING PLANETARY RADIATION AND ALBEDO EFFECTS, FOR A SPACECRAFT EMISSIVITY OF 0.3.

ANALYTIC PARAMETERS

SOLAR CONSTANT = 247.9 WATTS FT.² OR 846.7 BTU (HR. - FT.²)
 VENUS DIAMETER = 12,240 KM
 VENUS GM = 324,140 KM³ SEC⁻²
 SPACECRAFT SIZE = 1 FOOT SQUARE, THICKNESS NEGLIGIBLE

MASS = 100 LB
 SPECIFIC HEAT = 0.18 BTU(LB. - °F)
 THERMAL CONDUCTIVITY ASSUMED INFINITE

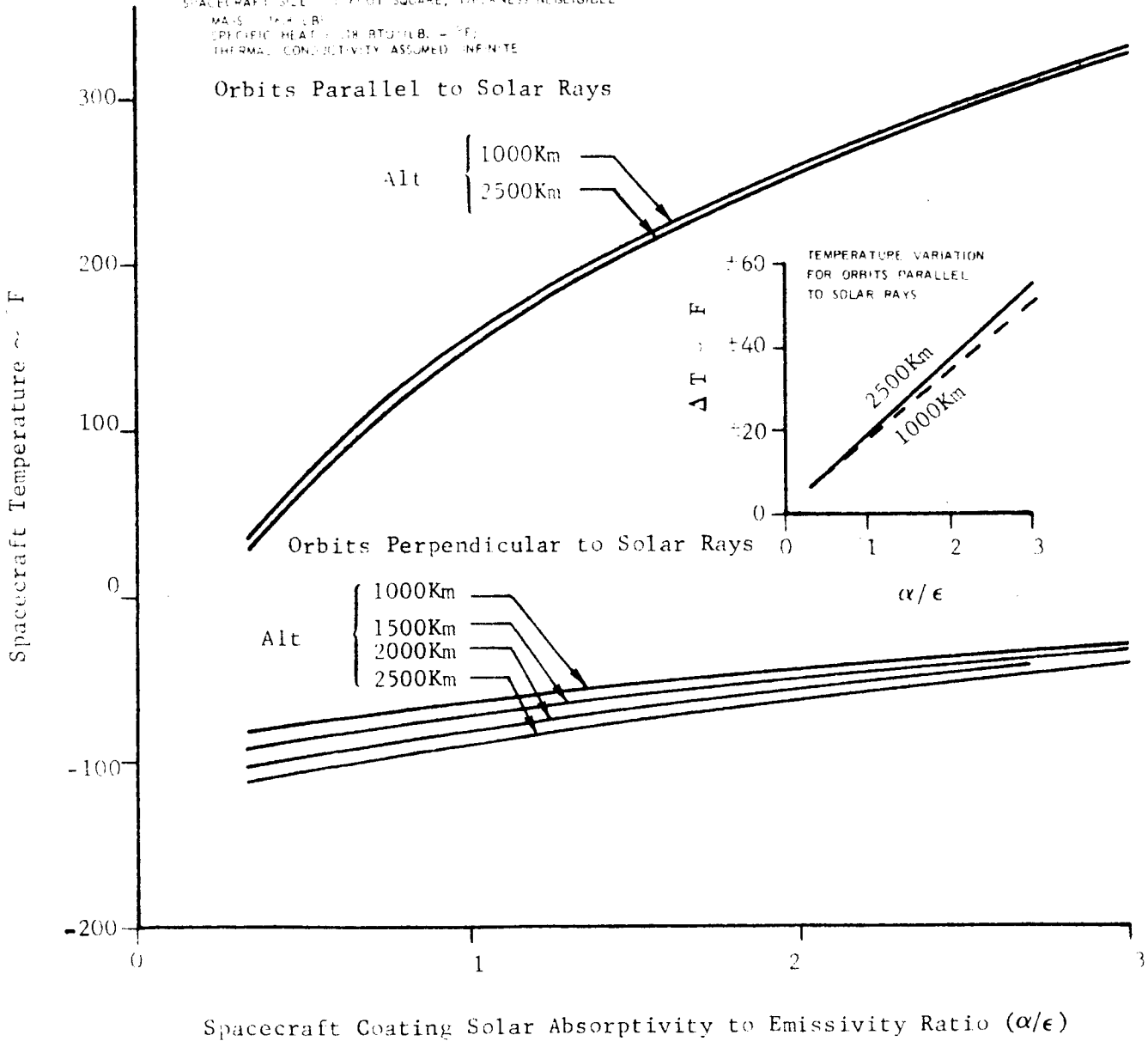


FIGURE II-53 MEAN TEMPERATURE OF A PLANETARY ORIENTED FLAT PLATE SATELLITE IN VENUS CIRCULAR POLAR ORBITS INCLUDING THE EFFECTS OF PLANETARY RADIATION AND AN ALBEDO OF 0.59, FOR A SPACECRAFT EMISSIVITY OF 0.3.

ANALYTIC PARAMETERS

SOLAR CONSTANT = 241.9 WATTS FT.² OR 846.7 Btu (HP. - FT.²)
 VENUS DIAMETER = 7624.0 KM
 VENUS OM = 91,230 KM² SEC²
 SPACECRAFT SIZE = 1 FOOT SQUARE, THICKNESS NEGLIGIBLE
 MASS = 100 LBS.
 SPECIFIC HEAT = 0.1 BTU (LB. - °F)
 THERMAL CONDUCTIVITY ASSUMED INFINITE

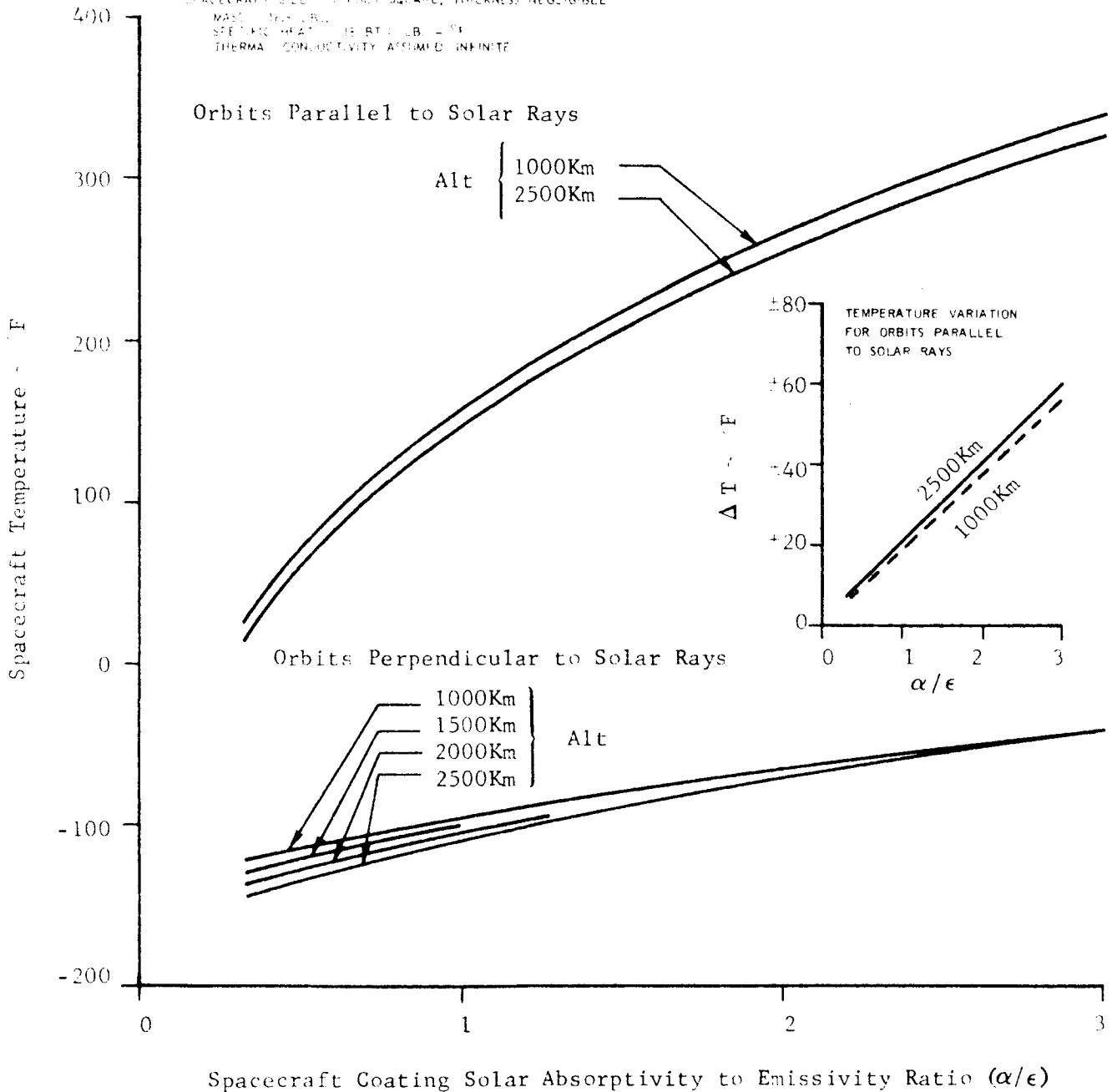


FIGURE II-54 MEAN TEMPERATURE OF A PLANETARY ORIENTED FLAT PLATE SATELLITE IN VENUS CIRCULAR POLAR ORBITS INCLUDING THE EFFECTS OF PLANETARY RADIATION AND AN ALBEDO OF 0.77, FOR A SPACECRAFT EMISSIVITY OF 0.3.

ANALYTIC PARAMETERS

SOLAR CONSTANT 247.9 WATTS FT.² OR 846.7 BTU (HR. - FT.)²
 VENUS DIAMETER 12 240 KM
 VENUS GM 324,280 KM³ SEC⁻²
 SPACECRAFT SIZE 1 FOOT SQUARE, THICKNESS NEGLECTIBLE
 MASS 16.8 LBS.
 SPECIFIC HEAT .18 BTU (LB. - °F)⁻¹
 THERMAL CONDUCTIVITY ASSUMED INFINITE

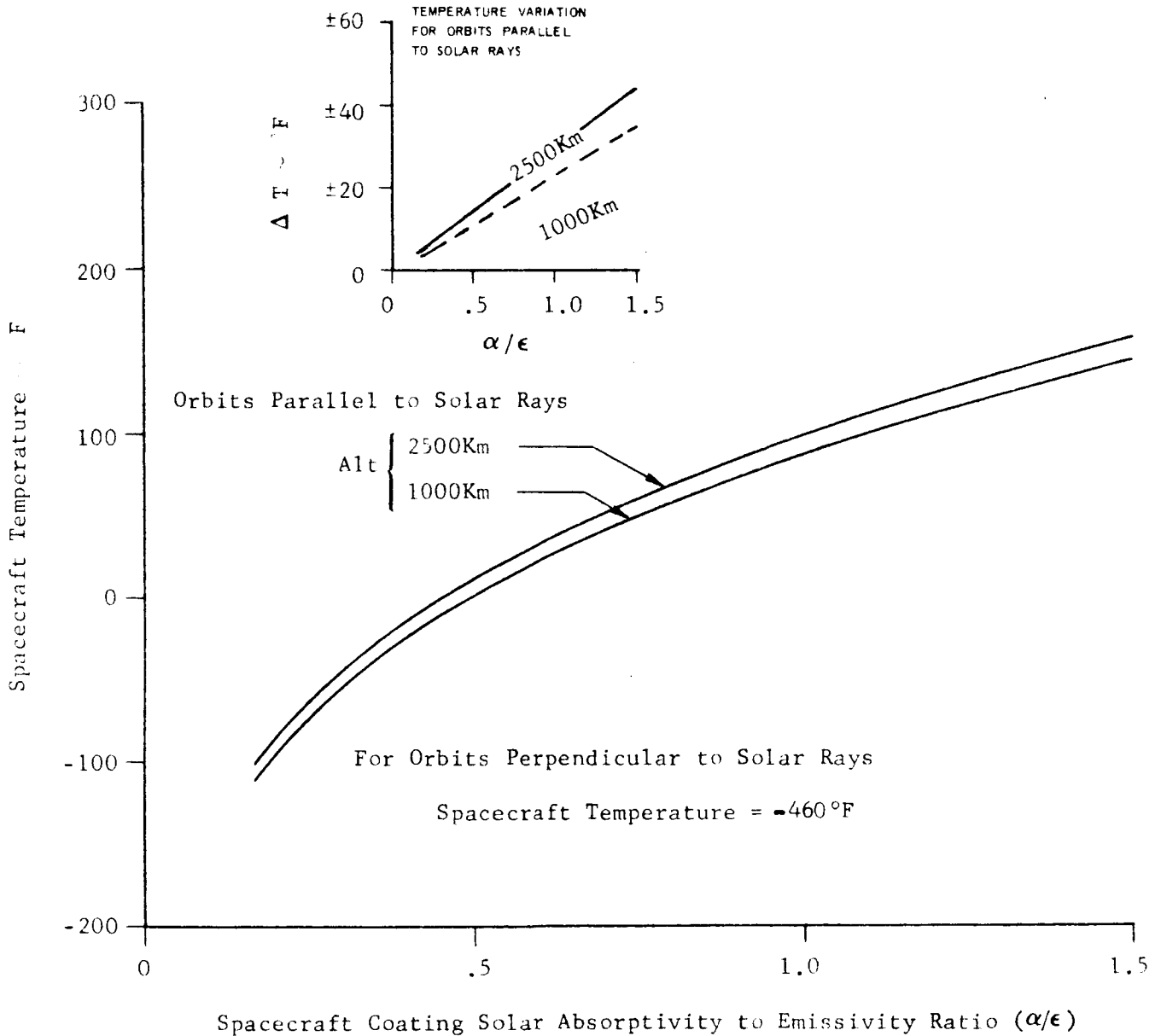


FIGURE II-55 MEAN TEMPERATURE OF A PLANETARY ORIENTED FLAT PLATE SATELLITE IN VENUS CIRCULAR POLAR ORBITS NEGLECTING PLANETARY RADIATION AND ALBEDO EFFECTS, FOR A SPACECRAFT EMISSIVITY OF 0.6.

ANALYTIC PARAMETERS

SOLAR CONSTANT = 247.9 WATTS/FT.² OR 846.7 BTU/(HR. - FT.²)

VENUS DIAMETER = 12,240 KM

VENUS GM = 324,270 KM³/SEC²

SPACECRAFT SIZE = 1 FOOT SQUARE, THICKNESS NEGLIGIBLE

MASS = 16.2 LBS

SPECIFIC HEAT = .18 BTU/(LB. - °F)

THERMAL CONDUCTIVITY ASSUMED INFINITE

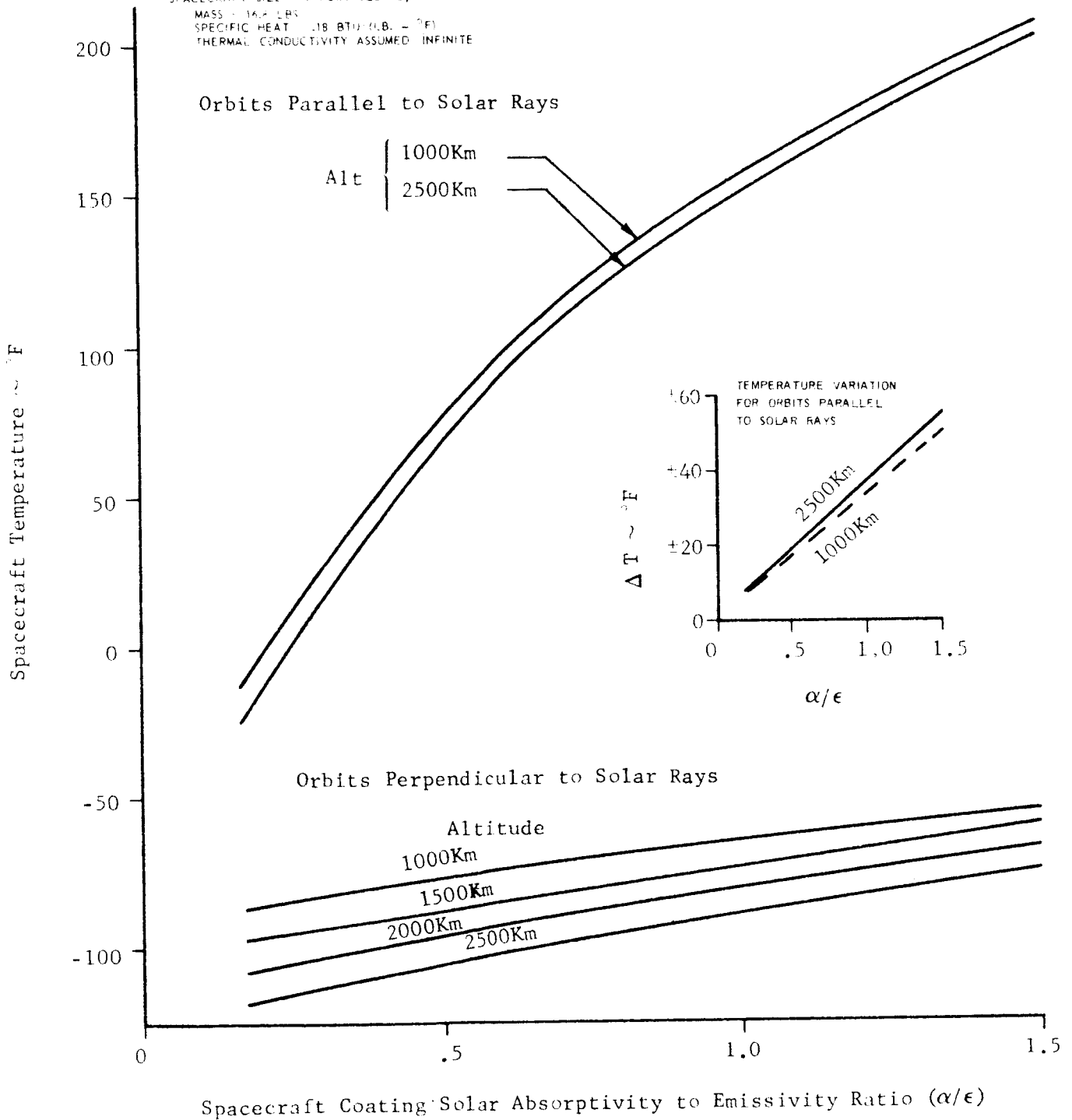
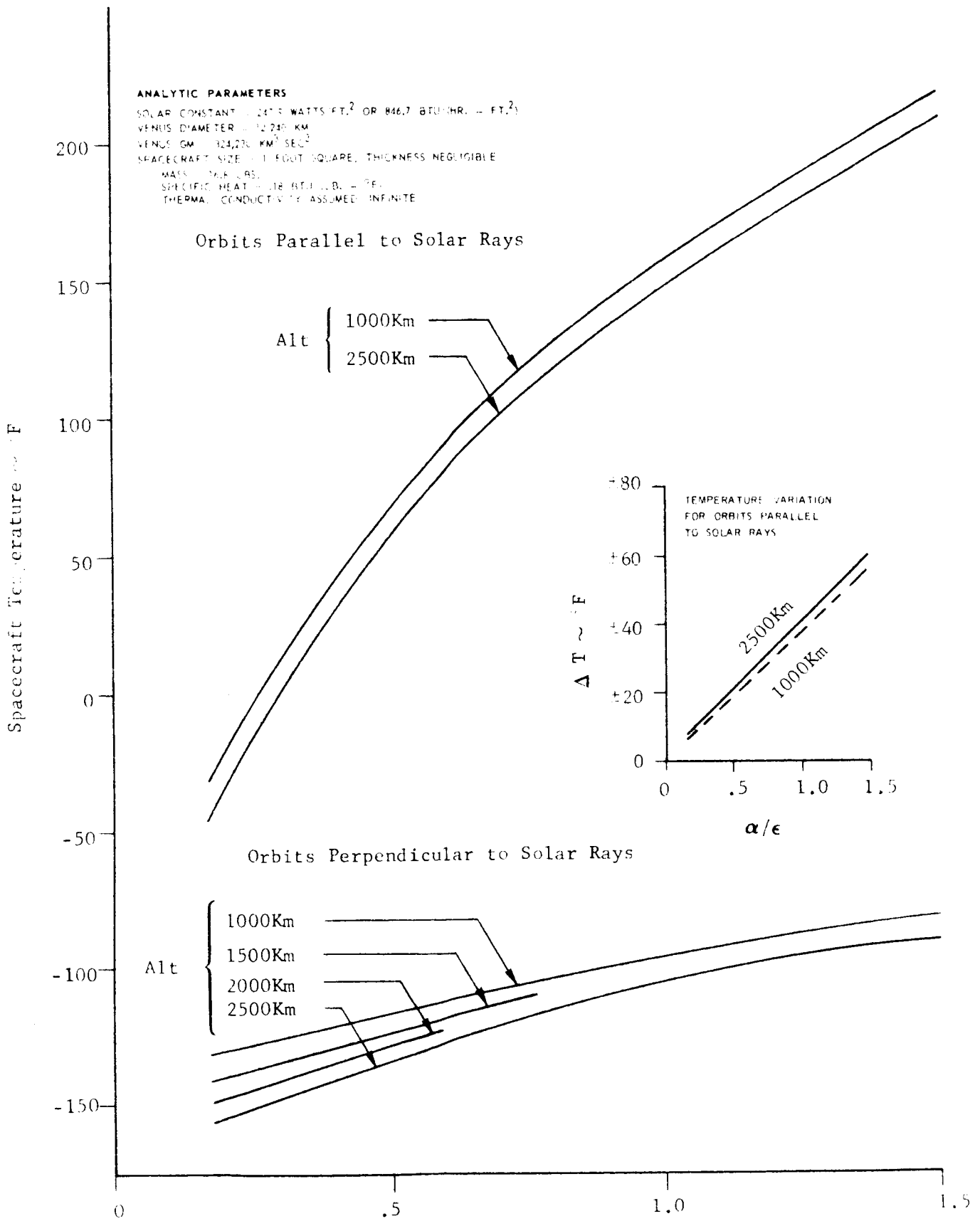


FIGURE II-56 MEAN TEMPERATURE OF A PLANETARY ORIENTED FLAT PLATE SATELLITE IN VENUS CIRCULAR POLAR ORBITS INCLUDING THE EFFECTS OF PLANETARY RADIATION AND AN ALBEDO OF 0.59, FOR A SPACECRAFT EMISSIVITY OF 0.6.



Spacecraft Coating Solar Absorptivity to Emissivity Ratio (α/ϵ)

FIGURE II-57 MEAN TEMPERATURE OF A PLANETARY ORIENTED FLAT PLATE SATELLITE IN VENUS CIRCULAR POLAR ORBITS INCLUDING THE EFFECTS OF PLANETARY RADIATION AND AN ALBEDO OF 0.77, FOR A SPACECRAFT EMISSIVITY OF 0.6.

ANALYTIC PARAMETERS

SOLAR CONSTANT = 247.9 WATTS FT.² OR 846.7 BTU/(HR. - FT.²)
 VENUS DIAMETER = 12 240 KM
 VENUS GM = 324,239 KM³ SEC⁻²
 SPACECRAFT SIZE = 1 FOOT SQUARE, THICKNESS NEGLECTIBLE
 MASS = 14.5 LBS.
 SPECIFIC HEAT = 0.16 BTU/1LB. - °F
 THERMAL CONDUCTIVITY ASSUMED INFINITE

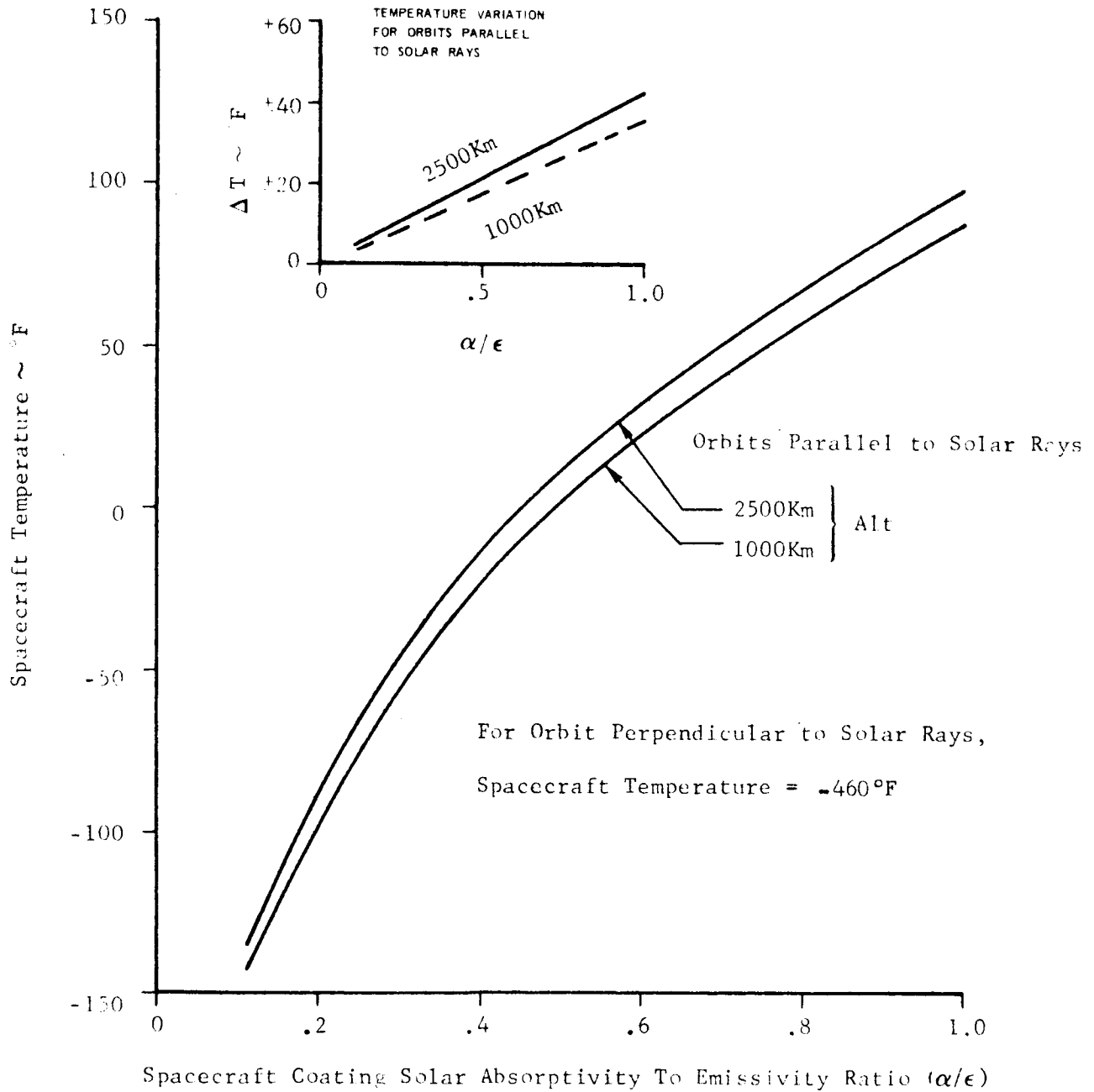


FIGURE II-58 MEAN TEMPERATURE OF A PLANETARY ORIENTED FLAT PLATE SATELLITE IN VENUS CIRCULAR POLAR ORBITS NEGLECTING PLANETARY RADIATION AND ALBEDO EFFECTS, FOR A SPACECRAFT EMISSIVITY OF 0.9.

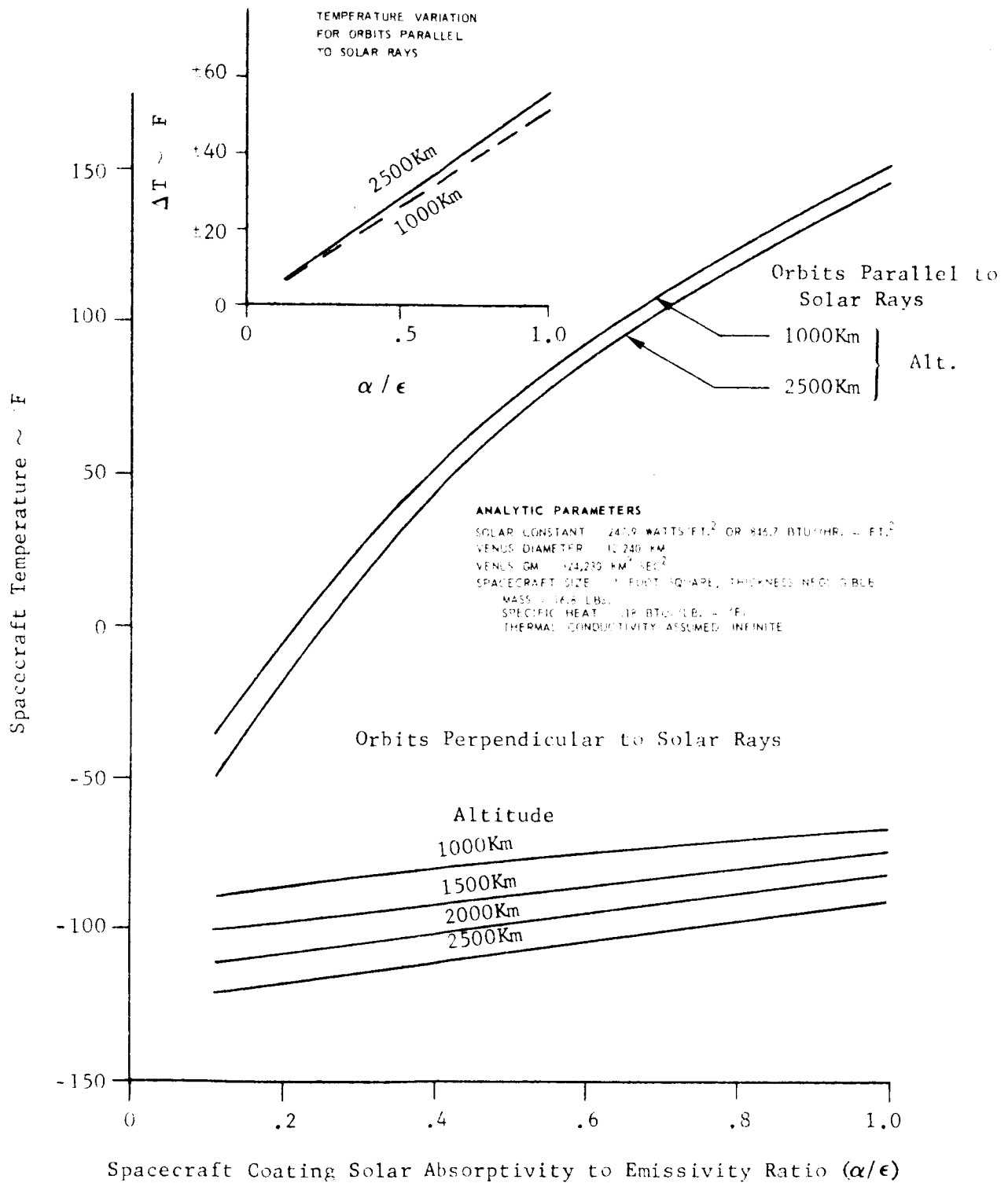


FIGURE II-59 MEAN TEMPERATURE OF A PLANETARY ORIENTED FLAT PLATE SATELLITE IN VENUS CIRCULAR POLAR ORBITS INCLUDING THE EFFECTS OF PLANETARY RADIATION AND AN ALBEDO OF 0.59, FOR A SPACECRAFT EMISSIVITY OF 0.9.

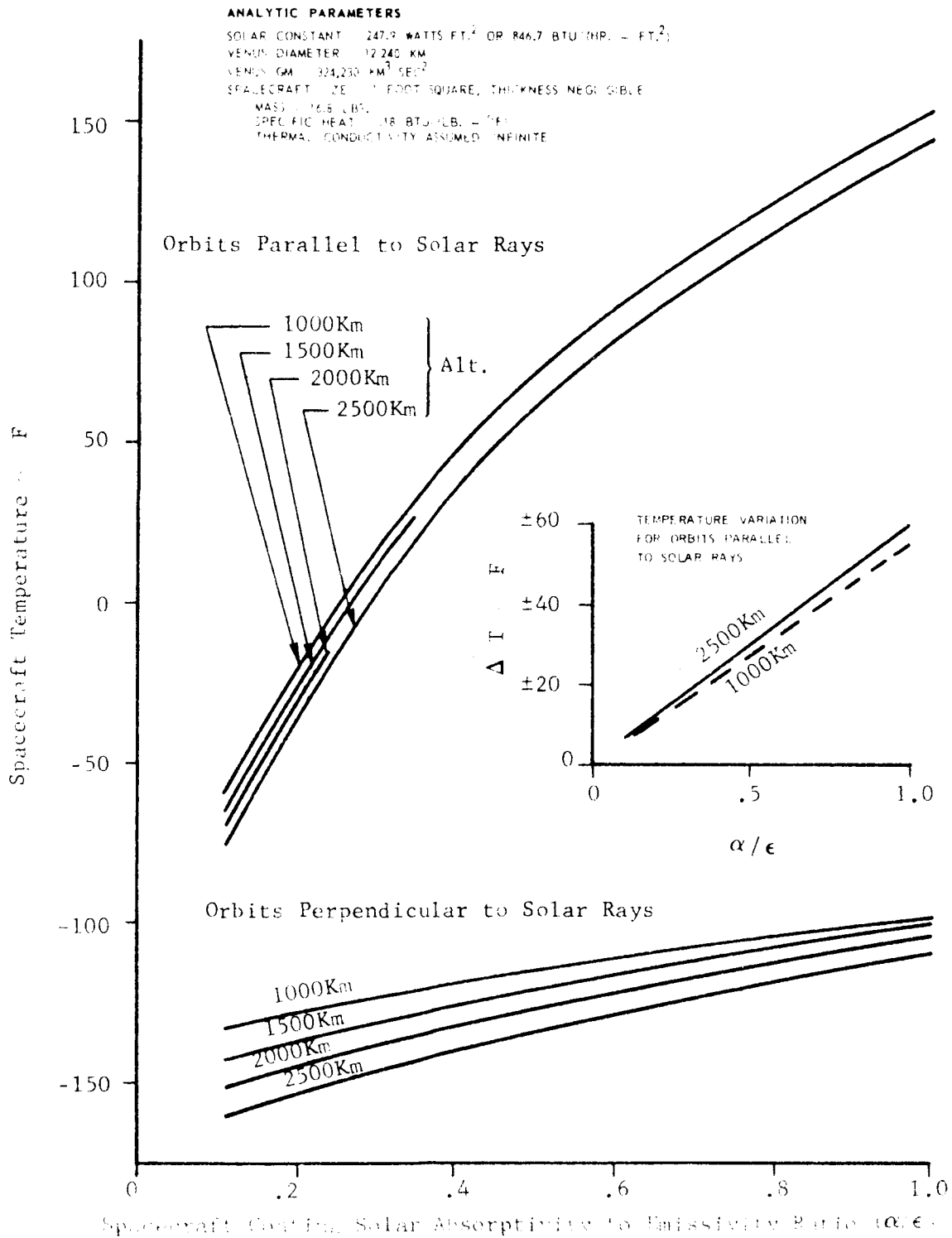


FIGURE II-77 MEAN TEMPERATURE OF A PLANETARY ORIENTED FLAT PLATE SATELLITE IN VENUS'S CIRCULAR POLAR ORBITS INCLUDING THE EFFECTS OF PLANETARY RADIATION AND AN ALBEDO OF 0.77, FOR A SPACECRAFT EMISSIVITY OF 0.9.

- - - Orbits Perpendicular to Solar Rays
- Orbits Parallel to Solar Rays

Analytic Parameters

Solar Constant = 247.9 Watts/Ft²

Venus Diameter = 12,240 Km

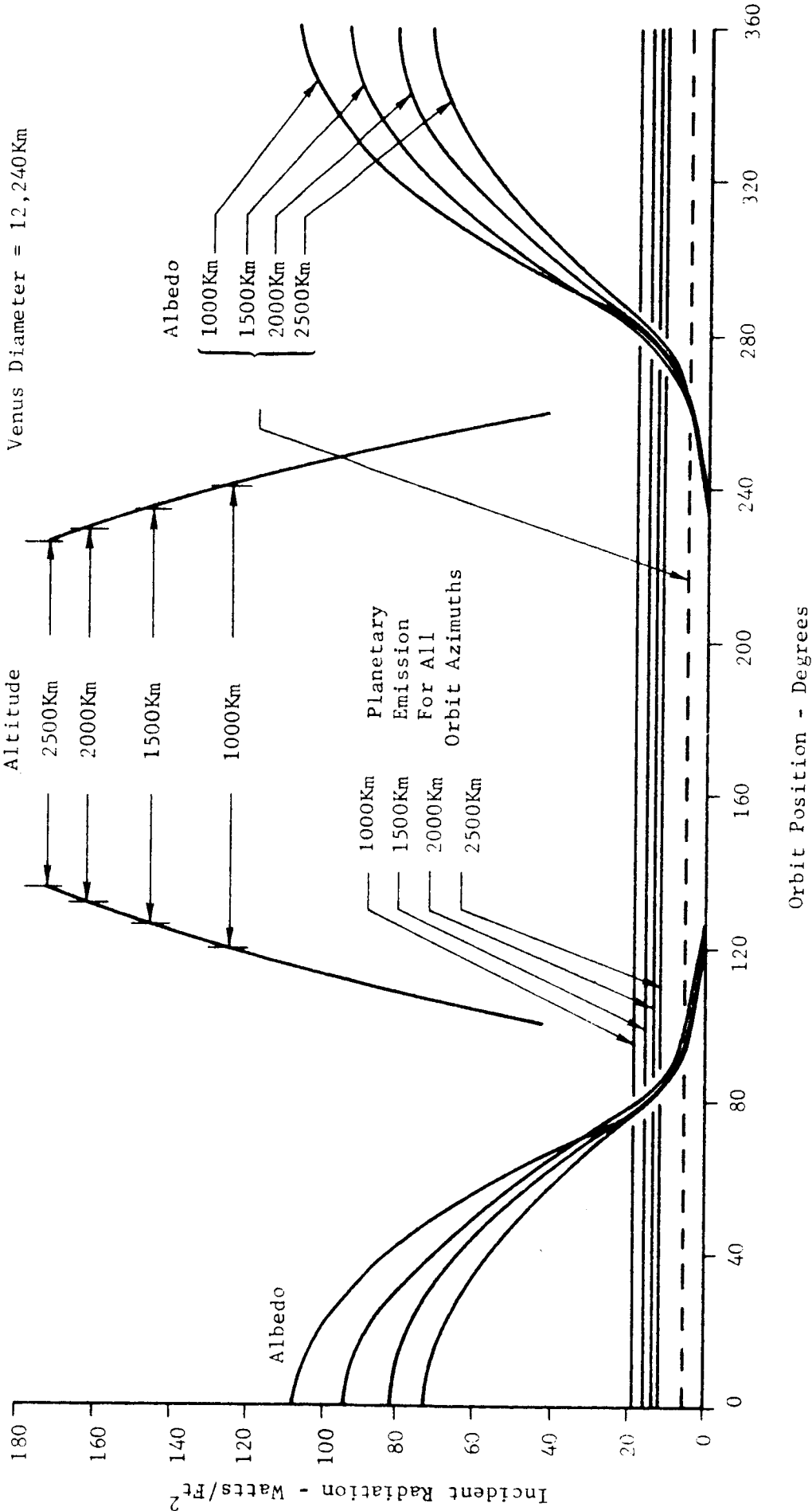


FIGURE II-61 INCIDENT RADIATION ON PLANET ORIENTED SIDE OF A 1 FOOT SQUARE FLAT PLATE IN CIRCULAR POLAR ORBITS AROUND VENUS WITH AN ALBEDO OF 0.59.

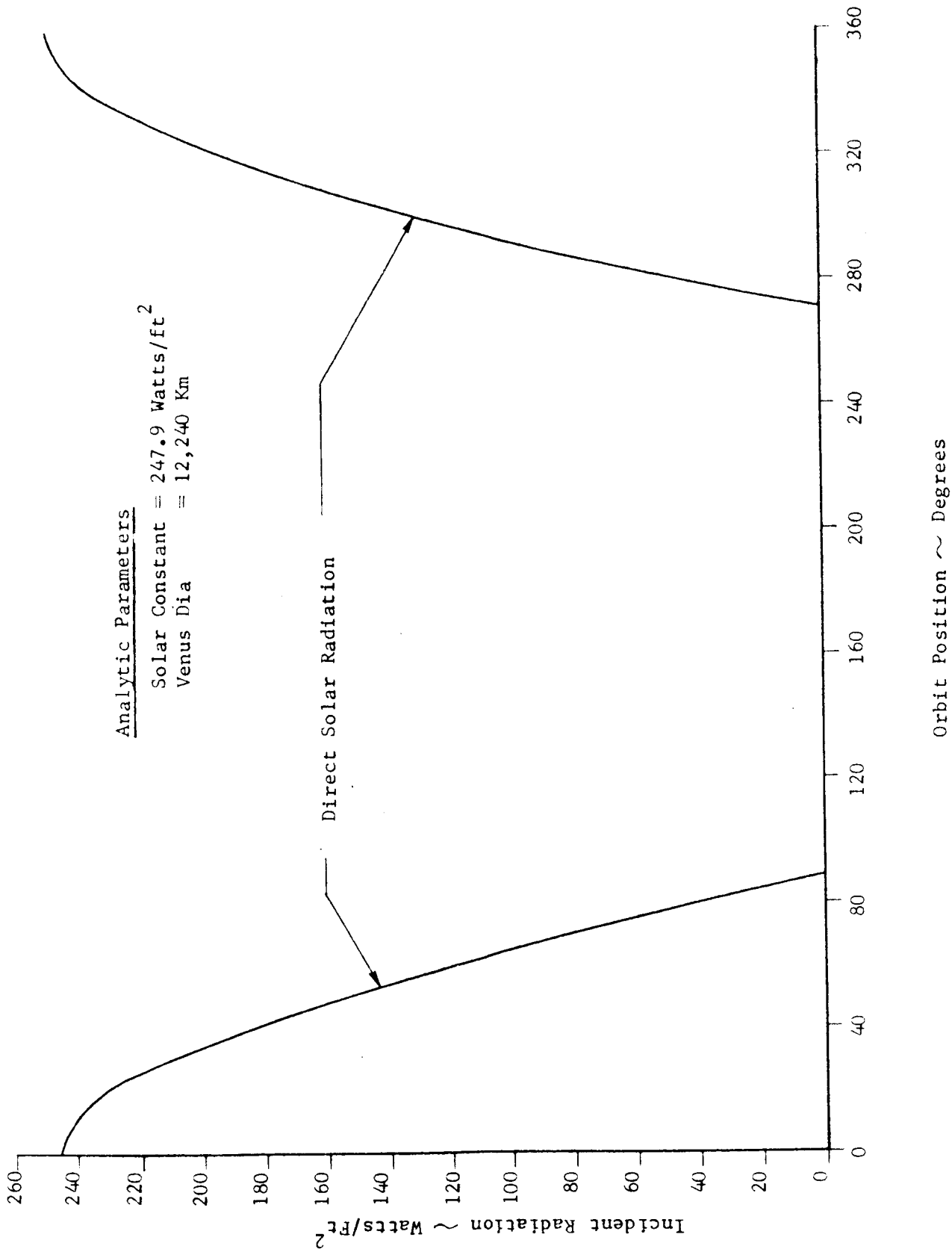


FIGURE II-62 INCIDENT RADIATION ON SIDE OPPOSITE PLANET ORIENTED SIDE OF A 1 FOOT SQUARE FLAT PLATE IN CIRCULAR POLAR ORBITS AROUND VENUS.

--- Orbits Perpendicular to Solar Rays
 — Orbits Parallel to Solar Rays

Analytic Parameters
 Solar Constant = 247.9 watts/Ft²
 Venus Diameter = 12,240Km

Shadow Period

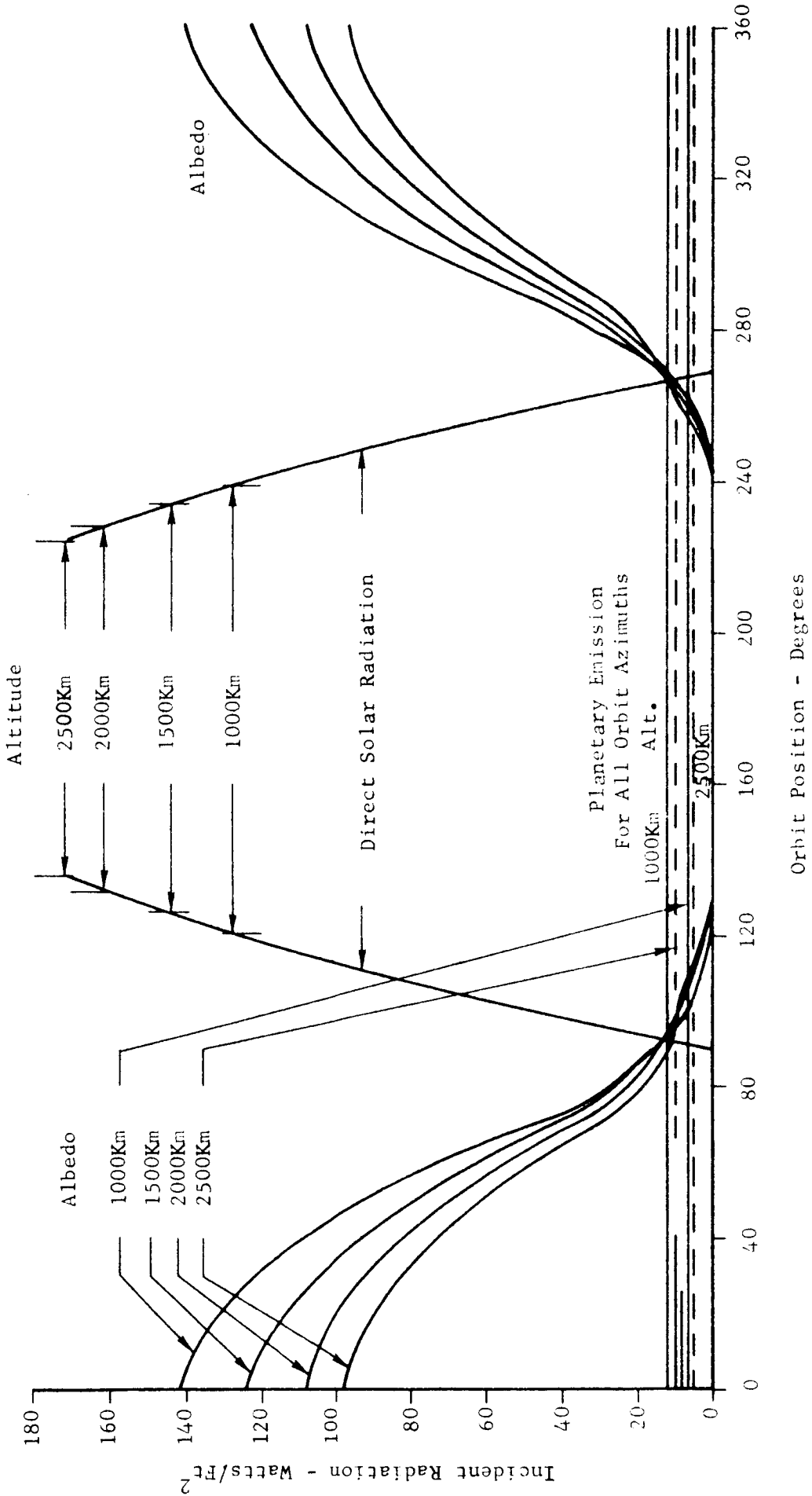
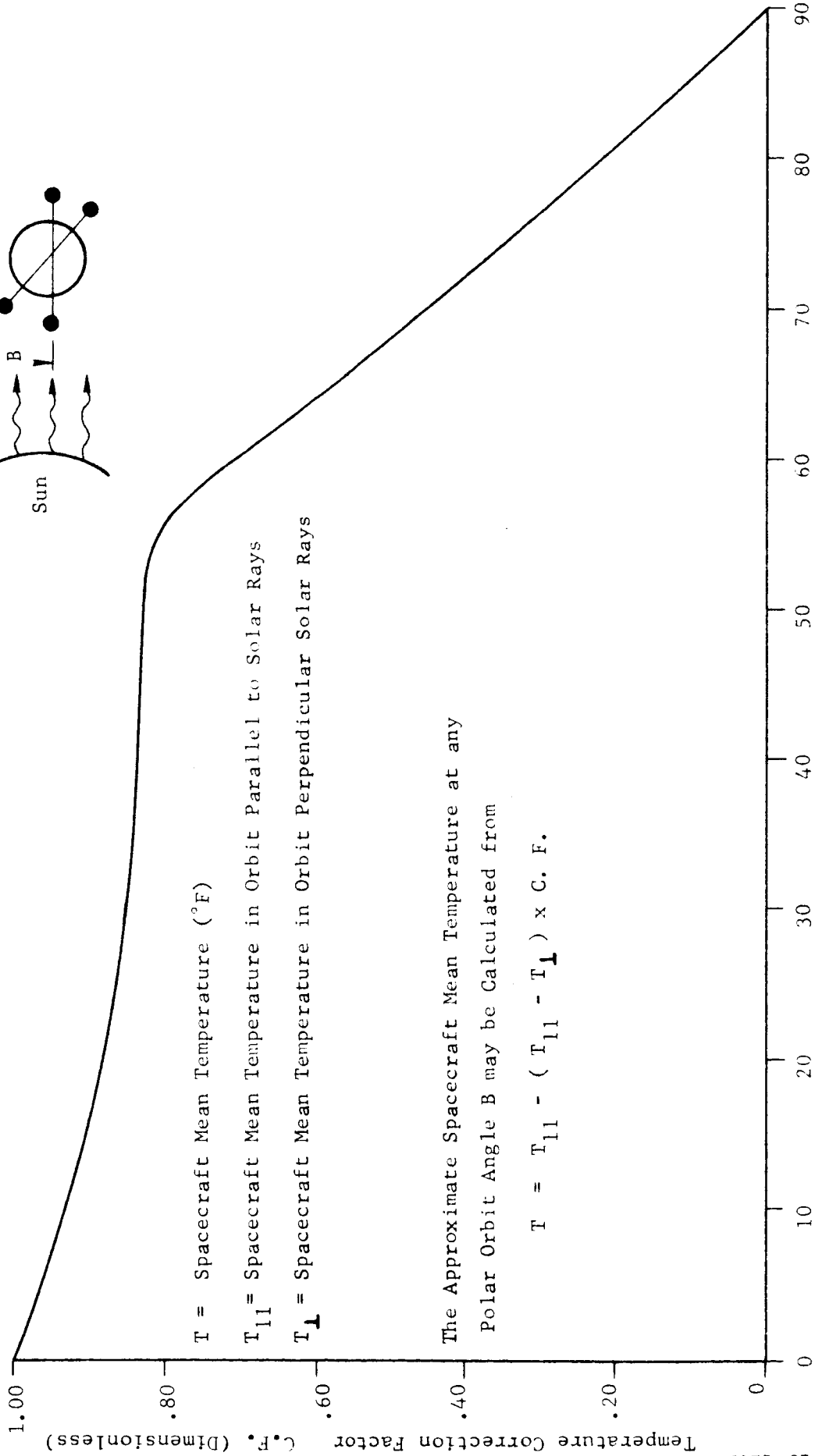
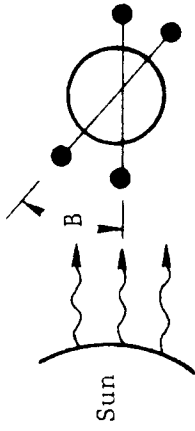


FIGURE II-63 INCIDENT RADIATION ON PLANET ORIENTED SIDE OF A 1 FOOT SQUARE FLAT PLATE IN CIRCULAR POLAR ORBITS AROUND VENUS WITH AN ALBEDO OF 0.77.

Azimuth Angle B = Angle of Polar Orbit Plane from Orbit Parallel to Solar Rays Toward the Orbit Perpendicular to the Solar Rays



T = Spacecraft Mean Temperature ($^{\circ}$ F)

T_{11} = Spacecraft Mean Temperature in Orbit Parallel to Solar Rays

T_{\perp} = Spacecraft Mean Temperature in Orbit Perpendicular Solar Rays

The Approximate Spacecraft Mean Temperature at any Polar Orbit Angle B may be Calculated from

$$T = T_{11} - (T_{11} - T_{\perp}) \times C.F.$$

Azimuth Angle B - Degrees

FIGURE II-64 FLAT PLATE TEMPERATURE DETERMINATION FOR CIRCULAR POLAR ORBITS AS A FUNCTION OF AZIMUTH ANGLE.

NORTHROP SPACE LABORATORIES

SECTION III

SIMULATION TECHNIQUES

The data survey and analytic study phases of this report have provided representative values for albedo factors, effective radiating temperatures, and spectral energy distribution. With the effect of radiosity (combined albedo and planetary emission) on the overall thermal balance demonstrated, this section will consider the factors and characteristics which will enter into the specification of a planetary radiosity simulation system, and will review and evaluate the techniques and equipment for construction of a practical simulator.

The simulator should produce the equivalent thermal effects on the spacecraft as the actual environment even if the actual conditions are not exactly duplicated. Acceptability of deviations from perfect duplication or simulation of the desired effects enters into the technical and economic evaluation, planning and design of a system. Also, to be of value for testing purposes, a simulation system should not introduce any unknown or indeterminate effects, and performance characteristics should be controllable within desired ranges.

DESIRED SIMULATION CHARACTERISTICS

In evaluating possible radiosity simulation techniques, the characteristics of the actual environment which effects the thermal balance of a spacecraft in planetary orbit will provide the starting point for planning an integrated simulation system. The environmental characteristics include the solar energy incident directly on the spacecraft, the space heat sink, the planetary albedo and the planetary thermal emission energy. The effects of the thermal environment are also dependent on orbital characteristics, and spacecraft configuration.

Solar Energy

The solar energy requirements for a planetary simulator system will be similar to those for a deep-space simulator, except that additional provisions

must be made for on-off programming of the solar beam to simulate the eclipsing conditions.

Space Heat Sink

The heat sink requirements for a planetary simulation system are similar to those for a deep-space simulator where the test item is completely surrounded by highly absorptive cold surfaces. Therefore, in the design, both of solar simulators and planetary radiosity simulator systems, care must be taken to minimize non-absorbing areas and to preclude any direct reflection of energy from chamber components to the specimen.

Planet Radiosity

In planetary orbit a spacecraft will receive thermal energy input due to the planet radiosity. The radiosity includes the albedo energy which is essentially the percentage of solar energy reflected by the planet and the planetary thermal emission resulting from the effective temperature of the planet. The planet as seen from an orbiting satellite can be assumed to act as a diffuse (Lambert) reflecting or radiating surface. The total radiosity energy intercepted by a spacecraft will diminish with increasing orbital altitude due to the changing field angle of the planetary source as viewed from the craft. For a given altitude the planetary emission will provide a constant and symmetrical energy distribution on the satellite, while the albedo energy input will vary as the illuminated hemisphere is viewed from various positions in orbit. Even for low orbits, the radiation reaching the craft comes from a large distance and produces uniform illumination on various elements of the craft. This condition is difficult to produce in a simulator system due to the limited distance to radiating sources in relation to the physical extent of the test specimen.

The spectral energy distribution for the albedo and the planetary radiation differ greatly because of the difference in source temperatures. The solar spectrum is nominally equivalent to that of a 6000°K black body. The planetary albedo may be essentially of the same spectrum as that of the Sun though reduced

in intensity, or may show some selective reflection as in the case of the reddish appearance of the planet Mars. The planetary radiation of Mars and Venus has a spectrum which falls in the range of that from a black body at 210 to 260°K. This places the spectrum of solar energy and of planetary albedo into the visible region, and that of planetary emission broadly into the far infrared. Since spacecraft surfaces such as black, white, or polished metal will reflect or absorb these energies in a spectrally selective manner, spectrally correct simulation of the two components of radiosity is desirable.

For planning of a planetary orbit thermal simulation system, values for the planetary albedo and radiation energy are needed. Data for the planets Mars and Venus are summarized in Figures III-1* and III-2. These data include spectral distribution and integrated energy levels for the solar energy, maximum zero-altitude albedo energy, and constant zero-altitude planetary radiation energy. These values serve as the basis for determining the energy levels and distribution on a spacecraft for various altitudes, and orbital positions and orientations.

The energy inputs to specific spacecraft structural shapes, or to elemental spacecraft areas, can be determined by the application of "illumination factors" (shape or geometry factors) to the zero-altitude radiosity levels. These factors are based on strict geometric relations between diffusely reflecting or radiating planetary surfaces and orbital altitude, positions, and orientations. Although generally expressed for varying altitudes above the Earth, in Reference 7, tabulated values of illumination factors can be normalized to apply to orbits around any planet. Application of these factors will define the steady-state and the programmed variation in radiosity energy distribution which must be approached in a simulation system design.

Examples of the illumination factors for elemental areas distributed around a spacecraft and for various positions in an orbital plane which includes the planet-Sun line, are shown in Figures III-4 and III-5, using the coordinate notation outlined in Figure III-3. Figure III-4 shows the general energy

* Referenced Figures are grouped as the final entry in this section.

distributions for various normalized orbital altitudes which apply either for albedo energy at the sub-solar orbital point only, or for emission energy at any position over the uniformly radiating planet. The albedo energy diminishes and becomes asymmetrical for alternate orbital positions as shown in Figure III-5, which corresponds to a 1000 Km orbit over Mars. In comparison to these curves which show that the radiosity energy will generally be distributed more than ± 90 degrees around the craft, the solar energy input will extend only ± 90 degrees from the craft-Sun line following a direct cosine distribution.

As further examples of the distribution, variations, and interrelated orientations of input energy components, Figure III-6 shows polar plots of the summed energies for various positions in a 1000 Km Mars orbit. This also illustrates the requirements that a radiosity simulator system provide control or adjustment of the relative orientation of the radiosity sources with respect to the solar simulation, and also be coordinated with solar eclipsing and changing energy levels and distribution asymmetry for the albedo component. An actual simulation system will also require means for adjusting or programming the orientation of the test specimen with respect to the solar and planetary radiation sources to simulate planned random movement or stabilized orbital conditions. Thermal analysis verification requirements will determine the need for simulation of only the limiting conditions of energy variation and orientation or for more complex installations which would include gimbaling of craft or radiosity sources and programming through simulated orbital cycles.

Summary of Simulation Requirements

As has been shown, the thermal balance on a spacecraft in planetary orbit involves more complex interrelations of energy levels, energy spectrum and distribution effects, and positional and time variations, than the deep-space situation. In summary, the design of a practical planetary simulator system should consider the degree to which the following contributing factors and variables must be simulated to produce realistic thermal effects in a test installation:

1. Solar energy input including planet eclipsing.
2. Total absorption of energy radiated from the spacecraft, without reflection.
3. Different spectral distribution of albedo and planetary emission energy.
4. Spatial uniformity of radiosity energy across the spacecraft.
5. Variations in intensity and angular distribution of albedo energy with respect to orbital altitude and position.
6. Variations in intensity and angular distribution of planet emission energy with respect to orbital altitude only.
7. Cyclic variations in directional relation between solar and radiosity energy, and interrelation with spacecraft orientation.

An examination of the relative importance of the above characteristics for specific planetary missions, indicates some simplifications and simulation compromises which may be applied to the design of a practical planetary simulation system. The magnitudes of energy contributions across the boundary of a one-foot diameter (0.785 square foot projected area) spherical test volume for simulation of Mars and Venus orbits are shown in Figures III-7 and III-8. Examination and comparison of these figures can lead to the following general conclusions and considerations to be applied in the planning of practical simulation systems:

1. For Mars orbits below approximately 3000 Km, both albedo and planetary emission are important energy contributions and will require reasonable simulation.
2. For Venus orbits below approximately 10,000 Km, albedo is a major energy contribution and will require detail simulation including programmed variations.
3. For any Venus orbit, planetary emission is a minor energy contribution and can possibly be omitted from the simulation requirements.
4. Simulation requirements for Mars and Venus are sufficiently different to require separate designs rather than the additional complexity of a "universal" simulator.

5. Despite complexity in energy distribution and variation programming, the energy levels required for radiosity simulation are within the general capability of practical radiation sources.

Having considered the actual environmental characteristics and parameters which define the thermal balance on spacecraft in planetary orbits, and having defined the general characteristics of actual simulation systems, the following portions of this report section will further consider details of possible radiosity simulation methods and relations to testing objectives.

CURRENT TECHNIQUES

A survey of current techniques applicable to simulation of planetary albedo and radiation was performed. In addition to a review of References 40 through 44, a letter questionnaire and telephone survey was performed, details of which are given in Appendix A.

Simulation of the thermal effects of planets can be approached in two ways:

1. Duplication of the thermal radiation fields which would exist in the vicinity of the satellite.
2. Providing heat to the satellite surfaces to provide the required analytically-determined thermal inputs.

The first approach, if executed to perfection, would require the exact shape factors, intensities and spectral energy distribution. However, the only way to exactly duplicate these factors would be to provide a simulator the size of the planet being simulated. Therefore, attempts to reproduce the radiant thermal environment in a practical sized space chamber require compromises in simulation accuracy.

Most radiosity simulators used to date were developed for simulating the heating effect on satellites near the Earth or the Moon. These have been fairly unsophisticated systems which produce the approximate heat input, without attempting to duplicate the energy input distribution and the spectral

character. The methods used included heated radiating panels, infrared lamps, reflection of the simulated solar beam and contacting heaters.

Walt Camack of the Philco Corporation devised a more advanced system. His approach establishes a simulated thermal radiation field as it would exist in the vicinity of a spacecraft "seeing" the planet albedo and radiation. This is accomplished by an arrangement shown in Figure III-9. Within a reflective hemispherical cavity a diffuse radiation field simulating the spectral energy distribution of the albedo is generated by interreflections between the diffusely reflective cavity walls. The cavity is covered by a "radiation director" plate, i.e., a thick plate perforated by many conical holes which direct the light forward to the specimen. The holes shape the radiation into numerous conical beams of radiation, as shown in Figure III-9. Within the test volume above this simulator a uniform illumination field will exist. As a point moves across a test plane parallel to the perforated plate, the same number of holes illuminate it at all times. As a point moves away from the plate, the number of holes seen increases by the square of the distance from the plate, yet the illumination from each hole diminishes by the inverse square of the distance, resulting again in constant illumination.

The energy sources in this system can be selected to yield a combination of planet albedo and radiation. The diffusely white painted hemisphere reflects short wave length albedo radiation and can perform an integration of several spectral varieties of sources because of multiple and diffusive inter-reflections. The temperature of the hemisphere can be controlled to produce the desired level of long wave length planetary radiation.

The Conformal Lamp Bank or Wrap-Around Approach of supplying the required heat input to the surface of a craft is to shape the radiating sources to fit the envelope of the spacecraft and then program the lamps on and off, or control the power level, to achieve the desired heat input, possibly even including the simulated solar thermal input.

A modification of this wrap-around approach is to install banks of lamps on a moving frame to allow orientation of the albedo with respect to the sun

which is simulated separately. In this approach, the lights are grouped to simulate as nearly as possible the energy distribution on the specimen which would be received from a planet. In addition to the rotation of the entire assembly, the lights can be programmed to simulate various orbital conditions and altitudes.

COMPONENTS OR ELEMENTS OF A RADIOSITY SIMULATOR SYSTEM

The following components are considered for application to the simulation of planetary thermal environments:

Heated Shrouds

Heated surfaces can contribute radiant energy proportional to the area of radiation surface and the temperature to the fourth power, and with a location of the spectral energy peak dependent on temperature in accordance with Wien's Displacement Law. To get energy with the proper spectral distribution and at the proper intensity level, a large surface area at an equivalent planet temperature would be required. Intensification of low temperature radiation energy without change of the spectrum can be accomplished only by making the shape factor larger. It is not practical to collect and focus, or collimate this energy. The difficulty arising in simulation because of this effect is illustrated by Figure III-10.

The shape factors at points 1, 2 and 3 are quite different and as a result the radiation intensity will also vary drastically for vertical planes throughout the test volume. The intensity and direction of illumination on other parallel planes, as illustrated by points 4 and 5, will also vary drastically. If the specimen is of compact geometry filling most of the test volume, the importance of this variation will be reduced by the averaging effects of thermal diffusion within the specimen. But, if the specimen is a "spider" type, many surfaces may be illuminated improperly.

An approach which will enable better simulation of the desired intensity distribution is to replace the solid shroud with strips or rings at a higher

temperature. For example, increasing the absolute temperature by a factor of three increases the radiation energy of a surface by a factor of $3^4 = 81$, while shifting the spectral energy distribution curve toward the shorter wave length by a factor of $\frac{1}{3}$. This increased energy capacity makes it possible to use 81 times less surface in the simulator to provide the required energy level. This then allows the distribution of the radiating elements around the specimen to provide more nearly uniform intensities to parallel surfaces and better distribution of energy around the specimen. The use of smaller sources may also allow the use of reflectors to beam the radiation to achieve a better simulation. Whether or not the shift of the spectral energy toward the short wave length will change the thermal balance of a specimen will depend on the specimen being tested. If the reflectance and absorptance of surface finishes are not greatly different for the shifted spectrum, the thermal balance will not be significantly changed.

Bare Filaments

Bare filaments can be used in a vacuum to provide radiant energy of high intensity which can be directed with reflecting surfaces. The spectrum of energy would fall generally between that of reflected solar energy and the planet radiated energy. Depending again on the characteristics of the specimen, this spectrum may be suited for simulation of full radiosity energy, partial simulation, or none. The advantages of a bare filament as a source is its simplicity and economy for installation and maintenance. It occupies very little volume and it is easy to provide power and to control the power level.

Graphite Fabric

Newly marketed for heating purposes by National Carbon Company is a graphite cloth which can be used in vacuum at temperatures up to 3000°K . This material can be used to provide very high radiant energy flux.

Incandescent Lamps (Tungsten Filament)

A large variety of lamps can be used to provide radiant energy. The

main advantage of mass produced lamps is their low cost, ease of installation and replacement, and the low cost of power and controls. Lamps with built-in reflectors focus the beam into a cone with cross-sections similar to those shown in Figure III-11.

Photo-flood lamps operating up to color temperatures of 3400°K (location of spectral energy peak at approximately 0.85 micron) can provide near simulation of albedo spectrum, but the rated life is low (4 to 10 hours).

Quartz-iodine lamps give very long life at their rated power level with a color temperature of 3000°K and, because of the iodine cycle which prevents the tungsten from depositing out on the quartz envelope, the intensity remains essentially constant throughout the lamp life. These lamps can, at the penalty of shortened life, be overpowered to yield a higher temperature as shown in Figure III-12. By raising the power by 70%, for example, to increase the color temperature from 3000°K to 3450°K (15% increase), the life can be expected to be reduced from 2000 hours to 25 hours (a factor of 80).

Fluorescent and Vapor Lamps

Fluorescent lamps were considered for supplementing the visible light spectrum of albedo because of their high efficiency in producing light in the 0.3 to 0.6 micron range. However, a 40 watt fluorescent lamp is quite large and produces only about 8 watts in the desired range. As a result, more lamps would be required to develop a practical energy level than can be physically placed into the area around a specimen.

Color-corrected mercury lamps provide a visible light spectrum similar to the fluorescent but in a smaller envelope. However, the high proportion of infrared energy and the poor control characteristics make this type of source also rather impractical. About 20 minutes are required to achieve full brilliance on start-up of mercury lamps and where the lamp is turned off after a period of operation, it needs to cool for several minutes before it can be restarted. These lamps are also somewhat temperature sensitive both from starting and operating standpoints, and because the envelope operates at a very

high temperature it must be protected against temperature shock. It is probable that they could be operated in a vacuum, although there would be hazards from lamp failure and explosion.

Both Sylvania and General Electric have announced the development of new and improved vapor discharge lamps having a 50% improvement in efficiency over standard mercury lamps because of the use of additional metal vapors. These lamps have a broad spectral energy spread in the visible range.

Gas-Arc Lamps

Both long-arc and short-arc gaseous discharge lamps with suitable filtering can be used to produce high intensity energy with essentially a 6000°K source spectral distribution. The short-arc sources provide a point source which can be located at a reflector focus and provide a suitable beam for specimen illumination. However, it is questionable that they could be operated reliably within a vacuum environment. The long-arc lamp operates with lower electrode and envelope temperatures, and as indicated by the Ozram Company data, and Reference 44, these lamps can probably be operated in vacuum at reduced power levels.

Contact Heaters

Heaters built into the specimen cannot actually contribute to the simulation of a radiosity environment and have not been considered in devising a radiosity system. However, specimen temperature simulation is the final goal of thermal environment simulation. In certain instances it might be simpler to predict the amount of heat which would be absorbed by a surface and provide this input by contact heaters within the specimen rather than from radiation sources.

Optical Elements

Reflecting surfaces to be used in radiosity simulators will generally be highly polished metallic surfaces, possibly protected with thin transparent films. These reflecting surfaces, especially those with protective coatings,

may have spectrally selective reflectance, i.e., they may reflect some wave lengths better than others. This may, in some cases, cause degradation of the spectral energy distribution, or may be used for controlled selective reflectance to improve the desired spectrum.

Interference filters can be deposited on flat surfaces to give a reflectivity of from 80 to 95% in the visible range while rejecting most of the energy in the infrared region. The control of deposition on curved surfaces is difficult and may result in a lower efficiency. The cutoff wavelength of interference filters is controlled by the spacing of the surfaces and it appears possible to approach the type of reflectance which might be required to make color correction for the Mars albedo spectrum.

Another example of selective absorption of some of the infrared spectrum from a 3400°K source to shift the apparent energy spectrum toward that of a higher temperature source is the use of a white painted surface. Its temperature could also be controlled to provide low temperature radiation to simulate planetary radiation.

Selective filtering in a vacuum environment should generally be accomplished by spectrally selective reflector surfaces rather than selective transmission. If the filtering is accomplished by window elements, absorbed energy in a vacuum will be dissipated by radiation. For example, the glass window in Figure III-13, intended to filter out the infrared portion of the light beam, must get hot enough to re-radiate all the energy absorbed. This may result in a spectrum more or less acceptable than the original unfiltered beam. Water filters can provide essentially the filtering desired and by the addition of certain chemicals such as copper sulphate (as indicated on page 256 in the Science of Color - Reference 45), further color correction can be achieved. If water is used for filtering, circulation will provide a means of temperature control. Heating or draining the water to prevent freezing when the lamps are turned off may be necessary in a chamber with LN₂ shrouds.

SIMULATION PHILOSOPHY

Objectives

The objective of simulating the thermal environment of a planet on an orbiting spacecraft is to determine the specimen temperature response to the expected mission environment and to confirm functional integrity of the spacecraft equipment during the test period. To accomplish this, it is necessary to provide reasonably accurately the thermal input to the specimen without altering its emitting properties. Solar simulation as a part of the total thermal input to a spacecraft must be included in a thermal balance test and the directional relationship between the solar and planetary inputs must be defined and provided. The actual degree to which the thermal input factors need to be reproduced depends on the specific test purposes and the specimen characteristics. Further, the simulator has to be integrated with a suitably sized vacuum chamber in a time period and at a cost which can be justified by the test requirements.

Test Approaches

The need for performing tests to aid, supplement, and verify analytical predictions of the thermal response of a spacecraft is due to the difficulty in determining and describing the thermal response characteristics of the specimen. In the test or physical experiment, the specimen may be the actual spacecraft or a duplicate of it which copies the thermal response characteristics. However, in testing it becomes very difficult to provide all the diverse and varying thermal environments which can readily be described for thermal analytical calculations. Thermal test in a vacuum may be required: (1) to determine thermal responses of a specimen to allow improved calculations of the thermal response during space missions, (2) to determine the thermal response to specific environments, or (3) to perform qualification and equipment functional checks during simulated mission environments.

One approach to accomplish these results is to simulate the extremes of thermal environments. By inducing step inputs of environments, the specimen

thermal responses can be determined and a period of stabilization will determine either the time required to reach permissible temperature limits or determine what maximum temperature extremes are achieved at steady state. Equipment function checks can be made in conjunction with the thermal check.

A second approach is the simulation of periodic time averages of thermal environments. This approach permits steady state testing without hazarding out-of-tolerance temperatures to sensitive components. This, again, can be applied in step functions to determine the specimen responses.

A third approach to thermal testing is simulation of all the cyclic variations of the thermal space environment. This would give the best check of proper equipment functioning. The main problem in attempting to simulate the total cyclic space thermal environment is the extreme difficulty encountered in attempting to adequately simulate all aspects and time dependent changes of the space environment.

To evaluate the value of a simulation technique it is necessary to consider the results desired from tests, all the environment variations to be simulated, and the test chamber and specimen factors.

Spacecraft Factors

Many of the characteristics of the spacecraft can be factors in determining the requirements for simulation. Inversely, test limitations may restrict the design selections. The size, weight, thermal conductivity, and specific heat of a spacecraft will affect its sensitivity to rapid transients of inputs and will also determine the need for uniformity of illumination. A large craft with heavy structure having a high thermal diffusivity and a high specific heat will not respond readily to short period transients of heat input. Even if the heat is not distributed uniformly or correctly, the high diffusivity and thermal inertia of the craft will tend to average out the discrepancies. A light weight craft on the other hand will quickly respond to variations of heat input.

The shape or configuration of a spacecraft is a factor in determining the requirement for accurate reproduction of the energy distribution around and

through the test volume. A specimen with many separated and loosely connected experiments will require that the thermal inputs have nearly correct view angles and intensities for all exposed surfaces. A flat-sided specimen with no voids or cavities could tolerate a thermal input of any view angle, as long as the flux was uniform across the flat surface. With a "solid" specimen, the requirement for a flux uniformity with depth is also reduced.

The thermo-optical surface properties of the spacecraft determine the need for matching the simulated radiosity spectral energy distribution to that of the actual space environment. Surface properties can also affect the thermal balance for varying angles of incidence of the radiosity.

The placement of components within a spacecraft, the temperature limits of the components, and the methods of controlling temperatures will also affect the simulation accuracy requirements. The required duration of test runs determines the life rating required for radiation sources.

Error Analysis

The thermal environment of space or the radiosity field can be described in vector terms of direction or field of view, intensity, and spectral energy distribution. The energy intercepted by a spacecraft, however, is usually measured in terms of flux incident to various surfaces. Errors in spacecraft temperature response during tests will occur because of deviations in simulation.

The following potential deviations from desired energy input and the associated spacecraft factors will determine the error factors and consequently the importance of accurate simulation.

1. Total intensity or energy level deviation from required level.
2. Non-uniformity of intensity across a plane.
3. Non-uniformity of intensity with depth of field.
4. Deviation from proper intensity at various angles.
5. Deviation from desired spectral match.
6. Fluctuation of energy intensity and spectral match with time.

A deviation of the basic energy level will affect the specimen temperature by a factor of one-fourth that of the energy error as shown by the equation

$$\frac{dT}{T} = \frac{1}{4} \frac{dE}{E}, \text{ derived by differentiating the radiation relationship } E = A\sigma\epsilon T^4.$$

The actual temperature errors resulting from improper energy distribution and spectral mismatch will not be as high as indicated by this equation because of the averaging and integrating effect of the spacecraft as discussed above.

Other factors which need to be considered with the simulation of planetary radiosity are the solar thermal input, the simulated space cold sink, the vacuum facility and the specimen support structure and instrumentation. Since the distribution of radiant energy around the specimen is very dependent on the direction of the thermal inputs, errors can result from improper positioning of the radiosity sources relative to the simulated solar radiation.

Trade-Offs in Simulation

The importance for providing the various features of radiosity simulation should be determined from the specimen properties and the test results required, and then established to the best degree allowed by the limitations imposed by time, cost, and compatibility between simulation features.

Table III-1 lists desirable features, with some approaches for achievement, and illustrates that designs which optimize one requirement may sacrifice others.

TABLE III-1 Desired Radiosity Simulation Features

DESIRABLE RADIOSITY SIMULATION FEATURES	POTENTIAL TECHNIQUES FOR ACHIEVEMENT
Wide range of intensity with control or modulation and rapid on-off control; absence of uncontrolled variations or fluctuations.	Use sources with a wide range of power control which can be turned on and off quickly in the extreme temperature and vacuum environments to be encountered.
Uniformity of intensity in all parallel planes.	Many small sources located a long distance from the specimen.
Proper distribution of energy for various angles (shape factor or view angle).	Set power levels and control the beam width of sources or the source distribution.
Change of view angle or energy distribution.	Change power levels and source beam widths or the source locations.
Motion of the radiosity simulator relative to the specimen and the solar simulation.	Program the sources around the chamber or rotate the array (make the array light-weight and simple). Specimen gimbaling may also be required to achieve full relative positioning.
Radiosity spectral match and changing spectrum for various phases.	Use sources with appropriate color temperature. Use filtering. (Heat removal will be required.) Study specimen properties to establish the degree of match required.
Avoid shielding the specimen from the Sun or space heat sink simulators.	Small sources and arrays with restricted or no motion.
Compatibility with a vacuum facility long life and reliability.	Locate radiosity sources close to specimen. Use rugged long life sources and elements.

Presently Used and Proposed Systems

The systems presently used in planetary and lunar simulation have been designed to partially simulate the thermal environments of the planet Earth or of the Moon. Their limitations are recognized and the measured response is effectively corrected by analytical methods.

Some of the proposed systems are more sophisticated but still quite restricted in their ability to fully simulate varying altitudes or provide correct spectral simulation of planet albedo and radiation. These systems will be more effective in partially simulating the required environment. The thermal balance achieved by the specimens using these more advanced simulators will be much nearer that encountered in space, than it would be without inclusion of the planetary radiosity simulation, and with analytic corrections close predictions will be possible for the actual temperatures encountered in a space mission.

SUGGESTED SIMULATION APPROACHES

Tailored Design

Because of the many ramifications to be considered in simulation of planetary radiosity and because improving one feature may tend to degrade others, the simulator system design should be tailored to accommodate specific specimen types and specific mission environments. By anticipating the probable specimens and prediction of their properties, the thermal environment features which will most affect the thermal balance can be predicted and a practical simulator designed.

Thermal Energy Sources

To achieve distribution of thermal energy to a specimen and simulate reasonably the uniformity and view angle requirements, it is desirable to spread many small sources over a wide area. The energy flux to the specimen may be controlled by varying the number of sources on full power, rather than varying power input rate from all sources. This requires that the smallest

number of sources on full power provide adequate distribution and uniformity. This technique allows better control of spectral energy simulation. However, if distribution and uniformity is disturbed by this technique it will be necessary to control the source power input or otherwise restrict the radiation flux.

Optics Distribution and Motion

The optics to be used with planetary radiosity simulators should, if possible, be restricted to reflector elements. These should have high reflection efficiency in order to get the maximum source energy directed toward the specimen and reduce heating of the reflector. Reflectors must be temperature controlled to avoid radiation at undesired wavelengths. Figure III-14 shows some approaches to achieving distribution of energy to a spacecraft. Figure III-14 (a) shows several collimated sources directing energy toward the specimen from different angles. It can be seen that this design achieves uniformity of illumination on parallel planes throughout the test volume. As was shown by Fitz and Mayer (Ref. 41), the distribution of energy around a specimen from five collimated banks closely simulates the distribution desired. If a sufficient number of arrays could be provided at the proper intensities and spectrum, a radiosity field very similar to that encountered by the craft in orbit would be produced. However, the optics for this type of a system would be very complex and costly and the arrays probably would be less movable than the solar simulator. Further, it is not possible to collimate the low temperature planetary radiation.

Figure III-14 (b) shows projection systems wrapped around a test volume. The intensity of illumination can be seen to vary with depth because surfaces further from the projection source receive energy reduced proportionally to the square of the distance from the source. The distribution of energy across a plane in the test volume which is essentially parallel to the array will depend principally on the energy spread in the source beams. If the beam is more intense toward the center, the center of the test volume will receive more energy than the sides.

As the number of full projection lamps is increased, as shown by Figure III-14 (c), the distribution of energy around the surface of a spherical test specimen or volume can be made very nearly that which would be encountered in space. The uniformity with depth, however, will still vary. And, in order to achieve the distribution around the far side of a test volume some back lighting of surfaces on the near side will occur.

The approach depicted in Figure III-14 (d), as proposed by W. Camack (Ref. 42) provides essentially correct illumination to the specimen volume for one orbital altitude and position. Uniformity on all parallel planes in the test volume is provided due to the fact that as the illumination to a plane decreases because of distance from one source, the illumination increases in the same proportion because the number of sources in a specific view angle increases by the square of the distance from the sources. The distribution of energy around the specimen will depend on the beam shape of the individual source. If the planet being simulated is assumed to have a diffusive or cosine distribution for radiated or reflected energy, the individual beams should be shaped to that configuration by reflectors or other devices. A technique devised by W. Camack for application of this approach has been previously discussed and is shown in Figure III-9.

The approach shown in Figure III-14 (e) has combined the wrap-around approach with the shaping and directing of beams to achieve good uniformity and good distribution around the specimen. The figure shows the simulation for the sub-solar orbital position, and the beams toward the edge of the simulator are narrower and directed toward the far side of the specimen surfaces on the side nearest to the planet simulator. In this design, the distribution around the specimen is more dependent on the number and placement of sources than on the shape of the beam.

Because there are apt to be a large number of sources in a simulator they should be kept simple to reduce their weight, volume and cost. They should be designed to avoid extensive and tedious adjustments. The efficiency should be high to avoid the necessity for complicated and costly cooling systems to

remove large amounts of waste heat. Further, it is anticipated that even very unsophisticated optical systems may display unexpected distribution of energy because it may not be practical to use point sources of radiation for radiosity simulation. In the radiosity simulator the necessity for a large number of sources to provide energy distribution has been pointed out. This large number will also help to average out irregularities in lamp beams. Some methods suggested for directing radiant energy are illustrated in Figure III-15.

Standard filament lamps with built-in spherical or parabolic reflectors are designed to provide a wide variety of beams from narrow spots to wide flood angles. The long-life lamps have fairly long and wide-spread filaments and as a result the beam has some irregularities as illustrated, (Fig. III-15). It is possible with fairly simple elements to further modify such light beams. A cone surrounding a lamp beam tends to trim the edges and reinforce the center portion of the beam. A flat mirror can split a beam and redirect the light to the opposite side. This flat mirror could be moved back and forth mechanically to change the beam shape. An internally reflecting sphere with a hole in one side sized to shape the beam to the desired field angle has been suggested to achieve high efficiency.

Figure III-14 (f) depicts a simulator for a spacecraft at 60° from subsolar. At a shifted orbital position three main changes in the planetary thermal input occur: (1) the center of the simulated apparent planet disk rotates; (2) the intensity will reduce, (3) non-symmetrical illumination, dependent on the altitude, will occur. If an altitude change coincides with the orbital position change, a further change in the intensity and energy distribution results. Physical rotation can accomplish the first requirement of rotating the planetary disk center relative to the sun, but for all others it becomes necessary to change or regulate the emission from the sources. On and off programming of the sources around a test specimen can also produce the simulation of rotation required, and since the other orbital changes may require switching of sources, it appears desirable to study this approach to accomplish

the total change without physically rotating the planetary simulation array.

If the specimen to be tested essentially fills the test volume so that continuous surfaces of a sphere, cube or similar shape receive the radiative energy inputs, the wrap-around approach can be used with the sources distributed to provide proper energy distribution to just the outside surface of the specimen. Concern for the distribution of energy to the far sides of the specimen will be omitted since the specimen would shield those surfaces from receiving radiation in space as well as in the chamber. When a specimen has discontinuities or voids in its structure which allow radiation to pass through or past parts of the specimen to additional surfaces, it becomes more necessary to use the approach shown in Figure III-14 (e) to assure that surface S_1 receives energy from a larger number of sources to compensate for the fact that it is further away and to assure that surface S_2 (back side) does not receive undesirable energy.

One problem created by attempting to switch control of the planet simulator to create the rotation simulation is the requirement for changing the beam shapes. One possible way to accomplish this is to use mechanical adjustment of the lamp directions or to use mechanical motion on reflectors to shape the beams. Another method is to have the total beam composed of double or multiple sources and switch on only those which give the desired beam shape. This might also be part of the total intensity control.

Assuming that the specimen is on a double ring gimbal which will allow any surface to face the Sun, it will be necessary to rotate planetary albedo from the sub-solar position through one axis of rotation, only, to the simulation of a position near the terminator, or to the point where the magnitude of albedo becomes negligible. Simulation of the planetary radiation theoretically should be continued around to and through the Sun position. However, the Sun is eclipsed during this period so the gimbal device can be used to position the planet radiosity simulator relative to the specimen.

One limit imposed on the motion of the planetary radiosity simulator

relative to the solar simulator occurs when one extreme edge of the planetary simulator would eclipse the solar beam. As illustrated in Figure III-16, the actual satellite receives both solar radiation and planetary radiosity. When the planetary simulator is devised to yield similar shape factors, part of the planetary radiosity array eclipses part of the solar beam. This limit exists for either a physically rotated array or a switch programmed array. A compensating factor is that in restricting the simulated rotation of the planet simulator to avoid eclipsing the Sun, the only portion of the planet radiation which needs to be sacrificed is rendered less consequential because it overlaps the solar radiation.

Mars System

For a Mars radiosity simulator first consideration will be given to simulation of the planetary radiation because as was shown in the discussion of requirements, the low albedo of Mars makes the planet radiation relatively more significant. The generation of the required amount of long wavelength radiant energy demands a large area of radiating surface. Also, the shape factor between the specimen and the simulator is not constant with distance when the simulator is located close to the specimen, as is necessary in a chamber.

The examples in Figure III-17 shows the simulator disk split into several rings each having different shape factors toward various portions of the test volume. It is thus possible to improve the distribution of this type of energy to specimens. Changes in orbital position and altitude could be produced by cooling sections of the simulator to reduce its radiation to the specimen. Radiant sections could also be made up of louvers which could be turned to present more or less of a radiating surface toward the specimen. This will reduce response time in simulation of the effect of changing positions and altitudes.

As previously discussed, increase in the temperature of the radiators will increase the energy per unit area greatly at a small sacrifice of correct

spectral distribution. This allows reduction of the amount of radiating area required to produce the required energy levels and helps achieve better distribution and faster modulation. Infrared radiation will also be emitted by the albedo sources at a spectrum depending on their temperature which can be controlled by their cooling systems. The distribution of the albedo sources should approximate that required for planet radiation. It is possible that for planet radiation without albedo, as would occur during the eclipse, a very low power supply level to the albedo sources will provide adequate radiation.

The "red" planet Mars appears to have a spectrally selective reflectance which modifies the solar spectrum so that the peak of albedo energy occurs at a wavelength of 0.8 micron. This spectral distribution cannot necessarily be reproduced by a 3200°K black body radiator because the energy reflected by Mars is deficient in energy in the long wavelengths. Possible approaches for generating this energy spectrum are: (1) the use of standard (long life) filament type lamps, (2) the use of high temperature (3400 to 3600°K) tungsten or carbon filament lamps, or (3) the use of gas arc lamps. In all three cases, it would be possible to employ filtering to improve the spectrum toward the expected Mars albedo.

Venus System

Venus radiosity is predominantly the result of albedo. The spectrum is apparently quite similar to that of the Sun. The planet emission, while it is numerically in the order as that of Mars, is much less significant relative to the higher albedo and solar energies at Venus. Because of this, and because this low temperature radiation is difficult to simulate in correct spectral and lateral distribution, priority should be given to good albedo simulation and planet radiation requirements be satisfied as best as practical. It is expected that one problem will be the reduction of unwanted infrared excess from the albedo system and some of this excess can probably be used to simulate planet radiation to the accuracy required. Venus albedo simulation will require sources either 10 times brighter, or 10 times as many sources, than will be required for Mars. Design of one facility to simulate the environment of both

planets would require a great number of compromises in the simulation for both cases. If the simulator is designed to Venus criteria, it would be very difficult to restrict the input sufficiently to achieve reasonable simulation for Mars. However, such a unit would also encompass the range of environment effects encountered in Earth orbit.

Because of the high energy requirement and the need for the 6000°K temperature equivalent, consideration should be given to using gas arc lamps as sources for a Venus albedo simulator. With this type of lamp, it will probably be necessary to sacrifice some of the uniformity of energy distribution and control of phase and orbital altitude changes.

CONCEPTS FOR SPECIFIC APPLICATIONS

For the purpose of applying Mars and Venus planetary simulation techniques to a specific case, a specimen will be assumed having the following characteristics:

Size and Weight:	10 foot diameter - 5000 lbs.
Shape:	Approximately spherical except having voids and projections to cause shadowing.
Structure:	Outer shell conductivity equivalent to 1/8" thick aluminum.
Surface Thermal Optical Properties:	Black, polished aluminum, and white paint ($\alpha/\epsilon = 1/5$) with the emissivity change occurring essentially linearly between 3 μ and 6 μ wavelength.

It will be assumed that an elliptical equatorial orbit will carry the craft from 1000 kilometers to 8000 kilometers of altitude. The craft will be assumed to be planet oriented (one side of the craft always facing the planet).

A space chamber with the clear test volume of approximately a 20 foot diameter sphere with a fixed-position 10 foot diameter solar simulation beam will be assumed to be the facility to which a planet simulation system shall be added.

The requirement for the craft to face one side constantly toward the planet makes it necessary to provide a two-axis gimbal with a 180° motion capability in each axis. Figure III-18 shows how the combined solar and planetary simulator could be phased to simulate a 360° orbit.

The specimen is rotated 180° around a Sun planet axis at the sub-solar and at anti-solar position. This avoids the need for placing a planetary simulator completely around the chamber.

Mars Simulator

For the Mars Planet simulator the maximum intensities of reflected and radiated energy and the direct solar energy at 1000 kilometer altitude at the sub-solar point intercepted by a 10 foot diameter sphere are, per Figure III-7:

Planet albedo	= 900 watts (based on albedo = 0.295)
Planet radiation	= 585 watts (based on 211°K planet temperature)
Solar radiation	= 4400 watts

The sources to be used for the albedo simulator are tungsten filament lamps operated at 3000°K with filtering used to modify the spectrum to nearly match that of the Mars albedo. On Figure III-19 it can be seen that the spectrum of a 3000°K filament source considerably exceeds the Mars spectrum in the infrared region when the total intensity is raised so that the levels are equal at the expected Mars peak of 0.8 μ .

The filtering required is approximately 50% of the total energy from the source. The filtering or optics should have essentially the characteristics shown in Figure III-20.

Several materials have characteristics approaching the desired curve. Blue filter elements tend to color correct in the required manner and certain "white" paints have selective absorptivities increasing rapidly toward longer wavelengths. It is expected that the total efficiency of the elements will be

somewhat reduced by unwanted absorption in the required spectrum. Additional losses will be encountered because of the collection efficiency and because of beam shaping requirements. The beam forming devices will be spherical reflectors as shown in Figure III-21. The color correction capability of the double reflector unit is greater because all energy is reflected at least one time and some two times.

The total efficiency of the albedo system is the product of the lamp efficiency (approximately 80%), the collection and filtering efficiency (25% estimated) due to deliberate rejection and inadvertent losses, and the efficiency of directing and shaping the beams to give the desired shape factor and energy distribution (estimated at 50%).

$$\text{Total efficiency} = 0.8 \times 0.25 \times 0.5 = 10\%$$

To furnish the 900 watts for the 10 foot spherical test volume at 1000 kilometers, a total input of 9 kilowatts is required. Thirty 300 watt iodine quartz lamps would supply this power. Figure III-22 shows 37 lamps distributed on a hemispherical dome essentially in a projected close-pack pattern on 40" centers. The reflectors will direct energy in such a manner that points on the far side of the chamber receive energy from more lamps than those on the near side thus maintaining nearer to a uniform distribution with depth. The number of lamps used in this distribution cannot give entire uniformity to the energy distributed on the specimen surface nor to the uniformity with depth. The flux at specimen surfaces perpendicular to the axes of symmetry of the simulator is approximately 9.5 watts per square foot for the orbital conditions called for. An accurate calculation of energy distribution and uniformity could be made provided full definition of actual beam pattern and other variables would be available.

To achieve the required motion of the albedo simulator relative to the Sun, fifteen additional lamps will be distributed around one side of the chamber, some of them overlapping the existing array but at a different angle to produce the shape factor from the planet at a different direction. These lamps will be located up to the maximum angle which does not cause them to

obstruct the solar simulator assumed to be 10 feet in diameter.

The Mars view angle for an altitude of 1000 kilometers is approximately 105° . To simulate higher altitude conditions it is necessary to restrict the sources to a narrower angle of view and to reduce the intensity. For an altitude of 8000 kilometers, the view angle is approximately 30° and the total planetary thermal input is approximately 10% of that at 1000 kilometers. If this simulation is accomplished by turning off 90% of the sources, only four will be left on. It is doubtful that a good lateral distribution of energy to the specimen could be effected with only four lamps. Furthermore, the lamps toward the center of the simulator have greater total energy than those at the sides, so it appears necessary to use both the shutting off of some lamps to reduce the view angle and a diminishing of the emission of those left on, to reduce the total energy. One method available is the reduction of the power level to the lamp. This will change the spectrum of the albedo, and may be unacceptable. However, if the determination at the lower orbit simulation determines the relative effect of the spectrum, it might be possible through analysis to ascertain the effect at the new altitude condition. Further, since the albedo input does become less significant when compared with the solar input (roughly 2% at this altitude), accuracy of albedo simulation becomes relatively less important.

Other techniques for reducing the thermal input of the simulated albedo are to pulse it "on" and "off" periodically in periods long enough to assure full brilliance of the sources, but short compared to the thermal response periods of pertinent items on the specimen. In this way, a 10 to 1 reduction in thermal input from the albedo simulator could be approached by reducing the number of lamps "on" to 30% and then switching these "on" for one minute and "off" for two minutes for another 30% reduction.

The amount of energy emitted from the source could be mechanically reduced by means of an iris diaphragm or a shutter.

Because 9000 watts were introduced to the chamber and only 900 watts

were usable for albedo simulation, it will be necessary to reject some of the excess heat. The excess energy can be used to provide planetary radiation simulation. The temperatures desired will then be considerably above liquid nitrogen temperature and it will not be necessary to cool surfaces with LN₂ during operation. (However, when the chamber is used for deep space simulation and planetary radiation is not required, it will be desirable to cool these surfaces to LN₂ temperature to effectively remove them as radiant heat sources.)

The reflection elements of the albedo simulation sources are designed to absorb infrared radiation and will be good sources of simulated planetary radiation. If the 37 reflectors used in the 20 foot diameter hemisphere are each one foot in diameter, their total area is only approximately 5% of the area of the hemisphere.

The shape factor from the reflectors to the specimen volume is approximately .07 if the reflectors radiate in all directions. Approximately 5000 watts of the total 9000 watts for albedo will be absorbed by the reflector elements and then re-radiated at a temperature of approximately 460°K. This means that only 350 watts will be received at the specimen volume. To increase this to the necessary 585 watts it will be necessary either to increase the temperature to approximately 520°K, shifting the peak of the black body spectral distribution curve from the desired 14 μ to 5.6 μ . Modification to the spectral distribution can probably be better tolerated than a poor lateral energy distribution and the change in shape factor which would occur if a greater area at lower temperature were used as simulated planetary radiation source.

Desired temperature increase could be accomplished by restricting back-side radiation (by providing a low emissivity polished metal finish) or by increase of the total heat input to the radiating reflectors.

A simulation of the 8000 kilometer altitude position calls for a reduction of planetary radiation to 10% of that at 1000 kilometers. This can be accomplished with 30% of the sources in use, reduced to a temperature of approximately 400°K to further reduce the radiation by a factor of 3.

Venus Simulator

For a satellite in a 1000 kilometer orbit around Venus, the maximum energies intercepted by a 10 foot diameter spherical specimen are, per Figure III-8:

Planetary albedo	14,000 watts (based on albedo .76)
Planetary radiation	1,140 watts (based on 231°K planet temperature)
Solar radiation	19,500 watts

The very high intensity Venus albedo apparently has a spectrum very nearly matching the Sun's. The approach which was used to generate color corrected albedo for Mars by absorbing the excess infrared energy from an oversized 3000°K source becomes rather impractical for Venus. As shown by Figure III-23 the excess infrared resulting from oversizing the source approximately four times to bring the level up to that of the Venus albedo spectrum peak at 0.5μ results in an excess of 10 times the desired energy. This, coupled with the inefficiencies of the optics, makes it impractical to try to absorb and reject all the excess energy. Even when a 3400 to 3600°K filament source is used, with the resultant radical reduction in lamp life, the excess energy makes this approach unattractive for spectrally correct albedo for Venus.

If spectral match can be compromised, filament sources are the easiest to install and control to provide the total flux. For Venus the total planetary albedo and radiation intercepted by a 10 foot diameter satellite at 1000 kilometers is 15 kw or 10 times that for a Mars satellite at the same altitude. By using an approach similar to that used for Mars, but not attempting to color correct, a thermal flux simulator could be built. If 1000 watt lamps are used with lamp efficiencies of 90%, collector efficiency of 50% and a beam distribution efficiency of 50%, 225 usable watts could be realized from each lamp. Forty-five lamps would be required for the sub-solar position energy. This results in an excess energy of 35 kilowatts in the chamber which needs to be absorbed in some way. Much of this will be picked

up by the LN_2 shrouds due to spurious radiation. Some can be taken out by water cooling or by some other relatively high temperature fluid. With poorer distribution of energy tolerated, the efficiency of the distribution system could be improved to reduce some of the excess energy.

To achieve nearly spectrally correct albedo simulation for Venus, it will be necessary to use a 6000°K source, e.g. a gas arc lamp. Information received through the courtesy of Mr. A. Landau, from the Ozram Lamp Company, indicates that a 6000 watt long-arc lamp can probably be operated in vacuum at a 3000 to 3500 watt level. It is not known what operation at this power level will do to the spectral energy distribution of the lamp, but it is expected that it will not change radically from the maximum energy state. Since these lamps have a high energy band in the infrared it is desirable to use some filtering with reflection, as was proposed with the Mars system, to improve the spectrum. Since the long arc is not a point source, it is not practical to use a spherical reflector, but instead a cylindrical reflector will be used to shape the radiation and filtering will be accomplished by absorption of a percentage of the excess infrared.

Gas arc lamps have efficiencies of approximately 50%. The collection and beaming efficiency is expected to be 40% with a filtering efficiency of 70%. The total usable energy from a 3 kw operating lamp will then be approximately 400 watts. To provide the required 14,000 watts for albedo, 35 lamps will be required. These will be spaced in concentric rings around the hemisphere of the simulation chamber.

Figure III-24 shows 37 gas arc lamps and reflector elements distributed on the bottom hemisphere of a chamber. It will be necessary to optimize the spacing, the displacement from the specimen, and the shape of the beams to achieve acceptable energy distribution around the specimen. It will also be desirable to mix Xenon and Mercury-Xenon lamps to achieve improved spectral match with minimal filtering required.

Rotation of the albedo simulation relative to the solar beam will be

accomplished by turning off most of the main array below the specimen and turning on some above. Simulation of a higher altitude will be simulated by selectively turning lights "off" and by reducing the power to those remaining "on". It is not known how far the power can be reduced before the lights extinguish, nor what effect the further reduction in power will have on the spectrum.

It will be necessary to fluid-cool the lamp electrodes to reduce the infrared heat radiation. The reflectors should also be cooled to as low a temperature as practical. Cooling the reflectors to 300°K will reduce the heat input to the specimen to a total of approximately 1000 watts, which is actually the planetary radiation level requirement. However, radiation from the lamp envelopes and electrodes received by the specimen is expected to exceed 4000 watts. The problem becomes that of minimizing the infrared emission more than providing it. It may be possible to use a cooled double reflector as shown in Figure III-21 to further shield the infrared radiation and to help accomplish additional beam shaping.

For simulating conditions of planet radiation only, as in the eclipse position, the reflector elements can be controlled at the proper temperature to produce the heat required for the altitude being simulated. For simulation of deep-space it will be desired to cool the reflector elements to liquid nitrogen temperature to simulate the heat sink of space.

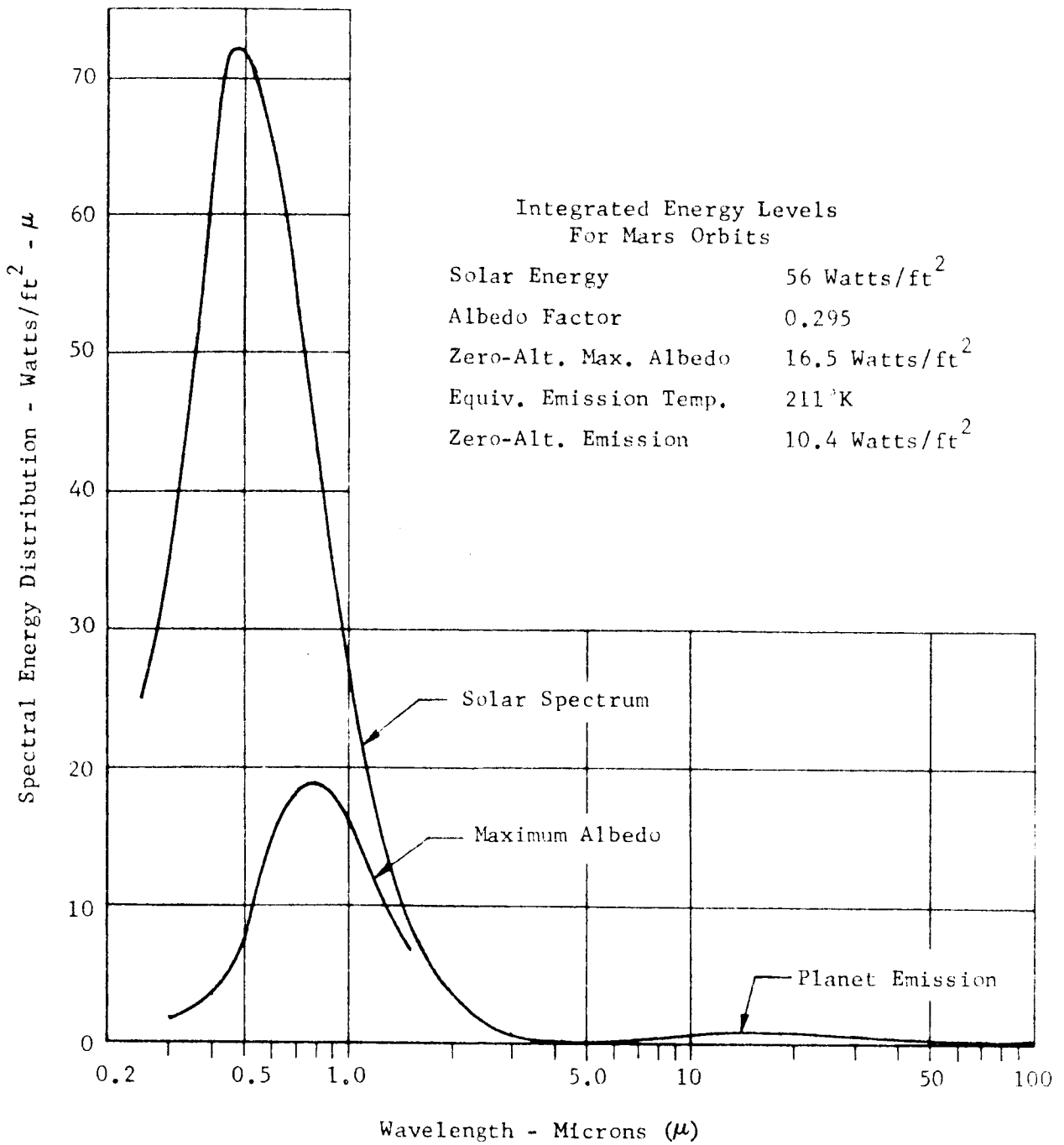


FIGURE III-1 ENERGY CHARACTERISTICS - MARS ORBITS

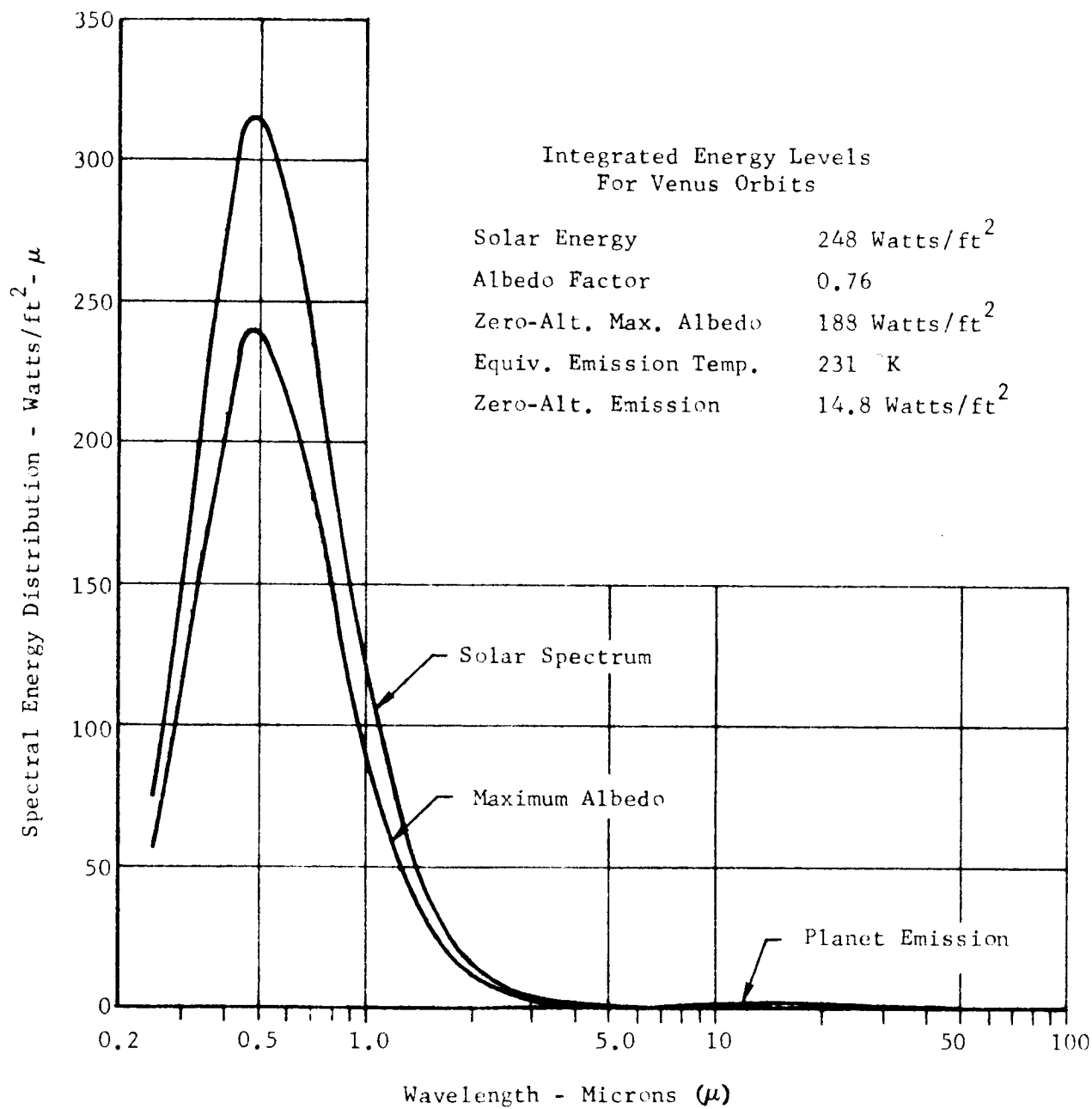
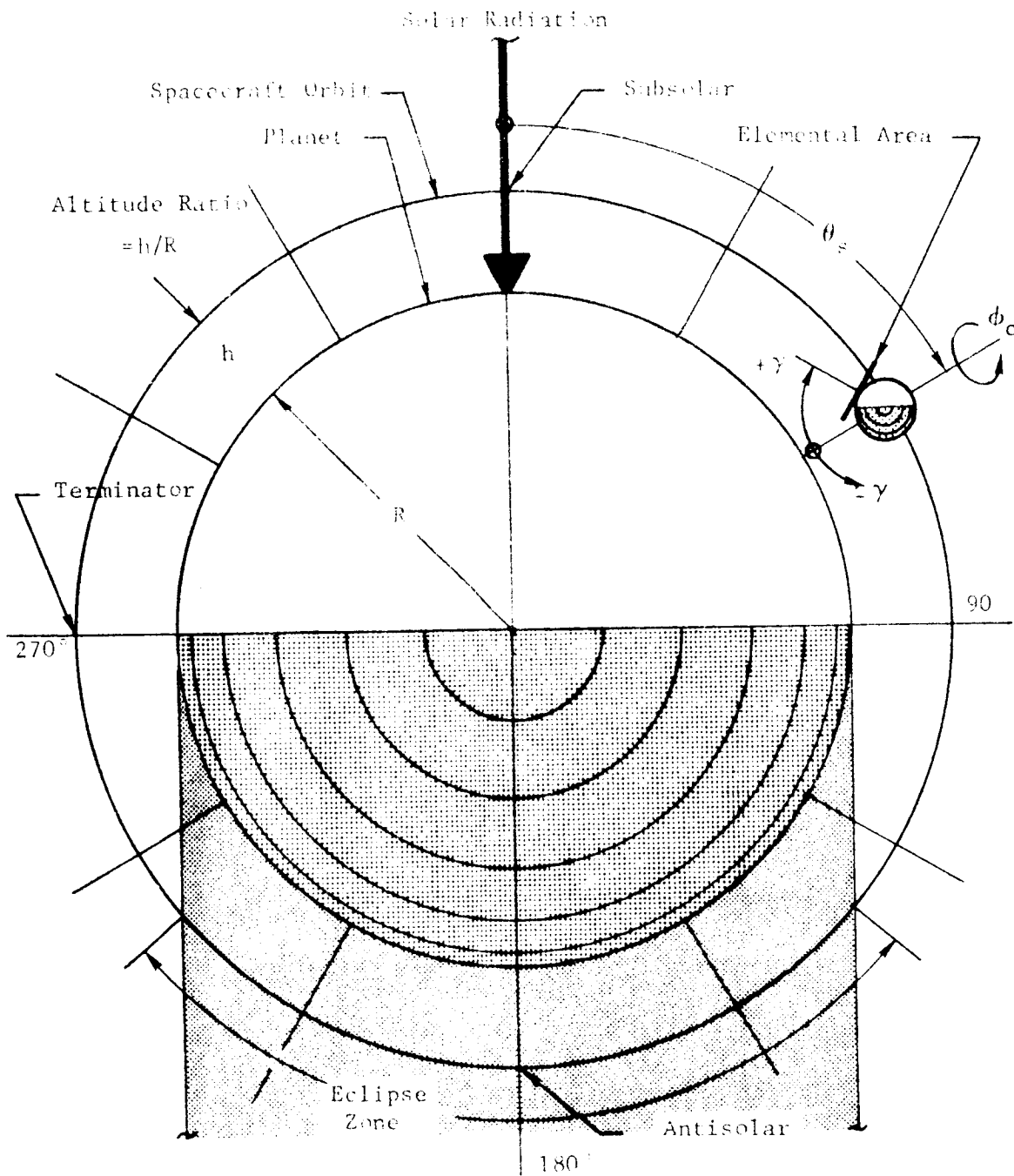


FIGURE III-2 ENERGY CHARACTERISTICS - VENUS ORBITS



- θ_s = Spacecraft Orbital Position From Subsolar
- $\pm\gamma$ = Pitch of Elemental Area From Normal to Planet
- $\pm\phi_c$ = Roll of Elemental Area About Normal to Planet

FIGURE III-3 SPACECRAFT ORBITAL COORDINATES

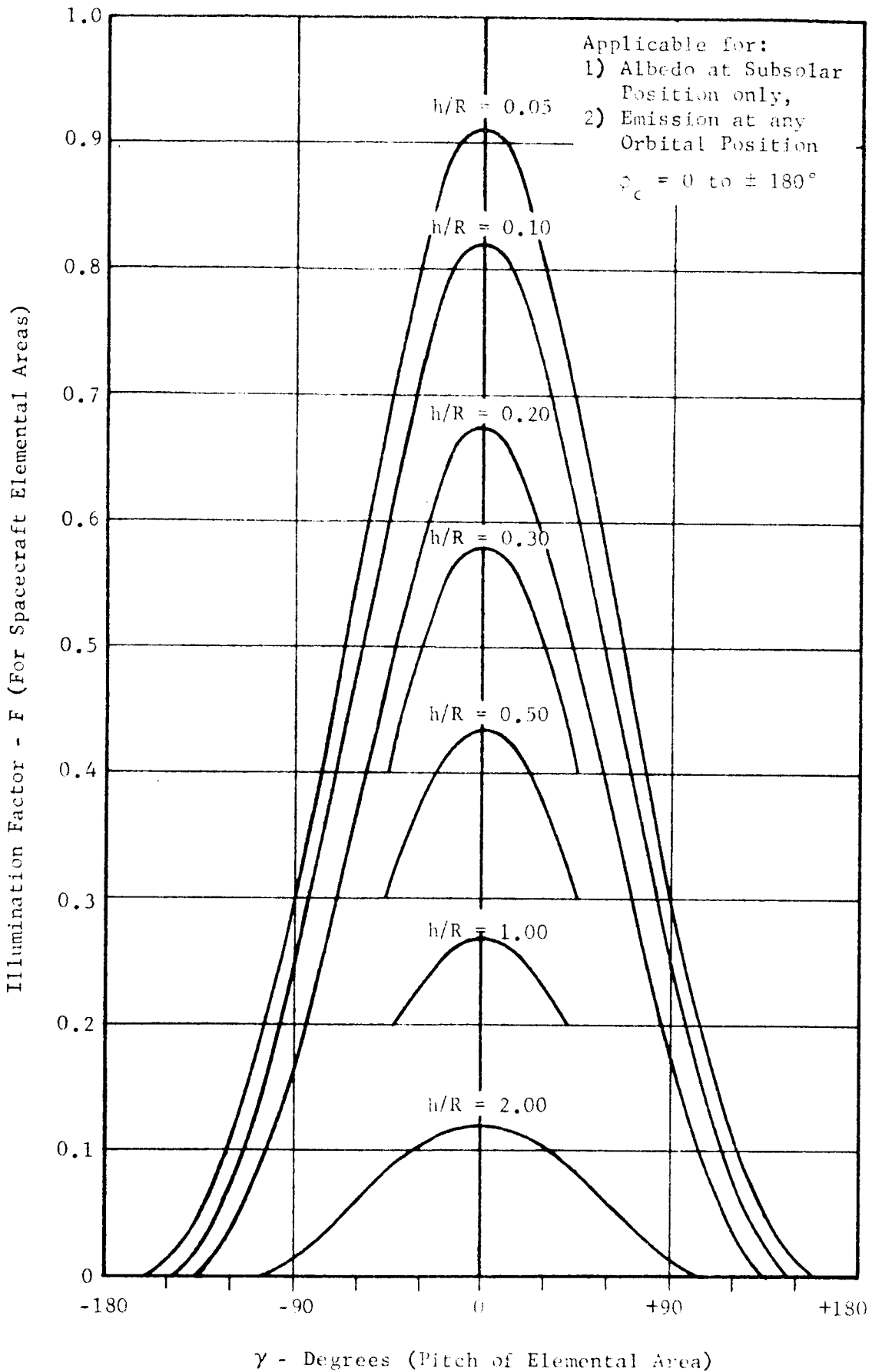


FIGURE III-4 ELEMENTAL AREA ILLUMINATION FACTORS -
 MAXIMUM ALBEDO AND PLANETARY EMISSION

NSI. 65-5

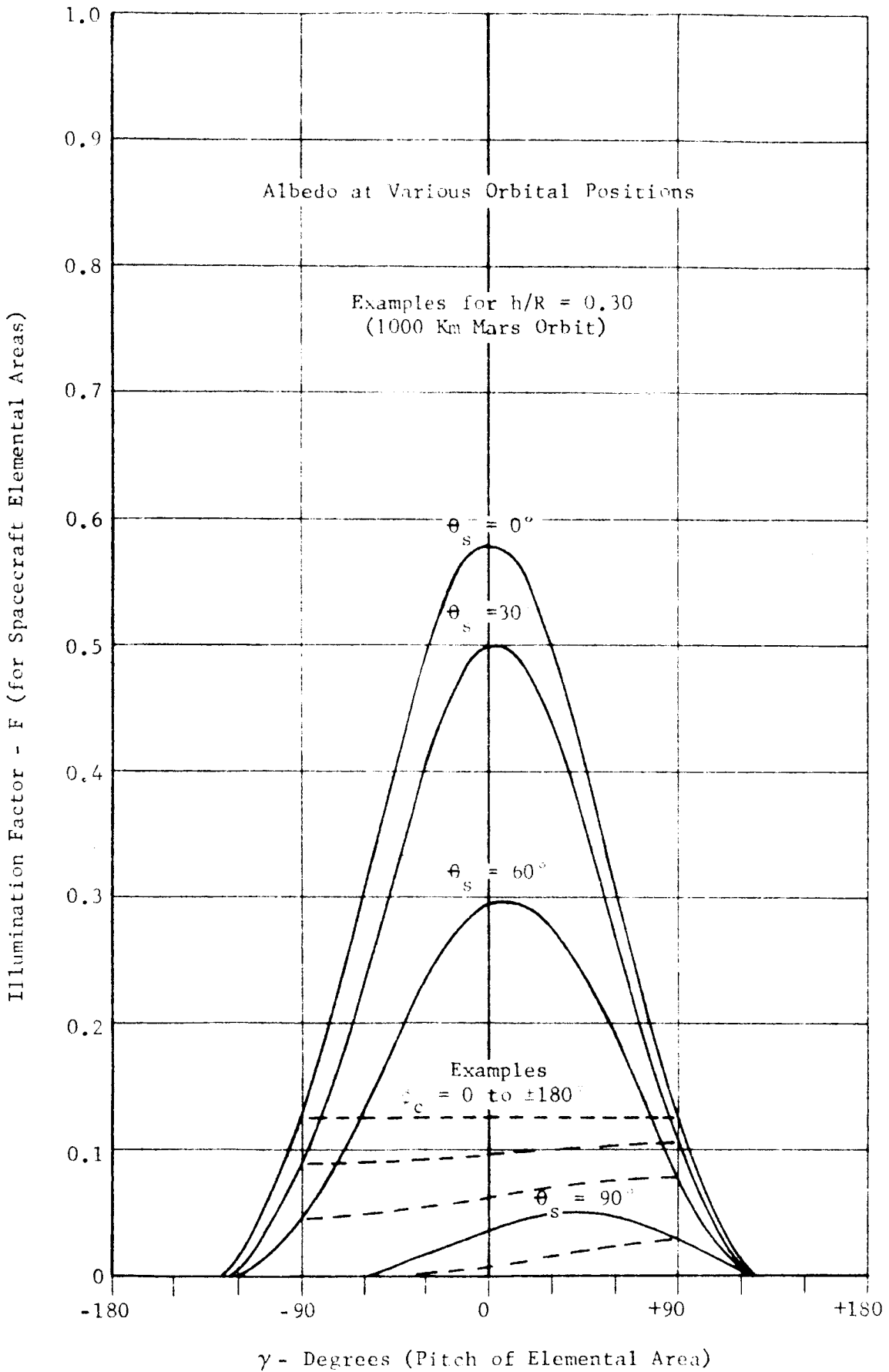


FIGURE III-5 ELEMENTAL AREA ILLUMINATION FACTORS -
PLANETARY ALBEDO
III-37

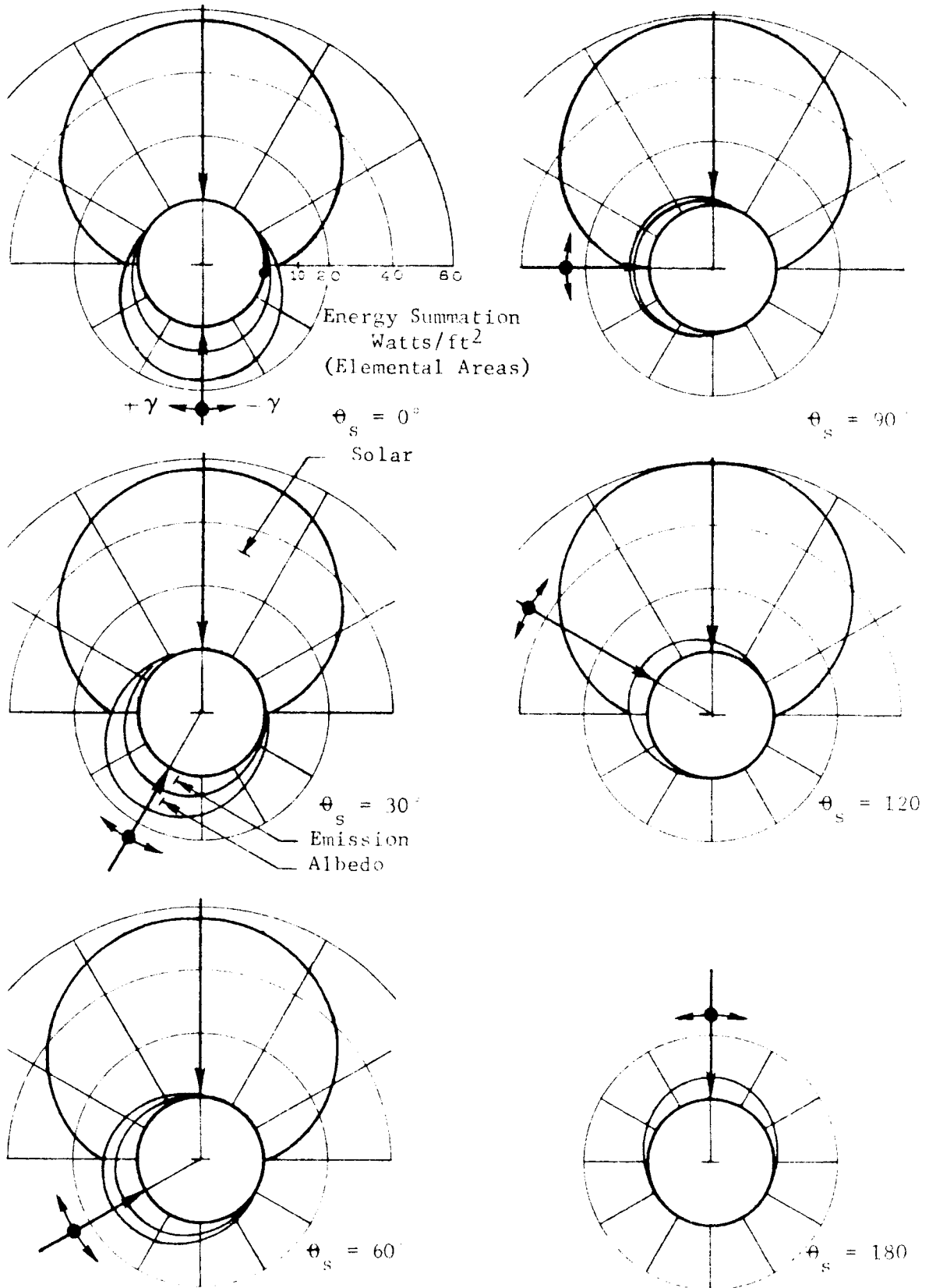


FIGURE III-6 POLAR ENERGY DISTRIBUTIONS -
1000 KILOMETER MARS ORBIT

Energy Incident on One-Foot-Diameter Spherical Test Volume
 (0.785 ft² Projected Area)

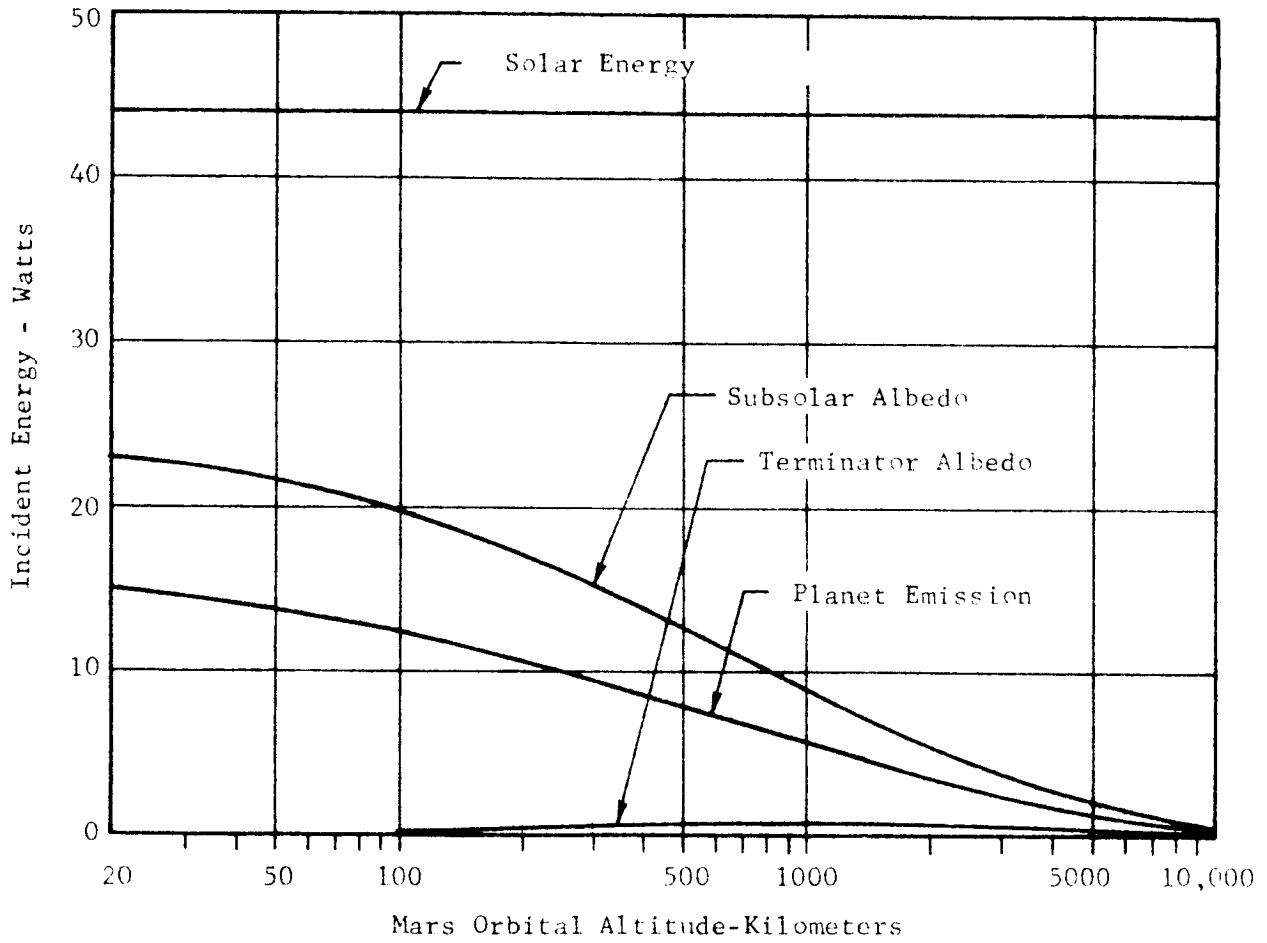


FIGURE III-7 ENERGY CONTRIBUTIONS - MARS ORBITS

Energy Incident on One-Foot-Diameter Spherical Test Volume
 (0.785 ft² Projected Area)

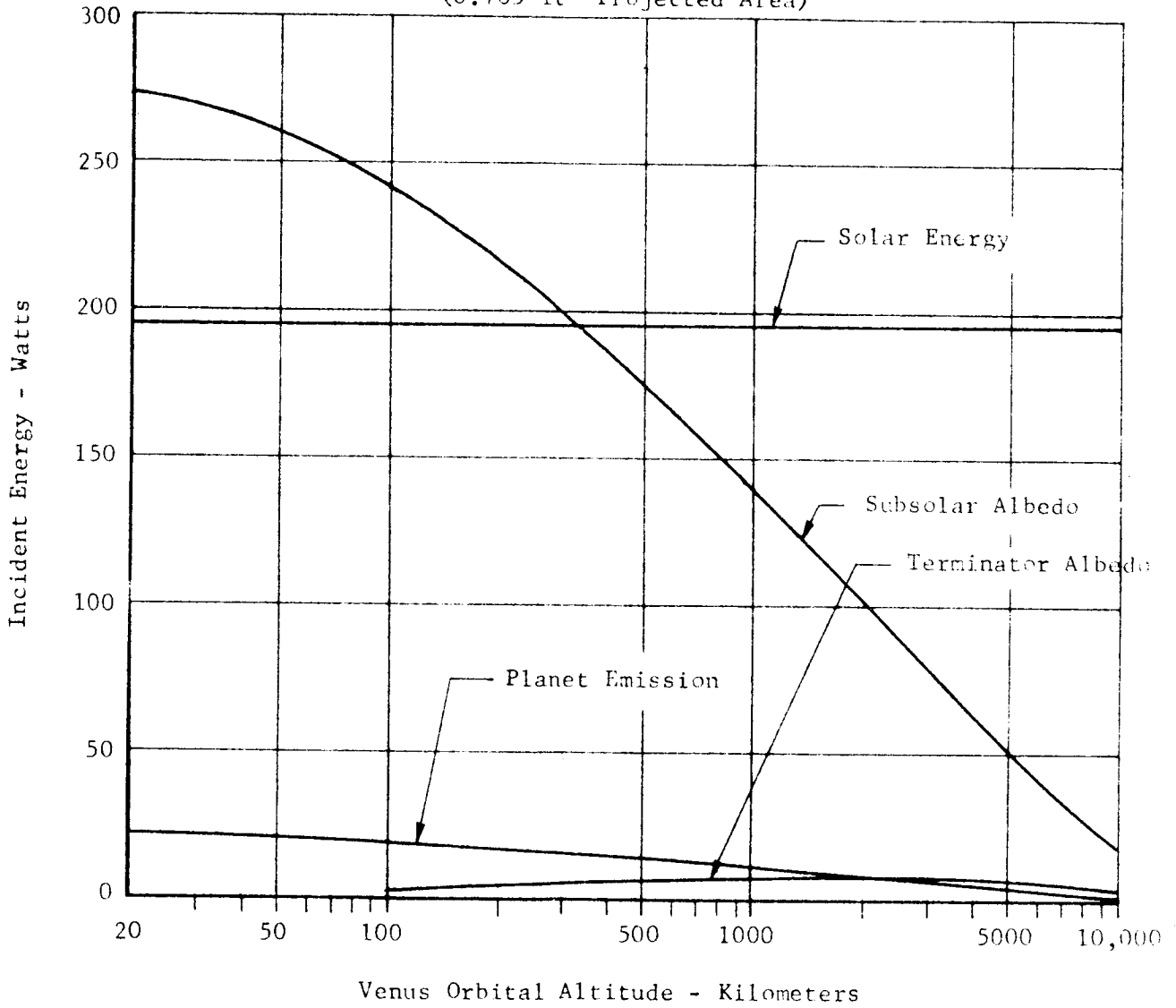


FIGURE III-8 ENERGY CONTRIBUTIONS - VENUS ORBITS

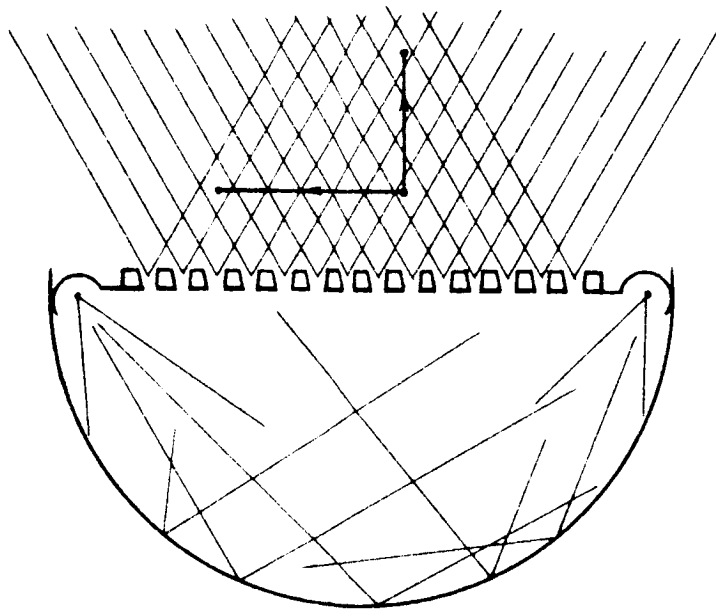


FIGURE III-9 RADIOSITY FIELD SIMULATOR

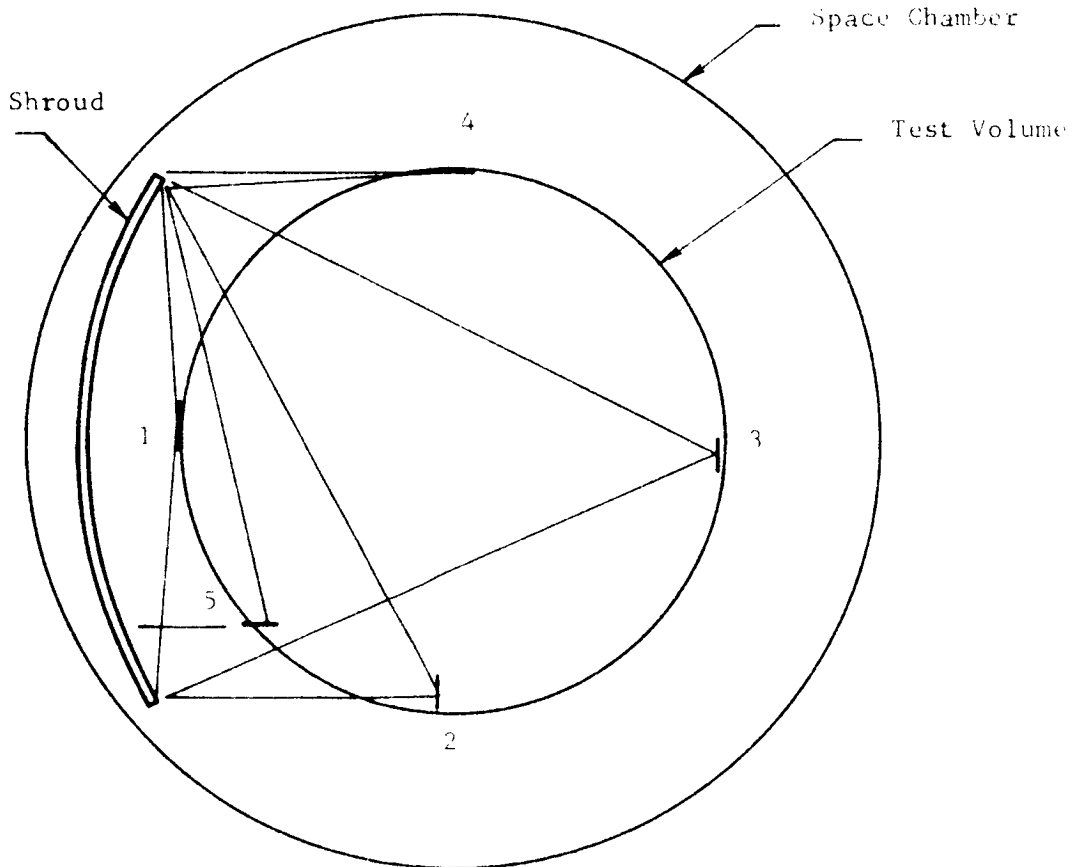


FIGURE III-10 SHROUD SIMULATOR

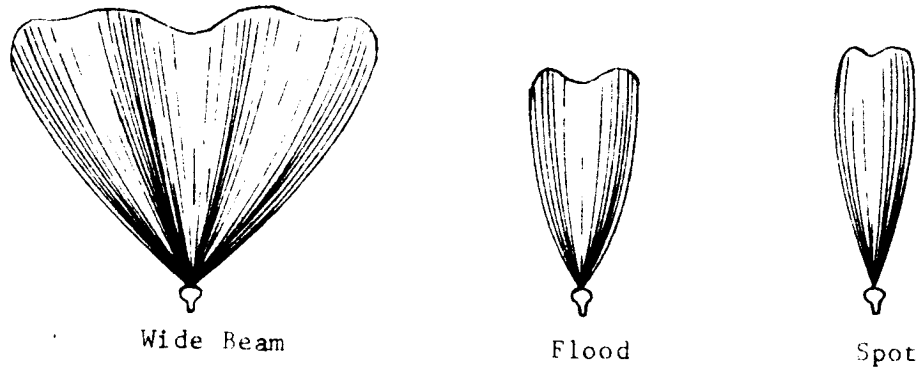


FIGURE III-11 LAMP BEAMS

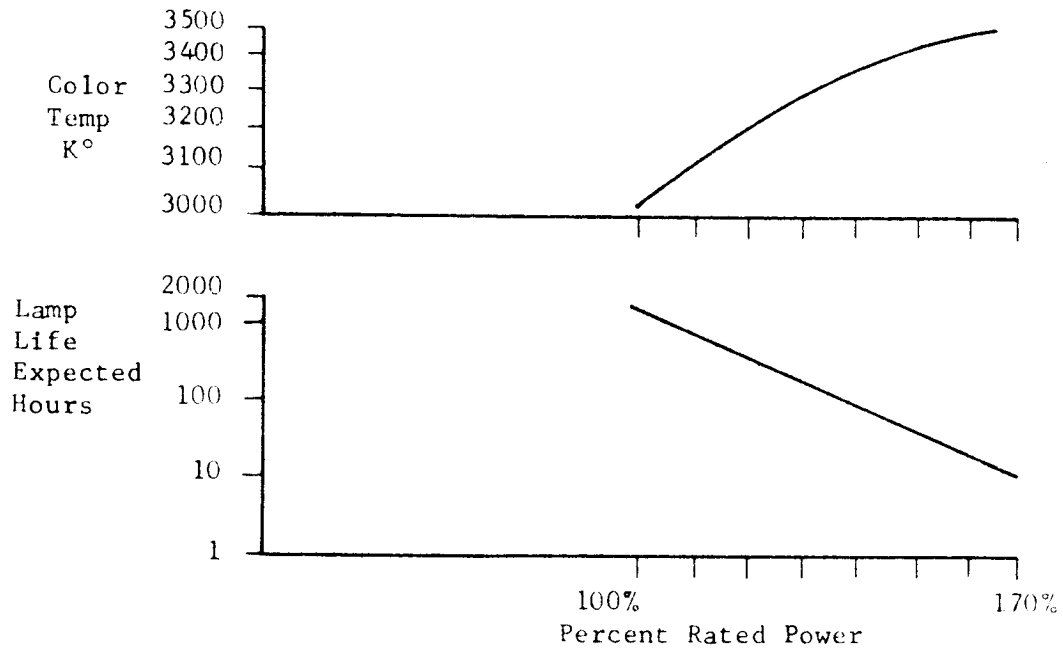


FIGURE III-12 INCANDESCENT LAMP CHARACTERISTICS

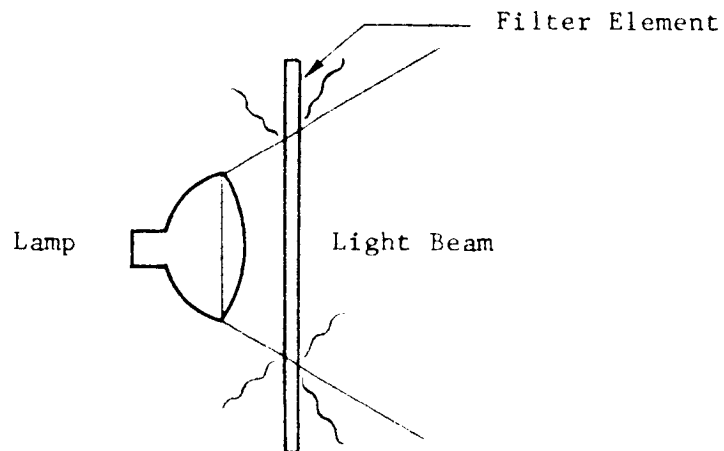


FIGURE III-13 WINDOW TYPE FILTER

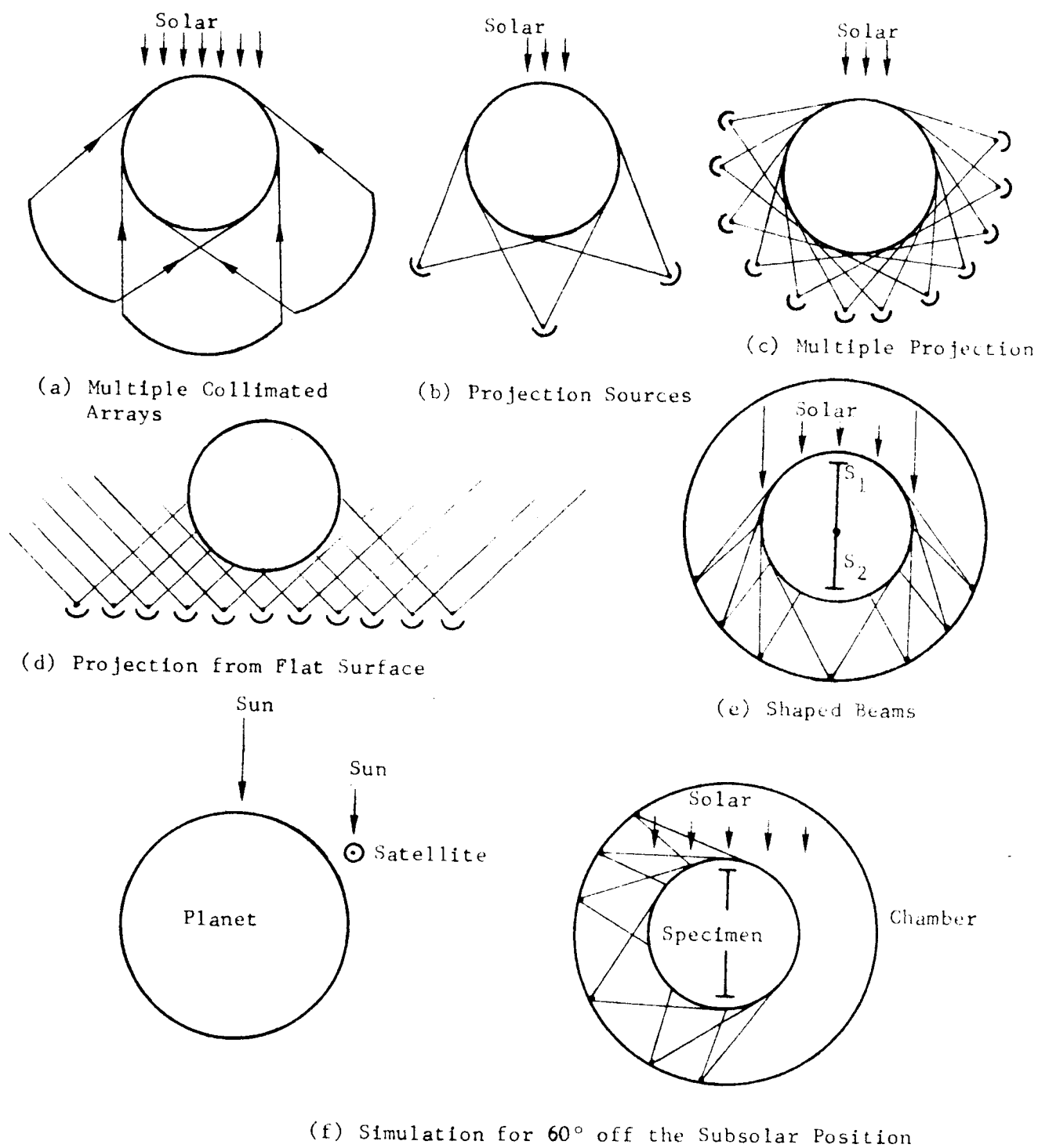


FIGURE III-14 SIMULATION ENERGY DISTRIBUTION APPROACHES

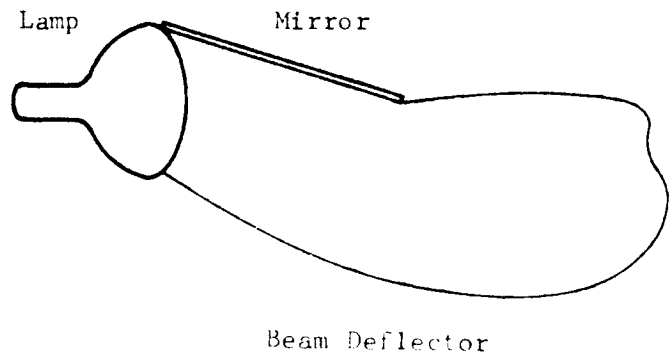
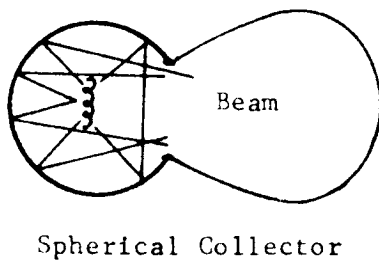
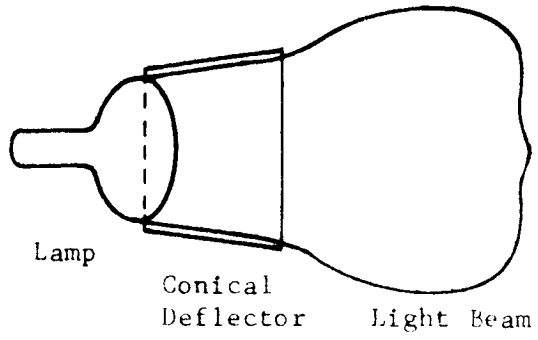
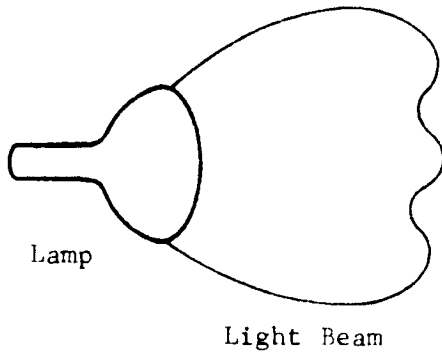


FIGURE III-15 BEAM SHAPING

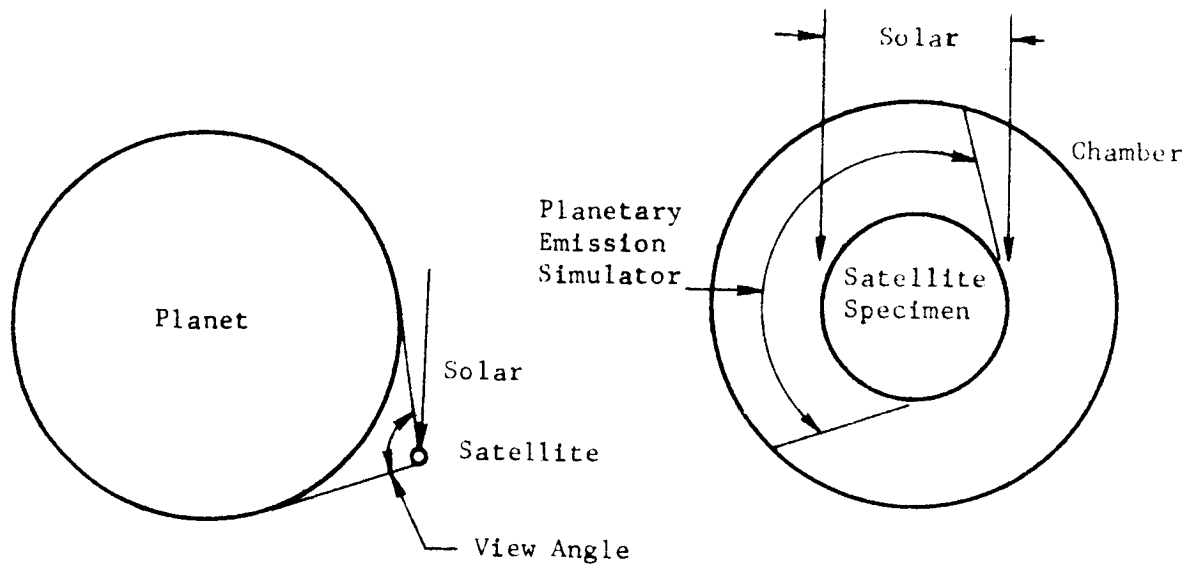


FIGURE III-16 PLANETARY SIMULATION NEAR ECLIPSE

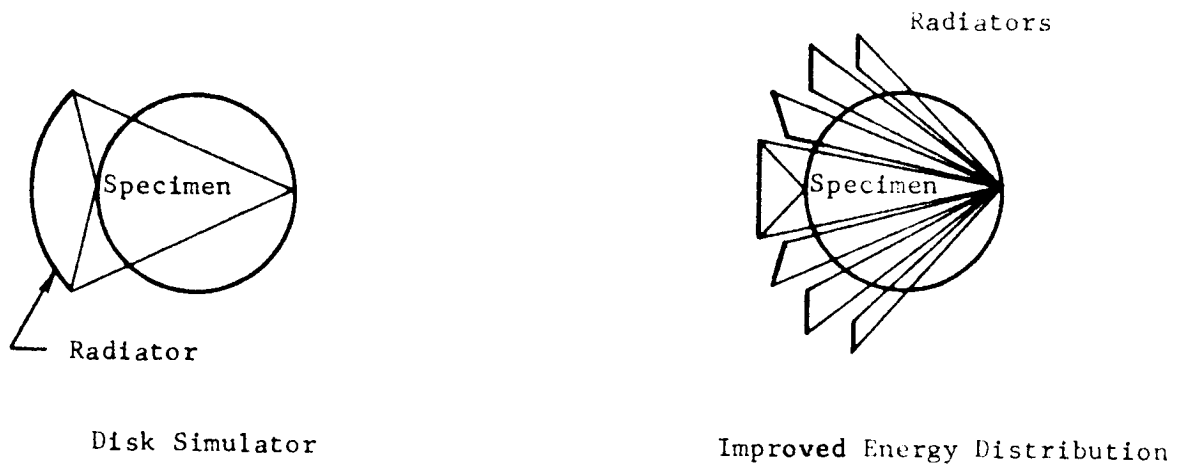


FIGURE III-17 DISTRIBUTED RADIATION SIMULATOR

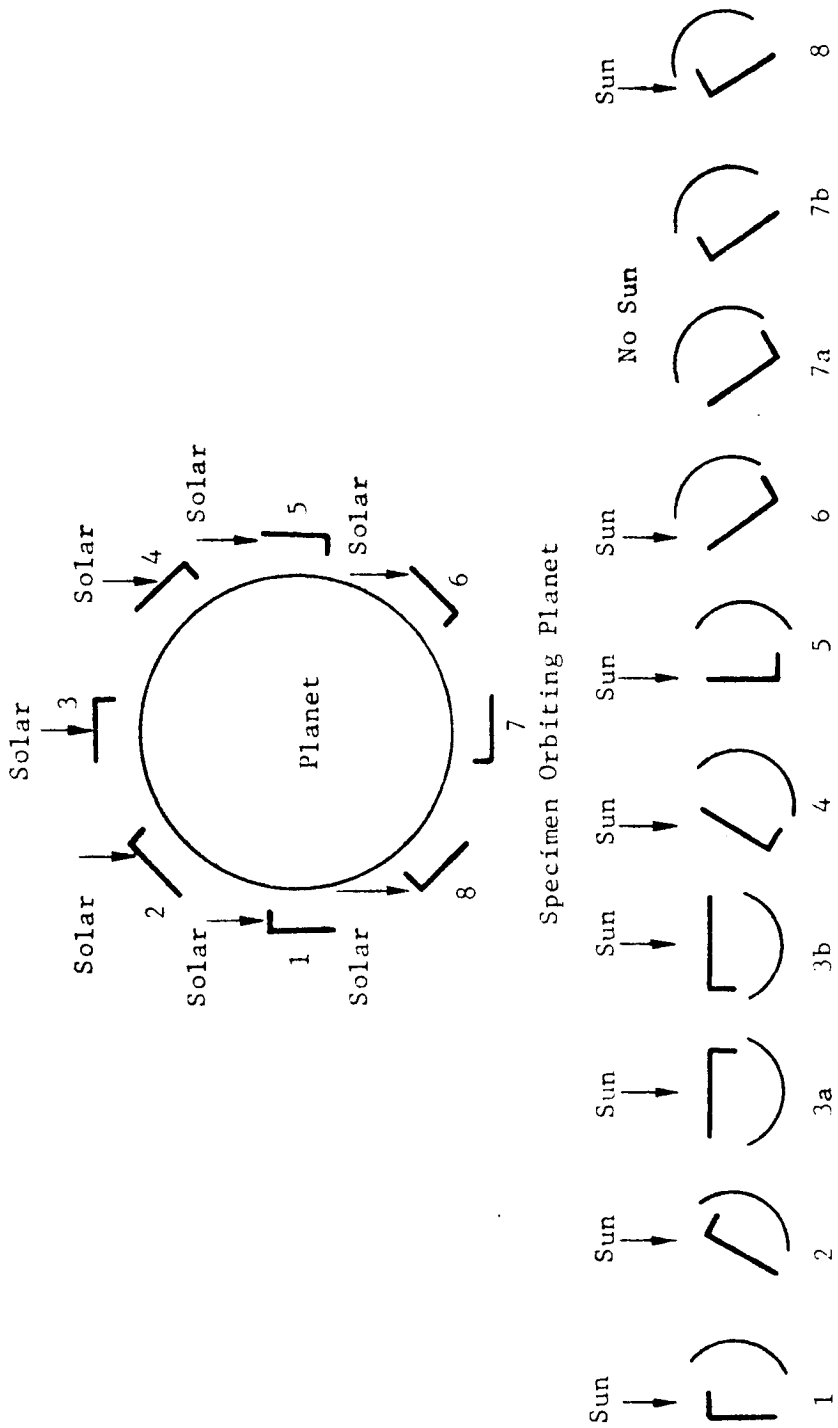


FIGURE III-18 METHOD FOR PROGRAMMING 360° ROTATION SIMULATION

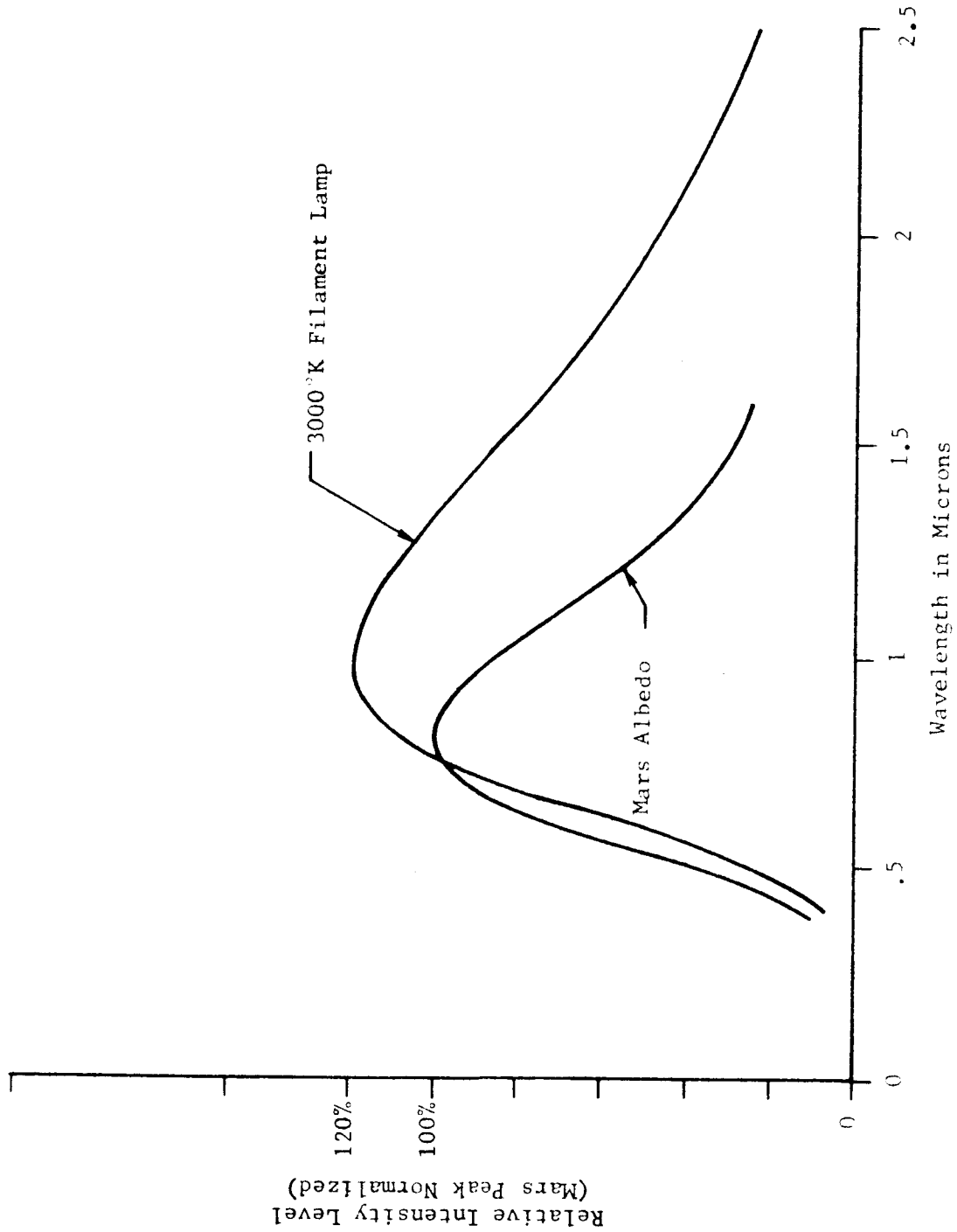


FIGURE III-19 COMPARISON OF MARS ALBEDO & 3000 K SOURCE

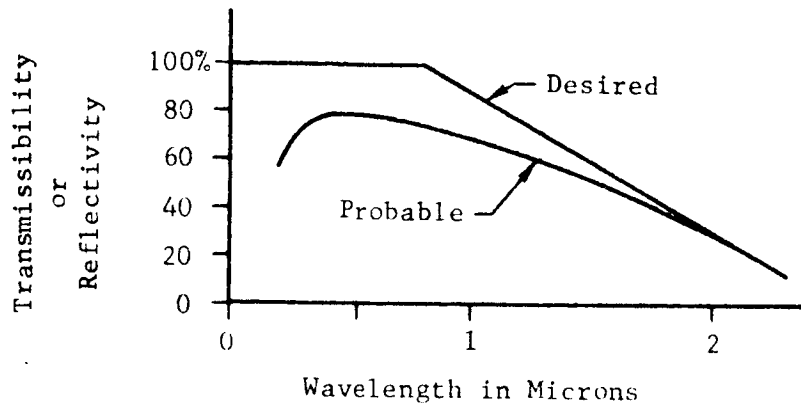


FIGURE III-20 FILTERING FOR MARS ALBEDO

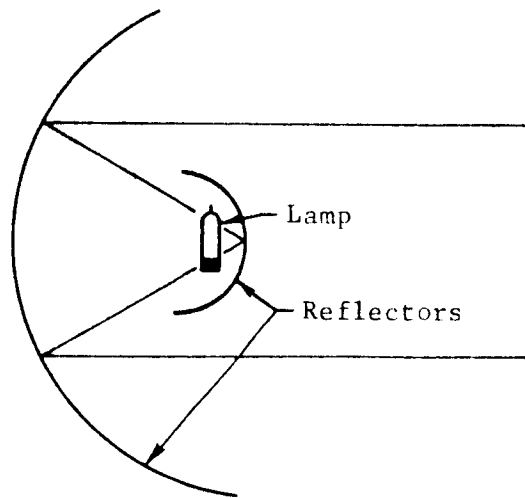


FIGURE III-21 BEAM REFLECTOR

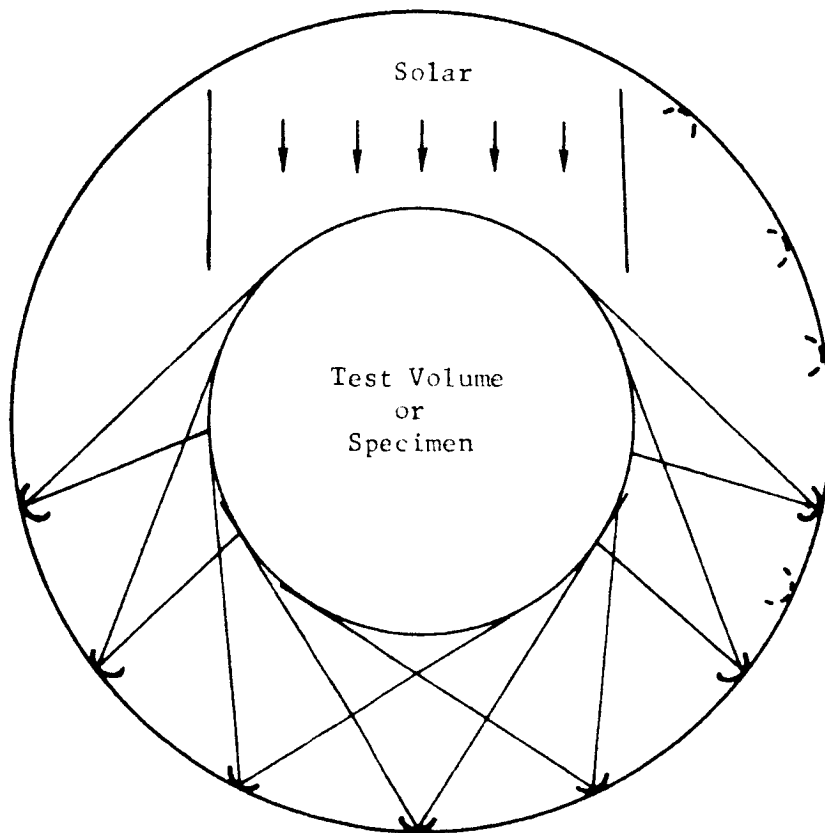
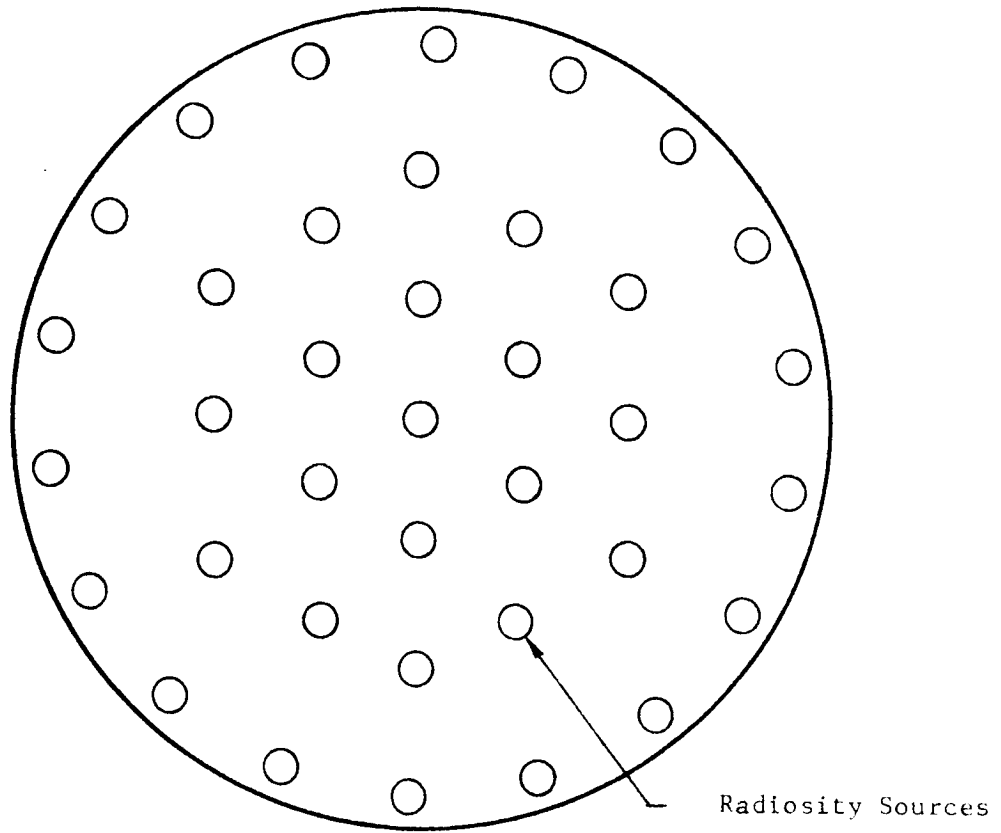


FIGURE III-22 MARS SIMULATOR

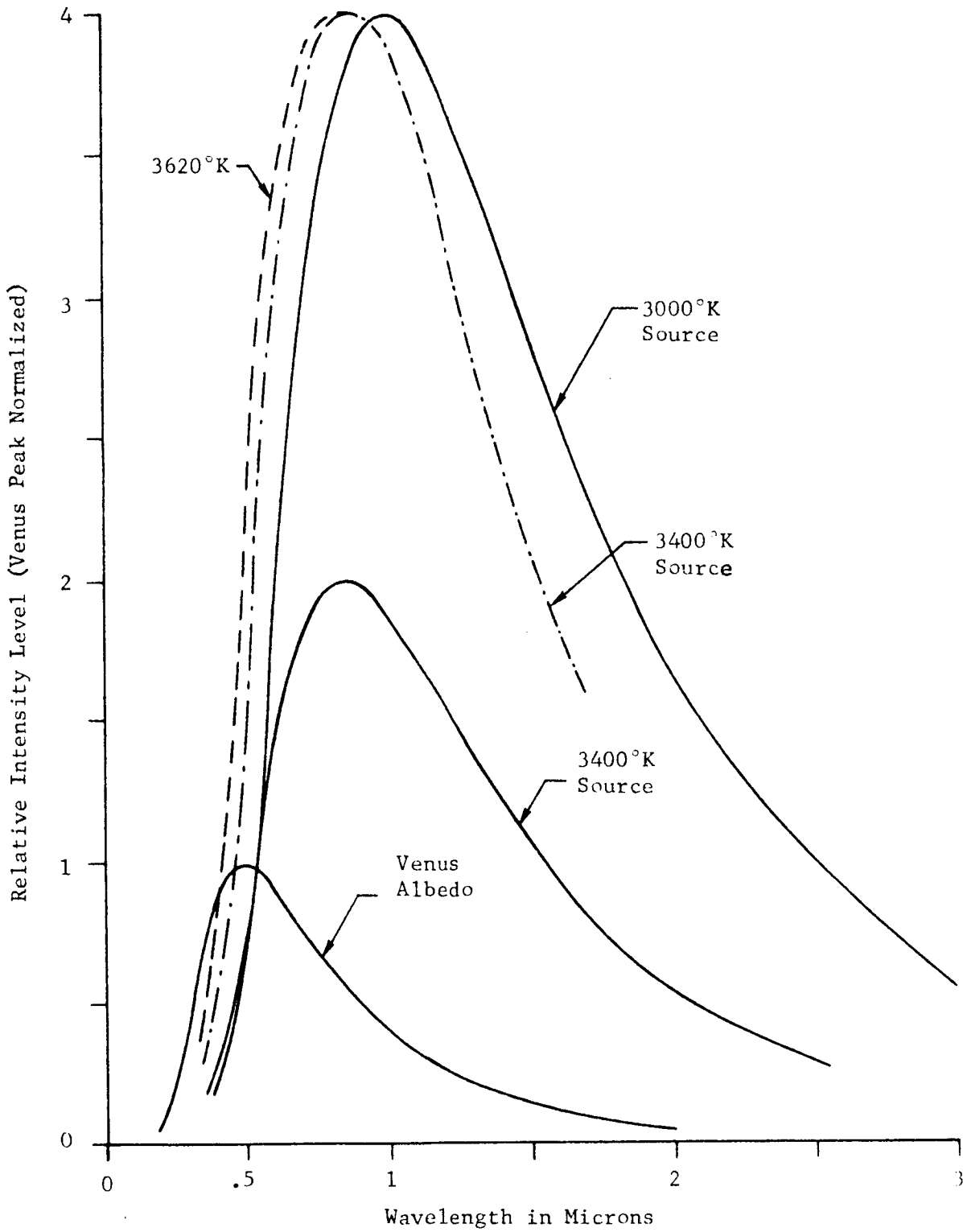


FIGURE III-23 COMPARISON OF VENUS ALBEDO AND TUNGSTEN FILAMENT SOURCES

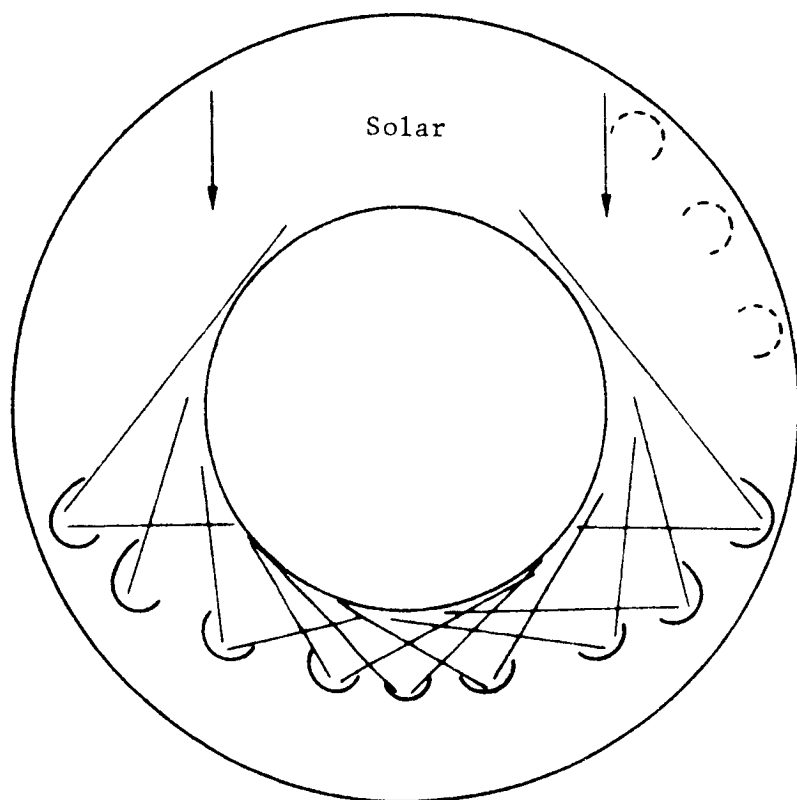
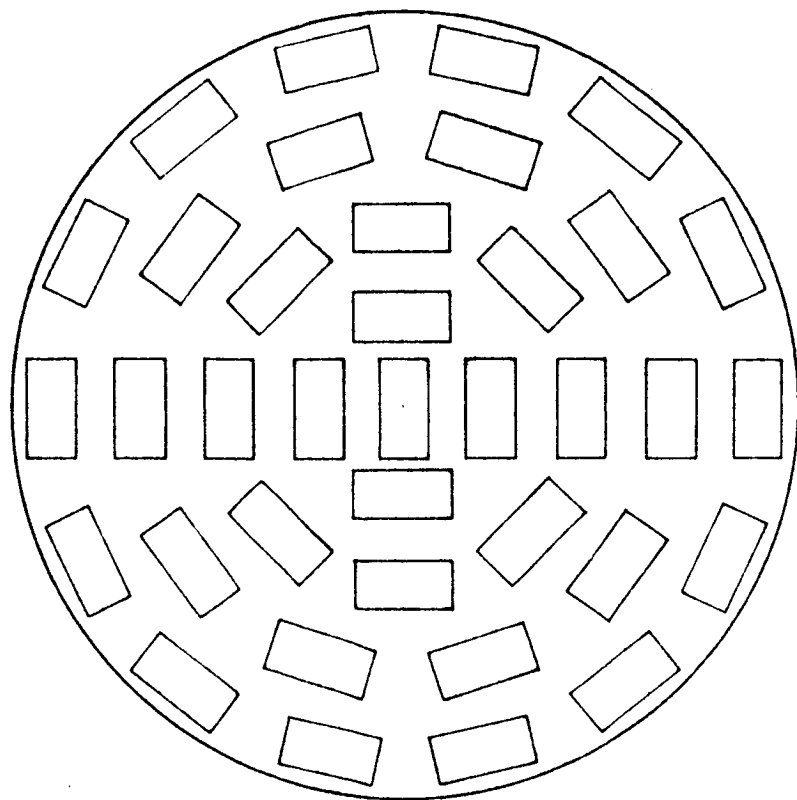


FIGURE III-24 VENUS SIMULATOR

NORTHROP SPACE LABORATORIES

SECTION IV

CONCLUSIONS AND RECOMMENDATIONS

THERMAL ANALYSIS

The results of the thermal analysis have shown that the effects of planetary radiation and albedo are significant and must be considered in the design and test of space vehicles in close circular orbits around Mars and Venus. Thermal analysis to determine thermal effects on spacecraft orbiting these planets in highly elliptical orbits is recommended for further study. Such a study should be restricted to those elliptical orbits and spacecraft configurations which are considered for Mars or Venus missions. The temperature of a spacecraft in a highly elliptical orbit is less affected by the planetary radiation and albedo than a spacecraft in a close circular orbit and simulation of these effects may be unnecessary. This is to be expected since the planetary radiation and albedo effects diminish with increasing altitude and a spacecraft in an elliptic orbit would spend much of the orbit time at altitudes where such effects are negligible.

SIMULATION TECHNIQUES

An ideal planetary simulator would be one which could provide variable simulation to produce the thermal effects of all phases of orbits around any of the planets or their moons, and be integrated in a space simulation facility. Practical limits do not even make the combination of Mars and Venus radiosity simulation attractive. Even with the design restricted to a single planet, the problems of simulating conditions for various orbital phases and altitudes make the simulator still complicated, and even for a fixed orbital condition, simulation of all the features of energy distribution and spectrum may be only achievable with adequate rather than perfect accuracy. The characteristics of a test specimen will determine the type and degree of simulation which is required. This leads to the conclusion that a simulation system should be tailored to a specific requirement related to the craft and its

mission and that an all-purpose planetary albedo and radiation simulator is not practical.

The basic limitation of presently conceived planetary radiosity simulators are:

- (1) The lateral distribution of energy on the test specimen may be in error in excess of 20% in many locations. For a craft with good thermal diffusivity this shortcoming is not serious. For very thin shelled satellites or for relatively isolated experiments, this may be more serious.
- (2) The simulation of higher altitude orbits requires a compromise in energy distribution and probably also in spectral match. (A compensation here is the fact that for higher altitudes planetary radiosity effects are a smaller percentage of the total space thermal input.)
- (3) The albedo reflector elements may cause some undesired reflection of by-passed solar energy.
- (4) Simulation of changing direction of planetary radiosity relative to the solar flux direction causes a disturbance of uniform energy distribution.
- (5) Simulated planetary radiation will be in a shorter spectral band than the real planetary radiation, if reasonably correct intensity and lateral distribution shall be achieved.

Further investigations and development are required and recommended in the following areas:

Reflector Devices

Reflector elements generally used are highly polished metallic surfaces with protective coatings. The properties of these surfaces may result in spectrally selective reflectance which may be detrimental or beneficial to the desired performance. Through the selection of coatings and finishes for the reflectors, it is possible to achieve desirable color correction for the reflected energy. The approach used by General Electric in producing

"Cool Beam" incandescent lamps is to eliminate much of the infrared energy by transmitting the light through multiple layer interference surfaces which mainly reflect the visible light. This approach could be used to improve the energy spectrum of sources for Mars albedo simulation purposes. If necessary, this may be supplemented by higher lamp filament temperatures at the expense of lamp life.

Further research to define the required reflectance characteristics, suitable coatings, filament temperature and lamp life penalties would provide basic information required for successful design of planetary albedo and radiation simulation facilities.

Beam Shaping Techniques

The simulation of planetary albedo requires beams of albedo energies from the sources to the specimen of varying shapes as the source location around the specimen changes. A program to determine the extent that various source and reflector combinations could affect this variation would be very useful.

Source Selection

The operation of potential radiation sources in a vacuum environment should be experimentally investigated to ascertain problems which might be encountered in system use. Gas-arc lamps should be tried in a vacuum environment to determine the cooling requirements, thermal stress resulting from radiant cooling of the envelope, amount of infrared energy emitted and the extent that it can be reduced with filtering.

Preliminary Facility Design

A simulator for a particular spacecraft and mission should be designed, capable to provide a specified degree of planetary simulation. After radiation sources are selected or developed, locating and controlling them to achieve a proper distribution of energy around and through a specimen volume is very complex. A combination of intuitive design and computer

calculations is required to develop and verify the distribution of energy for simulating various orbital positions and altitudes.

The specimen support and rotation problem is related primarily to the requirement for orientation relative to the solar simulation, but also needs to be considered with respect to possible shielding effects of planetary simulation devices.

NORTHROP SPACE LABORATORIES

APPENDIX A

ALBEDO SIMULATION SURVEY

A summary of the results from a survey made to collect information on albedo simulation techniques is presented in this Appendix.

Letter and Questionnaire

A letter and questionnaire requesting comments and recommendations on Albedo Simulation was sent to individuals at 28 companies or agencies known to have an interest in space simulation. Nine responses were returned. Of these, three companies indicates that they were unable to answer the questionnaire either because they did no planetary simulator work, or for other reasons. The six answers received are summarized here with the questions as submitted.

Question A. "Relative to solar simulation, how important is the inclusion of albedo simulation? What considerations have you given to including planetary albedo and planetary radiation simulation in space environment tests?"

- Answers:
1. Mandatory to simulate for low orbit.
 2. Simulate for thermal balance and optics calibration.
 3. The solution can often be obtained analytically.
 4. Very important for small scientific satellites.
 5. Essential for some tests.
 6. Depends on design - Plans call for inclusion as part of tests.

Question B. "What specific techniques are recommended for the simulation of planetary albedo (reflected) and planetary radiated thermal energy flux?"

- Answers:
1. Quartz lamps on bird-cage structure.
 2. Diffusing hemisphere source with conical holes.
 3. Quartz lamps.
 4. Radiating plate and direct skin heaters.

5. Black painted honeycomb (moon radiation).
6. Again specimen dependent. Tungsten lamps good where heat flux satisfactory. No satisfactory source found for precise spectral match.

Question C. "Which type of thermal balance tests with simulated solar radiations and planetary albedo and radiation is most useful, among the following, and why do you think so?"

- a. Simulation of maximum extreme conditions, determination of transient responses and stabilization times, or time to reach allowable limits...
- b. Time averaging of radiation environments...
- c. Duplication of cyclic variations of thermal environments...

Answers:

1. a. For qualification tests on small vehicles.
b. For large long time constant vehicles.
c. Ideal but difficult and costly hence utility questionable.
2. a and b. Generally
c. In some cases.
3. c. Assuming adequate analysis accompanies.
4. a. Second in importance.
b. Most useful.
c. Useful in verifying orbital variation.
5. a. Most useful for verifying calculation and assumption.
c. Useful for environmental testing.
6. All appropriate for certain circumstances.
a. Gives satisfactory design information and go-no-go indication.
b. Of limited value.
c. Best but normally impractical.

Question D. "What is the order of importance of planetary albedo and radiation simulation parameters, among the following?"

- a. Intensity or flux density...
- b. Uniformity of the flux...
- c. Shape factor or view angle...

d. Spectral distribution energy match.

Answers:

	<u>First</u>	<u>Second</u>	<u>Third</u>	<u>Fourth</u>
1.	a.	c.	b.	d.
2.	a. b. & c.	d.		
3.	a. & d.			
4.	c.	a.	b.	d.
5.	a.	c.	d.	b.
6.	a.	b.	c.	d. (normally)

Question e. "Present simulation of solar spectral distribution is less than perfect. Does this cause you to minimize the effects of spectral simulation error by restricting the selection of thermal control coatings to those that will yield representative test results? From your experience, how serious do you consider these limitations to be?"

Answers:

1. No restriction on thermal control materials foreseen.
2. Thermal behavior factors are selected to avoid sophisticated tests.
3. Analytic methods are used to compensate for test limitations.
4. Analysis can predict true temperatures.
5. Thermal coatings are not generally narrow band devices and 10% to 5% spectral match can be achieved.
6. NO, do not restrict selection for test validity. Satisfactory spectral simulation is available where care is used in data analysis.

Question F. "What instrumentation is recommended for monitoring albedo and planetary radiation simulator performance?"

Answers:

1. Continuous intensity monitoring at widely separated points, measurement of the look angle and spectrum periodically, and uniformity measurement at test beginning or end.
2. Instrumentation depends on simulator characteristics. Excellent design can reduce the instrument requirement to a single sensor.
3. Disc calorimeter, and measure all coating properties.

NORTHROP SPACE LABORATORIES

4. Total energy sensor plus spectral discriminating sensor such as a solar cell if two types of sources are used.
5. Total energy sensor plus black body source temperature.
6. Calorimeters monitoring absolute flux at vehicle location and a beam monitor to sample source spectrum where small changes may be important.

Telephone Contacts

Telephone conversations with twenty-three individuals indicated that most had an interest in the simulation of planetary thermal effects but had not given much thought to actual implementation of simulation devices. Several suggested the use of infrared lamps and heated surfaces to provide the required heat inputs. Some rather unique and well-engineered simulation system proposals were encountered.

REFERENCES

1. Sinton, W. M. and Strong, J., Astroph. J., 131,470, 1960(a)
2. Sinton, W. M. and Strong, J. "Observations of the Infrared Emission of Planets and Determination of Their Temperatures" Progress Report of Johns Hopkins University, Laboratory of Astrophysics and Physical Meteorology, April 15, 1960(b)
3. General Electric NSVD "Space Facts - A Handbook of Basic and Advanced space Flight and Environmental Data for Scientists and Engineers" copyright 1960
4. Kaplan, L. D., Planet. Space Sci. 8, 23, 1961.
5. Kellogg, W. W. and Sagan, C. "The Atmospheres of Mars and Venus" National Academy of Sciences, National Research Council, Publ. 944, Washington, D.C., 1961
6. Pettit, E. and Sinton, W. M. "Planets and Satellites" Chapters 10 and 11, University of Chicago Press, Chicago, Ill., 1961
7. Stevenson, J. A. and Grafton, J. C., "Radiation Heat Transfer Analysis for Space Vehicles" ASD TR61-110, Part 1, Dec., 1961
8. Warner, B. "The Clouds of Venus" J. of Brit. Astro. Assoc., Vol. 71, No. 5, 1961, pp 200-201
9. Jastrow, R. and Rasool, S. I. "Radiative Transfer in the Atmospheres of Venus and Mars" Proc. of the Third Int. Space Sci. Sympos., Washington, D.C., May 2-8, 1962
10. Öpik, E. J. "Atmosphere and Surface Properties of Mars and Venus" Progress in Astron. Sci., Vol. 1, 1962, pp 261-342
11. Sinton, W.M. paper presented at the Sympos. of Planet. Phys., Liege, Belgium, 1962
12. Wyckoff, R. C. "Scientific Experiments for Mariner R-1 and R-2" Calif. Inst. of Tech. Jet Propul. Lab. Tech. Rept. No. 32-315, 15 July 1962

13. Briggs, M. H. and Mamikunian, G. "Venus - A Summary of Present Knowledge" J. of Brit. Interpl. Soc., V. 19, No. 2, March-April, 1963
14. Chase, S. C., Kaplan, L. D., and Neugebauer, G. "The Mariner 2 Infrared Radiometer Experiment" J. of Geophysical Research, V. 68, No. 22, 15 November 1963
15. Murray, B. C., Wildey, R. L., and Westphal, J. A. "Infrared Photometric Mapping of Venus Through the 8-14 Micron Atmospheric Window," Div. of Geological Sciences, Calif. Inst. of Tech., Pasadena, Calif., Contribution No. 1172, May 13, 1963
16. Rasool, S. I. "Structure of Planetary Atmospheres" A.I.A.A. Jour., V. 1, No. 1, Jan. 1963
17. Rea, D. G. and Welch, W. J. "The Reflection and Emission of Electromagnetic Radiation by Planetary Surfaces and Clouds" Space Science Reviews, Vol. 11, No. 4, Oct., 1963
18. Sinton, W. M. "Recent Infrared Spectra of Mars and Venus" J. of Quant. Spectrosc. Radiat. Transfer, Vol. 3, pp 551-558, 1963
19. Pettit, E. and Nicholson, S. B. "Radiation Measures on the Planet Mars" Publ. of the Astron. Soc. of the Pacific, 36, 1924, pp 269-272
20. Coblentz, W. W. "Temperature Estimates of the Planet Mars" Astronomische Nachrichten, 224, No. 5374, col 361-78, 1925
21. de Vaucouleurs, G. "Physics of the Planet Mars" Faber and Faber Limited, 24 Russell Square, London, England, copyright 1954
22. Schilling, G. F. "A Note on the Atmosphere of Mars" J. of Geoph. Res., Vol. 67, No. 3, March, 1962
23. Kellogg, W. W. and Sagan, C. "The Terrestrial Planets" Annual Review of Astr. and Astroph., Vol. 1, 1963, pp 235-266
24. Kreith, F. "Radiation Heat Transfer for Spacecraft and Solar Power Plant Design" International Textbook Co., Scranton, Pa., 1962
25. de Vaucouleurs, G. "Geometric and Photometric Parameters of the Terrestrial Planets" Rand Corp. Memo RM-4000-NASA, March, 1964
26. Guérin, P. "Spectrophotometric Study of the Reflectivity of the Center of the Martian Disk at Opposition, and the Nature of the Violet Layer" Planet. and Space Sci., Vol. 9, March, 1962

27. Coulson, K. L. and Lotman, N. "Molecular Scattering of Solar Radiation in the Atmosphere of Mars," J. of Geophys. Res., Vol. 68, No. 20, 15 Oct. 1963
28. de Vaucouleurs, G. "Multicolor Photometry of Mars in 1958" Planetary and Space Sci., Pergamon Press, 2, 1959, pp. 26-32
29. Kuiper, G. P. "The Atmospheres of the Earth and the Planets" University of Chicago Press, Chicago, Ill., 1949 Edition and 1952 Edition
30. Kozyrev, N. A. "Molecular Absorption in the Violet Region of the Spectrum of Venus" Publ. Crimean Astroph. Obs. 12, 177-181, 1954
31. Kurchakov, A. V. "Optical Properties of the Atmosphere and Surface of the Planet Mars" A. R. S. J. Suppl., March 1962, pp 490-495
32. Moroz, V. I. "The Infrared Spectrum of Venus (1-2.5 μ)" Soviet Astronomy, Vol. 7, No. 1, July-August, 1963
33. Woolley, R. v.d.R. "Monochromatic Magnitudes of Mars in 1952," Mon. Not. Royal Astr. Soc. 113, 521-525, 1953
34. de Vaucouleurs, G. Proc. Lunar Planet. Explor. Colloq., 1959, 2 (1), 42
35. Russell, H. N. "On the Albedo of the Planets and Their Satellites" Astroph. J. 43, 173-196, 1916
36. Allen, C. W. "Astrophysical Quantities" University of London, The Athlone Press, 1963, 2nd Edition
37. Martynov, D. Ya "On the Radius of Venus" Soviet Astronomy, Vol. 6, Jan.-Feb., 1963, pp 511-517
38. "American Ephemeris and Nautical Almanac for the Year 1965" U.S. Govt. Printing Office, Washington, D.C.
39. McCue, Gary A., Program for Determining the Thermal Environment and Temperature History of Orbiting Space Vehicles, ASD TN 61-83, February 1961.
40. Wallace, D. A., Kelley, L. R., Garber, D. L., Bottorff, M. R., Lovejoy, E. F., "Design of a Thermal Simulation Unit for the Naval Missile Center Hyperaltitude Chamber" USGEC Report 104-101, U.S. Navy Contract No. NBy-33536.
41. Fitz, C. D. and Mayer, E. A., "Evaluation of Methods for Simulating the Earth's Albedo and Planet Radiation", AEDC-TDR-63-217, October 1963.

42. Camack, W. G., "Method for Simulating Planetary Radiation", Philco Western Development Laboratories, November 1964.
43. "Final Report Engineering Design Study of Albedo Simulator System and Apollo Spacecraft Gimbal Support System", TD No. H-6196-3, prepared for NASA/MSC, Contract No. NAS9-2976 by Honeywell, Inc.
44. Landau, A., "Improved Solar - Albedo - IR Radiation Module", unsolicited proposal XPS260, Aerospace Controls Corporation, 8 November 1963.
45. Jones, L. A., et al; "The Science of Color", Optical Society of America, Washington 36, D. C.